Investigating the interplay between excitatory neurotransmission and GABAa receptor expression and trafficking in the stargazer mutant mouse

Payne, Helen Louise

Investigating the Interplay between Excitatory Neurotransmission and $GABA_A$ Receptor Expression and Trafficking in the Stargazer Mutant Mouse

Helen Louise Payne

A thesis submitted to the University of Durham in accordance with the requirements for the degree of Doctor of Philosophy

School of Biological and Biomedical Sciences,
University of Durham

2006

ABSTRACT:

The stargazer mutant mouse is an animal model of human absence epilepsy and cerebellar ataxia. The stargazer mutation results in the complete ablation of expression of TARPγ2, an AMPA receptor (AMPAR) auxiliary subunit. Results of the current study provide evidence for the involvement of TARPγ2 in the regulation of expression and trafficking of specific $GABA_A$ receptor (GABAR) subtypes in the cerebellum and hippocampal formation.

Expression of total GABARs (γ2 and δ-containing) in stargazer cerebellum was found to be reduced to 70 ± 10% of control levels. *In situ* [^{3}H] muscimol autoradiography revealed that this loss of GABARs was entirely restricted to the cerebellar granule cell (CGC) layer. Total numbers of γ2-containing GABARs were only slightly reduced in the stargazer cerebellum (90 ± 6% of control levels), which was entirely attributable to a reduction in the benzodiazepine-insensitive (BZ-IS) subtype of γ2 containing GABARs, conferred by α6βγ2 receptors which are located entirely within the CGC layer (to 78 ± 10% of control levels). The benzodiazepine-sensitive subtype of GABAR, largely represented by α1βγ2 receptors, was unaffected. This data implied that the extrasynaptic α6ββδ GABARs were dramatically affected by the mutation. This was further supported by semi-quantitative immunoblotting analysis which demonstrated a reduction in GABAR α6 and δ subunit expression to 39 ± 22% and 36 ± 21% of control levels respectively.

Cultured cerebellar granule cells (CGCs) from control (AMPAR and kainate receptor-competent) and stargazer (AMPAR-incompetent but kainate receptor-competent) mice were employed as a model system to investigate how the stargazer mutation evoked aberrant α6ββδ GABAR expression and trafficking. The studies described herein demonstrated that AMPAR activation resulted in L-type voltage-gated calcium channel-dependent up-regulation of GABAR δ subunit expression and cell surface trafficking which was not detected in CGCs derived from stargazer animals. This offers a partial explanation for the abnormalities observed *in vivo*.

This investigation also provides evidence of a switch in GABAR expression in response to hyper-excitability in the dentate gyrus of the stargazer mutant, where a combination of *in situ* autoradiographical, immunohistochemical and immunoblotting analyses indicated that $\alpha4\beta\gamma2$ GABARs arose at the expense of the $\alpha4\beta\delta$ subtype. Hence, there is a potential switch from extrasynaptic GABARs in favour of synaptic GABARs, which may reflect an adaptive response to high frequency spike-wave discharges that enter the DG in the stargazer mutant.

Overall the results of this study support the hypothesis that neural networks in both the cerebellum and the hippocampus are able to undergo homeostatic GABAergic plasticity in response to alterations in excitatory inputs.

ACKNOWLEDGEMENTS

First and foremost I would like to acknowledge the constant support and guidance that I have received over the duration of my PhD from my supervisor, Dr Chris Thompson. I am truly thankful to you for having given me the opportunity to be part of your lab.

I would also like to acknowledge the support of my family; my parents, Sara and Lily, without whom none of this would have been possible. I would also like to thank my partner, James, who has been a great support through the highs and the lows of my PhD.

Last but by no means least I would like to thank the other members of the lab, past and present; Dr Victoria Hann, Peter Donoghue, Dr Clare Young and Dr Jane Ives. I would also like to acknowledge financial support from Merck, Sharp & Dohme and technical support from the staff of the LSSU.

DECLARATION

I confirm that no part of the material presented has previously been submitted for a degree in this or any other university. If material has been generated through joint work, my independent contribution has been clearly indicated. In all other cases, material from the work of others has been clearly indicated, acknowledged and quotations and paraphrases indicated.

H. Payne 19/5/06

CONTENTS

LIST OF FIGURES

LIST OF TABLES

ABBREVIATIONS

AMPA	α-amino-3-hydroxy-5-methylisoxazole-4-propinoic acid
AMPS	Ammonium persulphate
BDNF	Brain-derived neurotrophic factor
$BDNF^{-/-}$	Brain-derived neurotrophic factor knockout
B_{MAX}	Maximum number of binding sites per mg protein
bp	Base pair(s)
BSA	Bovine serum albumin
BZ	Benzodiazepine
BZ-S	Benzodiazepine-sensitive
BZ-IS	Benzodiazepine-insensitive
°C	Degrees Celsius
cDNA	Complimentary DNA
CGC	Cerebellar granule cell
Cl^-	Chloride ions
CNQX	6-cyano-7-nitroquinoxaline-2,3-dione
CNS	Central nervous system
CO_2	Carbon dioxide
Da	Dalton
DAB	3,3'-diaminobenzidine tetrahydrochloride
DEPC	Diethyl pyrocarbonate
DG	Dentate gyrus
DGC	Dentate granule cell
dH_2O	Distilled water
DIV	Days *in vitro*
DMSO	Dimethyl sulphoxide
DNA	Deoxyribonucleic acid
dNTPs	Deoxynucleotide triphosphates
dpm	Disintegrations per minute
DTT	Dithiothreitol

E	Embryonic (day)
EDTA	Ethylenediaminetetracetic acid
ECL	Enhanced chemiluminescence
EEG	Electroencephalogram
EGL	External granule cell layer
EGTA	Ethylenebis(oxyethylenenitrilo)tetracetic acid
EPSCs	Excitatory postsynaptic currents
ER	Endoplasmic reticulum
ERC	Entorhinal cortex
FCS	Foetal calf serum
FDU	5-Fluoro-2'-deoxyuridine
g	Gram
g	Gravitational force
GABA	γ-aminobutyric acid
GABAR	$GABA_A$ receptor
GC	Granule cell
GlyR	Glycine receptor
H_2O_2	Hydrogen peroxide
HCl	Hydrochloric acid
HEBSS	HEPES containing Earle's balanced salt solution
HEK-293	Human embryonic kidney-293
HEPES	N-2-hydroxyethylpiperazine-N'-2-ethane sulphonic acid
HRP	Horseradish peroxidase
5-HT	5-hydroxytryptamine receptor
Hz	Hertz
IC_{50}	Concentration of the ligand giving 50% inhibition of specific binding
IGL	Internal granule cell layer
IML	Inner molecular layer
IPSC	Inhibitory postsynaptic current

Kb	Kilo base
KCl	Potassium chloride
K_D	Dissociation constant
KDa	Kilodalton
Luminol	5-amino-2,3-dihydro-1,4-phthalazinedione
M	Molar
MEM	Modified eagle medium
mEPSC	Miniature excitatory postsynaptic current
mg	Milligram
$MgSO_4$	Magnesium sulphate
mIPSC	Miniature inhibitory postsynaptic current
ml	Millilitre
mM	Millimolar
Mr	Molecular weight
mRNA	Messenger ribonucleic acid
nAChR	Nicotinic acetylcholine receptor
NaCl	Sodium chloride
NaOH	Sodium hydroxide
nCi/mg	Nanocuries per mg
NGF	Nerve growth factor
NHS-SS-biotin	Sulfosuccinimidyl 2-(biotinamido)ethyl-1,3-dithioproprionate
nm	Nanometre
nM	Nanomolar
NMDAR	*N*-methyl-D-aspartate receptor
NSE	Neuron specific enolase
NT-3	Neurotrophin-3
NT-4	Neurotrophin-4
NT-5	Neurotrophin-5
OD	Optical density
OML	Outer molecular layer
P	Postnatal (day)
PBS	Phosphate buffered saline
PCR	Polymerase chain reaction

PDZ	Postsynaptic density-95, discs large, zonula occludens
Pmoles/mg	Picomoles per milligram
PMSF	Phenylmethylsulphonyl Fluoride
P4S	Piperidine-4-sulphonate
PSD	Postsynaptic density
PSD-95	Postsynaptic density protein of 95 kDa
PTZ	Pentylenetetrazole
RNA	Ribonucleic acid
RT-PCR	Reverse transcription polymerase chain reaction
SAP-97	Synapse-associated protein of 97 kDa
SDS	Sodium dodecyl sulphate
SDS-PAGE	Sodium dodecyl sulphate polyacrylamide gel electrophoresis
SEM	Standard error of mean
Stg	Stargazer
SWD	Spike-wave discharge
TARP	Transmembrane AMPA receptor regulatory protein
TBE	Tris-borate buffer
TBS	Tris buffered saline
TEMED	N,N,N',N-teramethylethylenediamine
THIP	4,5,6,7-tetrahydroisothiazolo-[5,4-c]pyridin-3-ol
Tris	Tris(hydroxymethyl)methylamine
Triton X-100	Iso-octylphenoxypolyethoxyethanol
Tween-20	Polyoxyethylenesorbitan monolaurate
µg	Microgram
µg/ml	Micrograms per millilitre
µl	Microlitre
µm	Micrometre
µM	Micromolar

UV	Ultraviolet
V	Volts
VDCC	Voltage-dependent calcium channel
v/v	Volume/volume
w/v	Weight/volume

CHAPTER 1. INTRODUCTION

1.1. Epilepsy

Epilepsy is the commonest type of neurological disorder, affecting approximately 1% of the population (Letts *et al.*, 1998; Brodie *et al.*, 2005). Epilepsies are a heterogeneous group of disorders characterised by recurrent spontaneous seizures. Seizures can be classified depending on the pattern of neuronal involvement and the clinical features of the seizure. The two main classes of seizure are partial and generalised. Partial seizures originate in a focal region of the cortex and are divided into those that impair consciousness (complex partial) and those that do not (simple partial). Generalised seizures can be characterised by widespread involvement of the cortical regions and usually involve an impairment of consciousness. Subtypes of generalised seizures include absence, myoclonic, clonic, tonic and atonic seizures (Brodie *et al.*, 2005).

Absence seizures commonly affect children and manifest as a sudden onset of staring and impaired consciousness with or without eye blinking and a characteristic electroencephalogram (EEG) demonstrates a 3 Hz spike-wave pattern (Brodie *et al.*, 2005). A number of mouse mutants show characteristics of absence epilepsy with ataxia and a form of spike-wave discharge associated with behavioural arrest (Letts *et al.*, 1998). A number of these mutants possess mutations in genes encoding calcium channel subunits, including tottering (α1A subunit mutation), leaner (α1A subunit), ducky (α2/δ2 subunit), lethargic (β4 subunit mutation) and stargazer, (putative calcium channel γ2 subunit mutation) (Letts *et al.*, 1998; Sharp *et al.*, 2001).

Epilepsy results from an imbalance between excitatory and inhibitory neurotransmission, which can occur as a consequence of an increase in excitatory neurotransmission, via glutamate receptors or a deficiency in inhibitory neurotransmission mediated by GABA receptors. Here follows an introduction to excitatory (Non-NMDA: AMPA and Kainate) receptors and inhibitory ($GABA_A$) receptors in terms of their structure and function in the central nervous system (CNS) which is essential for the understanding of the work herein.

1.2. γ-Aminobutyric Type A ($GABA_A$) Receptors

1.2.1. Structure of the $GABA_A$ Receptor (GABAR)

In the central nervous system, the principal mediator of inhibitory neurotransmission is the GABA receptor. GABA receptors can be subdivided into $GABA_A$ (ligand-gated chloride ion channel receptors), $GABA_B$ (G-protein coupled receptors) and $GABA_C$ (ligand-gated ion channel receptors) receptors. The $GABA_A$ receptor (GABAR) is a member of the superfamily of ligand-gated ion channels which also includes the nicotinic acetylcholine receptor (nAChR), the glycine receptor (GlyR) and the 5-hydroxytryptamine receptor ($5HT_3$) (Sieghart *et al.*, 1999).

The $GABA_A$ receptor is a hetero-pentameric glycoprotein which is encoded by a family of 18 separate genes, grouped according to their sequence homology, α (1-6), β (1-4), γ (1-4), δ, ε, π and θ. ρ (1-3) form $GABA_C$ receptors which are prominent in the retina (Barnard *et al.*, 1998). Each GABAR subunit consists of four putative transmembrane (TM) domains, a large extracellular N-terminus, an extracellular C-terminus and a large intracellular loop between TM3 and TM4 domains (figure 1.1.). The subunit composition of the GABAR determines the pharmacological and electrophysiological properties and the cellular location of the receptor. The predominant subunit combination in the brain exists in a pentameric organisation, consisting of 2α, 2β and a γ2 subunit. The major GABAR subtypes in the cerebellum include α1βxγ2, representing approximately 40% of the total GABAR in

the brain, α6βxγ2 (7%), α1α6βxγ2 (22%), α6βxδ (18%) and α1α6βxδ (10%) (McKernan and Whiting, 1996; Pöltl *et al.*, 2003).

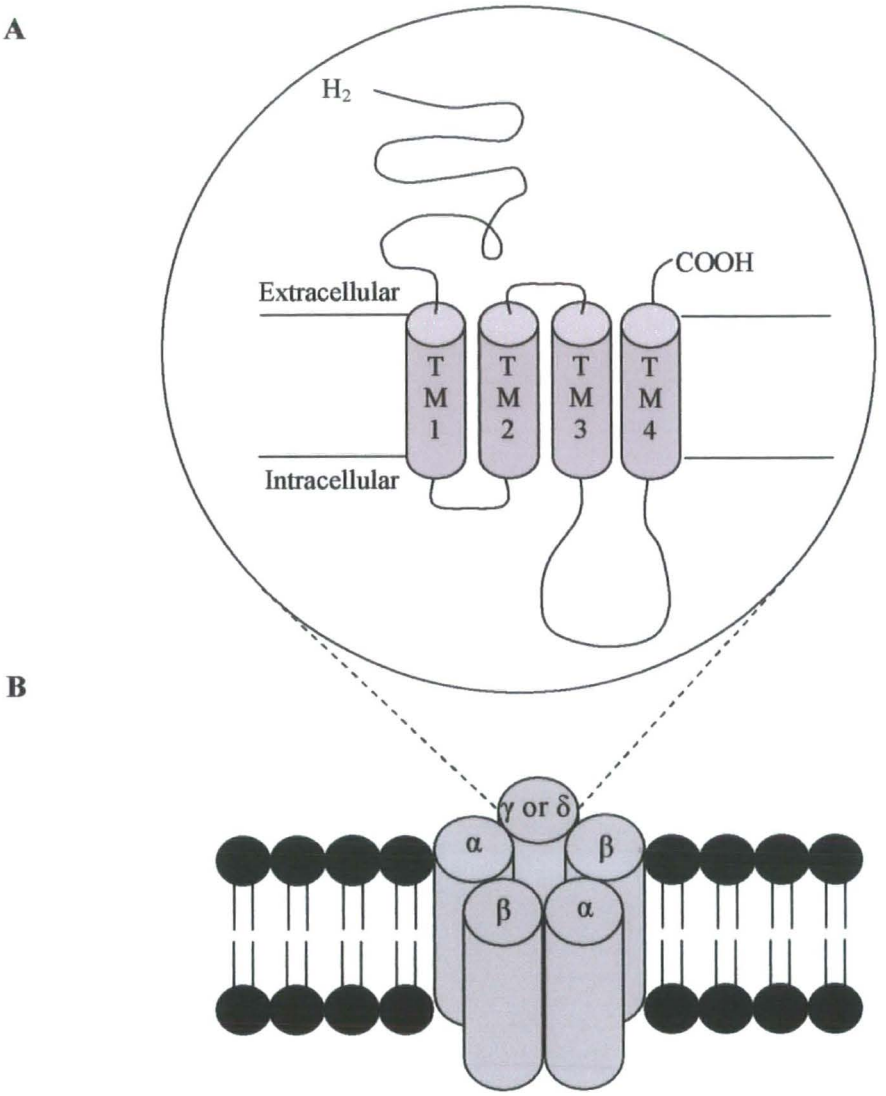

Figure 1.1. Structure of a $GABA_A$ Receptor

A: Structure of a GABAR subunit, consisting of four transmembrane domains with extracellular amino and carboxy termini. A long intracellular loop links transmembrane domains 3 and 4.

B: Structure of a $GABA_A$ receptor, composed of a pentameric arrangement of GABAR subunits, most commonly, 2α, 2β and either a γ or δ subunit.

The genes encoding the GABAR subunits have been demonstrated to occur in clusters of 3-4 genes at each locus on the chromosome. Each cluster contains genes of the α, β and γ or ε subunit classes, corresponding to GABAR composition. GABAR subunits α2, α4, β1 and γ1 occur on human chromosome 4 (4p13-q11), subunits α1, α6, β2 and γ2 have been mapped to human chromosome 5 (5q34-q35), α5, β3 and γ3 subunits are localised on human chromosome 15 (15q11-q13), while the GABAR δ subunit has been mapped to human chromosome 1 (1p) (For review see Barnard *et al.*, 1998)

1.2.2. Expression of GABAR subunits

The expression of GABAR subunits is regulated in a temporal and spatial manner, which allows for a potentially diverse population of pentameric receptors. The maturation of the cerebellum involves the migration of cerebellar granule cells from the external to the internal granule cell layer. Precursor cells in the germinative zones of the outer surface of the cerebellum (EGL) begin to divide and become post-mitotic in the first postnatal weeks (Qiao *et al.*, 1996, 1998; Mellor *et al.*, 1998). The cerebellar granule cell precursors migrate along Bergmann glial cell processes to pass through the molecular and Purkinje cell layers and finally come to rest in the internal granule cell layer (IGL) where the cells mature and extend dendritic processes (Gao *et al.*, 1995).

During the development of the cerebellum the expression of $GABA_A$ receptor subunits change. Dividing precursor cells and post-mitotic, premigratory cells express α2, α3, β3, γ1 and γ2 subunits, which are replaced by α1, α6 and δ subunits as cells reach the IGL (Laurie *et al.*, 1992; Mellor *et al.*, 1998). This switch in $GABA_A$ receptor subunit expression occurs at approximately postnatal day 6-7 (P6-7) (Laurie *et al.*, 1992). Therefore, the expression level of the α6 subunit provides a marker of the level of maturity of the cerebellum (figure 1.2.).

In the hippocampus, in contrast to the cerebellum, the predominant expression of

adult GABAR subunits is established from the early embryonic stage (Laurie *et al.*, 1992). Increases in GABAR α1, α2, α5, β1, β3, γ2 and δ are observed from embryonic day 14-19 (E14-E19) to adult age. Continuous low levels of expression of GABAR α3 and β2 subunits have been reported from E19-adult age. In contrast, GABAR γ1 subunit mRNA expression levels decrease after P6, while γ2 mRNA levels peak around P6 and α3, α4, β1 and γ3 subunit mRNA levels peak at P12 (Laurie *et al.*, 1992) (figure 1.2.).

The cerebellum demonstrates a diverse range of GABAR subunit immunoreactivities. The granule cell layer has been reported to express high levels of GABAR α1, β2, β3 and δ subunit protein. Most notably, the GABAR α6 subunit is expressed solely in the cerebellar granule cell (CGC) layer. Staining for other GABAR, α2, α3, α4, α5, β1, γ1 and γ3 are absent or are observed at low levels in the cerebellum (Pirker *et al.*, 2000). The Purkinje cell layer demonstrates high levels of α1, β2 and γ2 immunoreactivity. Staining in the molecular layer for GABAR α2, α3, α5, β1, β2, γ2 and γ3 has been reported to be mostly diffuse. Dendrites demonstrate high levels of α1 immunoreactivity, while β2 subunit expression is observed in single perikarya (Pirker *et al.*, 2000).

Abundant staining for the GABAR α1, α2, α4, α5, β1, β2, β3 and γ2 subunits were reported in the hippocampus by Pirker *et al.*, in 2000. High levels of GABAR α1, β2 and γ2 subunits were observed in the stratum oriens and radiatum of the CA1 and CA3, while immunoreactivity for the α2, α4 and δ subunits was reported in the dentate gyrus molecular layer. Moderate staining for the α1, β1, β2, β3 and γ2 subunits were also reportedly noted in the molecular layer. GABAR β2 subunit staining is equally distributed in the Ammon's horn, β3 subunit immunoreactivity has been reported to be enriched in the CA1 and CA3, with β1 subunit expression concentrated in the CA2 (Sperk *et al.*, 1997; Pirker *et al.*, 2000). Interneurons in the polymorph cell layer of the dentate gyrus were shown to be labelled with α1, α3, β1, β2, γ2 and δ subunit-specific antibodies (summarised in table 1.1.).

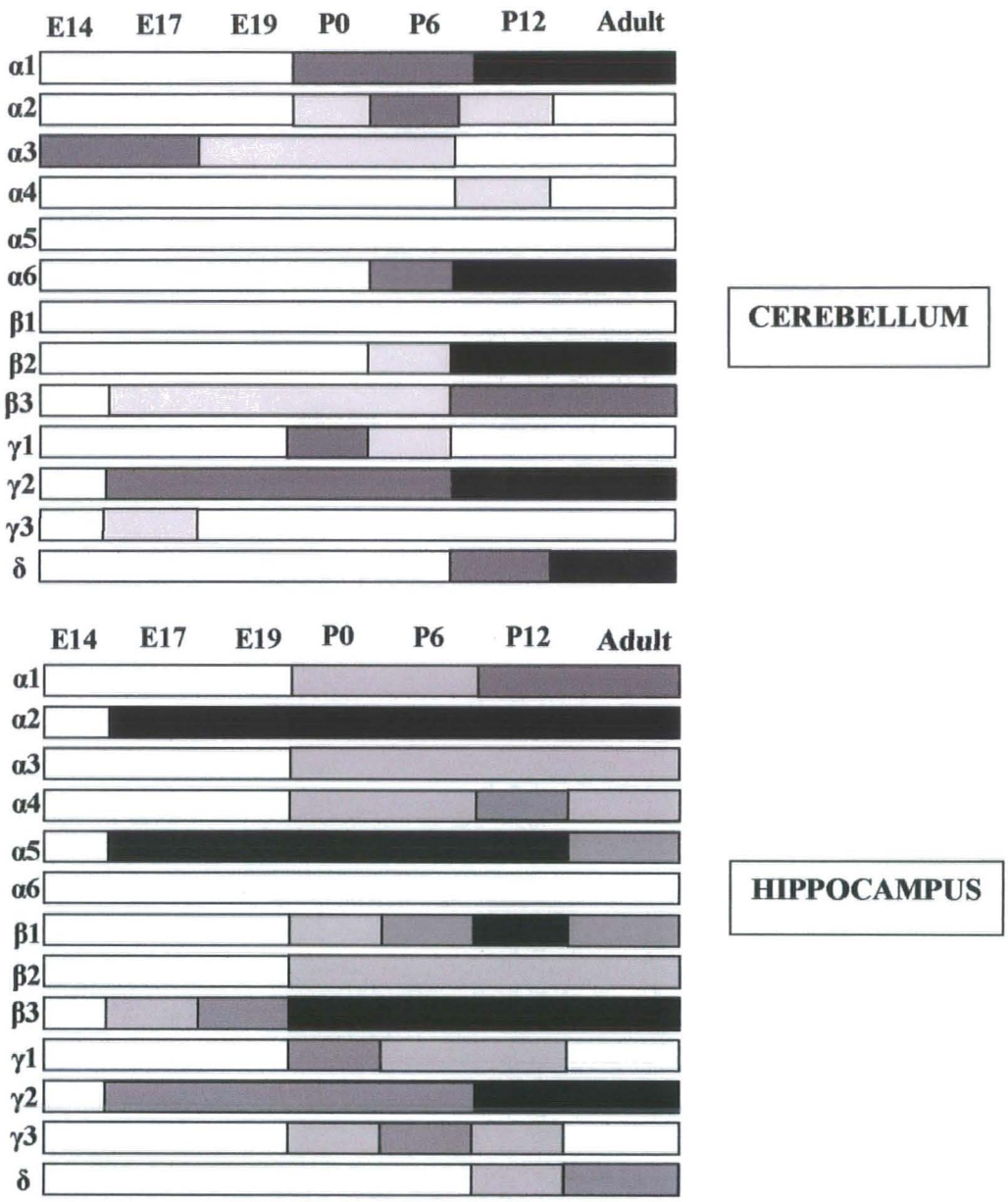

Figure 1.2. Developmental expression profiles of GABAR subunits in the cerebellum and hippocampus from embryonic (E) to postnatal (P) to adult age

White bar: No expression, Light grey bar: Low expression, Grey bar: Medium expression, Black bar: High expression (Laurie *et al.*, 1992).

Table 1.1. Expression of the GABAR subunits in the adult cerebellum and hippocampus

GABAR SUBUNIT	CEREBELLUM			HIPPOCAMPUS		
	CGC	ML	PL	DG	CA1	CA3
α1	++	++	++	+	++	+
α2	-	+	-	++	+	+
α3	-	+	-	+	-	-
α4	-	-	-	++	+	-
α5	-	+	+	+	++	+
α6	+++	-	-	-	-	-
β1	-	+	-	+	+	-
β2	++	++	++	+	++	++
β3	+++	-	-	++	++	++
γ1	-	-	+	-	-	-
γ2	++	++	++	++	++	++
γ3	-	+	+	-	-	-
δ	+++	-	-	++	-	-

-: No expression, +: Low expression, ++: Moderate expression, +++: High expression. CGC: Cerebellar granule cell layer, DG: Dentate gyrus, ML: Molecular layer, PL: Purkinje cell layer.

Adapted from Pirker *et al.*, 2000

1.2.3. GABAR trafficking and targeting

GABAR constitutively recycle between the cell surface and microtubule-dependent perinuclear endosomal compartment by clathrin-dependent mechanisms (Tehrani *et al.*, 1997; Connolly *et al.*, 1999a; Moss and Smart, 2001; Kneussel *et al.*, 2002). Assembly of GABAR subunits is reported to occur in the endoplasmic reticulum (ER), involving interactions with chaperone molecules such as calnexin and Ig binding protein (BiP), molecules which hold glycoproteins in the ER until folding and assembly is complete (Connolly *et al.*, 1996a). Heterologous expression of GABAR subunits has demonstrated that expression of GABAR at the cell surface requires the combination of an α and a β subunit in the presence or absence of a γ subunit to produce GABA-gated currents (Connolly *et al.*, 1996a, 1996b, 1999).

Localisation of GABAR to the synapse is controlled by association of GABAR with interacting proteins such as gephyrin and $GABA_A$ receptor-associated protein (GABARAP). Gephyrin is a ubiquitous protein which binds to polymerised tubulin, acting as a scaffolding protein shown to co-localise with the GABAR α2, β2/3 and γ2 subunits, to stabilise γ_2-containing GABAR at postsynaptic sites (Kneussel *et al.*, 1999, 2001; Sassoe-Pognetto and Fritschy, 2000; Kittler *et al.*, 2001a; Jacob *et al.*, 2005). Studies on gephyrin-deficient mice ($geph^{-/-}$) demonstrated a complete loss of synaptic γ2 subunit-containing GABAR (Kneussel *et al.*, 1999).

GABARAP shares sequence homology with GATE16, a protein which participates in vesicular membrane transport through interaction with *N*-ethylmaleimide-sensitive factor (NSF), a protein critical for vesicular fusion. GABARAP is enriched in the trans-golgi network and has previously been proposed to facilitate intracellular transport from the Golgi apparatus to synaptic sites (Wang and Olsen, 1999; Chen *et al.*, 2000; Kittler *et al.*, 2001).

The GABAR γ2 subunit is mostly dispensable for assembly and membrane insertion of functional GABAR, but is essential for accumulation of GABAR at synapses, and

for the recruitment of gephyrin to postsynaptic sites. Keller *et al.*, in 2004 reported a novel γ2 subunit interacting protein, the Golgi-specific DHHC zinc finger protein (GODZ), a member of the superfamily of DHHC cysteine-rich domain membrane proteins, which have been characterised as palmitoyltransferases. GODZ interacts with a cysteine-rich 14 amino acid domain which is conserved in the cytoplasmic loop (TM3-4) of the GABAR γ1-3 subunits. Co-expression of GODZ and GABAR in HEK-293 cells resulted in the palmitoylation of the GABAR γ2 subunit in its cytoplasmic domain. This highlights a novel post-translational modification selective for γ subunit-containing GABAR important for the regulation of trafficking in the secretory pathway (Keller *et al.*, 2004).

Rathenberg *et al.*, in 2004 identified a role for palmitoylation of GABAR in the synaptic clustering of GABAR containing the γ2 subunit in cultured hippocampal neurons. More recently, the roles of distinct domains of the GABAR γ2 subunit have been identified in mediating clustering and synaptic function of GABAR and gephyrin (Alldred *et al.*, 2005). Analysis of GABAR α2/γ2 chimeras where extracellular, transmembrane and intracellular domains of the γ2 subunit were replaced with homologous domains from the α2 subunit were employed to determine the domains of the γ2 subunit that critical for GABAR clustering and synaptic function. Transfection of the above chimeric constructs into GABAR γ2 subunit knockout ($\gamma2^{-/-}$) neurons revealed that the fourth transmembrane domain of the γ2 subunit is necessary for postsynaptic clustering of GABARs, whereas the fourth transmembrane domain and the cytoplasmic loop contribute to the recruitment of gephyrin to the postsynaptic membrane.

GABAR expression and function can be modulated by phosphorylation. GABAR phosphorylation can act to cause diverse functional effects, from enhancement to inhibition of function depending on the receptor subunit composition and the location of the phosphorylation site within the subunit (Lin *et al.*, 1996; McDonald *et al.*, 1998). GABAR β1-3 and γ2 subunits are targets for cAMP-dependent protein

kinase A, protein kinase C, cGMP-dependent protein kinase and calcium/calmodulin-dependent protein kinase II (CaMKII) (Krishek *et al.*, 1994; McDonald *et al.*, 1994; McDonald *et al.*, 1998).

GABAR β subunits play a unique role in function modulation, as they possess conserved sites for protein kinase A (PKA) phosphorylation (McDonald *et al.*, 1998). Expression of GABAR with varying β subunits in human embryonic kidney cells 293 (HEK-293) cells revealed that phosphorylation of serines 408 and 409 enhanced GABA-activated currents, while phosphorylation of the β1 subunit at serine 409 acted to reduced GABA-activated currents. In contrast the β2 subunit was not affected by PKA phosphorylation (McDonald *et al.*, 1998). The GABAR β subunit therefore plays a critical role in the modulation of GABAR function. Furthermore, the GABAR β subunit is not only essential for the cell surface targeting of functional GABAR but also for the targeting of GABAR to cellular locations (Connolly *et al.*, 1996a, 1996b). Expression of GABAR containing the β3 subunit were shown to target to the basolateral domain of madin-darby canine (MDCK) cells, analogous to the somatodendritic surface of neurons, via the apical surface, corresponding to axonal surfaces in neurons. In contrast, GABAR containing the β2 subunit were targeted directly to the basolateral domain (Connolly *et al.*, 1996b).

Heterologous expression systems have provided evidence that protein kinase C (PKC) activity can interfere with recycling of receptors to the cell surface from late endosomes (Brandon *et al.*, 1999; Connolly *et al.*, 1999; Moss and Smart, 2001). Furthermore, GABAR β subunits have been reported to be phosphorylated by PKC-dependent signalling pathways to modulate neuronal GABAR function in neurons (Poisbeau *et al.*, 1999).

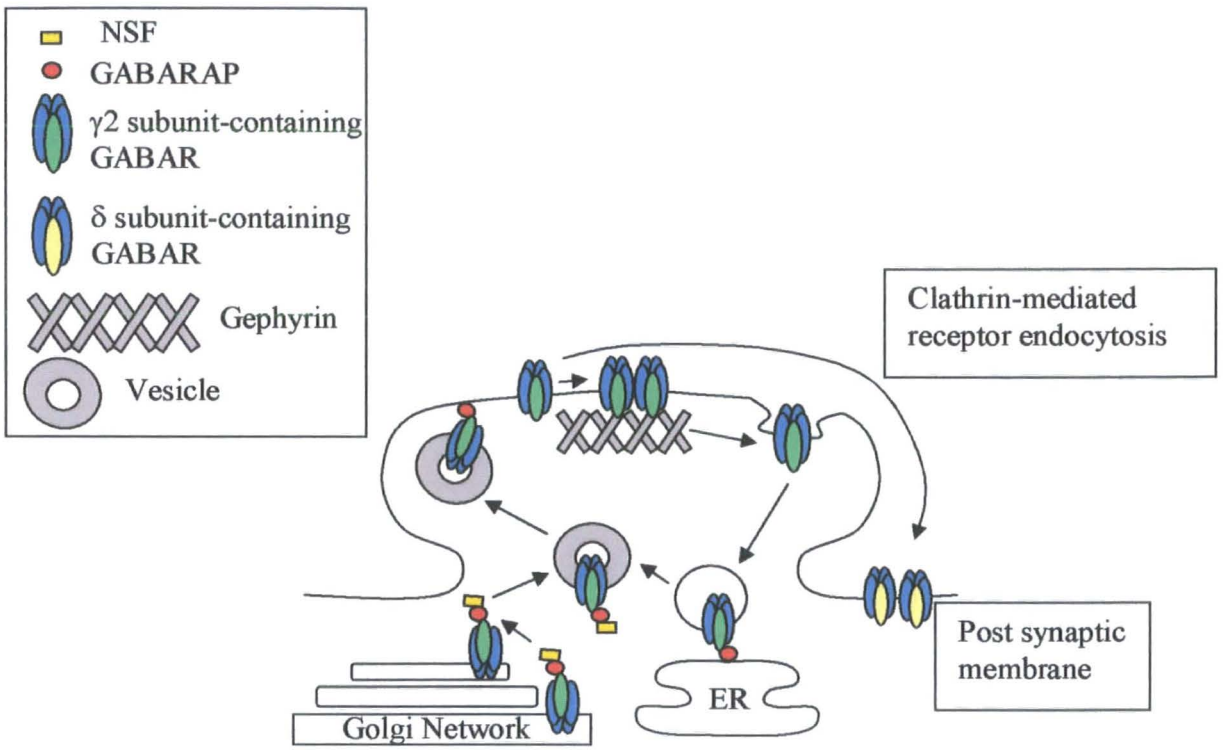

Adapted from Kneussel (2002)

Figure 1.3. Constitutive recycling of GABAR to the cell surface

Proteins reported to interact with GABARs to influence cellular trafficking are Plic-1 which interacts with α and β subunits of GABAR acting to limit the degradation of GABAR by the proteosome, thereby acting to increase GABAR surface expression (Bedford *et al.*, 2001). $GABA_A$ receptor interacting factor-1 (GRIF-1) is a 913 amino acid protein identified by the yeast-2 hybrid system to specifically interact with the GABAR β2 subunit and kinesins to function in trafficking β2 subunit-containing GABAR to the synapse along microtubules (Beck *et al.*, 2002; Brickley *et al.*, 2005). Huntingtin-associated protein 1 has recently been identified as a protein important in the modulation of synaptic GABAR number by inhibiting receptor degradation and facilitating receptor recycling (Kittler *et al.*, 2004).

1.2.4. Localisation of GABAR to synaptic and extrasynaptic sites

In cerebellar granule cells (CGCs), two types of $GABA_A$ receptor-mediated inhibition exist, phasic and tonic (Brickley *et al.*, 1996, 1999; Nusser *et al.*, 1998). GABAR have been shown to be segregated to synaptic and extrasynaptic sites to mediate phasic and tonic inhibition depending on their subunit composition. Nusser *et al.*, in 1998 reported that γ2 subunit containing GABAR were enriched in GABAergic Golgi synapses, while GABAR containing the δ subunit were present on the extrasynaptic, somatic and dendritic membranes in CGCs. δ-containing GABAR have been proposed to mediate tonic inhibition, as a result of their characteristic pharmacological properties and extrasynaptic location. δ subunit-containing GABAR have distinct properties in that they do not desensitise in the presence of GABA while they display a high affinity for the ligand. δ subunit-containing GABAR also confer a small single channel conductance and a long open time of the channel (Nusser *et al.*, 1998; Brown *et al.*, 2002).

In hippocampal neurons δ subunit-containing GABAR, are targeted to perisynaptic domains where they respond to overspill of GABA from the synapse (Wei *et al.*, 2003). With the exclusive non-synaptic presence of the subunit, it is a prime candidate for the mediation of tonic inhibition, to regulate passive membrane properties (Nusser *et al.*, 1998).

Table 1.2. Properties of γ2 and δ subunit-containing GABAR

RECEPTOR PROPERTY	GABAR γ2 SUBUNIT	GABAR δ SUBUNIT
Cellular Localisation	Synaptic	Extrasynaptic/Perisynaptic
Single Channel Conductance (Nusser *et al.*, 1998)	30 ps α1β1γ2	22 ps α1β1δ
Channel open time (Nusser *et al.*, 1998)	5 msec α1β1γ2	400 msec α1β1δ
Desensitisation in the presence of GABA (Nusser *et al.*, 1998)	Fast 10 msec	Slow 5-8 msec
Sensitivity to zinc (Brown *et al.*, 2002)	High IC_{50}=2.0 μM α4β3γ2	Low IC_{50}=3.1 μM α4β3δ
Affinity for GABA (Nusser *et al.*, 1998)	EC_{50}=13 μM α1β3γ2	EC_{50}=0.27 μM α6β3δ
Sensitivity to neurosteroids (Brown *et al.*, 2002)	THDOC=297% potentiation α4β3γ2	THDOC=524% potentiation α4β3δ

Phasic inhibition in CGCs has been attributed to the activation of synaptic $\alpha_1\beta\gamma_2$, $\alpha_6\beta\gamma_2$ and $\alpha_1\alpha_6\beta\gamma_2$ receptors, in response to synaptic release of GABA (Sieghart *et al.*, 1999). Phasic inhibition, in the form of postsynaptic currents, involves the synchronous opening of 18-32 synaptic GABAR. In contrast, tonic inhibition involves the persistent opening of several GABAR channels, providing a background level of inhibition within a CGC (Nusser *et al.*, 1998). Figure 1.4. depicts the arrangement of the cerebellar circuitry and the cellular localisation of GABAR subtypes either synaptically or extrasynaptically.

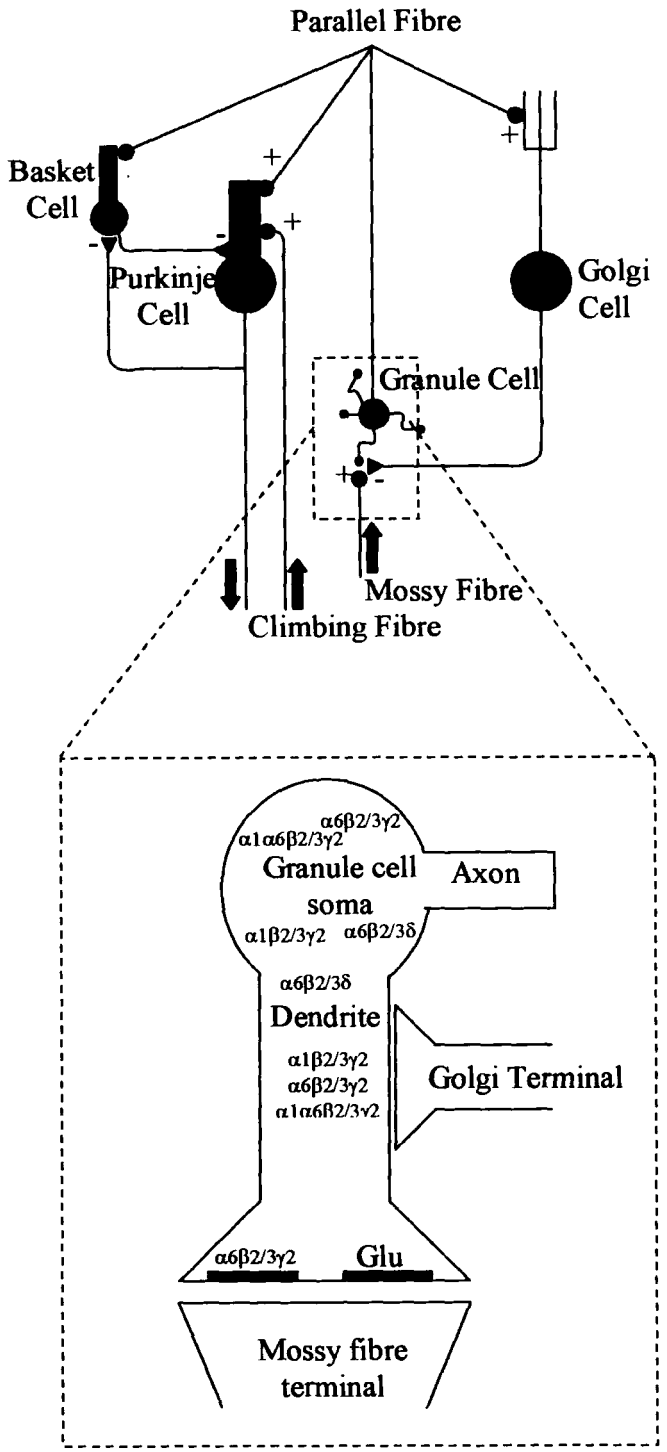

Figure 1.4. Cerebellar circuitry

Arrangement of circuitry within the cerebellum (Taken from Wisden *et al.*,1996)

Localisation of GABAR subtypes within a glomerulus (Adapted from Nusser *et al.*, 1998)

1.2.5. Modulation of GABAR function

$GABA_A$ receptors can be modulated by a number of different ligands including benzodiazepines, barbiturates, anaesthetics, convulsants and neurosteroids, which bind to distinct sites on the receptor to alter the ability of GABA to open the GABAR Cl^- channels.

Benzodiazepines (BZ) are commonly used for their anxiolytic, sedative and anticonvulsant properties. Benzodiazepines bind to the $GABA_A$ receptor on allosteric sites to modulate GABA-mediated Cl^- ion flow and hence inhibitory neurotransmission in the CNS. A BZ agonist acts as a positive modulator of the GABAR, to increase the frequency of opening of the Cl^- channel, increase net Cl^- ion flux and hence potentiate inhibitory neurotransmission (Rogers *et al.*, 1994). Conversely, a classical BZ antagonist, such as Ro15-1788 (flumazenil), acts to prevent the binding of benzodiazepine agonists to the receptor, with no intrinsic activity of its own. Inverse agonists act as negative modulators, to decrease the opening frequency of the channel (Turner *et al.*, 1991; Smart T., 1998). Ro15-4513 is a partial inverse agonist at GABAR, which has high affinity for the α4 and α6 GABAR subunits and proconvulsant properties (Barnard *et al.*, 1998).

Sieghart *et al.*, in 1987 reported that BZ pharmacology can be divided into two classes of binding site, benzodiazepine-sensitive (BZ-S) which can be blocked by diazepam and benzodiazepine-insensitive (BZ-IS) which are unaffected by BZ binding. It is the subunit composition of the $GABA_A$ receptor that confers its pharmacology. The combination of α1, α3, α5, β and γ2 subunits confers benzodiazepine sensitivity. The BZ-IS subtype of receptor is a subpopulation of receptors located predominantly in the cerebellum, with minor populations in the hippocampus and cortex. Turner *et al.*, in 1991 proposed that BZ-IS receptors are composed of α4 or α6, β and γ2 subunits. The α subunit thus influences the receptor's benzodiazepine pharmacology. Type I pharmacology is indicative of α1βγ2, present in the adult cerebellum. Type II pharmacology is conferred by the α2,

α3 and α5 subunits and is the predominant subtype expressed in the developing cerebellum.

It is possible to distinguish between γ2 and δ-subunit containing GABAR in the cerebellum by using a combination of radioligands in binding studies. [^{3}H] Ro15-4513 binds to γ2-containing GABAR only, while, [^{3}H] muscimol has high affinity for both γ2 and δ-containing receptors. Therefore, by difference analysis, it is possible to determine contributions of both γ2 and δ-containing GABAR to a receptor population.

Brown *et al.* in 2002 characterised the pharmacological differences between human $\alpha_4\beta_3\delta$ and $\alpha_4\beta_3\gamma_2$ GABAR in a stable cell line (mouse L9-tk) cells). δ-containing GABAR were shown to exhibit a higher sensitivity for GABA when compared to γ_2-containing receptors, but also δ-containing receptors had a higher efficacy for GABA partial agonists, piperidine-4-sulphonate (P4S) and 4,5,6,7-tetrahydroisothiazolo-[5,4-c]pyridin-3-ol (THIP). It was also proposed that δ-containing receptors have a greater sensitivity to lanthanum (a cation) than γ_2-containing receptors and a low sensitivity for zinc. The δ subunit has been proposed to confer slow desensitization to GABA, insensitivity to modulation by benzodiazepine ligands and enhanced sensitivity to neurosteroids (Spigelman *et al.*, 2002, 2003; Stell and Mody, 2003).

1.3. Non-NMDA Receptors: α-amino-3-hydroxy-5-methyl-4-isoxazoleproprionic (AMPA) Receptors and Kainate Receptors

Non-NMDA receptors mediate fast excitatory neurotransmission in the central nervous system (CNS). α-amino-3-hydroxy-5-methylisoxazole-4-propinoic acid receptors (AMPAR) are heterotetrameric structures composed of GluR1-4 subunits (also known as GluRA-D). Kainate receptors consist of GluR5-7 and KA1-2 subunits (For review see Bettler and Mulle, 1995). Each subunit consists of a large extracellular amino terminal domain, four membrane-associated domains where the

second transmembrane domain forms a re-entrant loop, to result in an intracellular carboxy terminus (see figure 1.5.).

The extracellular and transmembrane domains of the AMPAR subunits are similar, sharing 68-74% amino acid identity, while the intracellular C-terminal tail is distinct between subunits, forming splice variants (Song and Huganir, 2002). The GluR1, GluR4 and GluR2L possess long cytoplasmic tails, while the predominant splice variant of the GluR2 subunit, GluR3 and the alternative splice form of GluR4 which is predominant in the cerebellum, possess short cytoplasmic tails (For review see Malinow and Malenka, 2002).

AMPAR are dynamic in their association with the post-synaptic density in that they are able to translocate into and out of the postsynapse. Modulation of AMPAR synaptic transmission underlies forms of synaptic plasticity, examples of which are long-term potentiation (LTP) and long-term depression (LTD), models of learning and memory (Malenka and Nicoll, 1999; Malinow and Malenka, 2002; Song and Huganir, 2002).

Proteins which interact with AMPAR can be separated into two groups, those that contain postsynaptic density-95, discs large, zonula occludens (PDZ) domains and those that interact via non-PDZ domains (Braithwaite *et al.*, 2000; Henley, 2003). Association of AMPAR with interacting proteins, via the C-terminal tail is important for AMPAR trafficking-dependent forms of plasticity, providing a mechanism for clustering of ion channels and receptors at the plasma membrane and also to direct kinases and phosphatases towards their substrates (Braithwaite *et al.*, 2000; Chen *et al.*, 2000; Henley, 2003). Proteins important in signalling, trafficking and targeting belong to the PDZ protein superfamily which bind with high affinity to short PDZ-binding motifs in the intracellular domain of the AMPAR subunits (Kittler and Moss, 2001b).

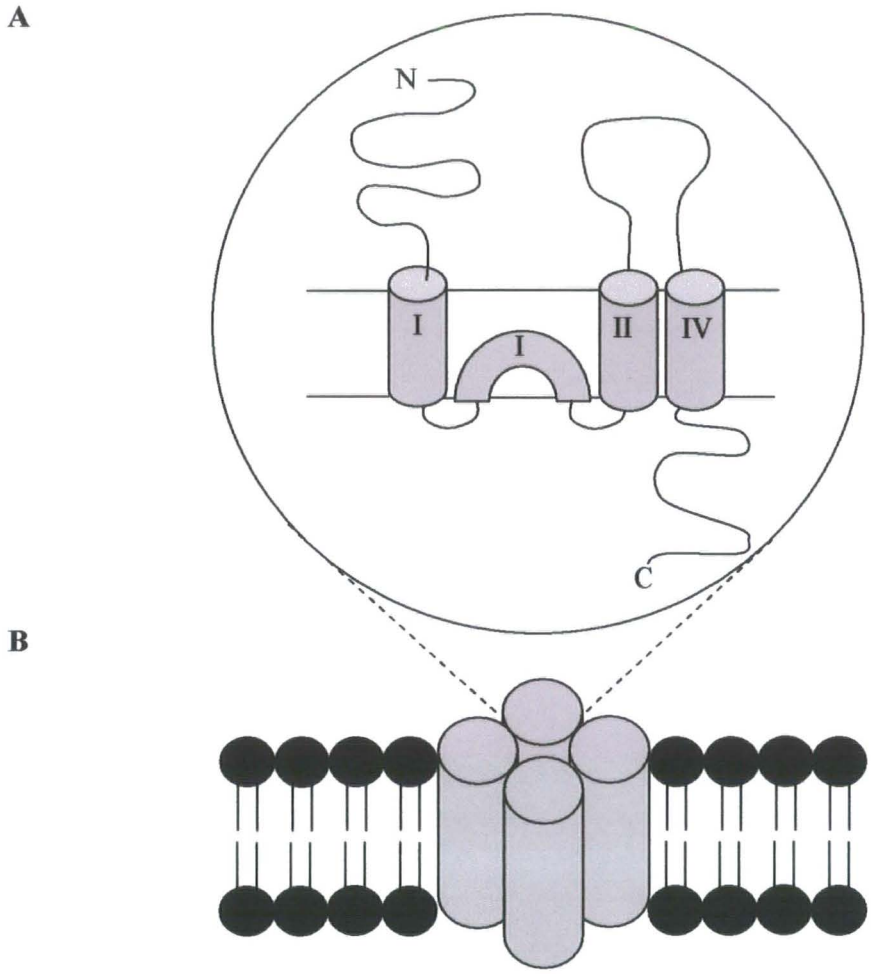

Figure 1.5. Structure of an AMPA receptor

A: Structure of an AMPAR subunit, consisting of four membrane-associated domains with extracellular amino terminus and intracellular carboxy terminus. B: Structure of an AMPA receptor, composed of a tetrameric arrangement of AMPAR subunits, of GluR1-4.

Glutamate receptor interacting protein (GRIP) was the first protein shown to interact with AMPAR by yeast two-hybrid analysis. GRIP is a 130 kDa protein which contains seven PDZ domains, the third, fifth and sixth of which bind to the C-termini of the AMPAR GluR2 and GluR3 subunits (Dong *et al.*, 1997). AMPA receptor binding protein (ABP) shares a 64-93% homology in PDZ domains to GRIP. ABP

similarly contains seven PDZ domains, of which the third, fifth and sixth PDZ domains interact with the C-termini of GluR2 and GluR3 (Srivastava *et al.*, 1998). The exact function of GRIP/ABP is not fully resolved, although it has been proposed to serve a scaffolding function, stabilising AMPAR at the synapse (Liu and Cull-Candy, 2005).

Protein interacting with C-kinase (PICK1) is a further PDZ-containing protein which has been shown to interact with AMPAR GluR2, GluR3 and GluR4 subunits via a single PDZ domain within its structure (Dev *et al.*, 1999; Xia *et al.*, 1999). PICK1 is a postsynaptic scaffold protein which in heterologous expression systems has been shown to aggregate AMPAR (Bredt and Nicoll, 2003).

Synapse associated protein of 97 kDa (SAP97) is a member of the synapse associated protein family, which includes SAP90 (PSD-95), chapsyn110 (PSD-93) and SAP102, which have been shown to interact with NMDA receptor subunits (Henley, 2003). SAP97 is the only PDZ protein currently known to interact directly with the C-terminus of the AMPAR GluR1 subunit (Sans *et al.*, 2001). It has been proposed that SAP97 has a role in AMPAR targeting and acts to cluster GluR1-containing AMPAR, but not in endocytosis, and therefore may fulfil a chaperone function (Braithwaite *et al.*, 2000; Sans *et al.*, 2001; Henley, 2003).

Non-PDZ protein interactions with AMPAR include *N*-ethylmaleimide-sensitive factor (NSF) which binds to the C-termini of GluR2 and GluR3 subunits, acting to play a role in regulating membrane insertion and stabilisation of AMPAR (Nishimune *et al.*, 1998; Song *et al.*, 1998). Neuronal activity-regulated pentraxin (Narp) is a neuronal immediate early gene product, forming a member of a secretory family of proteins, the pentraxins. Narp interacts with all AMPAR subunits via the extracellular domain of the subunit, acting to increase synaptic clustering of AMPAR (Henley, 2003; Bredt and Nicoll, 2003). 4.1 proteins are a family of cytoskeletal components. 4.1N and 4.1G interact with the C-terminus of the GluR1 subunit at the synapse. It has been proposed that the 4.1 proteins act to provide a link between

GluR1 and the actin cytoskeleton (Shen *et al.*, 2000). Lyn is a src-family non-receptor protein tyrosine kinase, which couples to the AMPAR GluR2 and GluR3 subunits to initiate signalling via the mitogen-activated protein kinase (MAPK) signalling cascade. This in turn activates transcription of DNA encoding brain-derived neurotrophic factor (BDNF) which has been shown to be involved in synaptic plasticity and the development of the nervous system (see section 1.4.4.1) (Hayashi *et al.*, 1999).

Table 1.3. Summary of AMPAR interacting proteins

INTERACTING PROTEIN	INTERACTING DOMAIN	AMPAR SUBUNIT
SAP-97	PDZ	GluR1
GRIP	PDZ	GluR2, GluR3
ABP	PDZ	GluR2, GluR3
PICK1	PDZ	GluR2, GluR3, GluR4
NSF	Non-PDZ	GluR2, GluR3
Narp	Non-PDZ	GluR1, GluR2, GluR3, GluR4
4.1N	Non-PDZ	GluR1
4.1G	Non-PDZ	GluR1
Lyn	Non-PDZ	GluR2, GluR3

The first transmembrane AMPAR interacting protein identified was stargazin, the protein mutated in the stargazer mutant mouse (Letts *et al.*, 1998).

1.4. The stargazer mutant mouse

The stargazer mutant mouse is an animal model of human absence epilepsy and cerebellar ataxia. The stargazer mutation arose spontaneously in the A/J inbred mouse line at The Jackson Laboratory, Maine, USA, and was recognised by its distinctive head tossing and ataxia. The recessive mutation was mapped to mouse

chromosome 15 and was determined to result from a 6 kb early viral transposon insertion into intron 2 of the stargazin gene (Noebels *et al.*, 1990; Letts *et al.*, 1998). The insertion of the transposon results in the premature transcriptional arrest of the stargazin gene which encodes a membrane-spanning protein, stargazin of 323 amino acids with a molecular weight of 36-41 kDa (Letts *et al.*, 1998; Sharp *et al.*, 2001). Stargazin mRNA distribution was determined by RT-PCR to be brain-specific, no expression was observed in heart, spleen, lung, liver, skeletal muscle, kidney or testis (Letts *et al.*, 1998). High levels of expression were observed in the cerebellum, olfactory bulb, cerebral cortex, striatum, pons, thalamus, CA3 and dentate gyrus of the hippocampus (Letts *et al.*, 1998; Klugbauer *et al.*, 2000; Sharp *et al.*, 2001).

Stargazin protein was determined to share a similar putative secondary structure with the γ subunit of skeletal muscle voltage-dependent calcium channel, γ1, comprising four transmembrane domains and cytosolic amino and carboxy termini. A 25% sequence identity in primary structure was also observed between the two proteins. Heterologous expression of stargazin demonstrated that the protein had relatively minor effects on P/Q, L- and T-type calcium channel kinetics and cell surface trafficking (Letts *et al.*, 1998; Klugbauer *et al.*, 2000; Rousset *et al.*, 2001; Green *et al.*, 2001). Stargazin was therefore proposed to be a neuronal counterpart of the skeletal muscle-specific calcium channel subunit, γ1 and was termed γ2 (Letts *et al.*, 1998).

1.4.1. The CACNG family of γ subunits

Voltage-dependent calcium channels are heteromultimeric complexes of α1, β, α2δ and γ subunits which assemble in a 1:1:1:1 subunit stoichiometry. The α1 subunit forms the central pore of the channel and thereby determines the major function of the channel. All auxiliary subunits act to modulate the voltage-dependence and kinetics of the channel (Burgess *et al.*, 1999; Chu *et al.*, 2001). The discovery of stargazin expanded the calcium channel γ subunit family to include a neuronal-specific γ subunit, in contrast to the skeletal muscle-specific γ1. To date, a total of

eight calcium channel γ subunits have been identified γ1-γ8 (genes: CACNG1-8), which have distinct tissue distributions in mouse and human, summarised in table 1.3. (Burgess *et al.*, 1999 (human γ2, γ3, γ4, γ5); Klugbauer *et al.*, 2000 (mouse γ3, γ4, γ5); Moss *et al.*, 2001 (γ7); Chu *et al.*, 2001 (rat γ6, γ7, γ8)). Chu *et al.*, in 2001 suggested that the calcium channel γ subunit family could be functionally subdivided into two groups, based on sequence similarity, tissue distribution and evolutionary relationships. The first group of γ subunits are those that could act as auxiliary subunits to associate with calcium channels (γ1 and γ6). A second subgroup are those that have a role in mediating protein trafficking, such as γ2 in targeting AMPAR to postsynaptic sites via an interaction with PDZ proteins. Analysis of sequence similarity within the γ subunit family identified a common PDZ binding domain at the C-terminus of γ2, γ3, γ4 and γ8, which are also robustly expressed in the brain.

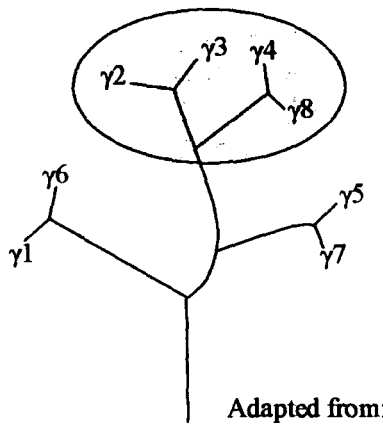

Adapted from: Qiao and Meng, 2003

Figure 1.6. Phylogenetic tree of the putative calcium channel γ subunit family
Common branching points represent shared ancestor sequences. Pairs indicate higher sequence identity than to other members of the family. Shaded area indicates members of the transmembrane AMPA receptor regulatory protein (TARP) family (Burgess *et al.*, 1999; Klugbauer *et al.*, 2000; Chu *et al.*, 2001; Moss *et al.*, 2001; Tomita *et al.*, 2003).

Table 1.4. The CACNG family of calcium channel subunit mRNA and protein expression

	γ1	γ2	γ3	γ4	γ5	γ6	γ7	γ8
Distribution: Cerebellum	-	+++	-	+	-	-	++	-
Cerebral cortex	-	+++	+++	+++	-	-	++	++
Hippocampus	-	++	+	+++	-	-	++	+++
Midbrain	-	++	++	+++	-	-	-	-
Striatum	-	++	++	+++	-	-	-	-
Thalamus	-	++	+	+	-	-	++	-
Heart	-	-	-	-	+	+++	+	-
Liver	-	-	-	-	+++	-	-	-
Lung	-	-	-	-	+	+	+	-
Kidney	-	-	-	-	++	-	-	-
Skeletal muscle	+++	-	-	-	+	++	-	-
Testes	-	-	-	-	+	-	-	+
References:	Chu *et al.*, 2001	Klugbauer *et al.*, 2000 Sharp *et al.*, 2001	Klugbauer *et al.*, 2000 Sharp *et al.*, 2001	Klugbauer *et al.*, 2000 Sharp *et al.*, 2001	Klugbauer *et al.*, 2000	Chu *et al.*, 2001	Chu *et al.*, 2001. Moss *et al.*, 2002	Chu *et al.*, 2001 Tomita *et al.*, 2003

1.4.3. Transmembrane AMPA receptor regulatory proteins (TARPs)

Tomita *et al.*, in 2003 defined the proposed subgroup of calcium channel subunits, as a family of transmembrane AMPA receptor regulatory proteins (TARPs). The identification of a calcium channel subunit as a member of the TARP family was based on the ability of the subunit to rescue glutamate-evoked responses in stargazer cerebellar granule cells (CGCs), CGCs that fail to express AMPAR at the cell surface as a result of ablation of stargazin expression. Subsequently, stargazin (γ2), γ3, γ4 and γ8 were identified as members of the TARP family (Tomita *et al.*, 2003).

Mapping of TARP isoform mRNA and protein distribution by a combination of *in situ* hybridisation and western blotting techniques demonstrated that TARPs had overlapping distributions in the brain, such that one cell type could possess a number of TARP isoforms (see table 1.1.). Furthermore, immunogold and immunofluorescence methods using pan-TARP antibodies revealed the selective location of TARPs at punctate sites on dendrites corresponding to excitatory synapses, evidenced by overlap of staining with AMPAR GluR2 subunit and postsynaptic density protein of 95 kDa (PSD-95) (Tomita *et al.*, 2003). Immunoprecipitations of Triton X-100 soluble brain extracts further confirmed the association of TARPs with AMPAR. Stargazin co-immunoprecipitated with AMPAR GluR1, 2 and 4 subunits in control cerebellum, γ3 co-associated with AMPAR subunits in cortex, γ4 in neonatal forebrain, and γ8 in hippocampus (See chapter 7; Tomita *et al.*, 2003; Rouach *et al.*, 2005).

1.4.3.1. Stargazin (TARPγ2)

Stargazin, also known as TARPγ2, whose expression is completely ablated in stargazer mutant mice, possesses four putative transmembrane domains and cytosolic N and C-termini. The C-terminus contains a PDZ binding motif (-RRTTPV), a protein–protein interaction motif which interacts with PSD-95 at the synapse.

Chen *et al.*, in 2000 identified two mechanisms by which TARPγ2 functions to control AMPA receptor number at the synapse. TARPγ2 regulates the delivery of AMPAR to the membrane surface, a function which does not require the PDZ-domain of the protein. Stargazer cerebellar granule cells express reduced levels of AMPAR subunits GluR2 and 4 (Ives *et al.*, 2004), furthermore, functional receptors are not delivered to the cell surface. Transfection of TARPγ2 into these cells restored normal AMPAR function (Chen *et al.*, 2000a).

The second mechanism of AMPAR trafficking for which stargazin is responsible is the synaptic targeting of AMPAR. Deletion of the final four amino acids of the C-terminal tail of TARPγ2 protein (stargazinΔC) disrupted the association of TARPγ2 with PSD-95, indicating a critical role for the PDZ domain of TARPγ2 in the synaptic clustering of AMPAR (Chen *et al.*, 2000). Chimeric analysis, by systematically switching sections of the γ5 structure with TARPγ2 domains identified the first intracellular loop and intracellular tail of TARPγ2 critical in AMPA trafficking, more specifically, C-terminal residues 212-268 (Tomita *et al.*, 2004).

In support of the role of TARPγ2 in the synaptic targeting of AMPAR to the cell surface, Schnell *et al.*, in 2002, demonstrated that overexpression of TARPγ2 resulted in a selective increase in extrasynaptic AMPAR excitatory postsynaptic currents (EPSCs). Clustering of these receptors at the synapse required increased expression of the synaptic anchor, PSD-95. Transfection of the stargazinΔC clone, lacking the PDZ domain, into slice cultures resulted in decreased clustering of AMPAR and decreased AMPAR EPSCs (Schnell *et al.*, 2002).

Vandenberghe *et al.*, in 2005a identified TARPγ2 as an auxiliary AMPAR subunit in cerebellar extracts. TARPγ2 was shown to associate with all four AMPAR subunits, but only within a tetrameric receptor structure, no free TARPγ2 was detected in cerebellar extracts. Hence, two receptor populations were identified, a functional form which is associated with TARPγ2, and an apo-form which lacks TARPγ2.

AMPAR of the stargazer mutant cerebellum show an immature endoplasmic reticulum-type of glycosylation pattern, consistent with a role for TARPγ2 in the transport of AMPAR from the endoplasmic reticulum (ER). Furthermore, in a later study, Vandenberghe and coworkers revealed that the unfolded protein response is up-regulated in stargazer CGCs, a homeostatic pathway that up-regulates genes encoding ER chaperones such as Ig binding protein (BiP), to prevent accumulation of unfolded and unassembled proteins in the ER, indicating a role for TARPγ2 in ER processing of AMPAR (Vandenberghe *et al.*, 2005b).

Synaptic plasticity involves protein phosphorylation cascades that alter the number of AMPAR at the synapse. The cytosolic C-terminus of TARPγ2 contains a number of serine, threonine and tyrosine residues that may act as substrates for phosphorylation. Interestingly, the PDZ domain of the TARPγ2 C-terminal tail overlaps with the consensus sequence for phosphorylation by protein kinase A (PKA). TARPγ2 is basally phosphorylated at a critical threonine residue (T321) by PKA in the brain (Choi *et al.*, 2002). As a consequence of phosphorylation, TARPγ2 selectively loses its interaction with PSD-95. Choi *et al.*, in 2002 demonstrated that mutations mimicking phosphorylation at T321 disrupted interactions with PSD-95 and synapse-associated protein of 97 kDa (SAP-97) both in the yeast 2-hybrid system and biochemical associations and clustering of TARPγ2 and PSD-95 in heterologous cells. Furthermore, a TARPγ2 phosphomimic (Thr 321→ Glu) transfected into cultured hippocampal neurons acted to reduce the frequency and amplitude of AMPAR-mediated EPSCs (Chetkovich *et al.*, 2002).

In contrast, Tomita *et al.*, in 2005a proposed that only serine residues of the C-terminal tail of TARPγ2 are phosphorylated in cultured cerebrocortical neurons. The group demonstrated that phosphorylation of TARPγ2 was dynamically regulated by activation of calcium-calmodulin kinase II (CaMKII) and protein kinase C (PKC) to induce phosphorylation, whereas activation of protein phosphatases, PP1 and PP2B dephosphorylate serine residues. Phosphorylation of TARPγ2 facilitates synaptic

trafficking of AMPAR to the surface through interaction with PDZ proteins. Furthermore, phosphorylation of TARPγ2 was found to be important in hippocampal long-term potentiation (LTP), while dephosphorylation mediates long-term depression (LTD) (Tomita *et al.*, 2005a).

1.4.4. The phenotype of the stargazer mutant mouse

The phenotype of the stargazer mutant appears at postnatal day 14, and manifests in cerebellar ataxia, impaired eye-blink conditioning responses and a characteristic head toss, from which the mutant was named (star-gazing) (Qiao *et al.*, 1996; 1998). At P18, the mutant begins to exhibit spontaneous bilaterally symmetrical 6-7 Hz spike-wave discharges at a frequency of ~150 per hour which originate in the reticulothalamocortical circuit, acting to persistently activate neocortical and hippocampal networks (Qiao and Noebels, 1993).

1.4.4.1. Cerebellum

The ataxia observed in the stargazer mutant on a flat surface has been reported to be mild in the hind limbs, without obvious forelimb involvement, with a normal righting response (Qiao *et al.*, 1996). Stargazer mice are severely impaired in motor coordination and balance. In motor coordination and balance tests on a stationary balance rod, all stargazer mice tested fell off the rod after <5 seconds either when initiating movement or when the rod was rotated slowly. In contrast, all control mice tested were able to remain on the rod for the entire duration of the experiment (60 seconds) (Qiao *et al.*, 1996). Classical eyeblink conditioning is a form of sensorimotor learning that depends on the cerebellum and therefore allows for the determination of changes in cerebellar function that can be correlated with biochemical abnormalities (Thompson, 1990). The stargazer mutant is severely impaired in the acquisition of eyeblink conditioning when compared to control littermates (Qiao *et al.*, 1998).

The cerebellum of the stargazer mutant has been reported to be mildly hypoplastic in that the net wet tissue weight of the stargazer cerebellum was reduced by 14%. Qiao *et al.*, in 1996 reported no major cytoarchitectural abnormalities in the stargazer cerebellum, with a well defined laminar cortical structure and cerebellar foliation, indicating a generalised reduction in all anatomical elements, rather than a specific structural abnormality. However, an increased number of external granule cells were observed in the stargazer cerebellum at P15 (226% of controls), where granule cells demonstrated elongated oval shaped nuclei with few scattered lumps of coarse chromatin around the nuclear membrane, characteristic of migrating, immature CGCs (Qiao *et al.*, 1998).

Neurotrophic factors play an important role in the development of the nervous system and have been implicated in the proliferation, migration, differentiation and maturation of cerebellar granule cells (Segal *et al.*, 1992; Gao *et al.*, 1995; Das *et al.*, 2001; Borghesani *et al.*, 2002). The family of neurotrophins include nerve growth factor (NGF), brain-derived neurotrophic factor (BDNF) and the neurotrophins 3 and 4/5 (NT-3, NT-4/5). The neurotrophins have different spatiotemporal expression patterns in the developing brain. Das *et al.*, in 2001 proposed different roles for neurotrophic factors in cerebellar development, where in early development, these factors regulate the proliferation, differentiation and survival of CGCs. Whereas, in adulthood, their role becomes more functional in the regulation, maintenance and survival of CGCs.

Interestingly, levels of brain-derived neurotrophic factor (BDNF) mRNA were reported to be reduced by 70% in the whole stargazer cerebellum, with a near total ablation of BDNF mRNA expression in the cerebellar granule cell layer at P15, coincident with the onset of ataxia (Qiao *et al.*, 1996). Levels of neurotrophins NT-3 and nerve growth factor (NGF) and BDNF TrkB receptor mRNA and protein were found to be normal in the stargazer cerebellum. However, a reduction in constitutive and NT-4/5 induced tyrosine phosphorylation of PLCγ1, a trkB signal transduction protein, suggested a deficit in trkB signalling in the stargazer mutant cerebellum

(Qiao *et al.*, 1998).

A number of abnormalities in excitatory and inhibitory neurotransmission in the stargazer cerebellum have been reported, which could underlie the cerebellar ataxia and deficits in motor learning observed in the mutant (Qiao *et al.*, 1998). Excitatory postsynaptic currents (EPSCs) at mossy fibre-granule cell synapses are devoid of the AMPAR-mediated fast component of excitatory neurotransmission, without a significant change in the *N*-methyl-D-aspartate receptor (NMDAR) mediated slow component. This abnormality was proposed by Hashimoto and co-workers in 1999 to result from defects in postsynaptic AMPAR function rather than a failure of presynaptic glutamate release. Characterisation of AMPAR subunit mRNA and protein expression levels in control and stargazer mice has produced conflicting evidence. Hashimoto *et al.* in 1999 state that expression of the four AMPAR subunit mRNAs are comparable with those found in wild type mice, as revealed by ***in situ*** hybridisation. In contrast, Ives *et al.* in 2004 report differences in AMPAR subunit protein expression levels in stargazer mice, particularly in GluR2 expression.

Chen *et al.* in 2000 implicated TARPγ2, the mutated protein, in the regulation of the cell surface expression and synaptic targeting of AMPAR. Hence, AMPAR are not expressed at the cerebellar granule cell surface as a result of the failure in receptor trafficking and anchoring in the membrane through the interaction of the carboxyl terminus with PDZ domains of PSD-95, a postsynaptic density protein (see section 1.4.3.1.).

Abnormalities in the inhibitory GABAR profile of the stargazer mouse have also been reported by Thompson *et al.*, in 1998. During the maturation of the cerebellum, expression of the GABAR subunits is subject to temporal regulation, such that there is a switch in expression of subunits, from α2/α3 to α6 and δ (Laurie *et al.*, 1992). Subsequently, the GABAR α6 and δ subunits can be used as markers of maturity in the cerebellum. Thompson *et al.*, in 1998 reported a dramatic reduction in expression of the GABAR α6 and β3 subunits in the stargazer mutant cerebellum,

by western blot analysis (to 23 ± 8% and 38 ± 12% of control levels respectively). Furthermore, the benzodiazepine-insensitive subtype of [^{3}H] Ro15-4513 binding was reduced to 38 ± 10% of control levels, indicating a loss of $\alpha 6\beta 3\gamma 2$ GABAR in the stargazer mutant.

1.4.4.2. Hippocampus

In contrast to cerebellar granule cells, granule cells of the dentate gyrus (DG) are not electrically silent in the stargazer mutant. The stargazer mutant exhibits spontaneous bilaterally symmetrical 6-7 per second spike-wave discharges in cortical and hippocampal brain areas, which represent ~20% of total waking electroencephalographic (EEG) activity (See figure 1.7.; Qiao & Noebels, 1993). Onset of seizure activity has been shown to occur between postnatal days 16-18 (P16-18), with a frequency of ~150 bursts per hour (Qiao & Noebels, 1993). The spike-wave pattern of generalised synchronous activity has been shown to generate primarily in the thalamus and neocortex to activate synaptically linked brain areas, such as the hippocampus via the dentate gyrus.

Accumulation of continuous seizure activity has been shown to correlate with an increase in mossy fibre sprouting in the inner molecular-granule cell layer of the dentate gyrus, which occurs at 4-6 weeks following seizure onset (Qiao & Noebels, 1993). In contrast to convulsive seizure models such as kainic acid treatment, kindling and pentylenetetrazole (PTZ) which are associated with cellular injury, death and gliosis (Nahm & Noebels, 1998), no significant cell death of granule cells in the dentate gyrus (DG), CA3 pyramidal cells or hilar polymorph cells was noted following non-convulsive seizures in the stargazer mutant (Qiao & Noebels, 1993).

Chronic depolarisation in convulsive seizure models also results in an adaptive modification of inhibitory neurotransmission to balance increased excitation, manifesting in alterations in the function, pharmacology, targeting and clustering of GABAR (Brooks-kayal *et al.*, 1998; Clark, 1998; Cohen *et al.*, 2003; Peng *et al.*,

2004). No abnormalities in GABAR expression have been reported in the stargazer DG to date. However, a number of convulsive seizures have also been reported to induce rearrangements in the GABAR expression profiles in the hippocampus. The rat model of mesial temporal lobe epilepsy has been reported to result in an increase in spontaneous miniature inhibitory postsynaptic currents (mIPSCs) in dentate granule cells of epileptic rats compared to controls, suggesting an increase in GABAR number (Brook-kayal *et al.*, 1998; Shumate *et al.*, 1998; Cohen *et al.*, 2003). Furthermore, GABA responses were found to demonstrate minimal augmentation by zolpidem and increased blockade of the GABA response by zinc in epileptic rats (Brook-kayal *et al.*, 1998; Cohen *et al.*, 2003). This alteration in GABA responses was reported to be paralleled by a reduction in GABAR α1 subunit expression (54% of controls), responsible for the reduction in amplification of GABA responses to zolpidem and increases in GABAR α4 (175% of controls) and δ (225% of controls) subunit mRNA expression, conferring increased sensitivity to zinc blockade (Brook-kayal *et al.*, 1998).

In the pilocarpine model of temporal lobe epilepsy, Peng *et al.*, in 2004 reported a reduction in GABAR δ subunit protein in the molecular layer of the dentate gyrus, while a time-dependent increase in GABAR δ subunit immunoreactivity was noted in the many GABAergic interneurons. In the same temporal lobe epilepsy model, Leroy *et al.*, in 2004 demonstrated a 40% increase in GABAR-mediated IPSCs and a reduction in the effectiveness of diazepam (65% compared to controls) at increasing the decay time of GABAR-mediated mIPSCs 24-48 hours after pilocarpine treatment. Furthermore, a loss of neurosteroid sensitivity was reported, corresponding to a decrease in $\alpha4\beta\delta$ GABAR.

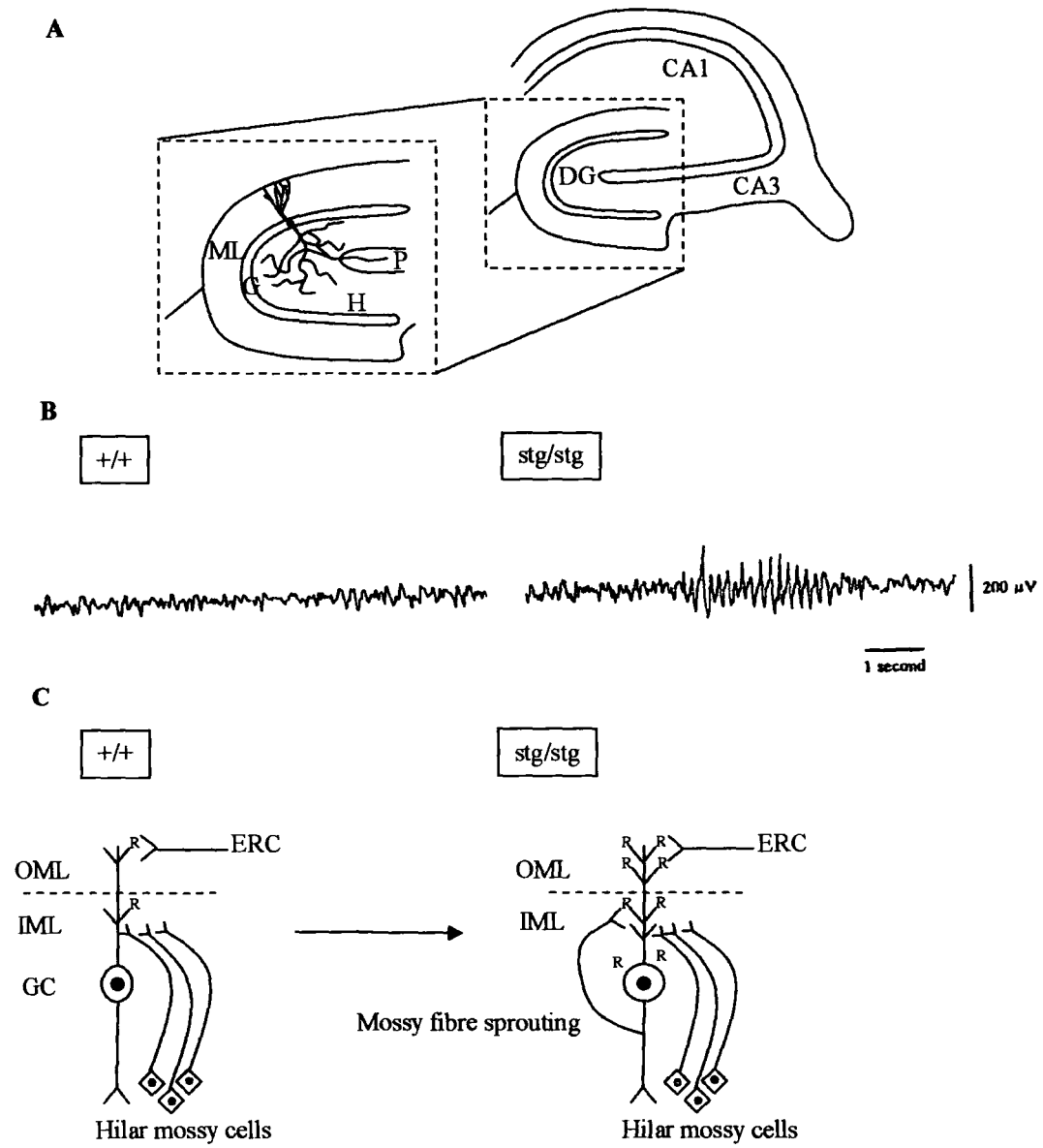

Figure 1.7. Effects of the stargazer mutation on the dentate gyrus circuitry

A: Structure of the hippocampus. DG: Dentate gyrus, G: Granule cell layer, H: Hilus, ML: Molecular layer,

B: Representative EEG traces from control and stargazer hippocampal brain areas, demonstrating spontaneous bilaterally symmetrical 6-7 per second spike-wave discharges in the stargazer mutant mouse (Qiao and Noebels., 1993)

C: Schematic representation of cellular differences between control and stargazer dentate gyri (DG). ERC: Entorhinal cortex, GC: Granule cell, IML: Inner molecular layer, OML: Outer molecular layer, P: Pyramidal cell. (Lynd-Balla *et al.*, 2004).

In contrast to decreased BDNF mRNA expression and trkB signalling in stargazer cerebellar granule cells (CGCs), the dentate granule cells (DGCs) of the stargazer mutant are subject to intermittent elevated BDNF expression (Chaftez *et al.*, 1995; Nahm and Noebels., 1998). Koyama *et al.*, in 2004 identified a role for BDNF signalling in the induction of mossy fibre sprouting. Activation of trkB signalling in the hippocampus has been shown to influence the maturation of GABAergic factors in cultured hippocampal neurons, including increased expression of GABAR β2/3 subunits (Yamada *et al.*, 2002), increased GABAR cluster number and synaptic localisation (Elmiariah *et al.*, 2004), as well as increased PKC phosphorylation, surface expression of GABAR β3 subunit containing receptors (Jovanovic *et al.*, 2004).

1.5. Aims of the study

Thompson *et al.*, in 1998 reported differences in the GABAR receptor complement expressed in the cerebellum of the stargazer mutant mouse. The abundance of total specific [^{3}H] Ro15-4513 binding sites was not found to differ significantly between control and stargazer mice. However, determination of the contribution of BZ-S and BZ-IS subtypes of receptor to the total receptor population indicated a reduction in the BZ-IS subtype of receptor to 38 ± 10% of control levels. The GABAR α6 subunit-containing receptors are the principal contributors to this receptor subpopulation (Sieghart *et al.*, 1987). This decrease in BZ-IS binding correlated with the reported decrease in the expression of the GABAR α6 subunit to 23 ± 8% in the stargazer mutant cerebellum as determined by western blot analysis. The previous study did not use the appropriate background strain of mouse (C57BL/6J) compared to the C3B6Fe$^+$ strain used in the current study. Furthermore, the full complement of GABARs were not investigated, the study favoured the γ2-subunit containing GABARs, without investigating the extrasynaptic, δ subunit-containing GABARs. A mechanistic explanation for the abnormalities in GABAR expression in the stargazer mutant was also not offered in the previous study.

Therefore, the aim of the current study was to determine the effects of the stargazer mutation on the complete GABAR complement in the stargazer mutant, using the appropriate background strain, with a particular focus on the expression and trafficking of the extrasynaptic GABAR δ subunit.

In the first instance, the GABAR subunit expression was to be determined quantitatively in control and stargazer cerebellum by western blotting and qualitative differences in distribution of GABAR subunits by immunohistochemical mapping using subunit-specific antibodies. Furthermore, radioligand binding techniques were to be employed to control and stargazer cerebellar membranes and tissue sections to determine the extent of any $GABA_A$ receptor deficits in the stargazer mutant.

Following *in vivo* characterisation of GABAR abnormalities in the stargazer mutant cerebellum, cerebellar granule cells were to be employed as a dynamic model system with which the trafficking and targeting of the GABAR δ subunit could be studied *in vitro*. Furthermore, to determine the effects of excitatory inputs on GABAR subunit expression by the comparison of GABAR expression in control ('AMPAR and kainate receptor-competent') and stargazer ('AMPAR-incompetent') CGCs by western blotting and radioligand binding techniques.

CHAPTER 2. MATERIALS AND METHODS

2.1. MATERIALS

Laboratory reagents purchased were of the highest quality available from VWR (Leicestershire, UK) or Sigma (Poole, Dorset, UK) with exceptions listed below.

2.1.1. Radiochemicals

[^{3}H] Muscimol (29.5 Ci/mmol) and [^{3}H] Ro15-4513 (20.0 and 28.3 Ci/mmol) were obtained from PerkinElmer Lifesciences (Boston, MA). Ro15-1788 and Flunitrazepam were a gift from Hoffmann LaRoche (Basle, Switzerland). Zolpidem was obtained from Tocris (Bristol, UK). [^{3}H] Flunitrazepam (91 Ci/mmol) and [^{3}H] Hyperfilm were purchased from Amersham Pharmacia (Aylesbury, Buckinghamshire, UK). Ecoscint and Decon 90 were obtained from National Diagnostics Ltd. (Hull, UK).

2.1.2. Antibodies

Anti-GABAR α1 (1-14Cys) subunit specific antibody used in immunohistochemical assays was provided by Professor F.A. Stephenson (School of Pharmacy, London, UK). Anti-GABAR α4 (1-14) (Ebert *et al.*, 1996), β1 (350-375) (Jechlinger *et al.*, 1998), β2 (351-405) (Jechlinger *et al.*, 1998), β3 (345-408) (Slany *et al.*, 1995), δ (1-44) (Jones *et al.*, 1997) and γ_2 (319-366) (Tretter *et al.*, 2001) subunit-specific antibodies were provided by Professor W. Sieghart (Brain Research Institute, University of Vienna, Austria). Affinity purified C-terminal anti-TARPγ2 (Cys DSLHANTANRRTTPV), anti-TARPγ8 (MESLKRWNEERGLW Cys) (Payne *et al.*, 2006 (in preparation)), anti-NMDAR NR1 (17-35), anti-GABAR α1 (1-15cys) (Thompson *et al.*, 2000) used in immunoblots and anti-GABAR α6 (1-15cys) (Ives *et al.*, 2002) subunit-specific antibodies were prepared in the laboratory as previously described by Pollard *et al.*, 1993. Anti-neuron-specific enolase (NSE) antibody was obtained

from Affiniti Research Products Ltd. (Nottingham, UK). Anti-β-actin antibody was obtained from Sigma. Anti-AMPAR GluR2 and anti-AMPAR GluR4 were obtained from Santa Cruz Biotechnology (Autogen Bioclear, calne, Wiltshire, UK). Anti-AMPAR GluR1 was provided by Cambridge Research Biochemicals (Billingham, UK).

2.1.3. PCR reagents

100 bp DNA ladder, Taq polymerase, and deoxynucleotides (dATP, dGTP, dCTP and dTTP) were obtained from Promega (Southampton, Hampshire, UK). Sequence specific primers were synthesised by Invitrogen (Paisley, UK).

2.1.4. Cell Culture

Modified Eagle Medium (MEM) + Earles salts - L-glutamine, Neurobasal A medium and B-27 supplement were obtained from Invitrogen/Gibco (Paisley, UK). Foetal calf serum was purchased from Perbio (Cheshire, UK). Sulfolink NHS-SS-biotin was obtained from Pierce (Chester, Cheshire, UK). Poly-L-lysine, insulin, FDU, nifedipine and streptavidin beads were obtained from Sigma (Poole, UK). Kainic acid, CNQX and verapamil were purchased from Tocris (Bristol, UK). Transferrin was obtained from Calbiochem (Darmstadt, Germany). L-glutamine was obtained from ICN (Ohio, USA).

2.1.5. Miscellaneous

Horseradish peroxidase-linked anti-rabbit secondary antibody, Horseradish peroxidase-linked anti-mouse secondary antibody, and ECL Hyperfilm, were purchased from Amersham Pharmacia (Aylesbury, Buckinghamshire, UK). Horseradish peroxidase-linked anti-goat secondary antibody was obtained from Pierce (Chester, Cheshire, UK). Vecta-stain *Elite* ABC kits (avidin-biotin-peroxidase method) were purchased from Vector Laboratories (Peterborough, UK). Prestained precision protein standards (10-250 kDa) were obtained from Bio-rad (Hertfordshire, UK). Nuclei lysis solution and protein precipitation solution were purchased from Promega (Southampton, Hampshire, UK).

2.2. ANIMALS

Wild type ($C3B6Fe^+$, +/+), heterozygous ($C3B6Fe^+$, +/stg) and homozygous stargazer mutant mice ($C3B6Fe^+$, stg/stg) were obtained from heterozygous breeding pairs originally obtained from The Jackson Laboratory (Bar Harbor, ME) and bred in the University of Durham vivarium on a 12 hour light/dark cycle with food and water freely available. All procedures were conducted according to the Animals (Scientific Procedures) Act 1986.

2.3. LABORATORY SOLUTIONS

Phosphate buffered saline (PBS)	4 mM Na_2HPO_4, 1.7 mM KH_2PO_4, 137 mM NaCl, 107 mM KCl, pH 7.4
Tris buffered saline (TBS)	50 mM Tris, 0.9% NaCl, pH 7.1
2x Electrode buffer	10 mM Tris, 800 mM Glycine, 0.2% SDS pH 8.8
2x Transfer buffer	25 mM Tris, 100 mM Glycine, 20% Methanol
3x Sample buffer	20 mM Dithiothreitol (DTT), 30 mM NaH_2PO_4, 30% Glycerol, 0.05% bromophenol blue, pH 7.4, 7.5% SDS
1x Solubilising buffer	50 mM Tris, 2 mM EDTA, 2% SDS pH 6.8
10x TBE	0.9 M Tris, 0.9 M boric acid, 40 mM EDTA, pH 8.0
SS buffer (Hall R.A., Soderling T.R., 1997)	137 mM NaCl, 5.3 mM KCl, 0.17 M Na_2HPO_4, 0.22 M KH_2PO_4, 10 mM HEPES, 33 mM glucose, 44 mM sucrose, pH 7.3
Luminol	1.25 mM in 0.1 M Tris-HCl, pH 8.5
P-coumaric acid	68 mM
Lowry reagent A	2% sodium carbonate, 0.1 M NaOH, 0.5% SDS
Lowry reagent B	2% sodium potassium tartrate
Lowry reagent C	1% copper sulphate
6 x Loading buffer	0.25% bromophenol blue, 30% glycerol, 60 mM EDTA, pH 8.0

2.4. GENOMIC SCREENING OF MICE

2.4.1. Background

Adult (2-6 months) and neonate (P3-4) mice are routinely screened for possession of the mutated stargazin gene, in order to classify each animal as a control mouse (+/+:+/stg) or stargazer mutant (stg/stg). Genomic DNA is extracted from tail biopsy, PCR amplification of specific sequences is undertaken using sequence-specific primers (See section 2.4.3.). Amplification products are separated by agarose gel electrophoresis, stained with ethidium bromide and viewed using a UV transilluminator.

The screening of adult mice is important for the pairing of heterozygous (+/stg) mice for the maintenance of the stargazer breeding program, but also experiments to determine differences in GABAR between heterozygous (+/stg) and wild type (+/+) animals hinges on the accurate genotyping of the mice. It is necessary to screen neonate mice for primary cerebellar granule cell culture, as the characteristic phenotype of the stargazer does not become apparent until P14. Figure 2.1. is an example of a PCR screen carried out on neonates, which were later used for primary cerebellar granule cell culture, demonstrating the characteristic amplification products of heterozygote (300 bp and 600 bp bands), wild type (600 bp) and stargazer (300 bp) animals.

2.4.2. Genomic DNA extraction from tail biopsy

Tail biopsies (~2-3 mm) were taken from adult (2-6 months) or neonate mice (P3-4) and transferred to 1.5 ml eppendorfs. In order to allow the correct identification of mice after genotyping, in the case of the adult mice, different combinations of ear punches were made and noted, whereas for neonates, toe clips were taken.

Per biopsy, 500 µl nuclei lysis solution (Promega) was combined with 120 µl 0.5 M EDTA, pH 8 at 4°C. 600 µl, or 360 µl for neonate samples, of this solution was added to each tail biopsy. 17.5 µl (10.5 µl for neonates) of 20 mg/ml

Proteinase K was then added to the samples, vortexed and incubated at 55°C overnight to digest constituent proteins.

Protein precipitation solution (200 µl for adult samples or 120 µl for neonates) was added to each sample and incubated on ice for 5 minutes, following which, samples were centrifuged at 11 400 *g* for 5 minutes using a bench top (Eppendorf 5415C) microfuge. The resultant supernatant was retained and 600 µl (360 µl for neonates) isopropanol was added in order to precipitate DNA and samples were centrifuged at 11 400 *g* for 10 minutes. The pellet was washed with 100 µl 70% ethanol and centrifuged for a further 5 minutes at 11 400 *g*. The dried pellet was resuspended in 80 µl (40µl for neonates) deionised water and incubated at 65°C for 45-60 minutes in order to dissolve DNA. DNA samples were stored at -20°C until required.

2.4.3. Primers

Oligonucleotide primers for the amplification of the stargazin gene were:
109F: 5'-CATTTCCTGTCTCATCCTTTG-3',
EHt7: 5'-ACTGTCACTCTATCTGGAATC-3',
EtNOR: 5'-GCCTTGATCAGAGTCACTGTC-3'
(Letts *et al.*, 1998)

2.4.4. Genomic PCR amplification

PCR reactions were carried out in a total volume of 25 µl. Each reaction contained final concentrations of:

3 units Taq Polymerase,
15 mM $MgCl_2$,
25 pmoles EtNOR,
50 pmoles 109F,
50 pmoles EHt7,
2.5 mM dNTPs,

2.5 µl Mg-free 10 x reaction buffer (500 mM KCl, 100 mM Tris-HCl, 1% Triton X-100)
13.4 µl dH_2O
1 µl genomic DNA.

PCR reactions containing control DNA samples (+/+, +/stg and stg/stg) were included in each PCR, in order to correctly identify the genotype of test samples. Contamination of PCR solutions was monitored by including a PCR reaction containing deionised water as a 'no DNA' control. The amplification protocol was carried out using an applied biosystems GeneAmp 2700 PCR machine as follows:

95°C - 5 minutes
94°C - 1 minute
55°C - 2 minutes } 30 cycles
72°C - 2 minutes

Resultant PCR products were stored at -20°C until required.

2.4.5. Agarose gel electrophoresis

5 µl of each amplification product was diluted in 5µl dH_2O and 2µl 6x loading buffer. 100 bp DNA ladder (4 µl) was diluted in 6 µl deionised water and 2µl 6x loading buffer and loaded on the gel in order to size sample DNA fragments. Products were resolved on 1.5% agarose gels (1.2 g agarose in 80 ml 1xTBE buffer) for ~45 minutes at 90 mV using a Bio-rad electrophoresis power pac. DNA was stained with ethidium bromide (0.2% v/v) for 10-15 minutes, followed by de-staining in deionised water for ten minutes. Gels were analysed using the Quantity one (4.0.3) software for the GelDoc system (Bio-Rad, Hertfordshire, UK).

A

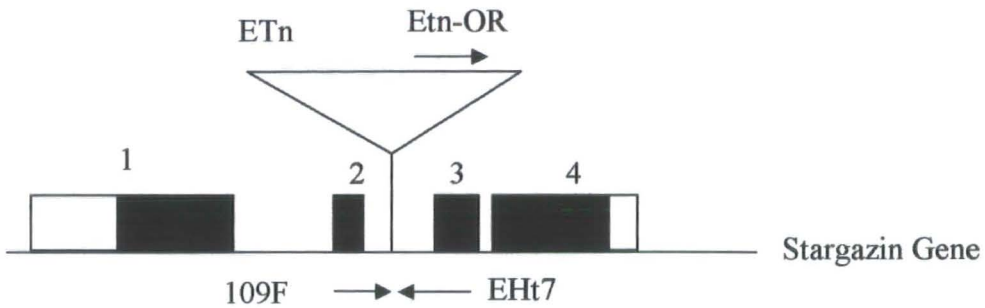

B

AMPLICONS: 109F + EHt7 = 600 bp
Etn-OR + EHt7 = 300 bp

C

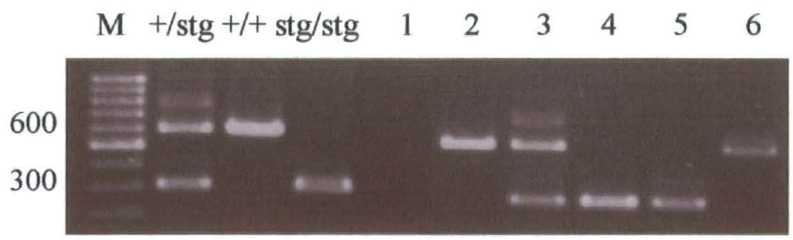

FIGURE 2.1. GENOMIC PCR SCREENING OF TAIL BIOPSIES

A: Schematic representation of the stargazin gene indicating the site of transposon insertion (6 kb) in stargazer mice. Boxed areas represent exons, with shaded regions on the stargazin gene representing coding exons. (Letts *et al.*, 1998). ETn: Early transposon insertion.

B: Amplicons resulting from the amplification of DNA extracted from tail biopsy with sequence specific primers, to produce bands of 600 bp and 300 bp.

C: M is 100 bp DNA ladder. Lane 1 is a 'no DNA' control lane. Lane 3 represents a heterozygote (300 and 600 bp). Lanes 2 and 6 represent wild type mice (600 bp). Lanes 4 and 5 represent stargazer mice (300 bp).

2.5. PREPARATION OF CEREBELLAR MEMBRANE HOMOGENATES FOR RADIOLIGAND BINDING

Cerebellar membrane preparations were carried out according to the method of Mehta and Ticku (1999) with modifications. Cerebella were dissected from adult (2-6 months old) +/+: +/stg and stg/stg mice, flash frozen in liquid nitrogen, to avoid ice crystal formation and stored at -80°C.

Cerebella were rapidly thawed, weighed and suspended in a minimum of 10 volumes of ice-cold buffer to wet tissue weight (50 mM Tris-Citrate, pH 7.1, 1 mM EDTA, 1 mM EGTA, 2 mM Benzamidine, 0.02% (w/v) Sodium azide), usually ~20 ml per 10 cerebella. Protease inhibitors were then added to the tissue to prevent proteolytic degradation, which included 1 mM Phenylmethylsulphonyl Fluoride (PMSF), 2 μg/ml Aprotinin, 1 μg/ml Leupeptin and 1 μg/ml Pepstatin A. The tissue was homogenised (10 strokes) in a 50 ml homogeniser tube, using a Potter glass/Teflon homogeniser. The homogenate was then transferred to Beckman centrifuge tubes and balanced against each other with ice-cold buffer. The tissue was centrifuged at 78 000 *g* for 40 minutes at 4°C in a Beckman L-70 ultracentrifuge using a 70.1Ti rotor. The resultant supernatant was discarded and the pellet re-suspended in ~30 ml ice-cold buffer, including protease inhibitors as above.

Following homogenisation (10 strokes) the homogenate was transferred to centrifuge tubes and balanced using ice-cold buffer. The tissue was then re-centrifuged at 45 000 *g* for 35 minutes at 4°C using a JA20 rotor in a high speed centrifuge (Beckman JS-HC or JS-HS). The resultant pellet was re-suspended in ~30 ml buffer including protease inhibitors, homogenised (10 strokes), flash frozen in liquid nitrogen and stored at -20°C overnight.

The tissue samples were then thawed quickly in warm water, balanced using ice-cold buffer and centrifuged at 45 000 *g* for 35 minutes at 4°C. The supernatant was discarded and the resultant pellet was re-suspended, homogenised and centrifuged as above. The final pellet was suspended in ~5 ml ice-cold buffer,

aliquoted into 1 ml samples and stored at -80°C until required. An aliquot was removed for protein determination using the Lowry assay with bovine serum albumin (BSA) as a standard.

2.6. SOLUBILISATION OF CEREBELLAR MEMBRANES FOR IMMUNOBLOTTING

Cerebella were dissected from adult mice, flash frozen in liquid nitrogen and stored at -80°C until required. Each cerebellum was homogenised (10 strokes) individually in a 2 ml homogeniser tube using a potter glass/Teflon homogeniser in 2 x Solubilising buffer (100 mM Tris, 4 mM EDTA including protease inhibitors Aprotinin (4 μg/ml), Leupeptin (2 μg/ml) and Pepstatin A (2 μg/ml)). An aliquot of homogenate was removed for protein determination by Lowry assay. Following which, an equal volume of 4% Sodium dodecyl sulphate (SDS) was added to the remaining material and incubated at room temperature for 30 minutes with agitation. The homogenate was triturated with a 0.8 mm diameter needle in order to shear genomic DNA. Samples were flash frozen in liquid nitrogen and stored at -80°C until required.

2.7. SOLUBILISATION OF DENTATE GYRI FOR IMMUNOBLOTTING

Adult mice were deeply anaesthetised, perfused with PBS-nitrite (0.1% w/v) plus protease inhibitors and forebrain were dissected out and stored at 4°C (see section 2.14.2). 200 μm coronal sections were cut using a vibrating microtome and dentate gyri were dissected out using a light microscope at 4°C. 250 μl 1x solubilising buffer was added to each dentate gyrus in a 1.5 ml eppendorf and incubated at room temperature for 30 minutes with agitation. Constituent DNA was then sheared by trituration of the homogenate with a 0.8 mm diameter needle. Samples were assayed by the method of Lowry, to determine protein concentrations (see section 2.8.) and samples were precipitated and resuspended in 2x sample buffer to give a final concentration of 1 mg/ml for western blot analysis (see section 2.10.).

2.8. LOWRY ASSAY FOR PROTEIN CONCENTRATION DETERMINATION

Protein concentration was determined by the method of Lowry *et al.*, (1951) using bovine serum albumin as the standard protein. A stock solution of BSA (1 mg/ml) was serially diluted in deionised water to yield concentrations of 5, 10, 20 and 40 µg/ml, which were used as a range of standard protein concentrations to construct a standard curve. Lowry reagent A, B and C were mixed in a ratio of 50:1:1 to form lowry reagent D. 1 ml lowry reagent D was added to a total volume of 200 µl of sample (10-20 µl) and water (180-190 µl) and incubated for 10 minutes at room temperature. Samples were assayed in duplicate. 100 µl Lowry reagent E (1 part Folins ciocalteau reagent and 1 part water) was added to each sample and incubated at room temperature for 30 minutes. The OD at 750 nm was determined for each sample, using a spectrophotometer, employing the '0 µg/ml BSA' sample as a blank. A standard curve for BSA was constructed to allow the determination of sample unknown protein concentrations.

2.9. PROTEIN PRECIPITATION BY THE CHLOROFORM METHANOL METHOD

4 volumes of methanol, 1 volume of chloroform and 3 volumes of deionised water (dH_2O) were added to 1 volume of sample. The preparation was then vortexed for 10 seconds and centrifuged for 1 minute at 11 400 *g*. Following centrifugation, the preparation was seen to form three layers, the protein present within the mixture forming a solid interface between two liquid layers. The top liquid layer was discarded and 3 volumes of methanol were added to the remaining preparation. The preparation was then gently agitated in order to mix the component layers and centrifuged for two minutes at 11 400 *g*. The supernatant was removed and discarded and the resultant pellet was allowed to air-dry. Once dry, the pellet was suspended in 2x sample buffer to yield a final protein concentration of 1 mg/ml, heated for 5 minutes at 95°C and stored at -20°C until required.

2.10. SODIUM DODECYL SULPHATE-POLYACRYLAMIDE GEL ELECTROPHORESIS (SDS-PAGE) AND IMMUNOBLOTTING

Polyacrylamide gel electrophoresis was performed in 10% polyacrylamide slab mini-gels, loading 10 μg protein and fractions thereof per gel lane (Thompson *et al.*, 1998).

2.10.1. Solutions

3.5% Stacking gel 10 ml total volume:	0.09% Acrylogel-3 0.125 M Tris-HCl, pH 6.8 0.1% SDS 1 mg/ml Ammonium Persulphate (APS) 10 μl TEMED 7.61 ml dH_2O
10% Resolving gel (Makes 10 gels)	29.63 ml dH_2O 25.2% Acrylogel-3 24 μl TEMED 25.1% Running Buffer (1.5 M Tris, 8 mM EDTA, 0.4% SDS, pH 8.8 in 100 ml dH_2O) 1 mg/ml AMPS
Blocking buffer	5% Dried skimmed milk powder 0.2% Tween 20 in PBS
Incubation buffer	2.5% Dried skimmed milk powder in PBS

2.10.2. Preparation of 10% resolving gels

10x8 cm glass plates, alumina plates and 1 mm spacers were rinsed with 100% ethanol, once with acetone and allowed to dry. Plates were then assembled in a 10-gel caster. 10% resolving gel solution was prepared as in section 2.11.1 and poured into the gel caster to a volume ~2-3 cm from the top of the gel caster. 150 µl water saturated butanol was added to the surface of each gel to prevent dehydration and allowed to polymerise for 1 hour at room temperature. Gels were wrapped individually in tissue and stored at 4°C in a 25% running buffer solution until use.

2.10.3. SDS-PAGE

A 10% resolving gel was clamped into a Hoefer Mighty Small II vertical slab gel unit. 3.5% stacking gel solution was prepared (see section 2.10.1.) and degassed for 10 minutes. 10 µl TEMED was added to the stacking gel solution and poured above the resolving gel. A 0.75 mm 10 well comb was inserted into the stacking gel and allowed to polymerise. ~200 ml 1x electrode buffer was poured behind the gel and in the base of the unit to ~1 cm height. The comb was removed and wells were washed by expelling electrode buffer into the wells using a Hamilton syringe to remove excess gel. 10 µl (10 µg) protein sample or prestained protein standards (10-250 kDa) was loaded per gel lane using a hamilton syringe. Electrophoresis was carried out using an Amersham pharmacia power pac E300/E301 at 80V for ~45 minutes to allow protein samples to move through the stacking gel and then proteins were resolved at 100V for ~90 minutes.

2.10.4. Immunoblotting

Once SDS-PAGE was complete, components of the transfer cassette were equilibrated in 1x transfer buffer. The transfer cassette was assembled in the following order: sponge, 1 piece of whatman 3MM filter paper, resolving gel, nitrocellulose membrane, whatman paper and sponge. All components were assembled submerged in transfer buffer and care was taken to ensure no air

became trapped within the transfer layers. Once assembled, the transfer cassette was placed in a Hoefer TE series transphor unit containing 1x transfer buffer at room temperature and proteins were transferred to nitrocellulose membrane for 2 hours at 50 V.

Following transfer of proteins to nitrocellulose, the membrane was incubated in blocking buffer (see section 2.10.1.) for 1 hour at room temperature with gentle shaking. Primary antibody was diluted in incubation buffer (see section 2.10.1.) and the nitrocellulose membrane was incubated in a 50 ml falcon tube overnight at 4°C in primary antibody (see table 2.1. for antibody concentrations).

Table 2.1. Primary antibody concentrations used for immunoblotting

ANTIBODY	**CONCENTRATION (μg/ml)**
Anti-GABAR α1 (1-14Cys)	0.25-1
Anti-GABAR α4 (1-14)	0.5
Anti-GABAR α6 (1-15cys)	2-4
Anti-GABAR β2 (351-405)	0.5
Anti-GABAR β3 (345-408)	0.5
Anti-GABAR δ (1-44)	1
Anti-GABAR γ2 (319-366)	1
Anti-NSE	1:100 000
Anti-β-actin	1:2000
Anti-AMPAR GluR2	1:250-500
Anti-NMDAR NR1 (17-35)	1
Anti-stargazin C-terminus peptide sequence (Cys-DSLHANTANRRTTPV)	1-4
Anti-TARP γ8 (1-14cys)	4

After incubation in primary antibody, the nitrocellulose membrane was washed three times in wash buffer (see section 2.10.1) and incubated in horseradish peroxidase linked secondary antibody (anti-rabbit (1:1000) or goat (1:4000)) diluted in incubation buffer, for 1 hour at room temperature with gentle shaking. On completion of blocking non-specific binding sites, the nitrocellulose membrane was washed three times in wash buffer and twice in PBS, before allowing the membrane to dry. Prestained protein standards were marked with diluted horseradish peroxidase linked secondary antibody (1:100), to allow sizing of proteins on the membrane.

The enhanced chemiluminescence (ECL) western blotting system was used to detect immunoreactive species on hyperfilm. Processing of membrane involved incubation in a solution of 1.25 M luminol (10 ml), 68 mM p-coumaric acid (120 µl) and 30% H_2O_2 (6.67µl) for 1 minute. On removal of reagent, the membrane was wrapped in clingfilm and exposed to Hyperfilm ECL for 1-5 minutes. Immunoreactive species were detected using Kodak GBX developer and films fixed for ~5 minutes. Band intensity was quantified using Image J software.

2.10.5. Analysis of immunoblots

The intensity of immunoreactive bands were quantified using ImageJ software. Immunoblots were scanned using a flatbed scanner at high resolution (minimum 600 dpi). Values of mean gray-scale intensity were determined for each immunoreactive band from which mean background intensity was subtracted. Values are expressed as a ratio of mean intensity for the protein of interest over mean intensity for β-actin.

2.11. RADIOLIGAND BINDING ASSAYS

[^{3}H] Ro15-4513 and [^{3}H] Muscimol binding assays were conducted on cerebellar membrane homogenates prepared as described in section 2.5. (Thompson *et al.*, 1998).

[^{3}H] Ro15-4513		[^{3}H] Muscimol	
Binding buffer	Wash buffer	Binding buffer	Wash buffer
10 mM Tris-HCl, 150 mM NaCl, pH 7.4	10 mM Tris-HCl, 50 mM NaCl, pH 7.4	50 mM Tris-Citrate, pH 7.1	5 mM Tris-Citrate, pH 7.1

2.11.1. [^{3}H] Ro15-4513

The radioligand concentration range for saturation analyses for [^{3}H] Ro15-4513 was 0.3125-40 nM. Non-specific binding was determined in the presence of Ro15-1788 (10 μM), a benzodiazepine receptor antagonist. [^{3}H] Ro15-4513 binding in the presence of flunitrazepam (10 μM), a benzodiazepine full agonist, defined benzodiazepine-insensitive (BZ-IS) binding sites and hence benzodiazepine-sensitive (BZ-S) sites could be determined by subtraction of the BZ-IS binding sites from total [^{3}H] Ro15-4513 specific binding sites.

2.11.2. Zolpidem displacement of [^{3}H] Ro15-4513

A concentration of [^{3}H] Ro15-4513 of 10 nM was used for zolpidem displacement of [^{3}H] Ro15-4513 binding, which was co-incubated with varying concentrations of zolpidem. Half log dilutions of zolpidem were employed ranging from 1 nM to 10 μM. Levels of total, BZ-S and BZ-IS [^{3}H] Ro15-4513 binding were determined as in section 2.11.1., in order to determine the levels of displacement of BZ-S binding in the presence of zolpidem.

2.11.3. [^{3}H] Muscimol

The radioligand concentration range employed for [^{3}H] Muscimol was 0.5-40 nM. Non-specific binding sites were defined in the presence of 0.2 mM GABA. Experimental protocols were similar for both radioligands. The total assay volume per reaction was 0.5 ml, comprising binding buffer, radioligand and

membrane preparation. Each radioligand concentration was tested in triplicate and incubated in the presence of radioligand for an hour on ice. Following which the reaction was terminated by rapid filtration through Whatman GF/B filter paper pre-soaked in 0.03% Polyethylenimine, using a Brandel Cell Harvester. Filters were washed three times with ~3 ml wash buffer and allowed to dry. Filters were then transferred to scintillation vials with 4 ml scintillation fluid (Ecoscint) and subjected to scintillation counting for 3 minutes per sample.

2.11.4. Data analysis for saturation binding curves

Saturation binding curve data was analysed using GraphPad Prism 3.0 by non-linear regression and one-site binding hyperbola. K_D values were calculated according to the following equation:

$$Y = \frac{B_{MAX}\, X}{K_D + X}$$

Y = Specific bound [^{3}H] ligand
X = Concentration of [^{3}H] ligand
B_{MAX} = Maximum number of binding sites
K_D = Dissociation constant from saturation binding of [^{3}H] ligand

For Rosenthal transformations, saturation data was fit by linear regression to the line, using GraphPad Prism 3.0:

$$F(x) = ax + b$$

F(x) = Specific bound [^{3}H] ligand/Free [^{3}H] ligand
A = Slope – ($1/K_D$)
X = Specific bound [^{3}H] ligand
B = x-axis

2.12. RECEPTOR AUTORADIOGRAPHY

2.12.1. Receptor autoradiography to tissue sections

Sucrose-perfused (10% sucrose in PBS) adult whole mouse brain was frozen in isopentane over liquid nitrogen (3 minutes, -40°C) and sectioned (16 μm) in the horizontal plane using a cryostat at -21°C. Sections were immediately transferred to polysine coated slides (BDH). Two control and two stargazer sections were thaw mounted onto each slide, dried for a minimum of 12 hours, desiccated and stored at -20°C until required.

Slides were incubated in pre-incubation buffer for 15-20 minutes at 4°C. Following which, the slides were transferred into radioligand-containing or non-specific binding buffer (see table 2.2.) at 3 minute intervals and incubated for a total of 1 hour at 4°C. Slides were removed from ligand-containing buffer in the same order and immersed in three changes of wash buffer for 15 seconds, followed by 1 wash in dH_2O, all at 4°C. Slides were then dried under a stream of cool air to remove any excess buffer and hence prevent ligand dissociation and allowed to dry at room temperature overnight. Once dry, the slides were secured into a hypercassette and exposed to [^{3}H] Hyperfilm for 2 weeks to 2 months depending on ligand employed.

Table 2.2. Summary of component buffers for [^{3}H] Receptor Autoradiography

	PREINCUBATION BUFFER	LIGAND-CONTAINING BUFFER	NON-SPECIFIC BINDING BUFFER	WASH BUFFER
[^{3}H] Flunitrazepam	50 mM Tris-HCl, pH 7.4 120 mM NaCl	50 mM Tris-HCl, pH 7.4 120 mM NaCl 5 nM [^{3}H] Flunitrazepam	50 mM Tris-HCl, pH 7.4 120 mM NaCl 5 nM [^{3}H] Flunitrazepam 10 μM Ro15-1788	10 mM Tris-HCl, pH 7.4
[^{3}H] Muscimol	0.31 M Tris-acetate, pH 7.1	0.31 M Tris-acetate, pH 7.1 20 nm [^{3}H] Muscimol	0.31 M Tris-acetate, pH 7.1 20 nm [^{3}H] Muscimol 1 mM GABA	10 mM Tris-HCl, pH 7.4
[^{3}H] Ro15-4513	50 mM Tris-HCl, pH 7.4 120 mM NaCl	50 mM Tris-HCl, pH 7.4 120 mM NaCl 20 nM [^{3}H] Ro15-4513 (10 μM flunitrazepam)	50 mM Tris-HCl, pH 7.4 120 mM NaCl 20 nM [^{3}H] Ro15-4513 10 μM Ro15-1788	10 mM Tris-HCl, pH 7.4

2.12.2. Quantification of receptor autoradiographs

The level of radioactivity in the different brain areas were compared in control and stargazer tissue sections using ImageJ software. Autoradiographs were scanned using a flatbed scanner at high resolution (1200 dpi). A standard curve was constructed by analysis of gray-scale intensity of radioactive standards of known concentrations, exposed on each autoradiograph to be analysed. Calibration standards ranged from 0.1-109.4 nCi/mg. 5-10 measurements of gray-scale intensity were taken from within each brain structure to be analysed of 6 comparable sections per mouse strain to yield a mean intensity. Mean film background values were subtracted from mean intensities. The amount of radioactivity associated with each brain structure could then be determined from the standard curves and compared by student's t-test with $p<0.05$ considered to be statistically significant.

2.13. IMMUNOHISTOCHEMISTRY

2.13.1. Solutions

Phosphate buffered saline (PBS) and $NaNO_2$ (0.1% w/v), pH 7.4	137 mM NaCl 107 mM KCl 4 mM Na_2HPO_4 (anhydrous) 1.7 mM KH_2PO_4 0.1% w/v $NaNO_2$
4% paraformaldehyde in 0.1 M phosphate buffer	50% (v/v) 0.2 M Phosphate buffer 50% (v/v) 8% Paraformaldehyde

2.13.2. Perfusion fixation and tissue sectioning

A deeply anaesthetised mouse (100 µl per 100 g Pentobarbital (Euthatal)) is assessed by failed nictating reflex and pressure-induced retraction of the hind limb and pinned out with its ventral surface uppermost. The ribcage is exposed and retracted to reveal the heart. A 25 gauge microlance is pushed into the left

ventricle through which is perfused, via a peristaltic pump, ice-cold 0.1 M sodium phosphate buffer (pH 7.4) containing 0.1% (w/v) sodium nitrite. The right atrium is cut under slight positive pressure from the perfusate and the animal is exsanguinated in this manner for 5 minutes (~25 ml buffer). The perfusate is exchanged for freshly prepared, ice-cold fixative (normally 4% paraformaldehyde in 0.1 M phosphate buffer, pH 7.4 for immunohistochemical studies). The fixation procedure is continued for 20 minutes (100 ml fixative) after which the brains are dissected out and immersed in fixative at 4°C overnight. For light microscopic studies, brains are cryoprotected by sucrose infiltration. Fixed, PBS-washed brains are transferred to 10% (w/v) sucrose in PBS, pH 7.4 for 48 hours prior to sectioning. The sucrose solution is replaced every 12 hours.

Perfusion-fixed adult whole brain was frozen in isopentane over liquid nitrogen (1 minute, -70°C) and sectioned (30 μm) using a cryostat (-21°C). Sections were stored in PBS/0.02% NaN_3 until required.

2.13.3. Antigen retrieval

Prior to immunohistochemical staining for the GABAR δ subunit, free floating sections were processed by antigen retrieval methods initially characterised by Jiao *et al.*, (1999), in order to increase receptor staining while reducing background staining. Following incubation in 20% methanol, 20% H_2O_2 in TBS, as in the immnuohistochemical staining procedure, sections were incubated in 0.05 M sodium citrate, pH 8.6 for 30 minutes at room temperature and then heated to 90°C for 70 minutes. Sections were allowed to cool to room temperature and washed in TBS before further immunohistochemical processing.

2.13.4. Immunostaining

Brain sections were immunostained using the Vecta-stain *Elite* ABC kit (avidin-biotin-peroxidase method). Residual paraformaldehyde was quenched by incubation of freely floating sections in (0.2% w/v) TBS-glycine, pH 7.4 for 30

minutes at room temperature. Non-specific binding sites were blocked with 10% w/v goat serum in (0.2% v/v) TBS-Triton X-100 (TBS-T), incubated for 1 hour at room temperature with agitation. Sections were incubated in primary antibody diluted in PBS-goat serum (1% v/v) overnight at 4°C.

Table 2.3. Primary antibody concentrations used for immunohistochemistry

ANTIBODY	CONCENTRATION (μg/ml)
Anti-GABAR α1(1-14cys)	0.25
Anti-GABAR α4 (1-14)	0.5
Anti-GABAR α6 (1-15cys)	0.25
Anti-GABAR β1 (350-375)	1
Anti-GABAR β2 (351-405)	0.5
Anti-GABAR β3 (345-408)	0.5
Anti-GABAR δ (1-44)	0.25
Anti-GABAR γ2 (319-366)	2
Anti-stargazin C-terminus peptide sequence (Cys-DSLHANTANRRTTPV)	0.5

Following incubation in primary antibody, sections were allowed to equilibrate to room temperature for 1 hour in primary antibody, washed 3 times (5 minute washes) with TBS-T and incubated for 2 hours with anti-rabbit biotinylated secondary antibody, diluted in TBS-goat serum (1% v/v). Sections were then washed 3 times with TBS-T and incubated at room temperature for 1 hour with ABC reagent (5 ml TBS, 100 μl Solution A, 100 μl Solution B). Following which, sections were washed 3 times with TBS-T, twice with TBS and incubated with Horseradish peroxidase substrate (0.0667% (v/v) Hydrogen peroxide, 3,3-diaminobenzidine (0.5 mg/ml) in TBS) until an optimal signal was achieved (~2-4 minutes). HRP substrate was then removed, sections washed 2 times with deionised water and mounted on a glass slide using DPX mountant.

Sections were imaged using a Nikon DXM 1200 camera and Nikon diaphot 300 microscope at x 400 and x 1000 magnifications.

2.14. PRIMARY CEREBELLAR GRANULE CELL CULTURE

2.14.1. Solutions

H-EBSS	138.3 mM NaCl, 5.4 mM KCl, 25 mM HEPES, 4.2 mM $NaHCO_3$, 1 mM $NaH_2PO_4.H_2O$
Sol. 1H	50 ml H-EBSS, 7.3 mM Glucose, 3 mg/ml Bovine Serum Albumin (BSA) fraction V, 0.5 ml $MgSO_4$ (3.82% w/v)
Trypsin	10 ml Sol.1H, 2.5 mg Trypsin
Dilute DNAse I and trypsin inhibitor	10 ml Sol. 1H, 1.6 ml concentrated DNAse/Trypsin inhibitor
Concentrated DNAse/trypsin inhibitor	10 ml Sol. 1H, 0.1 ml $MgSO_4$, 1300 kunitz units DNAse I, 8 mg Trypsin inhibitor
Culture media	100 ml MEM containing 10% foetal calf serum, 2 mM glutamine, 0.5 mg/ml gentamycin, 2.5 ml 1.33M glucose, 0.025 mg/ml insulin, 0.01 mg/ml transferrin

2.14.2. Cell Culture

(Adapted from Dutton, 1990)

All cell culture techniques were conducted using aseptic technique using a category 2 Telstar laminar flow hood, with autoclaved instruments and solutions. All solutions employed for the culture of primary neurons were sterile filtered through 0.2 μm membrane filters before use.

24 hours before culturing neurons, 35 mm Petri dishes were treated under sterile conditions with poly-L-lysine (50 μg/ml in deionised water (dH_2O), 2 ml per 35 mm dish). Excess poly-L-lysine was aspirated on the day of the culture, dishes were washed three times with sterile dH_2O and allowed to dry.

Cerebellar granule cells were cultured from 5-7 day old (P5-P7) mouse neonates. Cerebella were dissected out under sterile conditions, the meninges were removed to minimise contamination of the culture with non-neuronal cells and the tissue was transferred to sol. 1H (see section 2.14.1.). Upon completion of the dissections, excess sol. 1H was aspirated from the tissue and the cerebella were cut into blocks using two scalpel blades. The material was then transferred into trypsin solution (10 ml) and incubated at 37°C for 15 minutes with gentle agitation, in order to break down the tissue further. Dilute DNAse I and Trypsin inhibitor were then added to the tissue to breakdown DNA and inhibit the action of the trypsin. The material was then centrifuged at 200 *g* for 2 minutes at 4°C and the supernatant was aspirated to leave the cell pellet.

Approximately 5 ml Concentrated DNAse/Trypsin inhibitor was added to the pellet and the material was triturated approximately 30 times using a sterile, siliconised, heat-polished glass pipette, until a homogenate was obtained. The upper cell suspension was retained and the remaining concentrated DNAse/Trypsin inhibitor was added to the undissociated tissue and re-triturated. Any further cell suspension was added to the original retained material. The cell suspension was overlaid over 4% BSA (5 ml) and centrifuged at 500 *g* for 5

minutes at 4°C. The supernatant was aspirated and the remaining pellet was resuspended in 10 ml culture media. Cell numbers were counted on a haemocytometer and cells were resuspended in an appropriate volume to plate at a density of $3.0x10^6$ cells per 35 mm dish in a volume of 3 mls.

Cells were then incubated at 37°C, 5% CO_2/95% air. After 48 hours, cells were treated with Fluoro-2-deoxyuridine (80 μM) to suppress the proliferation of non-neuronal cells.

2.14.3. Drug treatment of cultured cerebellar granule cells

24 hours after plating (1 DIV), cerebellar granule cells were treated with 100 μM kainic acid (30 μl of 10 mM stock per 35 ml culture dish), an ionotropic glutamate receptor agonist, in order to activate AMPA receptors within the culture and hence allow us to study the effects of depolarisation on the cultured cells. Alternatively, cells were treated with KCl (30 μl of 2M stock per 35 mm dish), to increase the extracellular potassium concentration to 25 mM and hence depolarise the cells by altering electrochemical and potassium ion concentration gradients.

In order to study the possible mechanisms by which depolarisation by kainic acid influences $GABA_A$ receptor expression profiles, cells were treated with 10 μM nifedipine (3 μl of 20 mM stock in DMSO) or 10 μM verapamil (3 μl of 20 mM stock in DMSO), L-type calcium channel blockers, to determine if calcium entry though L-type calcium channels was an important factor in $GABA_A$ receptor expression.

2.14.4. Harvesting of cultured cerebellar granule cells

Each 35 mm culture dish of cells to be harvested was washed three times in SS buffer (3 mls) and solubilised in 500 μl 1x solubilising buffer. Cells were scraped into the solubilising buffer, transferred into 1.5 ml eppendorfs, flash frozen in liquid nitrogen and stored at -20°C until required.

2.15. CELL SURFACE BIOTINYLATION

(Adapted from Archibald *et al.*, 1998)

Quenching buffer	192mM Glycine, 4% sucrose in 50 mM TBS, pH 8.0
Lysis buffer	0.1mM PMSF, 10 μg/ml aprotinin, leupeptin, pepstatin A, 2mM EDTA in TBS, pH 8.0 + 1% SDS + 1% triton x-100

7 DIV cerebellar granule cells 35 mm dishes were washed three times (1 ml) with ice cold PBS + 4% sucrose, pH 8.0 and incubated for 15 minutes at 4°C with 1 mg/ml EZ-link Sulfo-NHS-SS-biotin in cold PBS + 4% sucrose with gentle agitation (0.5 ml per 35 mm dish). Cells were washed once with ice cold PBS + 4% sucrose and incubated for 10 minutes at 4°C with quenching buffer. Cells were washed twice in cold PBS + 4% sucrose. Cells were solubilised in 166 μl lysis buffer + 1% SDS and samples were made up to 1 ml total volume with 833 μl lysis buffer + 1% Triton x-100. Samples were incubated with 100 μl of 50% slurry of streptavidin beads for 2 hours at 4°C with agitation. Samples were centrifuged at 10 000 *g* for 1 min and the supernatant retained as the unbound fraction, or intracellular component. Streptavidin beads were washed once with 1 ml lysis buffer + 1% triton x-100 and centrifuged for 1 min at 10 000 *g*. Followed by a further two washes with lysis buffer alone. Sample bound to the beads was eluted with 50 μl 2x sample buffer by heating at 95°C for 5 minutes. Streptavidin beads were centrifuged at 10 000 *g* for 1 minute and the supernatant retained as the bound fraction or surface protein. Samples were subjected to western blot analysis (see section 2.10.) to allow for the quantification of surface versus intracellular protein.

2.16. RADIOLIGAND BINDING TO CULTURED CEREBELLAR GRANULE CELLS

Radioligand binding was conducted on 7 DIV cultured cerebellar granule cells using [^{3}H] Ro15-4513 and [^{3}H] muscimol at a concentration of 40 nM for each ligand. Briefly, cell culture dished were washed rapidly three times with 3 ml SS buffer and incubated in 1 ml ligand for 1 hour at 4°C. Following incubation in ligand, dishes were washed a further three times with 3 ml SS buffer rapidly, to avoid ligand dissociation and allowed to dry at room temperature. 1 ml 0.2 M NaOH was applied to each dish and incubated overnight at room temperature with gentle agitation. The reaction was neutralised with 100 µl 2 M HCl and incubated at room temperature for 30 minutes with agitation. 700-800 µl sample was added to 4 ml scintillation fluid and subjected to scintillation counting for 3 minutes per sample. A further 100 µl of each sample was aliquoted for lowry assay.

2.17. STATISTICAL ANALYSES

Statistical analyses were performed using GraphPad Prism version 3.0 and Microscoft Excel, using an unpaired student's t-test with $p<0.05$ considered to be statistically significant.

CHAPTER 3. $GABA_A$ RECEPTOR SUBUNIT PROTEIN EXPRESSION IN THE STARGAZER MUTANT MOUSE

3.1. INTRODUCTION

Previous work by Thompson *et al.* in 1998 identified a series of cerebellar $GABA_A$ receptor abnormalities in the stargazer mutant. These included specific down-regulation of expression of the GABAR α6 and β3 subunits whilst α1 and β2 subunits appeared to be relatively spared. Since the GABAR α6 subunit is one marker of cerebellar granule cell maturation this data might imply that the stargazer cerebellum is restrained in an immature state (see section 1.2.2.).

The initial studies conducted by Thompson et al., 1998 were limited by (i) the availability of a sufficient number of animals to conduct a comprehensive analysis; (ii) access to an appropriate background strain of mice for control experiments and, (iii) high quality subunit-specific antibodies with which to screen all $GABA_A$ receptor subunits of interest (Thompson *et al.*, 1998). Therefore, the aim of this chapter was to re-evaluate and extend the previous observations by Thompson *et al.*, in 1998 using an appropriate background strain and to further comprehensively characterise the expression of all the principal $GABA_A$ subunits and receptors in the cerebellum of the stargazer mutant mouse. Immunohistochemistry was used to investigate, qualitatively, the distribution of the $GABA_A$ receptor subunits in the cerebellum of the stargazer mutant mouse and secondly to quantify the levels of expression of these subunits by semi-quantitative immunoblotting. The $C3B6Fe^+$ mouse strain was utilised in the current study, as opposed to the C57BL/6J strain used in initial studies, as the stargazer mouse strain is essentially raised on the $C3B6Fe^+$ background. This allowed us to determine whether the previously reported effects were due to mouse strain variability or as a consequence of the stargazer mutation.

3.2. RESULTS

3.2.1. Immunohistochemical mapping of $GABA_A$ receptor subunits in adult control (+/+:+/stg) and stargazer (stg/stg) cerebellum

Paraformaldehyde perfusion-fixed (4% w/v) horizontal and sagittal mouse brain sections (30 μm) were immunohistochemically stained by standard methods (see section 2.14), using GABAR subunit-specific antibodies, in order to map the distribution of each receptor subunit in control and stargazer cerebellum. For each antibody employed, a range of concentrations of primary antibody (0.125-2 μg/ml), were applied to a number of sections in order to determine the optimum concentration of antibody to achieve the optimal specific signal, with a minimum level of non-specific staining. (See table 2.3. for concentrations of antibody employed.) Controls performed included sections probed with secondary antibody only to determine non-specific binding of the secondary antibody and sections stained with diaminobenzidine (DAB) without primary or secondary antibodies to determine non-specific binding of DAB.

3.2.1.1. $GABA_A$ receptor subunit α1

Immunostaining for the GABAR α1 subunit was observed in all layers of the cerebellar structure to varying degrees, with the predominant immunoreactive staining found in the cerebellar granule cell and Purkinje cell layers (figure 3.1.). Weaker immunostaining was observed in the basket and stellate cells of the molecular layer. No qualitative difference in levels of immunostaining for the α1 subunit was detected in control and stargazer sections (n=5-8 sections from n=3 mice per strain).

3.2.1.2. $GABA_A$ receptor subunit α6

Intense immunoreactivity for the GABAR α6 subunit was observed in the cerebellar granule cell layer of the cerebellum in control brain sections. No specific immunostaining was detected in either the molecular or Purkinje cell

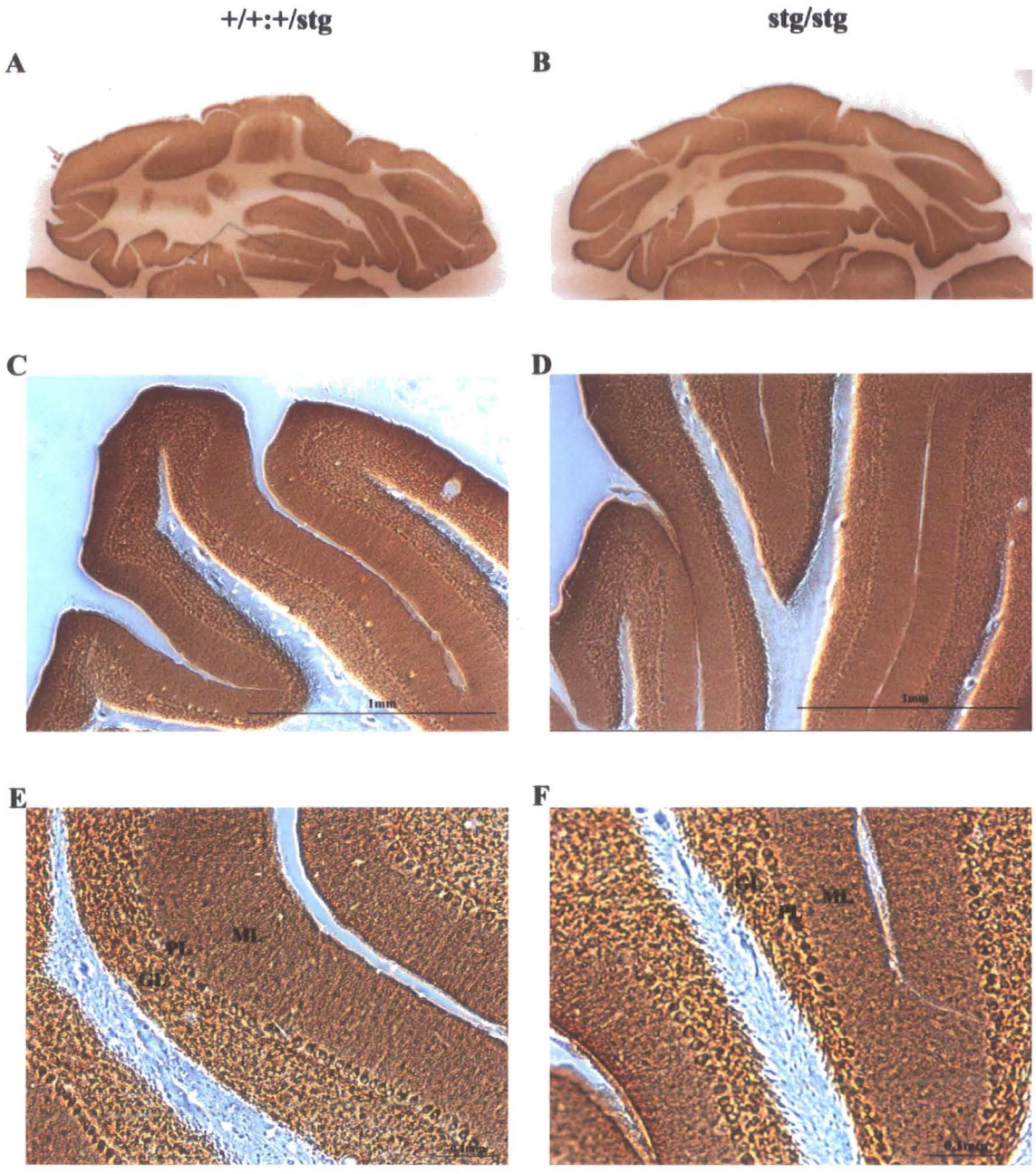

Figure 3.1. Immunohistochemical mapping of the $GABA_A$ receptor α1 subunit in adult mouse cerebellum

A&B: +/+:+/stg and stg/stg whole cerebella respectively
C&D: +/+:+/stg and stg/stg cerebella respectively at x40 magnification
E&F: +/+:+/stg and stg/stg cerebella respectively at x100 magnification

Note the intense staining in the granule cell layer (GL), Purkinje cell layer (PL) and the molecular layer (ML) in both control and stargazer cerebella.

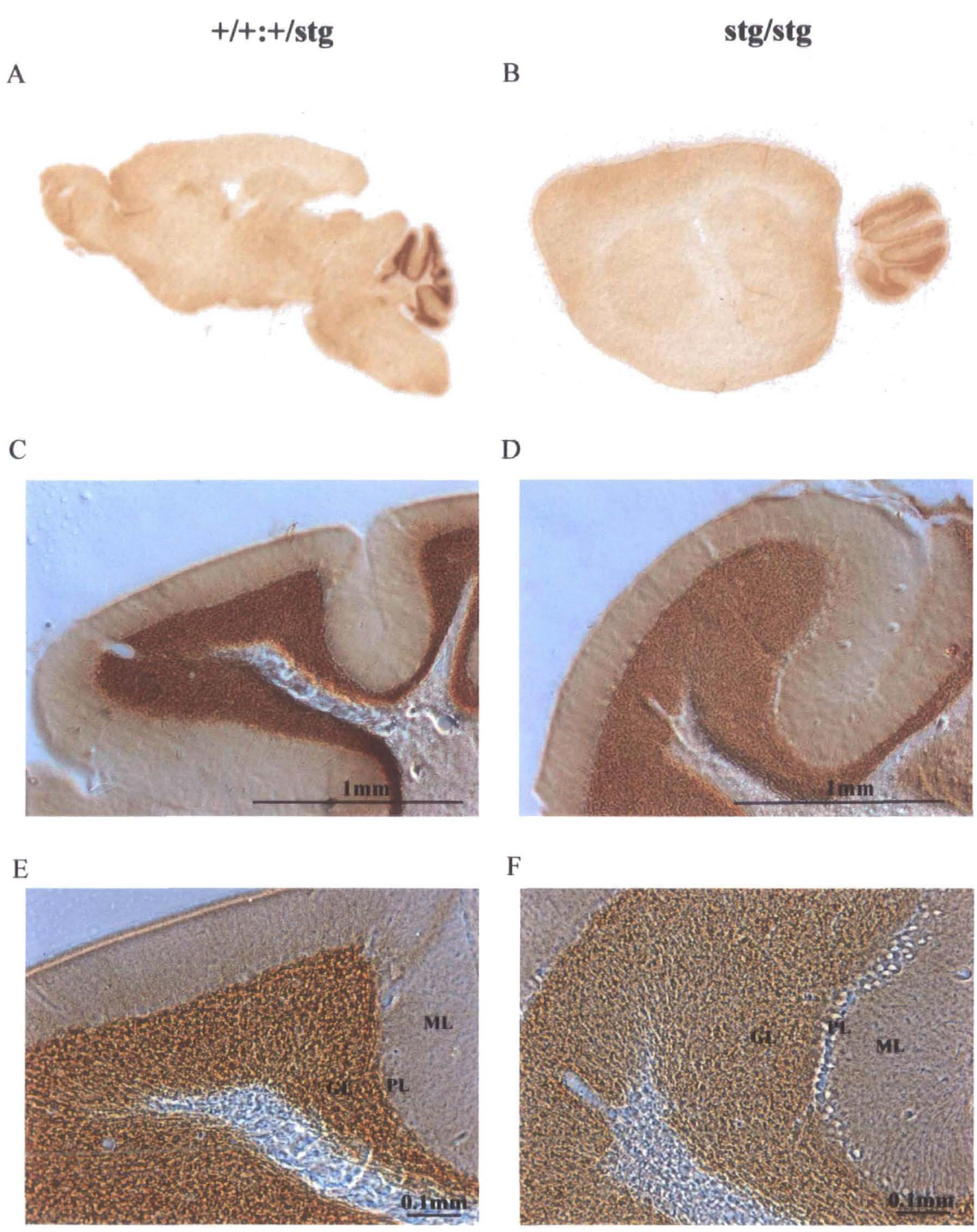

Figure 3.2. Immunohistochemical staining of $GABA_A$ receptor α6 subunit in adult mouse cerebellum

A&B: +/+:+/stg and stg/stg brain sections respectively at x40 magnification
C&D: +/+:+/stg and stg/stg brain sections respectively at x100 magnification

Note the decrease in intensity of staining in the granule cell layer (GL) of the stargazer tissue section. ML: Molecular Layer, PL: Purkinje Cell Layer.

layers. A dramatic decrease in immunostaining was noted in the cerebellar granule cell layer of stargazer sections when compared to controls, in all cerebellar folia (figure 3.2.) (n=5-8 from n=3 mice per strain)

3.2.1.3. $GABA_A$ receptor subunit β2

Strong immunoreactivity for the GABAR β2 subunit was observed in the cerebellar granule cell layer and to a lesser extent in the Purkinje cell layer and the basket and stellate cells of the molecular layer (n=5-8, from n=3 mice per strain). The level of immunostaining was greatly reduced uniformly in all cerebellar folia in stargazer tissue sections (figure 3.3.).

3.2.1.4. $GABA_A$ receptor subunit β3

Tissue sections probed with anti-GABAR β3 subunit specific antibody (0.5 μg/ml) displayed strong immunoreactivity in the cerebellar granule cell layer and to a lesser extent in the Bergmann glia cell bodies and processes in the molecular layer. No specific immunostaining was observed in the Purkinje cell layer (n=5-8 from n=3 mice per strain). The level of immunostaining was greatly reduced uniformly in all cerebellar folia in stargazer tissue sections when compared to control sections (figure 3.4.).

3.2.1.5. $GABA_A$ receptor subunit γ2

Various levels of immunostaining were observed in the cerebellar layers of control and stargazer tissue sections when probed with anti-GABAR γ2 subunit specific antibody (2 μg/ml). The most intense immunostaining was detected in the Purkinje cell layer, with strong immunoreactivity also in the granule cell layer and Purkinje cell dendrites of the molecular layer (n=5-8 from n=3 mice per strain). No obvious differences in intensity of staining were observed in control and stargazer sections (figure 3.5.)

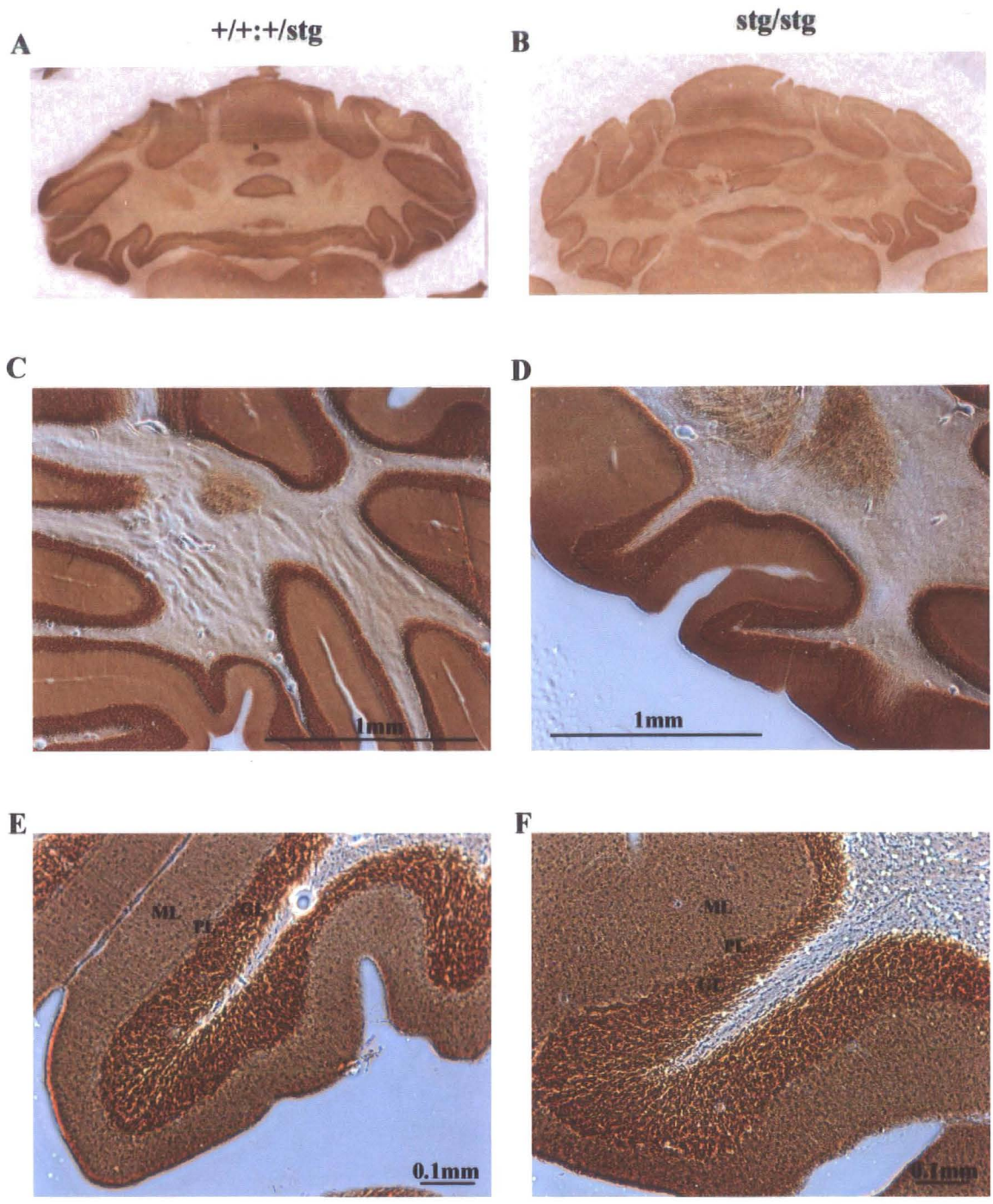

Figure 3.3. Immunohistochemical mapping of $GABA_A$ Receptor β2 Subunit in Adult Mouse Cerebellum

A&B: +/+:+/stg and stg/stg whole cerebella respectively
C&D: +/+:+/stg and stg/stg cerebella respectively at x40 magnification
E&F: +/+:+/stg and stg/stg cerebella respectively at x100 magnification

Note the reduction in staining in the granule cell layer (GL) of stargazer tissue sections. ML - Molecular Layer, PL - Purkinje Cell Layer

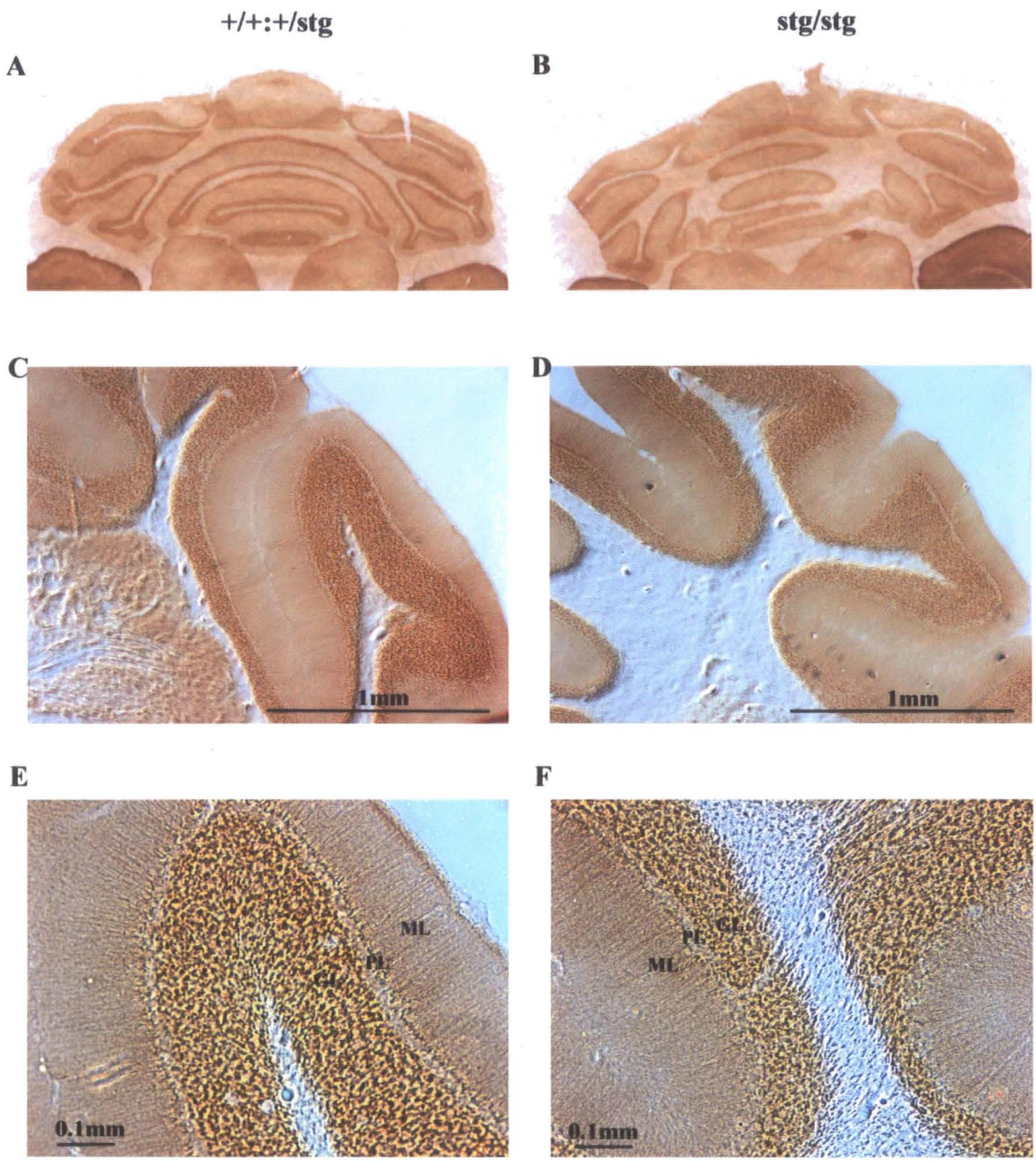

Figure 3.4. Immunohistochemical mapping of $GABA_A$ receptor β3 subunit in adult mouse cerebellum

A&B: +/+:+/stg and stg/stg whole cerebella respectively
C&D: +/+:+/stg and stg/stg cerebella respectively at x40 magnification
E&F: +/+:+/stg and stg/stg cerebella respectively at x100 magnification

Note the reduction in intensity of staining in the granule cell layer (GL) in the stg/stg cerebellum. ML: Molecular Layer, PL: Purkinje Cell Layer

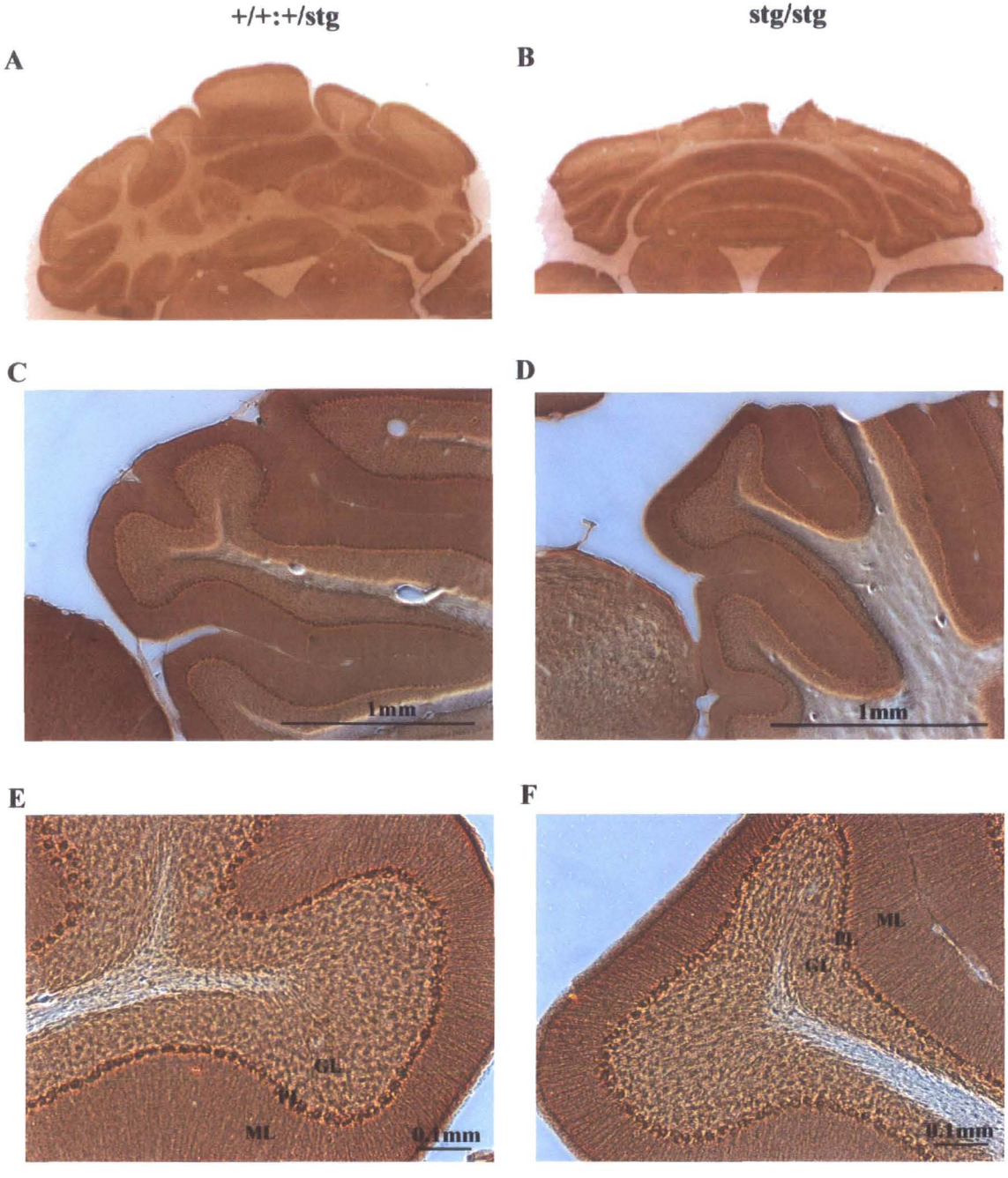

Figure 3.5. Immunohistochemical mapping of the $GABA_A$ receptor γ2 subunit in adult mouse cerebellum

A&B: +/+:+/stg and stg/stg whole cerebella respectively
C&D: +/+:+/stg and stg/stg cerebella respectively at x40 magnification
E&F: +/+:+/stg and stg/stg cerebella respectively at x100 magnification

Note the intense staining in the Purkinje cell layer (PL) and to a lesser extent in the granule cell layer (GL) and molecular layer (ML).

3.2.1.6. $GABA_A$ receptor subunit δ

Tissue sections probed for the localisation of the GABAR δ subunit (0.25 μg/ml) demonstrated the most intense immunoreactivity in the cerebellar granule cell layer, with no specific immunostaining present in the Purkinje cell or molecular layers. The level of immunostaining was dramatically reduced in the stargazer tissue sections when compared to controls (n=5-8 from n=3 mice per strain) (figure 3.6.).

The distribution of GABAR subunits studied were as expected from previous observations (Pirker *et al.*, 2000) and were compatible in both +/+:+/stg and stg/stg. However, immunohistochemical staining revealed an overall qualitative decrease in the expression of the GABAR subunits α6, β2, β3 and δ uniformly in all cerebella folia of the stargazer cerebellum.

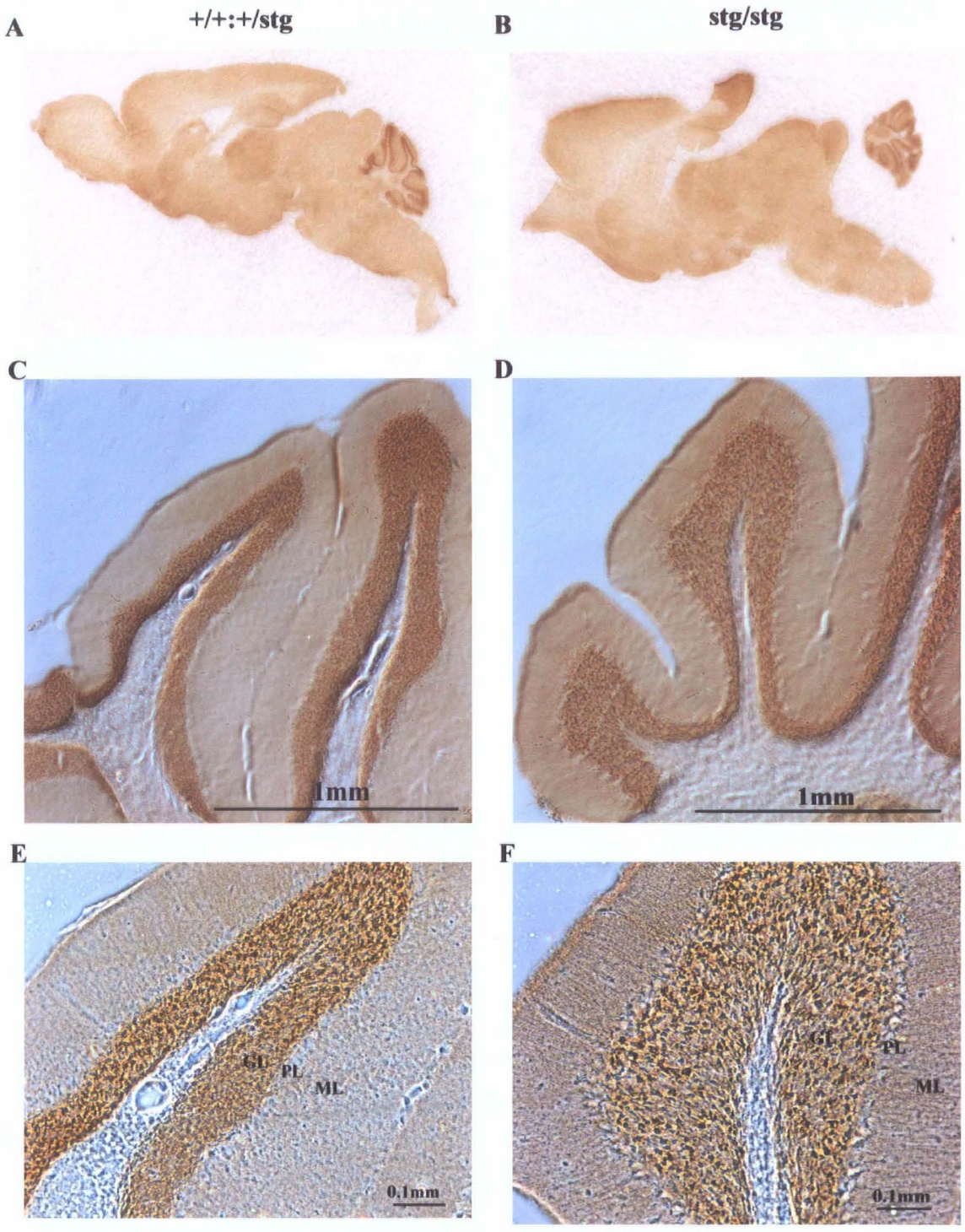

Figure 3.6. Immunohistochemical mapping of the $GABA_A$ receptor δ subunit in adult mouse cerebellum

A&B: Whole brain sections for +/+:+/stg and stg/stg mice respectively
C&D: +/+:+/stg and stg/stg cerebella respectively at x40 magnification
E&F: +/+:+/stg and stg/stg cerebella respectively at x100 magnification
Note the decrease in intensity of staining in the granule cell layer (GL) of the stg/stg cerebellum. ML: Molecular Layer, PL: Purkinje Cell Layer

Table 3.1. Immunohistochemical mapping of GABAR subunits in the adult mouse cerebellum

GABAR SUBUNIT	PURKINJE CELL LAYER		GRANULE CELL LAYER		MOLECULAR LAYER								STAINING INTENSITY IN STARGAZER SECTIONS COMPARED TO CONTROLS
	Purkinje cell bodies		Granule cells		Basket cells		Stellate cells		Bergmann glial cell bodies		Bergmann glial cell processes		
	+/+:+/stg	stg/stg	+/+:+/stg	stg/stg	+/+:+/stg	stg/stg	+/+:+/stg	stg/stg	+/+:+/stg	stg/stg	+/+:+/stg	stg/stg	
α1	+++	+++	+++	+++	++	++	++	++	-	-	-	-	=
α6	-	-	+++	+	-	-	-	-	-	-	-	-	↓↓
β2	+	+	++	+	+	+	+	+	-	-	-	-	↓
β3	-	-	++	+	-	-	-	-	++	++	+	+	↓
γ2	+++	+++	++	++	+	+	-	-	+	+	-	-	=
δ	-	-	+++	+	-	-	-	-	-	-	-	-	↓↓

+: Weak staining ++: Moderate staining +++: Strong staining -: No specific staining

3.2.2. Quantitative comparison of the expression of $GABA_A$ receptor subunits in adult mouse cerebellum by semi-quantitative immunoblotting

For each GABAR subunit to be studied, a range of protein concentrations of control and stargazer cerebellar membranes (0.125-10 μg) were subjected to immunoblotting and signals detected by the enhanced chemiluminescence (ECL) system. Immunoblots were exposed to hyperfilm ECL for most commonly 30 seconds, 1 minute and 2 minutes. The resultant immunoreactive bands were quantified by computer-assisted densitometry using ImageJ software in order to determine within which range of protein amounts the level of signal achieved was linear, i.e. the signal doubled when double the amount of protein was loaded. An amount of control and stargazer protein which fell within the linear range for each antibody was then loaded on subsequent sodium dodecyl sulphate-polyacrylamide gel electrophoresis (SDS-PAGE) gels to compare three separate control cerebella with three stargazer cerebella (see section 2.10.).

In order to normalise for the exact levels of protein loaded per SDS-PAGE gel and allow for the direct comparison of separate cerebella, the linear range forβ-actin was determined. A β-actin value for each separate control and stargazer cerebellum was determined in order to report the expression levels of each subunit as a ratio of protein of interest:β-actin signal.

3.2.2.1. $GABA_A$ receptor subunit α1

The linear range of protein for the GABAR α1 subunit was determined to lie between 2.5 and 5 μg for control cerebella and between 5 and 10 μg for stargazer cerebella (see figure 3.7.). Therefore, a comparison of 5 μg of each control and stargazer cerebellum was made by semi-quantitative immunoblotting using anti-α1-subunit specific antibody at 3 μg/ml.

No significant difference in the expression levels of the GABAR α1 subunit was observed between control and stargazer cerebella.

Figure 3.7. Determination of the linear range for cerebellar expression levels of $GABA_A$ receptor α1 subunit in control (+/+:+/stg) and stargazer (stg/stg) mutant mice

A: Western blot analysis of serially diluted +:+/+/stg and stg/stg cerebellar membrane homogenates probed with anti-GABAR α1 subunit antibody at a concentration of 1 μg/ml. n=3, immunnoblotting repeated twice.

B: Line graph showing the increasing intensity of immunoreactive band with increasing protein concentration by western blotting, quantified using ImageJ software (see section 2.10.5). Dotted lines indicate the linear range for +/+:+/stg and stg/stg membrane homogenates. The circled protein concentrations were used for subsequent comparison of control and stargazer cerebellar membranes.

A

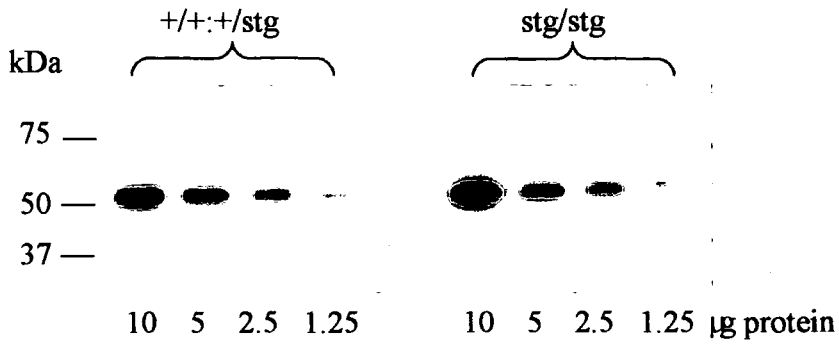
+/+:+/stg
stg/stg
kDa
75
50
37
10 5 2.5 1.25
10 5 2.5 1.25 µg protein

B

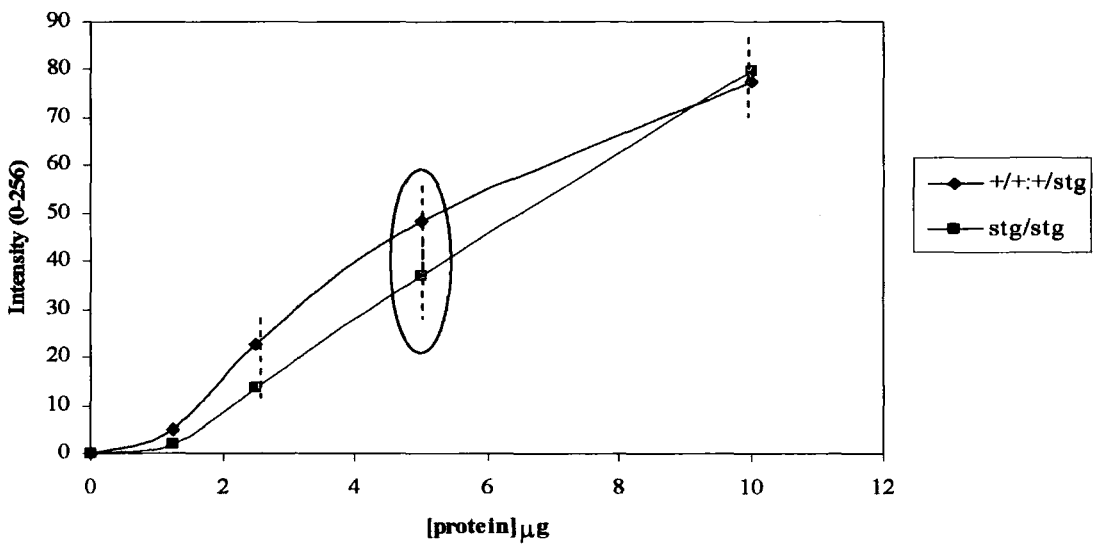
Intensity (0-256)
90
80
70
60
50
40
30
20
10
0
0 2 4 6 8 10 12
[protein] µg
+/+:+/stg
stg/stg

Figure 3.8. Quantification of cerebellar expression levels of GABAR α1 subunit in control (+/+:+/stg) and stargazer (stg/stg) mice

A: Western blot analysis of three control and three stargazer cerebella probed with anti-GABAR α1 subunit antibody at a concentration of 3 μg/ml.

B: Bar graph illustrating the relative levels of α1 subunit expression in control and stargazer cerebellum, expressed as a ratio of α1/β-actin. Values are mean ± SEM of n=3, immunoblotting repeated twice. Results indicate no significant reduction in α1 subunit expression in the stargazer cerebellum compared to control levels as determined by student's *t*-test (p=0.062).

A

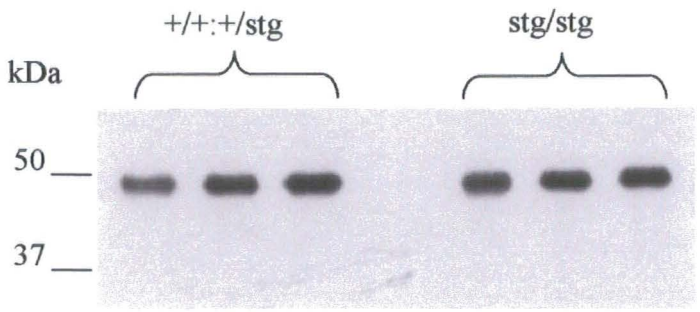

B

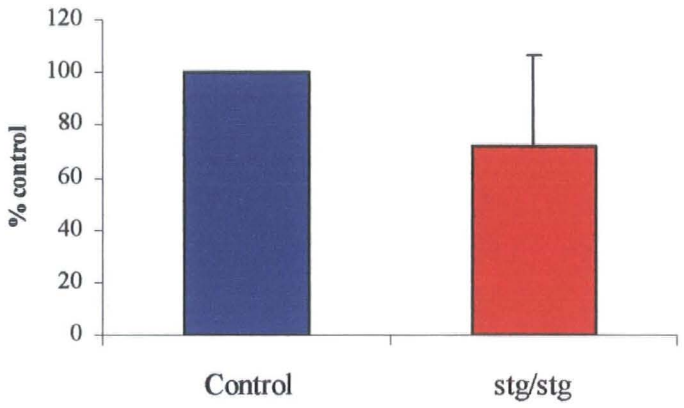

	Average ratio α1/actin	Percentage of control	P value
+/+:+/stg	0.89 ± 0.30	100	0.062
stg/stg	0.64 ± 0.06	72 ± 34	

Stargazer levels were determined to be 72 ± 34% of control levels (mean ± SEM, n=3, p=0.062) (figure 3.8.).

3.2.2.2. $GABA_A$ receptor subunit α6

The linear range for the GABAR α6 subunit was calculated to be between 2.5 and 5 μg protein for both control and stargazer cerebella (figure 3.9.). Hence, 5 μg of each control and stargazer cerebellum was compared by immunoblotting, probed with anti-GABAR α6 subunit specific antibody at 2 μg/ml.

Figure 3.10. demonstrates a dramatic reduction in the expression levels of the α6 subunit in the stargazer cerebellum to 39 ± 22% of control levels (n=3, p=0.013).

3.2.2.3. $GABA_A$ receptor subunit β2

Figure 3.11. summarises the western blot analysis conducted on serially diluted control and stargazer cerebella probed with anti-GABAR β2 subunit specific antibody at 0.5 μg/ml. The linear range for both control and stargazer cerebella was found to lie between 5 and 10 μg. Therefore, 5 μg of protein for each cerebellum was analysed by immunoblotting.

A significant reduction in the expression of the β2 subunit was found in stargazer cerebellum, to 45 ± 42% of control levels (p=0.012, n=3) (figure 3.12.).

3.2.2.4. $GABA_A$ receptor subunit β3

The linear range for the GABAR β3 subunit was found to lie between 2.5 and 5 μg protein for control cerebella and between 5 and 10 μg protein for stargazer tissue (figure 3.13). 5 μg protein of each cerebellum was analysed by western blotting, probed with anti-GABAR β3 subunit specific antibody at 0.5 μg/ml.

Figure 3.9. Determination of the linear range for cerebellar expression levels of $GABA_A$ receptor α6 subunit in control (+/+:+/stg) and stargazer (stg/stg) mutant mice.

A: Western blot analysis of serially diluted +:+/+/stg and stg/stg cerebellar membrane homogenates probed with anti-GABAR α6 subunit antibody at a concentration of 1 μg/ml. Arrow indicates GABAR α6 immunoreactive band. n=3, immunoblotting repeated twice. The immunoreactive band corresponding to the GABAR α6 subunit was identified by screening adult mouse forebrain membranes and GABAR α6 subunit immunopurified material by western blotting. The anti-GABAR α6 subunit antibody recognised only one band in the GABAR α6 subunit purified material of ~56 kDa, corresponding to the α6 subunit (data not shown).
B: Line graph showing the increasing intensity of immunoreactive band with increasing protein concentration by western blotting, quantified using ImageJ software (see section 2.10.5). Dotted lines indicate the linear range for +/+:+/stg and stg/stg membrane homogenates. The circled protein concentrations were used for subsequent comparison of control and stargazer cerebellar membranes.

A

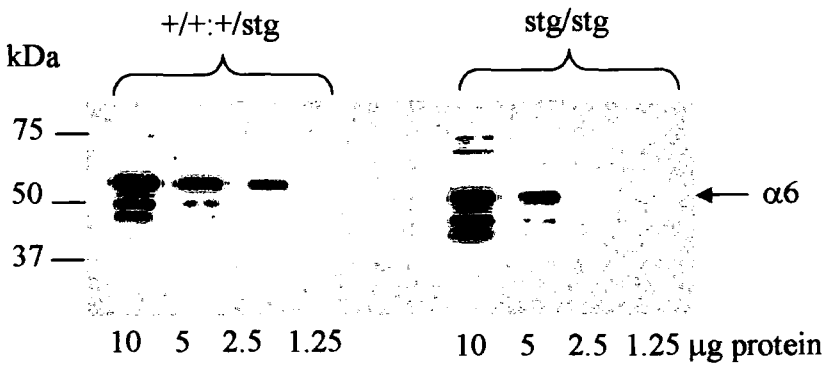
+/+:+/stg
stg/stg
kDa
75
50
37
α6
10 5 2.5 1.25
10 5 2.5 1.25 µg protein

B

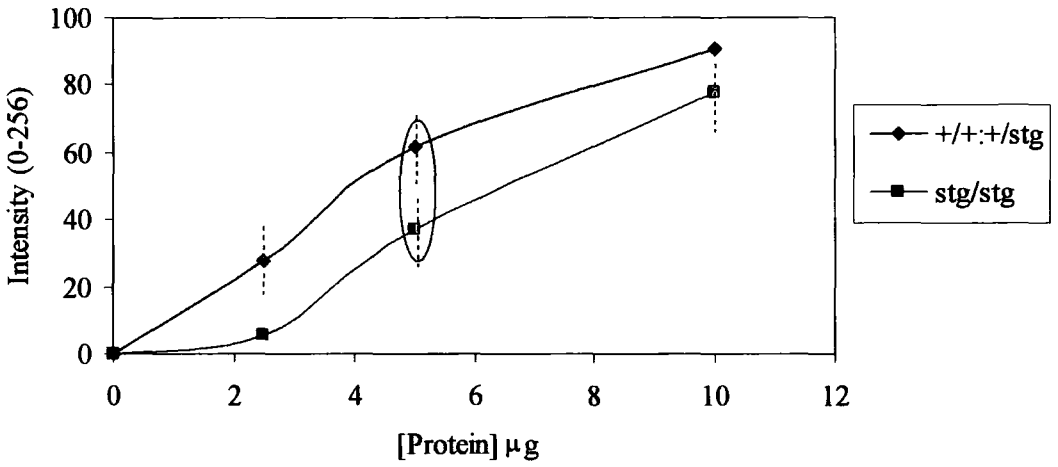
Intensity (0-256)
100
80
60
40
20
0
0 2 4 6 8 10 12
[Protein] µg
+/+:+/stg
stg/stg

Figure 3.10. Quantification of cerebellar expression levels of GABAR α6 subunit in control (+/+:+/stg) and stargazer (stg/stg) mice

A: Western blot analysis of three control and three stargazer cerebella probed with anti-GABAR α6 subunit antibody at a concentration of 1 μg/ml. Arrow indicates GABAR α6 immunoreactive band.
B: Bar graph illustrating the relative levels of α6 subunit expression in control and stargazer cerebellum, expressed as a ratio of α6/β-actin. Values are mean ± SEM of n=3, immunoblotting repeated twice. Results indicate a significant reduction in α6 subunit expression in the stargazer cerebellum to 39 ± 22% of control levels as determined by student's *t*-test ($p=0.013$).

A

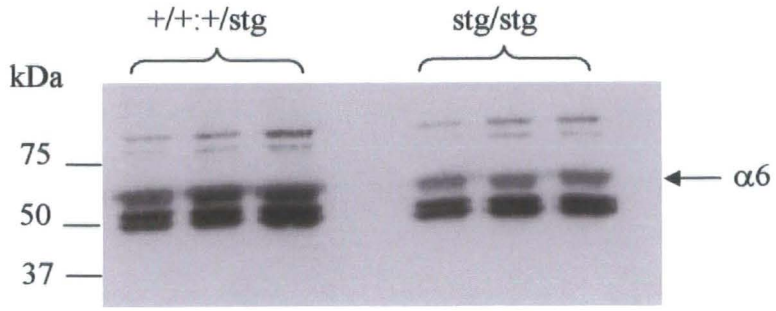

B

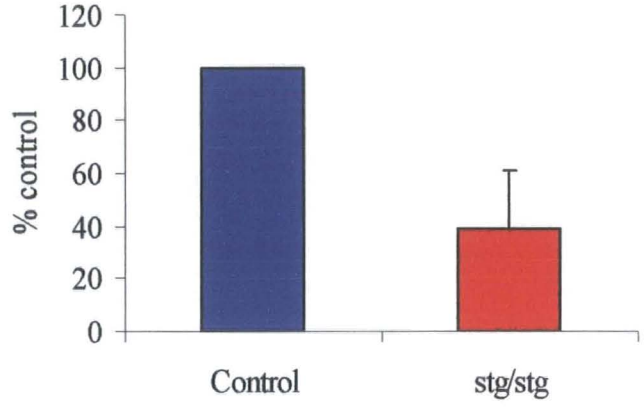

C

	Average ratio α6/actin	Percentage of control	P value
+/+:+/stg	1.35 ± 0.29	100	0.013
stg/stg	0.52 ± 0.07	39 ± 22	

Figure 3.11. Determination of the linear range for cerebellar expression levels of $GABA_A$ receptor β2 subunit in control (+/+:+/stg) and stargazer (stg/stg) mutant mice.

A: Western blot analysis of serially diluted +:+/+/stg and stg/stg cerebellar membrane homogenates probed with anti-GABAR β2 subunit antibody at a concentration of 0.5 μg/ml. n=3, immunoblotting repeated twice.

B: Line graph showing the increasing intensity of immunoreactive band with increasing protein concentration by western blotting, quantified using ImageJ software (see section 2.10.5). Dotted lines indicate the linear range for +/+:+/stg and stg/stg membrane homogenates. The circled protein concentrations were used for subsequent comparison of control and stargazer cerebellar membranes.

A

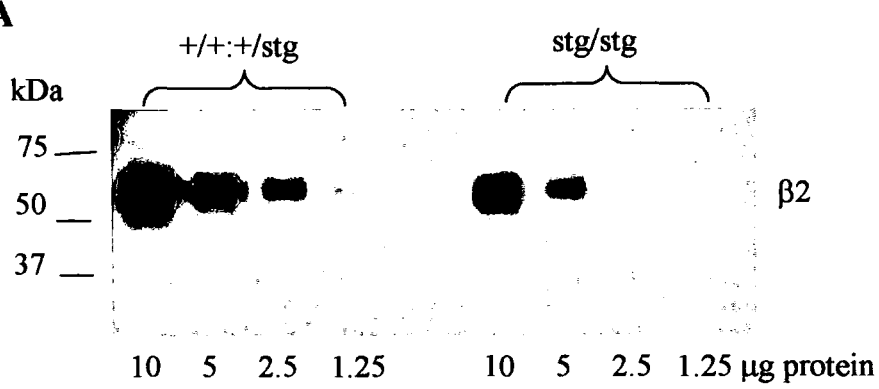
+/+:+/stg
stg/stg
kDa
75
50
37
β2
10 5 2.5 1.25
10 5 2.5 1.25 µg protein

B

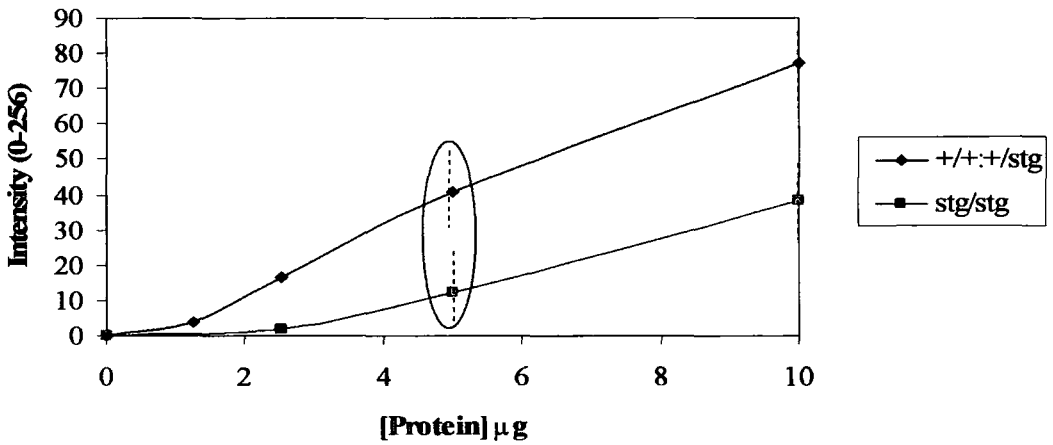
Intensity (0-256)
90
80
70
60
50
40
30
20
10
0
0 2 4 6 8 10
[Protein] µg
+/+:+/stg
stg/stg

Figure 3.12. Quantification of cerebellar expression levels of GABAR β2 subunit in control (+/+:+/stg) and stargazer (stg/stg) mice

𝔸: Western blot analysis of three control and three stargazer cerebella probed with anti-GABAR β2 subunit antibody at a concentration of 0.5 μg/ml.

𝔹: Bar graph illustrating the relative levels of β2 subunit expression in control and stargazer cerebellum, expressed as a ratio of β2/β-actin. Values are mean ± SEM of n=3, immunoblotting repeated twice. Results indicate a significant reduction in β2 subunit expression in the stargazer cerebellum to 45 ± 42% of control levels as determined by student's *t*-test (p=0.012).

A

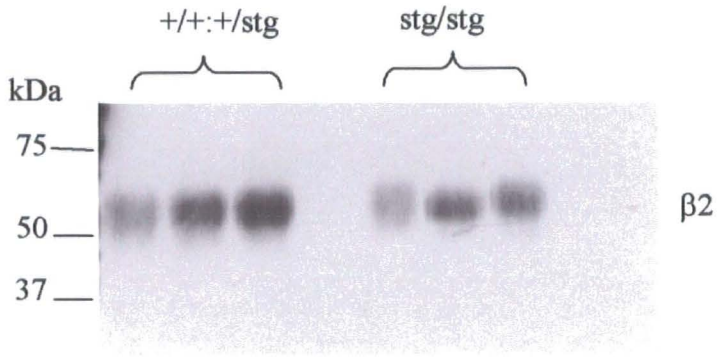

B

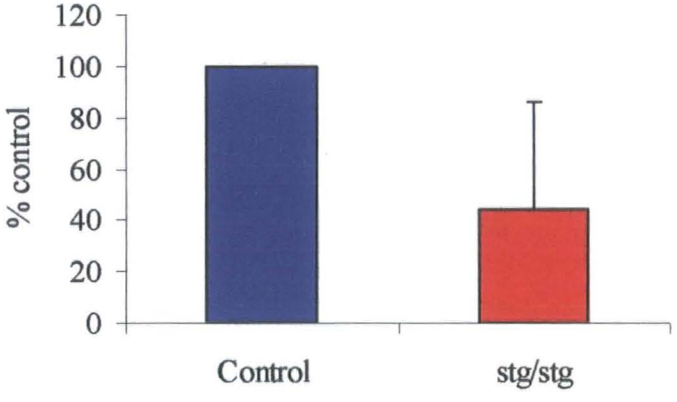

	Average ratio β2/actin	Percentage of control	P value
+/+:+/stg	0.71 ± 0.29	100	0.012
stg/stg	0.32 ± 0.09	45 ± 42	

Figure 3.13. Determination of the linear range for cerebellar expression levels of $GABA_A$ receptor β3 subunit in control (+/+:+/stg) and stargazer (stg/stg) mutant mice.

A: Western blot analysis of serially diluted +:+/+/stg and stg/stg cerebellar membrane homogenates probed with anti-GABAR β3 subunit antibody at a concentration of 0.5 μg/ml. n=3, immunoblotting repeated twice.

B: Line graph showing the increasing intensity of immunoreactive band with increasing protein concentration by western blotting, quantified using ImageJ software (see section 2.10.5). Dotted lines indicate the linear range for +/+:+/stg and stg/stg membrane homogenates. The circled protein concentrations were used for subsequent comparison of control and stargazer cerebellar membranes.

A

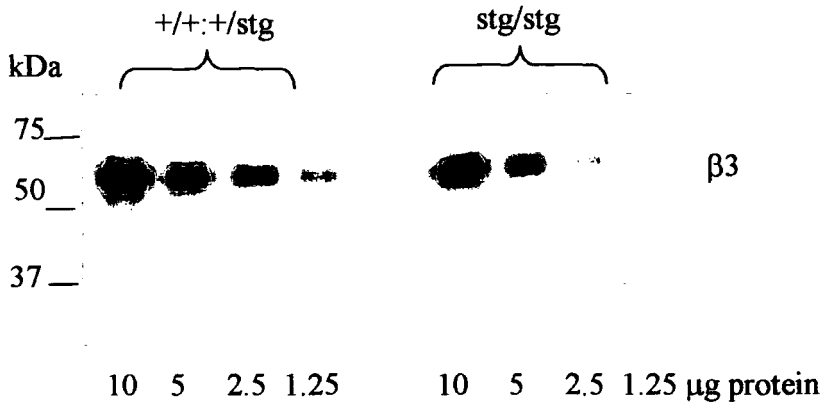
+/+:+/stg
stg/stg
kDa
75
50
37
β3
10 5 2.5 1.25
10 5 2.5 1.25 µg protein

B

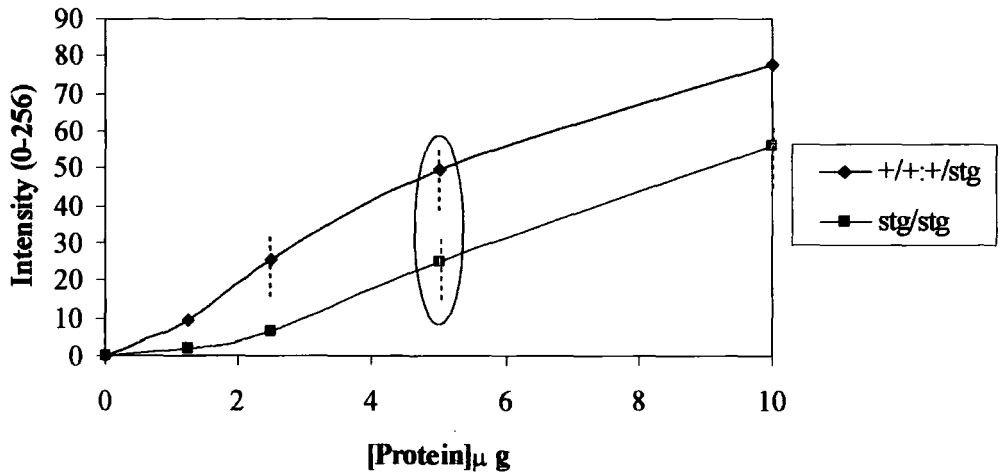
Intensity (0-256)
90
80
70
60
50
40
30
20
10
0
0 2 4 6 8 10
[Protein]µ g
+/+:+/stg
stg/stg

Figure 3.14. Quantification of cerebellar expression levels of GABAR β3 subunit in control (+/+:+/stg) and stargazer (stg/stg) mice

A: Western blot analysis of three control and three stargazer cerebella probed with anti-GABAR β3 subunit antibody at a concentration of 0.5 μg/ml.

B: Bar graph illustrating the relative levels of β3 subunit expression in control and stargazer cerebellum, expressed as a ratio of β3/β-actin. Values are mean ± SEM of n=6, immunoblotting repeated twice. Results indicate no significant reduction in β3 subunit expression in the stargazer cerebellum compared to control levels as determined by student's *t*-test (p=0.284).

A

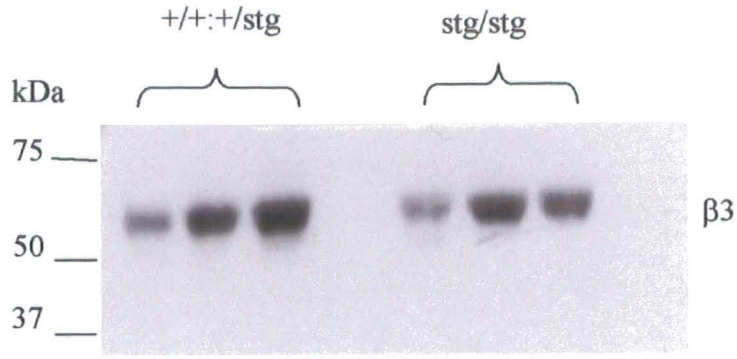

B

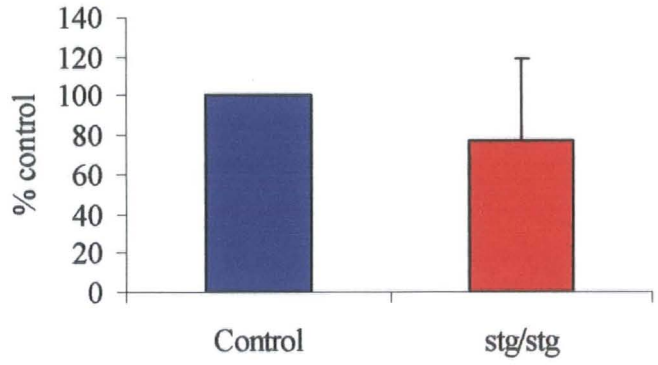

	Average ratio β3/actin	Percentage of control	P value
+/+:+/stg	0.93 ± 0.36	100	0.284
stg/stg	0.60 ± 0.15	77 ± 42	

Direct comparison of control and stargazer cerebella revealed no significant decrease in the expression levels of the β3 subunit in the stargazer mutant when compared to controls (77 ± 42% of control levels, n=6, p=0.283) (figure 3.14).

3.2.2.5. $GABA_A$ receptor subunit γ2

Figure 3.15 shows an example of a western blot performed in order to determine the range of cerebellar protein to be applied such that the GABAR γ2 subunit immunoreactive signal was in the quantitative range for control and stargazer cerebellum. The linear range was determined to be between 5 and 10 μg protein for both control and stargazer cerebella. Hence, 5 μg cerebellar protein was applied to subsequent immunoblots enabling the comparison of γ2 subunit expression between the two mouse strains.

No significant difference in γ2 subunit expression was observed in stargazer cerebellum (81 ± 26% of control levels, p=0.06, n=6) relative to controls (100%) (figure 3.16).

3.2.2.6. $GABA_A$ receptor subunit δ

The linear range for the GABAR δ subunit was determined to lie between 5 and 10 μg protein for both control and stargazer cerebella (figure 3.17.). 10 μg protein was employed for the direct comparison of GABAR δ subunit expression.

Figure 3.18. demonstrates the dramatic reduction in the expression of the δ subunit (Mr 54 000 Da) observed in stargazer cerebellum compared to control (36 ± 21%, p=0.011, n=3). A further immunoreactive band was observed with a molecular weight (Mr) of ~70 000 Da. This probably represents a non-δ subunit cross-reactive protein, since it was not observed on purified α6-δ subunit-containing GABARs (data not shown).

Figure 3.15. Determination of the linear range for cerebellar expression levels of $GABA_A$ receptor γ2 subunit in control (+/+:+/stg) and stargazer (stg/stg) mutant mice.

A: Western blot analysis of serially diluted +:+/+/stg and stg/stg cerebellar membrane homogenates probed with anti-GABAR γ2 subunit antibody at a concentration of 2 μg/ml. n=3, immunoblotting repeated twice.

B: Line graph showing the increasing intensity of immunoreactive band with increasing protein concentration by western blotting, quantified using ImageJ software (see section 2.10.5). Dotted lines indicate the linear range for +/+:+/stg and stg/stg membrane homogenates. The circled protein concentrations were used for subsequent comparison of control and stargazer cerebellar membranes.

A

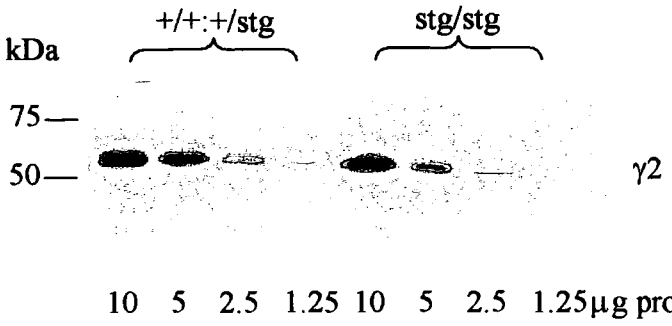
+/+:+/stg
stg/stg
kDa
75
50
γ2
10 5 2.5 1.25 10 5 2.5 1.25µg protein

B

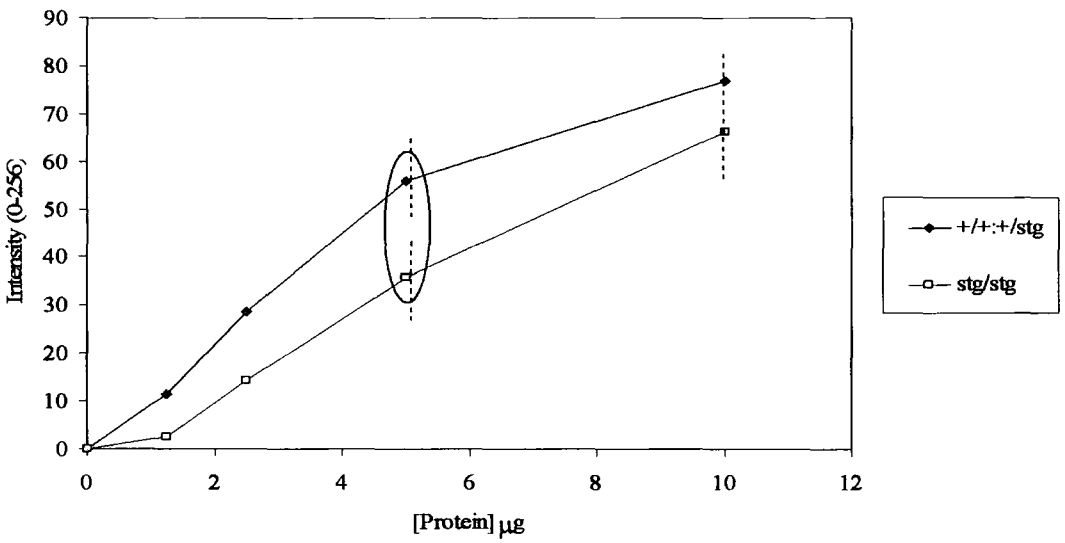
Intensity (0-256)
90
80
70
60
50
40
30
20
10
0
0 2 4 6 8 10 12
[Protein] µg
+/+:+/stg
stg/stg

Figure 3.16. Quantification of cerebellar expression levels of GABAR γ2 subunit in control (+/+:+/stg) and stargazer (stg/stg) mice

A: Western blot analysis of three control and three stargazer cerebella probed with anti-GABAR γ2 subunit antibody at a concentration of 2 μg/ml.

B: Bar graph illustrating the relative levels of γ2 subunit expression in control and stargazer cerebellum, expressed as a ratio of γ2/β-actin. Values are mean ± SEM of n=3 with immunoblotting repeated twice. Results indicate a significant reduction in γ2 subunit expression in the stargazer cerebellum to 81 ± 26% of control levels as determined by student's *t*-test (p=0.06).

A

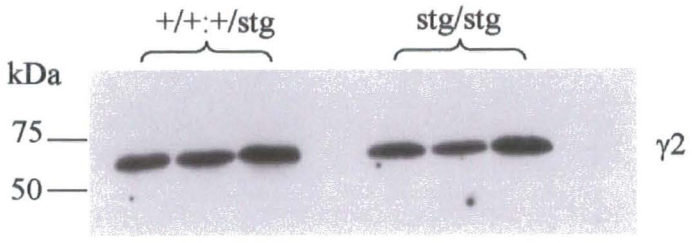

B

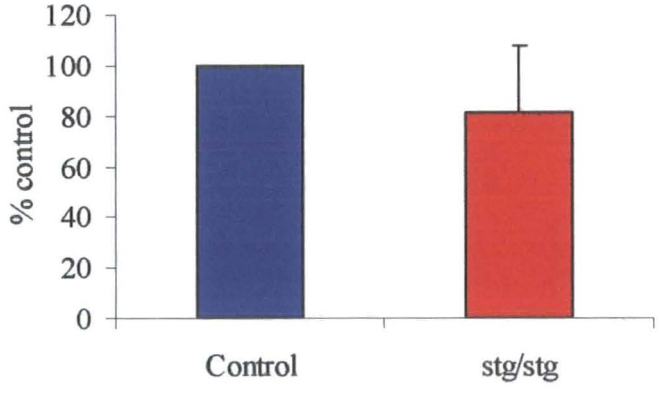

C

	Average ratio γ2/actin	Percentage of control	P value
+/+:+/stg	1.02 ± 0.19	100	0.06
stg/stg	0.83 ± 0.18	81 ± 26	

Figure 3.17. Determination of the linear range for cerebellar expression levels of $GABA_A$ receptor δ subunit in control (+/+:+/stg) and stargazer (stg/stg) mutant mice.

A: Western blot analysis of serially diluted +:+/+/stg and stg/stg cerebellar membrane homogenates probed with anti-GABAR δ subunit antibody at a concentration of 1 μg/ml. Arrow indicates GABAR δ immunoreactive band. n=3, immunoblotting repeated twice.
B: Line graph showing the increasing intensity of immunoreactive band with increasing protein concentration by western blotting, quantified using ImageJ software (see section 2.10.5). Dotted lines indicate the linear range for +/+:+/stg and stg/stg membrane homogenates. The circled protein concentrations were used for subsequent comparison of control and stargazer cerebellar membranes.

A

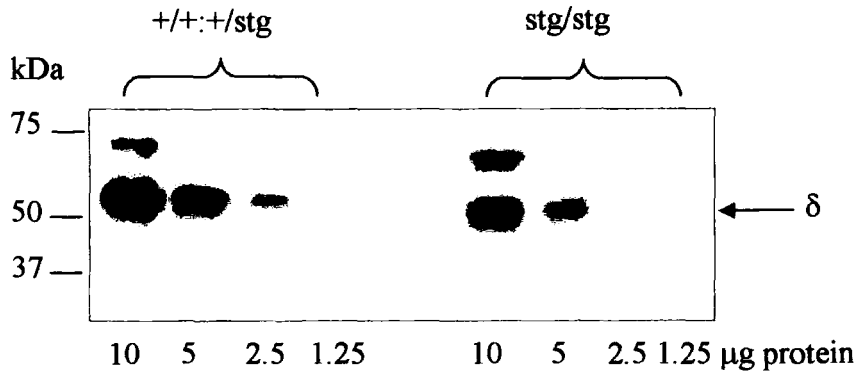
+/+:+/stg
stg/stg
kDa
75
50
37
δ
10 5 2.5 1.25 10 5 2.5 1.25 µg protein

B

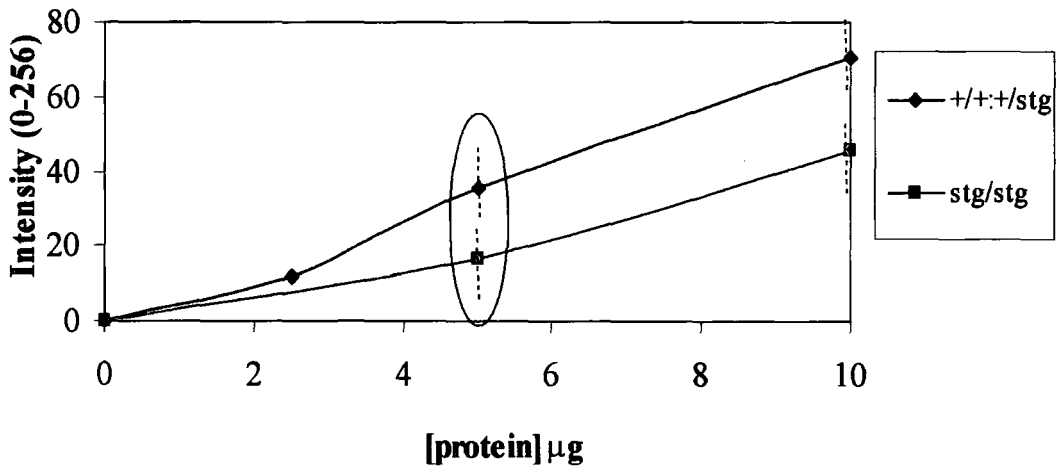
Intensity (0-256)
80
60
40
20
0
0 2 4 6 8 10
[protein] µg
+/+:+/stg
stg/stg

Figure 3.18. Quantification of cerebellar expression levels of GABAR δ subunit in control (+/+:+/stg) and stargazer (stg/stg) mice

A: Western blot analysis of three control and three stargazer cerebella probed with anti-GABAR δ subunit antibody at a concentration of 1 μg/ml. Arrow indicates GABAR δ immunoreactive band.
B: Bar graph illustrating the relative levels of δ subunit expression in control and stargazer cerebellum, expressed as a ratio of δ/β-actin. Values are mean ± SEM of n=3, immunoblotting repeated twice. Results indicate a significant reduction in δ subunit expression in the stargazer cerebellum to 36 ± 21% of control levels as determined by student's *t*-test (p=0.011).

A

B

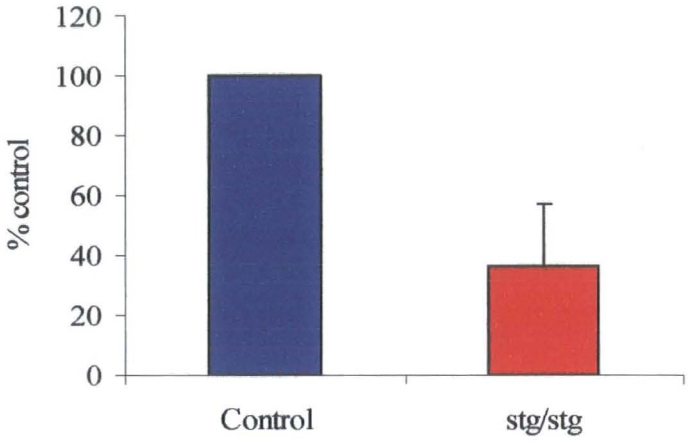

	Average ratio δ/actin	**Percentage of control**	**P value**
+/+:+/stg	1.37 ± 0.29	100	0.011
stg/stg	0.49 ± 0.05	36 ± 21	

Table 3.2. Quantitative comparison of GABAR subunit expression in adult control and stargazer cerebellum

GABAR SUBUNIT	CONTROL EXPRESSION LEVELS	STARGAZER EXPRESSION LEVELS AS PERCENTAGE OF CONTROL (MEAN ± SEM)	P VALUE
α1	100	72 ± 34	0.062
α6	100	39 ± 22	*0.013
β2	100	45 ± 42	*0.012
β3	100	77 ± 42	0.283
γ2	100	81 ± 26	0.06
δ	100	36 ± 21	*0.011

*statistically significant $p<0.05$.

Table 3.2. summarises, the expression levels of the GABAR subunits in the stargazer cerebellum. The α6, β2 and δ subunits were found to be significantly reduced in the stargazer cerebellum by semi-quantitative immunoblotting.

3.2.3. Zolpidem displacement of [^{3}H] Ro15-4513 binding to control and stargazer cerebellar membranes

Previous studies have implied that GABAR abnormalities in the cerebellum of stargazer mutant mice may result from compromised maturation of this brain region. The aim here is to determine whether GABARs undergo developmental transition expected in a normal maturing cerebellum-characterised by type II to type I transformation.

Zolpidem displacement of [^{3}H] Ro15-4513 binding (10 nM) to control and stargazer cerebellar membranes was conducted to determine the relative

proportion of type I and/or type II binding that may comprise the specific benzodiazepine-sensitive (BZ-S) subtype of binding sites. Type I pharmacology is indicative of expression of $\alpha 1\beta\gamma 2$ receptors, present in the adult cerebellum. Type II pharmacology is conferred by the $\alpha 2\beta\gamma 2$, $\alpha 3\beta\gamma 2$ and $\alpha 5\beta\gamma 2$ subunit-containing receptors, the predominant subtype expressed in the developing cerebellum (see section 1.2.5.).

Competitive displacement of [^{3}H] Ro15-4513 binding sites (10 nM) with zolpidem at concentrations of 1 nM to 10 μM revealed no difference in the type of binding sites present in control and stargazer cerebellar membranes. [^{3}H] Ro15-4513 binding to BZ-S binding sites was completely displaced by zolpidem with an IC_{50} of 40 nM and 42 nM for control and stargazer membranes respectively, consistent with type I pharmacology (see figure 3.19.)

3.3. DISCUSSION

The aim of this chapter was to re-evaluate and extend the previous studies that had shown that $GABA_A$ receptor subunit expression was compromised in the stargazer mutant mouse (Thompson *et al.*, 1998, Chen *et al.*, 1999).

3.3.1. Qualitative differences in GABAR subunit distributions in the stargazer mutant, determined by immunohistochemical studies

Immunohistochemical studies were conducted using subunit-specific antibodies to determine the cellular distribution of the $GABA_A$ receptor subunits in adult control and stargazer mouse cerebella.

The immunostaining observed matched previously described distributions for each of the $GABA_A$ receptor subunits in the cerebellum (Pirker *et al.*, 2000). GABAR $\alpha 1$ subunit immunoreactivity was observed in all layers of the cerebellar structure to varying degrees, with the predominant immunoreactivity in the cerebellar granule cell (CGC) and Purkinje cell layers.

Figure 3.19. Zolpidem displacement of [^{3}H] Ro15-4513 binding to adult control (+/+:+/stg) and stargazer (stg/stg) cerebellar membrane homogenates

Zolpidem displacement (half log concentrations ranging from 1 nM to 10 μM) of [^{3}H] Ro15-4513 binding (10 nM) to control and stargazer cerebellar membranes. n=3 measurements per zolpidem concentration, 10 cerebella per mouse strain. Data best fit a one-site binding model with calculated Hill coefficients (n_H) of -0.82 ± 0.07 and -0.85 ± 0.19 for control and stargazer respectively.

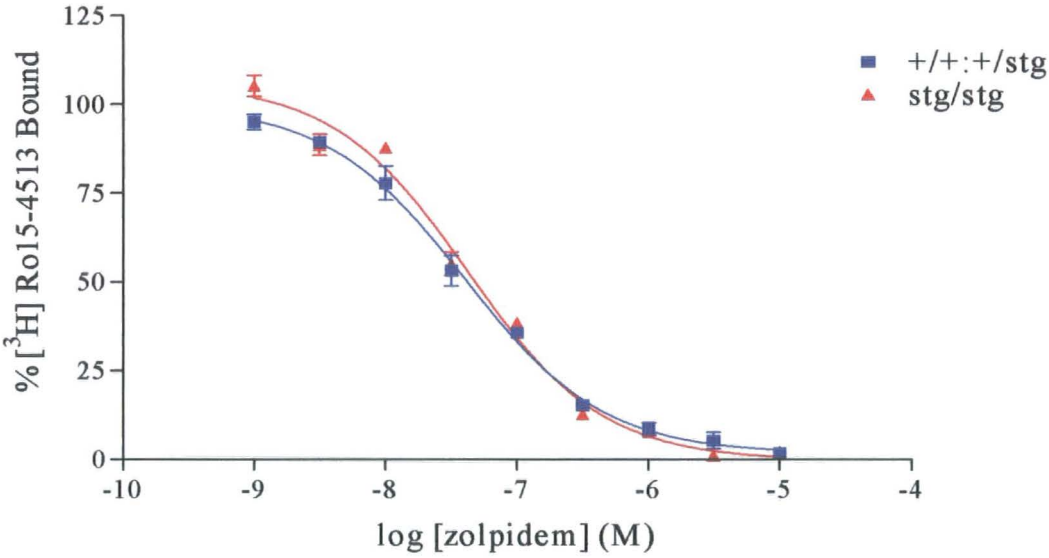
125
100
75
50
25
0
% [3H] Ro15-4513 Bound
-10
-9
-8
-7
-6
-5
-4
log [zolpidem] (M)
+/+:+/stg
stg/stg

Intense immunoreactivity for the α6 subunit was observed in the cerebellar granule cell layer of the cerebellum in control brain sections, with no specific immunostaining detected in either the molecular or Purkinje cell layers. Strong immunoreactivity was observed in the cerebellar granule cell layer and to a lesser extent in the Bergmann glia cell bodies and processes in the molecular layer for the β3 subunit with no specific immunostaining observed in the Purkinje cell layer. The most intense immunostaining for the γ2 subunit was detected in the Purkinje cell layer, with strong immunoreactivity also in the granule cell layer and Purkinje cell dendrites of the molecular layer. δ subunit immunoreactivity was most intense in the cerebellar granule cell layer, with no specific immunostaining present in the Purkinje cell or molecular layers. The current observations were also in agreement with reported *in situ* hybridisation data (Laurie *et al.*, 1992). CGCs were reported to possess high levels of α1, α6, β2, β3, γ2 and δ GABAR subunits, while Purkinje cells contained α1, β2, β3 and γ2 mRNAs only. The stellate/basket cells of the molecular layer were found to possess α1, β2 and γ2 mRNA only.

Qualitative decreases in the intensity of immunoreactive staining for the α6, β2, β3 and δ subunits were observed uniformly in all cerebellar folia in the cerebellar granule cell layer of the stargazer cerebellum.

3.3.2. Quantitative differences in GABAR subunit expression in the stargazer mutant, determined by immunoblotting studies

During the development of the cerebellum, there is a switch in the expression of $GABA_A$ receptor subunits, such that the expression of the α2, α3 and γ1 subunits are superceded by the adult GABAR subunit complement, α1, α6, β2, β3, γ2 and δ subunits (Laurie *et al.*, 1992; Thompson & Stephenson., 1994; Wisden *et al.*, 1996). *In situ* hybridisation studies of the adult rat cerebellum show that the expression of the α6 and δ subunits occurs postnatally at approximately P6 and continues to rise until adult levels of expression are reached at approximately P12 (Laurie *et al.*, 1992).

Semi-quantitative western blotting analyses indicated a decrease in the expression of GABAR α6, β2 and δ subunits in the stargazer mutant cerebellum to 39 ± 22%, 45 ± 42% and 36 ± 21% of control levels respectively.

Thompson *et al.*, in 1998 reported decreases to 23 ± 8% and 38 ± 12% of control levels in α6 and β3 expression respectively in the stargazer mutant whereas α1 and β2 expression was relatively spared. In the current study, a qualitative decrease in β3 subunit expression was observed by immunohistochemistry in the stargazer cerebellum. Quantitation of this decrease however revealed a reduction in expression to 77 ± 42% of control levels in the stargazer mutant, which failed to reach statistical significance (p=0.283, n=6).The discrepancy in the reported decreases in β3 subunit expression in the stargazer mutant in the initial study and the current investigation can possibly be attributed to differences in the background strains used in both studies. The current study utilised the appropriate background strain, the $C3B6Fe^{+}$ mouse strain whereas previously the C57BL/6J strain was used. Fujikawa *et al.*, in 2000 reported strain variations in the survival of cerebellar granule cells in culture under depolarising conditions, such that C57BL/6J CGCs did not survive in culture under physiological potassium concentrations (5 mM), but thrived under depolarising conditions. In contrast, CGCs derived from the Balb/C mouse strain survived both physiological and depolarising conditions (25 mM). Clearly cerebellar granule cells are different depending upon the strain of mouse from which they are derived. In this latter context it is interesting to note that $C3B6Fe^{+}$ mouse CGCs do survive at 5 mM KCl *in vitro*. So clearly C57BL/6J is not an ideal background strain.

Quantification of GABAR subunit expression levels in the stargazer mutant demonstrated that the levels of the α6 and δ subunits were reduced to 39 ± 22% and 36 ± 21% of control levels, respectively. The α6 and δ subunits preferentially co-assemble into receptors in the cerebellum (Quirk *et al.*, 1994; Jechlinger *et al.*, 1998; Pöltl *et al.*, 2003). Hence, it could be predicted that if a reduction in the expression of the α6 subunit is observed, there may be a concomitant reduction in the expression of the δ subunit. This hypothesis is

supported by investigations into the effects of the GABAR α6 subunit knockout mouse on other GABAR subunits (Jones *et al.*, 1997). The group report a dramatic reduction in the expression of the δ subunit protein in the α6 subunit knockout mouse to 25 ± 8% of control levels, as determined by western blot analyses. This hypothesis is tested later in this study in chapters 5 and 6.

Contrary to previous reports where expression of the β2 subunit was relatively spared (Thompson *et al.*, 1998), the expression levels of the β2 subunit were found to be dramatically decreased to 45 ± 42% of control levels in the stargazer cerebellum in the current investigation. However, Jechlinger *et al.*, in 1998 reported that in the cerebellum, 50-60% of the α6 subunits co-assemble with the β2 subunit, whereas only 20-30% co-assemble with the β3 subunit. Therefore, it may be predicted that with a loss of the α6 subunit in the stargazer mutant, a more dramatic loss of expression of the β2 subunit would be observed. We can only postulate that this discrepancy is due to an inappropriate background strain used in the previous study.

3.3.3. Is the GABAR profile of the stargazer mutant characteristic of a juvenile or adult cerebellum?

Segal *et al.*, in 1992 proposed that different neurotrophins act at different stages of cerebellar granule cell maturation. Brain-derived neurotrophic factor (BDNF) was found to be an essential requirement for the survival and maturation of immature cerebellar granule cells of the external granule cell layer (EGL) in dissociated rat cerebellar granule cell (CGC) cultures but also for the commitment of the granule cell to a neuronal phenotype. BDNF expression has been reported to be at higher levels in the internal granular layer than the external granule cell layer, forming a gradient of BDNF levels and hence, it has been proposed to act as a chemotactic factor, promoting the migration of the CGCs from the EGL to internal granule cell layer (IGL) (Borghesani *et al.*, 2002). The role of BDNF as a chemotactic factor in the cerebellum may explain the delay in migration of CGCs in the stargazer mutant mouse, which lacks BDNF expression in the CGC layer, as observed by Qiao *et al.*, 1996, 1998.

Investigations into the BDNF knockout mouse ($BDNF^{-/-}$) demonstrate an increase in the thickness of the EGL in the mutant when compared to wild-type controls, consistent with a slowing of the migration of CGCs from the EGL to IGL, highlighting the role of BDNF as a motogenic factor (Borghesani *et al.*, 2002). It might be predicted therefore that in the stargazer mutant differentiation of the GABARs may be compromised, such that immature GABAR subunits persist in the adult mutant.

Hashimoto *et al.*, in 1999 reported that stargazer CGCs exhibit electrophysiological characteristics that are compatible with an immature stage of development, with mossy fibre to granule cell synapses that are devoid of AMPAR-mediated excitatory postsynaptic currents (EPSCs). This observation is supported by studies on waggler mice, which are allelic to the stargazer, where GABARs expressed in Golgi cell to granule cell synapses have immature channel kinetics (Chen *et al.*, 1999) that might be explained by the loss of GABAR α6 subunit expression described by Thompson *et al.*, in 1998, which would be compatible with immature CGCs. However, in the current study, zolpidem displacement of [^{3}H] Ro15-4513 binding to adult control and stargazer cerebellar membranes showed the presence of GABARs with a Type I pharmacology (α1 subunit-containing $GABA_A$ receptors) expected to be present in adult mature cerebellum. Type II receptors which were clearly absent from stargazer are indicative of expression of α2 and α3 subunit-containing receptors, which are predominant in the immature cerebellum. Hence, it can be concluded that CGCs of the stargazer mutant differentiate as in control animals at least as far as the GABAR profile is concerned.

3.3.4. Conclusions

In conclusion, qualitative differences in GABAR subunit expression were determined using immunohistochemical techniques. Decreases in the α6, β2, β3, and δ subunits were observed in all cerebellar folia of the stargazer mutant cerebellum when compared to controls. The expression of the GABAR subunits were quantified in adult control and stargazer mouse cerebellum and revealed

significant decreases in expression of the GABAR α6, β2 and δ subunits in the stargazer mutant to 39 ± 22%, 45 ± 42% and 36 ± 21% of control levels respectively. This study demonstrates that the development of the GABAR profile of the stargazer mutant cerebellum is not impaired. The GABAR profile expressed in the stargazer cerebellum is not indicative of the immature complement of receptors expressed in the developing cerebellum (α2/α3/α5 subunit-containing receptors), as determined by zolpidem displacement of [^{3}H] Ro15-4513 binding, rather, the levels of expression of the α6 and δ subunit-containing GABARs present in the mature cerebellum, are dramatically reduced.

CHAPTER 4. $GABA_A$ RECEPTOR EXPRESSION IN THE CEREBELLUM OF THE STARGAZER MUTANT MOUSE

4.1. INTRODUCTION

Chapter 3 reported deficits in the expression of the GABAR subunits in the stargazer mutant mouse cerebellum as determined by immunohistochemistry and immunoblotting. The expression of the α6, β2 and δ subunits were found to be significantly reduced in the cerebellum of the stargazer mutant to 39 ± 22%, 45 ± 42%, and 36 ± 21% of control levels respectively.

The aim of the current chapter was to re-analyse the GABAR expression profile by radioligand binding to cerebellar membrane homogenates in the stargazer mutant mouse but using the appropriate background strain for control animals. $C3B6Fe^+$ mice were utilised in the current study, compared to the C57BL/6J strain used in previous investigations, as discussed in section 3.3.2 (Thompson *et al.*, 1998). This work was extended to analyse the distribution and abundance of receptor subtypes expressed in the stargazer mutant mouse brain by *in situ* receptor autoradiography. This approach also offered the ability to analyse δ-subunit containing GABAR that is difficult in radioligand binding assays on cerebellar membranes. Ultimately this would enable us to evaluate whether abnormalities in GABAR subunit expression translate into GABAR deficits in the stargazer mutant.

4.2. RESULTS

4.2.1. Determination of mouse genotype by genomic PCR screening

The accurate genotyping of adult (2-6 months old) mice is essential not only for the maintenance of the stargazer breeding programme for which heterozygotes are required, but is also essential for us to determine whether wild-type (+/+) and heterozygote (+/stg) mice could be combined for control material. Furthermore,

it is a necessity for the culture of control (+/+:+/stg) and stargazer (stg/stg) primary cerebellar granule neurons.

Heterozygote mice (+/stg) were used as breeders producing offspring in mendelian ratios of 1 +/+: 2 +/stg: 1 stg/stg. Tail biopsies were obtained from adult mice, DNA was isolated and subjected to multiplex polymerase chain reaction (PCR) using a combination of primers to yield characteristic amplicons of 300 base pairs (bp) corresponding to the mutated allele and 600 bp for the wild-type allele (as described in methods, section 2.4). The stargazer mutation arises from an early viral transposon insertion of 6 kb between introns 2 and 3 of the stargazin gene, located on mouse chromosome 15. Therefore, different combinations of primers were used to amplify different regions of the gene to include the transposon insertion if present (Noebels *et al.*, 1990; Letts *et al.*, 1998).

Heterozygote mice possess one copy of the normal allele (600 bp) and one copy of the mutated allele (300 bp), hence upon PCR screen, bands of both 300 and 600 bp were visualised by agarose gel electrophoresis. In comparison, a wild-type mouse possesses two copies of the normal allele and could therefore be identified by production of a single PCR product of 600 bp. The stargazer mutation is a recessive mutation. Hence, a stargazer mouse possesses two copies of the mutated allele and therefore only the 300 bp band can be visualised on an agarose gel (see figure 2.1.)

The validity of the genomic PCR screen was tested by allowing screened neonates to mature and observed the resultant progeny following mating of heterozygote mice. Neonates that were concluded to be heterozygotes did not demonstrate a stargazer phenotype but did go on to produce offspring that included stg/stg in mendelian ratios. Wild-type animals did not show any characteristics of the stargazer phenotype and produced a single 600 bp PCR product. Stargazer neonates did indeed demonstrate the characteristic head toss and cerebellar ataxia predicted of the mutant.

4.2.2. Radioligand binding to wild-type (+/+) and heterozygote (+/stg) cerebellar membranes

It has been previously reported that +/+ and +/stg animals fail to display any differences in any of the electrophysiological or molecular biological parameters studied to date and were therefore combined as control tissue (Qiao *et al.*, 1998; Hashimoto *et al.*, 1999). To establish whether this was suitable for our studies, pharmacological analyses were carried out to determine if wild-type and heterozygote animals could be grouped as control animals for our future experiments.

4.2.2.1. Cerebellar membrane homogenate preparation

Original methods developed in the laboratory for the preparation of cerebellar membrane homogenates incorporated an initial centrifugation step whereby homogenised tissue was spun at 10 000 *g* for 12 minutes. The resultant pellet containing whole cells and nuclei was discarded and the supernatant was utilised for the further preparation of cerebellar membranes. Upon determination of the [^{3}H] Ro15-4513 binding (20 nM) present in the pellet, it was found that 42 ± 11% of total specific binding sites, 39 ± 12% of benzodiazepine-sensitive (BZ-S) binding sites and 46 ± 10% of benzodiazepine-insensitive (BZ-IS) binding sites were contained within the pellet and were therefore discarded in the original protocol (figure 4.1.). According to Mehta and Ticku (1999) this was because cerebellar glomeruli were being spun down in the discarded fraction and probably contained CGC receptors which we proposed were compromised by the stargazer mutation and hence important for this investigation. Thus we adopted, with minor modifications the fractionation method of Mehta and Ticku.

4.2.2.2. [^{3}H] Muscimol

[^{3}H] muscimol acts as a GABA mimetic and hence binds with high affinity to the GABA binding site of the $GABA_A$ receptor, located at the interface between α and β subunits (Korpi *et al.*, 2002b).

Figure 4.1. Comparison of [^{3}H] Ro15-4513 binding in control cerebellar membrane preparation versus whole cell pellet

Bar graph demonstrates radioactivity bound to [^{3}H] Ro15-4513 binding sites (20 nM) obtained from cerebellar membrane homogenates and pellet discarded in the original membrane preparation protocol. Flunitrazepam (10 μM) was used to define BZ-IS and BZ-S sub-components of total specific binding. Ro15-1788 (10 μM) was used to define non-specific binding.

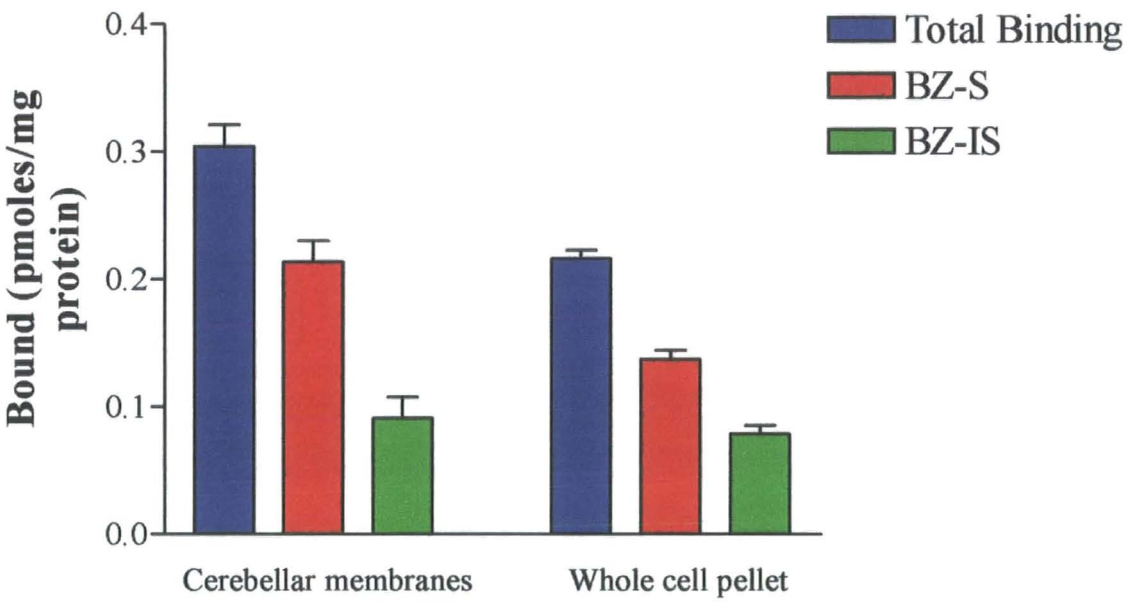
Total Binding
BZ-S
BZ-IS
Bound (pmoles/mg protein)
0.4
0.3
0.2
0.1
0.0
Cerebellar membranes
Whole cell pellet

Figure 4.2. [^{3}H] muscimol binding to wild-type (+/+) and heterozygote (+/stg) cerebellar membrane homogenates

A: Full saturation binding curves to wild-type and heterozygote cerebellar membranes using a concentration range of 0.5-40 nM [^{3}H] muscimol.
B: Bar graph to demonstrate the B_{MAX} values calculated for wild-type and heterozygote membranes. Results show no significant difference in B_{MAX}, i.e. total binding sites, in heterozygote cerebellar membranes (104 ± 28%) compared to wild-type, p=0.83.
C: Table summarising calculated B_{MAX} and K_D values for wild-type and heterozygote cerebellar membranes. Data is representative of mean ± SEM for n=2 experiments, membranes homogenates prepared from n=10 cerebella per mouse strain.

A

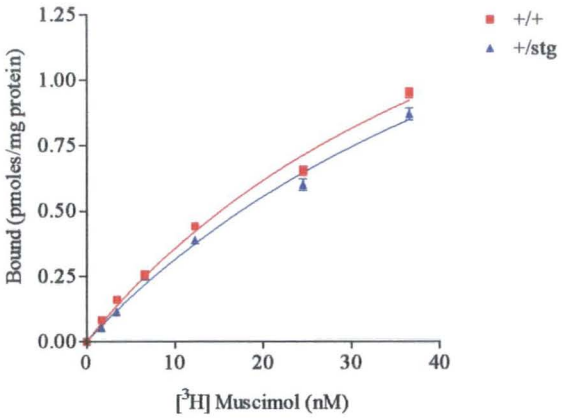

B

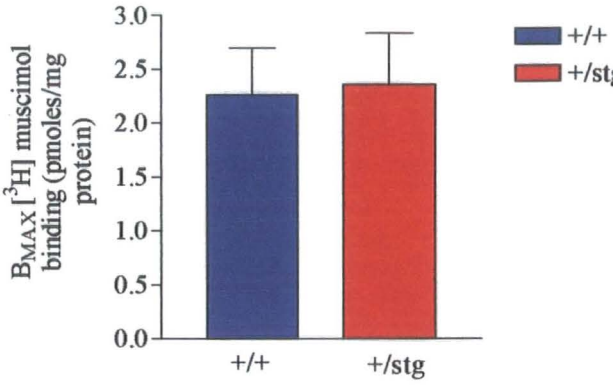

C

	+/+	+/stg
B_{MAX} (pmoles/mg protein)	2.3 ± 0.4	2.4 ± 0.5
K_D (nM)	53 ± 15	65 ± 19

Consequently, [^{3}H] muscimol will bind with high affinity to all GABAR, containing both γ2 and δ subunits. Interestingly, in autoradiography, the ligand has a degree of selectivity for specific GABAR in that it binds specifically to α6 subunit containing GABAR either directly or as a consequence of the presence of the δ subunit (Korpi *et al.*, 2002b).

Full-saturation [^{3}H] muscimol binding experiments were conducted to compare GABAR expression in wild-type (+/+) and heterozygote (+/stg) cerebellar membrane homogenates. Figure 4.2. demonstrates [^{3}H] muscimol binding curves to cerebellar membranes from wild type and heterozygote animals, using a concentration range of 0.5-40 nM ligand. Binding data was analysed using GraphPad prism 3.0 to construct Rosenthal transformations of the data and calculate the maximum number of binding sites per mg protein (B_{MAX}) and the dissociation constants (K_D) for each membrane preparation, summarised in figure 4.2. No significant difference in B_{MAX} for wild type and heterozygote animals was found in the current study. The B_{MAX} determined for wild-type and heterozygote mice were 2.3 ± 0.4 pmoles/mg protein and 2.4 ± 0.5 pmoles/mg protein respectively. K_D values calculated for wild-type and heterozygote mice were 53 ± 15 nM and 65 ± 19 nM respectively (figure 4.2). These values are contrary to published K_D values for [^{3}H] muscimol binding to mouse cerebellar homogenates, which are approximately 4-5 nM (Jones *et al.*, 1997; Tretter *et al.*, 2001). These results might be explained by the presence of endogenous GABA in the membrane preparation, despite the fact that the membrane preparation procedure was designed to wash out endogenous, competitive GABA. Hence, calculated K_D values from Rosenthal transformations of the data would be higher than expected. Nonetheless, the membranes were prepared identically for each strain and the binding curves were practically super-imposable (figure 4.2).

4.2.2.3. [^{3}H] Ro15-4513

Ro15-4513 is a partial inverse agonist at the GABAR, which binds to the BZ binding site of the receptor, located on the interface between α and γ subunits. Hence, the presence of the γ subunit within the GABAR is essential for binding

of Ro15-4513. Flunitrazepam (10 μM) was used to displace [^{3}H] Ro15-4513 bound to BZ-S GABAR (α1, α2, α3, α5, β and γ2 containing), to reveal labelling of BZ-IS GABAR containing the α4 and/or α6 subunits. Ro15-1788 (10 μM) is a competitive antagonist, which competes for specific Ro15-4513 binding sites, acting to displace [^{3}H] Ro15-4513 from GABAR for which it has high affinity, hence revealing non-specific binding.

In order to assess any differences in the contribution of γ2 containing GABARs to the receptor population of wild-type and heterozygote mice, full saturation [^{3}H] Ro15-4513 binding studies were conducted in the absence and presence of flunitrazepam (10 μM) and Ro15-1788 (10 μM) to generate total specific, BZ-S and BZ-IS parameters. Figure 4.3. shows [^{3}H] Ro15-4513 binding curves to cerebellar membranes from wild-type and heterozygote mice using a concentration range of 0.31-40 nM.

Calculation of B_{MAX} and K_D values for wild-type and heterozygote mice demonstrated no significant difference in the maximum number of binding sites (B_{MAX}), or the affinity of the ligand for its receptor (K_D) between the two preparations. B_{MAX} values for total [^{3}H] Ro15-4513 binding for wild-type and heterozygote mice were 1.53 ± 0.11 pmoles/mg protein and 1.40 ± 0.05 pmoles/mg protein respectively. For BZ-S binding, the maximum number of binding sites was determined to be 1.09 ± 0.10 pmoles/mg protein and 1.01 ± 0.05 pmoles/mg protein for wild-type and heterozygote mice respectively. B_{MAX} values for BZ-IS binding were 0.43 ± 0.02 pmoles/mg protein for wild-type membrane homogenates and 0.39 ± 0.02 pmoles/mg protein for heterozygote membrane homogenates.

In accordance with studies reported by others (Qiao *et al.*, 1998; Hashimoto *et al.*, 1999) we have determined that the GABAR pharmacology of wild-type and heterozygote animals is identical. Therefore, in all further experiments, both genotypes were grouped and used as control animals (+/+:+/stg).

Figure 4.3. [^{3}H] Ro15-4513 binding to wild-type (+/+) and heterozygote (+/stg) cerebellar membrane homogenates

A: Full saturation binding curves to wild-type cerebellar membranes using a concentration range of 0.3-40 nM [^{3}H] Ro15-4513. Non-specific binding was determined in the presence of Ro15-1788 (10 μM). [^{3}H] Ro15-4513 binding in the presence of flunitrazepam (10 μM), defined benzodiazepine-insensitive (BZ-IS) binding sites and hence benzodiazepine-sensitive (BZ-S) sites could be determined by subtraction of the BZ-IS binding sites from total [^{3}H] Ro15-4513 specific binding sites.

B: Full saturation binding curves to heterozygote cerebellar membranes using a concentration range of 0.3-40 nM [^{3}H] Ro15-4513.

C: Bar graph to demonstrate the difference in B_{MAX} values calculated for wild-type and heterozygote membranes. Results show no significant difference in B_{MAX} for total specific binding (100 ± 8% and 92 ± 9%, p=0.17), BZ-S binding (100 ± 10% and 93 ± 11%, p=18) or BZ-IS binding (100 ± 7% and 91 ± 7%, p=0.27) in wild-type or heterozygote membranes respectively.

D: Table summarising calculated B_{MAX} and K_D values for wild-type and heterozygote cerebellar membranes. Data is representative of mean ± SEM for n=2 experiments, membranes homogenates prepared from n=10 cerebella per mouse strain.

A

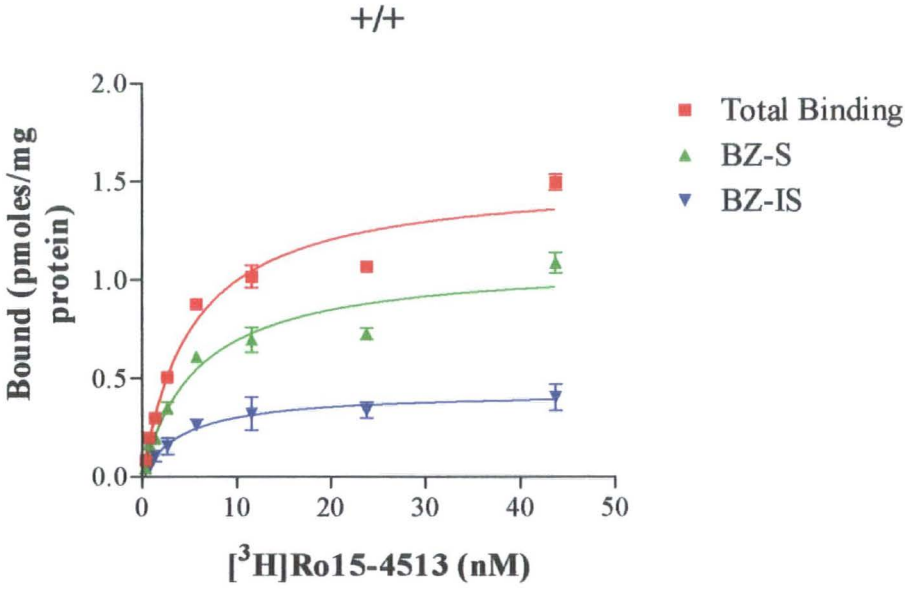
+/+
Bound (pmoles/mg protein)
2.0
1.5
1.0
0.5
0.0
0
10
20
30
40
50
[3H]Ro15-4513 (nM)
Total Binding
BZ-S
BZ-IS

B

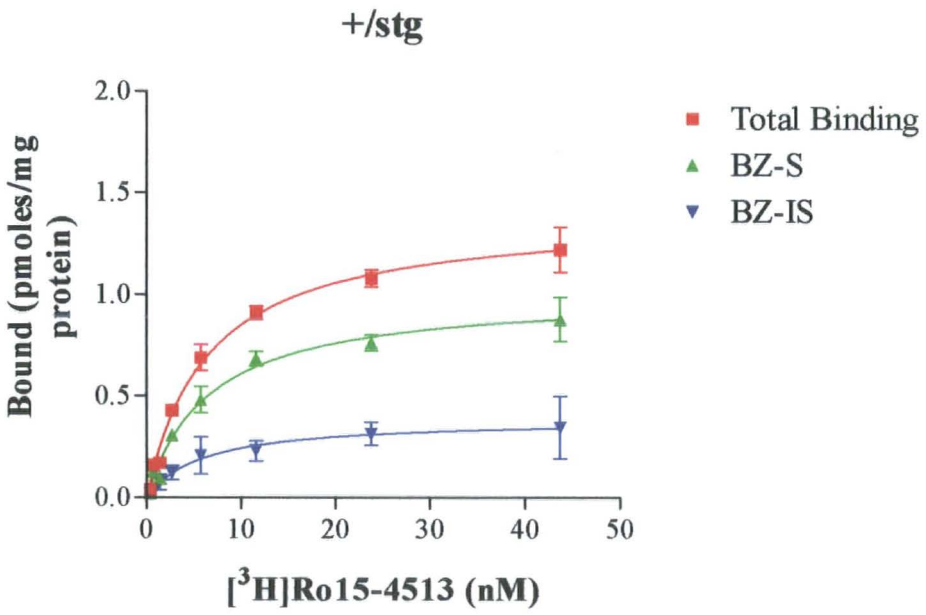
+/stg
Bound (pmoles/mg protein)
2.0
1.5
1.0
0.5
0.0
0
10
20
30
40
50
[3H]Ro15-4513 (nM)
Total Binding
BZ-S
BZ-IS

C

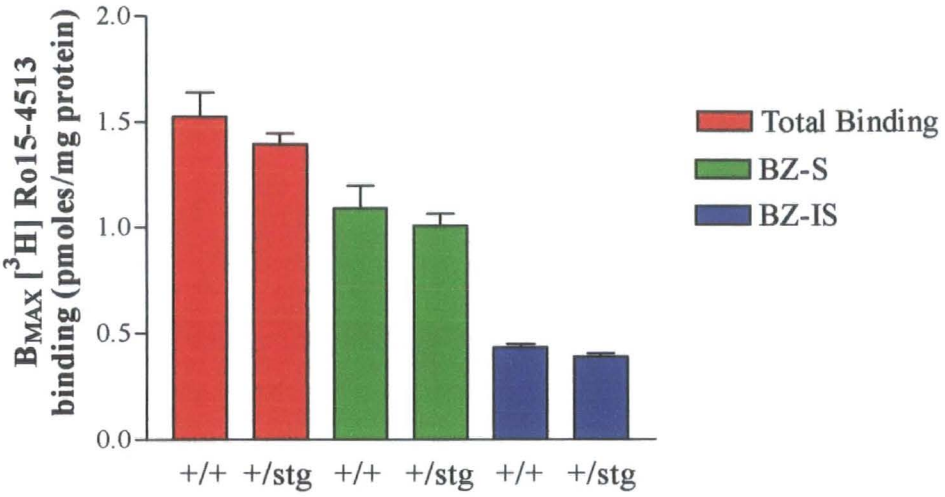

D

	+/+	+/stg
Total Binding B_{MAX} (pmoles/mg protein)	1.53 ± 0.11	1.40 ± 0.05
K_D (nM)	5.26 ± 1.26	6.40 ± 0.70
BZ-S B_{MAX} (pmoles/mg protein)	1.09 ± 0.10	1.01 ± 0.05
K_D (nM)	5.71 ± 1.72	6.54 ± 1.07
BZ-IS B_{MAX} (pmoles/mg protein)	0.43 ± 0.02	0.39 ± 0.02
K_D (nM)	4.32 ± 0.55	5.94 ± 0.83

4.2.3. Radioligand binding to control and stargazer cerebellum using [^{3}H] Muscimol

4.2.3.1. Cerebellar membranes

Full saturation binding experiments were conducted using a range of [^{3}H] muscimol concentrations of 0.5-40 nM ligand to control (+/+:+/stg) and stargazer (stg/stg) cerebellar membrane homogenates. Results are shown in figure 4.4. A significant reduction in B_{MAX} was calculated for the stargazer mutant, which was reduced to 70 ± 10% of control levels. No significant difference in K_D values were found between the two strains (2.98 ± 0.85 nM and 3.64 ± 0.74 nM for control and stargazer mice respectively), hence the affinity of the ligand for its receptor was not altered, rather, the total number of GABAR was found to be reduced in the cerebellum of the stargazer mutant mouse when compared to controls.

4.2.3.2. Receptor autoradiography

Adult control and stargazer tissue sections were subjected to receptor autoradiography, using [^{3}H] muscimol at a concentration of 20 nM. Non-specific binding was determined in the presence of 1 mM GABA.

Specific [^{3}H] muscimol binding was observed in the cerebellum, hippocampus, cortex, striatum and thalamus (see figure 4.5.). The levels of radioactivity were quantified in the cerebellar granule cell layer of both control and stargazer sections using ImageJ software. [^{3}H] standards of known radioactivities were exposed on [^{3}H] hyperfilm for the same length of time as the tissue sections, allowing for the construction of a standard curve of radioactivity versus intensity of pixels in a gray matter area. Quantification of the levels of radioactivity within the cerebellar granule cell layer of control and stargazer tissue sections revealed a reduction in [^{3}H] muscimol binding in the stargazer mutant to 54 ± 10% of control levels (n=6 sections per strain, 10 measurements per section, $p<0.01$.). Non-specific binding was determined to be at background levels of the film.

Figure 4.4. [^{3}H] muscimol binding to control (+/+:+/stg) and stargazer (stg/stg) cerebellar membrane homogenates

A: Full saturation binding curves to control and stargazer cerebellar membranes using a concentration range of 0.5-40 nM [^{3}H] muscimol.
B: Rosenthal transformation of specific [^{3}H] muscimol binding data to control and stargazer cerebellar membrane homogenates
C: Bar graph to demonstrate the difference in B_{MAX} values calculated for control and stargazer membranes. Results show a reduction to 70 ± 10%, p=0.03 of control levels in B_{MAX}, i.e. total binding sites, in stargazer cerebellar membranes.
D: Table summarising calculated B_{MAX} and K_D values for control and stargazer cerebellar membranes. Data is representative of mean ± SEM for n=2 experiments, membranes homogenates prepared from n=10 cerebella per mouse strain.

A

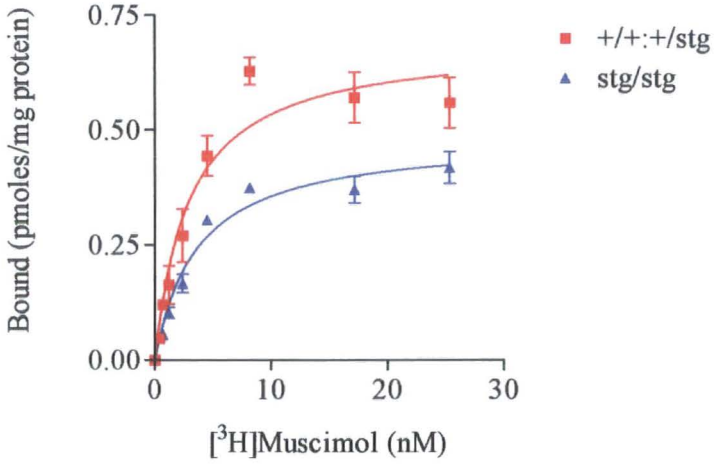

B

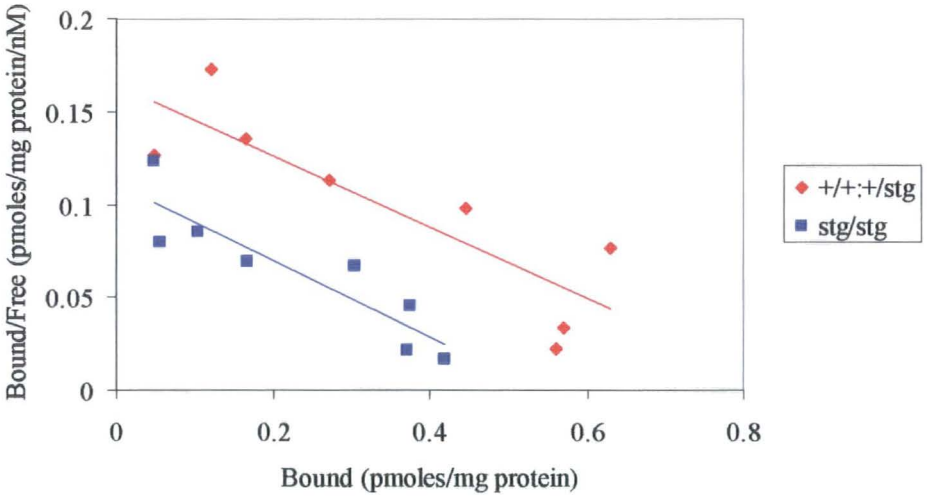

C

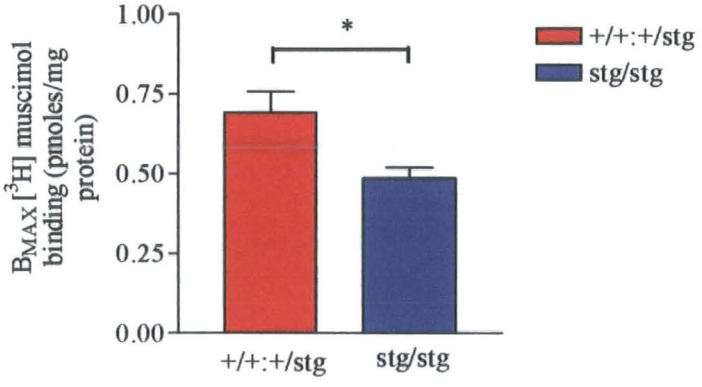

D

	+/+:+/stg	stg/stg
B_{MAX} (pmoles/mg protein)	0.69 ± 0.06	0.49 ± 0.03
K_D (nM)	2.98 ± 0.85	3.64 ± 0.74

Figure 4.5. [^{3}H] Muscimol binding (20 nM) to control (+/+:+/stg) and stargazer (stg/stg) adult mouse brain sections

A: Representative control and stargazer autoradiographs demonstrating high intensity of radiolabel in the cerebellar granule cell layer.

B: Standard curve of intensity versus radioactivity, constructed using ImageJ software to measure the intensity of [^{3}H] standards of known radioactivities (see section 2.12.2).

C: Column graph depicting the calculated radioactivities of the cerebellar granule cell layer of 6 control and 6 stargazer tissue sections, 10 measurements per section from n=2 mouse per strain.

D: Bar graph to demonstrate a significant decrease in [^{3}H] muscimol binding in the cerebellar granule cell layer of the stargazer mutant mouse, to 53 ± 10% of control levels, $p<0.01$.

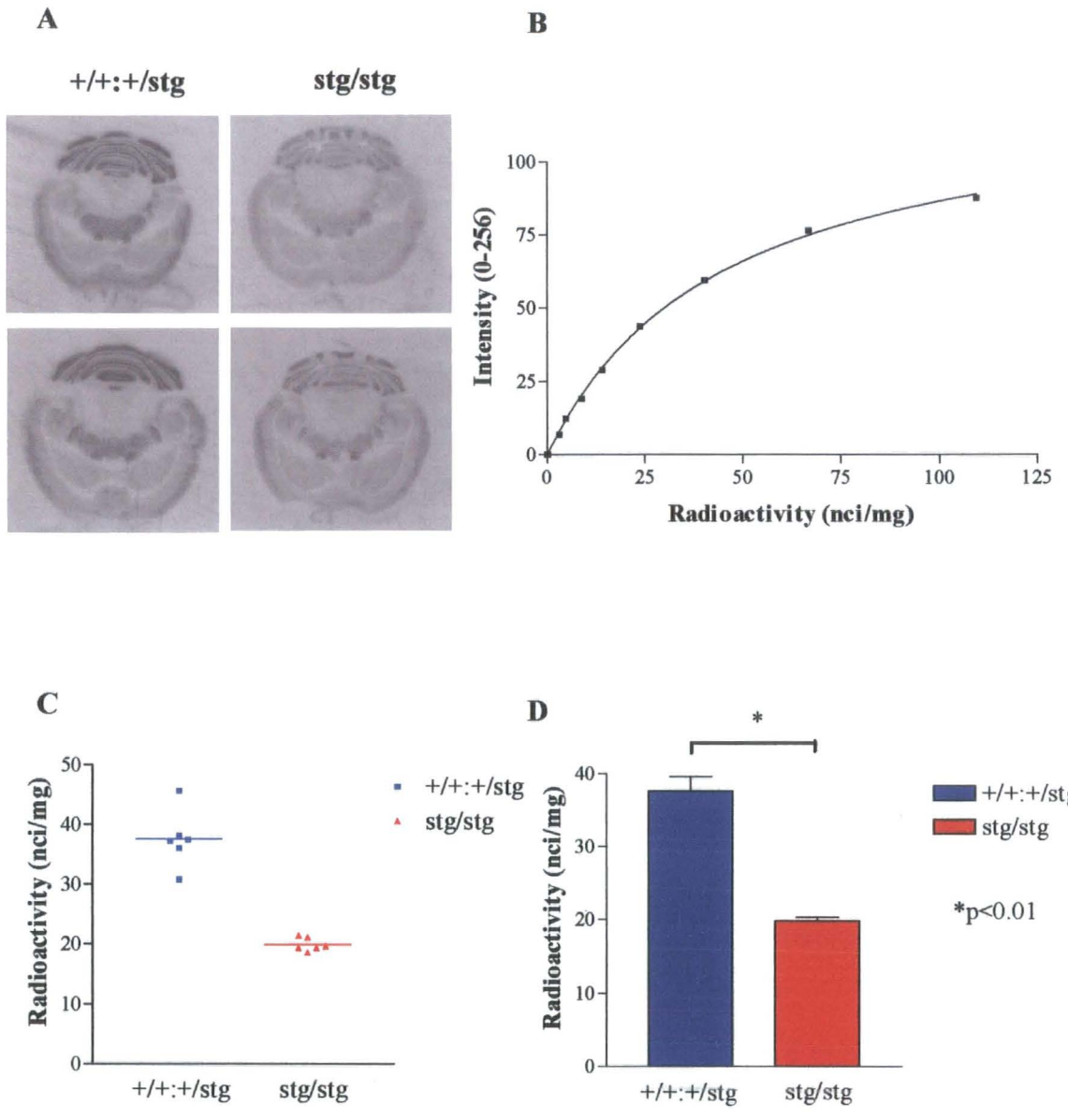
A
+/+:+/stg
stg/stg
B
Intensity (0-256)
100
75
50
25
0
0
25
50
75
100
125
Radioactivity (nci/mg)
C
Radioactivity (nci/mg)
50
40
30
20
10
0
+/+:+/stg
stg/stg
+/+:+/stg
stg/stg
D
*
Radioactivity (nci/mg)
40
30
20
10
0
+/+:+/stg
stg/stg
+/+:+/stg
stg/stg
*p<0.01

Hence, it can be concluded from [^{3}H] muscimol binding studies to control and stargazer cerebellar membrane homogenates and tissue sections that there is a significant reduction in the total number of GABAR in the stargazer mutant mouse, to 70 ± 10% of control levels and a reduction in α6-subunit containing GABAR to 54 ± 10% of control levels as determined by receptor autoradiography.

4.2.4. Radioligand binding to control and stargazer cerebellum using [^{3}H] Ro15-4513

4.2.4.1. Cerebellar membranes

Radioligand binding studies were conducted using a concentration range of 0.31-40 nM [^{3}H] Ro15-4513 to control and stargazer cerebellar membranes. Upon dissection of the resultant binding data into its pharmacological subtypes, it was found that the B_{MAX} of total [^{3}H] Ro15-4513 binding, representing α1βγ2, α6βγ2 and α1α6βγ2, was reduced to 81 ± 10% of control levels in the stargazer mutant (1.01 ± 0.05 and 0.82 ± 0.06 pmoles/mg protein for control and stargazer membranes respectively). The B_{MAX} of the BZ-S subtype of receptor, corresponding to α1βγ2 GABAR was reduced to 92 ± 15% of control levels (0.71 ± 0.08 and 0.65 ± 0.06 pmoles/mg protein for control and stargazer membrane homogenates). The BZ-IS subtype of receptor was dramatically reduced to 57 ± 13% of control levels (0.30 ± 0.76 pmoles/mg protein for controls and 0.17 ± 0.02 pmoles/mg protein for stargazer membranes), indicating a loss of α6βγ2 receptors in the stargazer mutant cerebellum (figure 4.6.).

4.2.4.2. Receptor autoradiography

Receptor autoradiography was conducted on adult control and stargazer tissue sections, using [^{3}H] Ro15-4513 at a concentration of 20 nM. 10 μM flunitrazepam was utilised to define BZ-IS binding and 10 μM Ro15-4513 to determine the contribution of non-specific binding.

Figure 4.6. [^{3}H] Ro15-4513 binding to control (+/+:+/stg) and stargazer (stg/stg) cerebellar membrane homogenates

A: Full saturation binding curves to control cerebellar membranes using a concentration range of 0.3125-40 nM [^{3}H] Ro15-4513. Non-specific binding was determined in the presence of Ro15-1788 (10 μM). [^{3}H] Ro15-4513 binding in the presence of flunitrazepam (10 μM), defined benzodiazepine-insensitive (BZ-IS) binding sites and hence benzodiazepine-sensitive (BZ-S) sites could be determined by subtraction of the BZ-IS binding sites from total [^{3}H] Ro15-4513 specific binding sites.

B: Full saturation binding curves to stargazer cerebellar membranes using a concentration range of 0.3125-40 nM [^{3}H] Ro15-4513.

C: Rosenthal transformation of total specific [^{3}H] Ro15-4513 binding data to control and stargazer cerebellar membrane homogenates

D: Rosenthal transformation of BZ-S [^{3}H] Ro15-4513 binding data to control and stargazer cerebellar membrane homogenates

E: Rosenthal transformation of BZ-IS [^{3}H] Ro15-4513 binding data to control and stargazer cerebellar membrane homogenates

F: Bar graph to demonstrate the difference in B_{MAX} values calculated for control and stargazer membranes. Results show differences in B_{MAX} for total specific binding (100 ± 8% and 81 ± 10%), BZ-S binding (100 ± 14% and 92 ± 15%) or BZ-IS binding (100 ± 7% and 57 ± 13%) in control or stargazer membranes respectively.

G: Table summarising calculated B_{MAX} and K_D values for control and stargazer cerebellar membranes. Data is representative of mean ± SEM for n=2 experiments, membranes homogenates prepared from n=10 cerebella per mouse strain.

A

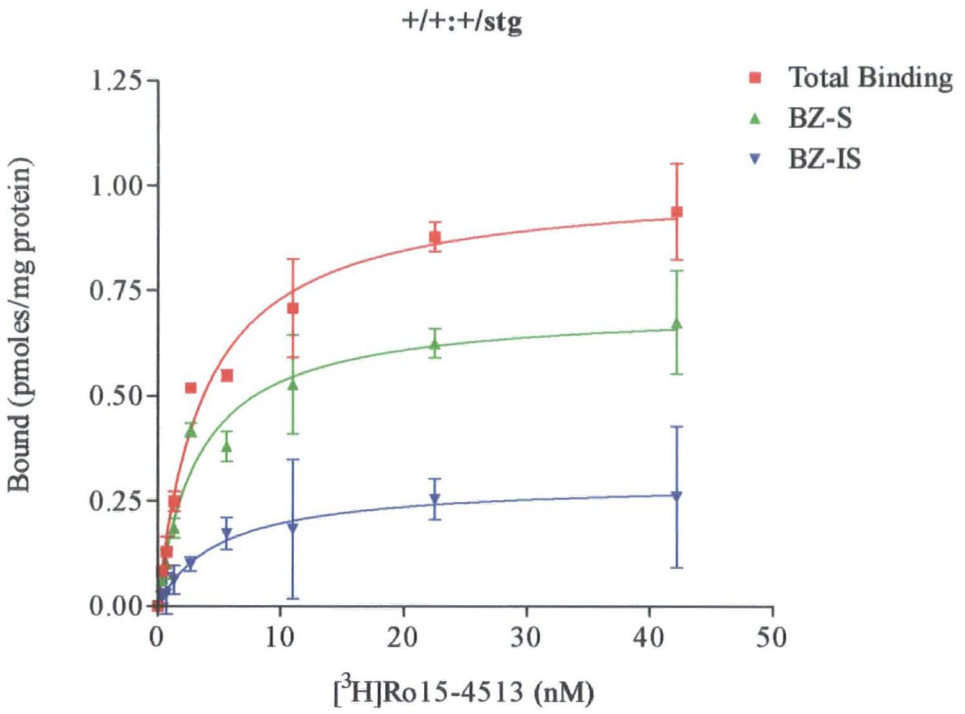
+/+:+/stg
Total Binding
BZ-S
BZ-IS
Bound (pmoles/mg protein)
1.25
1.00
0.75
0.50
0.25
0.00
0
10
20
30
40
50
[3H]Ro15-4513 (nM)

B

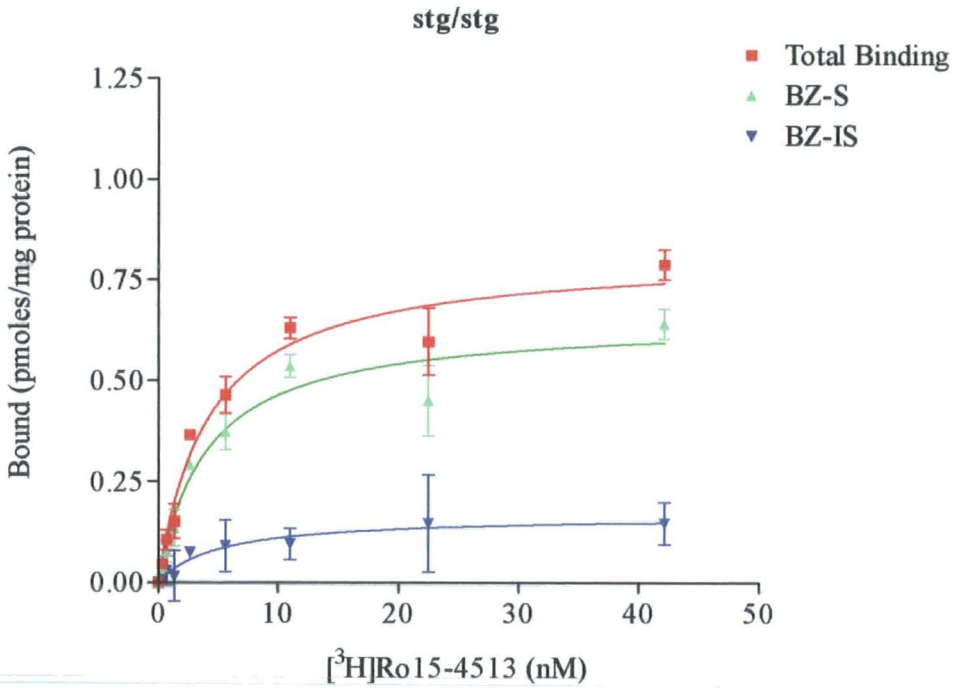
stg/stg
Total Binding
BZ-S
BZ-IS
Bound (pmoles/mg protein)
1.25
1.00
0.75
0.50
0.25
0.00
0
10
20
30
40
50
[3H]Ro15-4513 (nM)

C

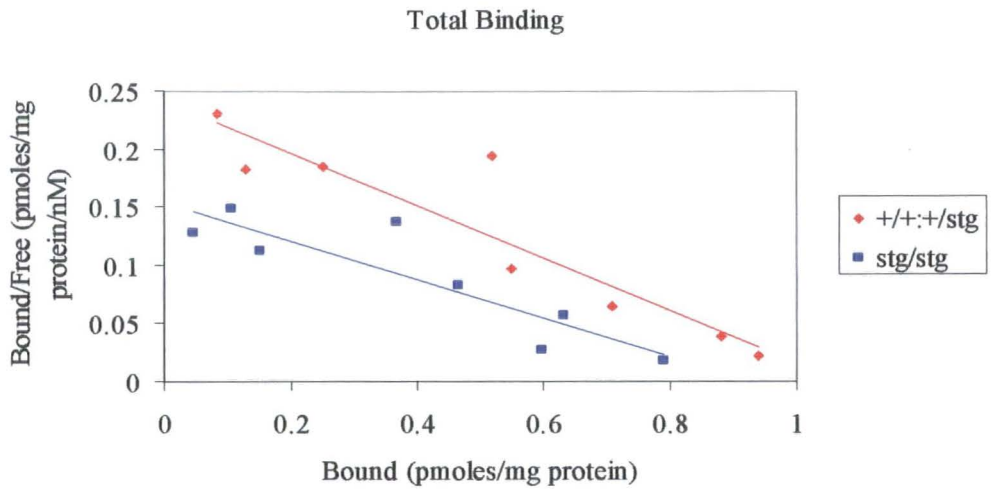
Total Binding
Bound/Free (pmoles/mg protein/nM)
0.25
0.2
0.15
0.1
0.05
0
0
0.2
0.4
0.6
0.8
1
Bound (pmoles/mg protein)
+/+:+/stg
stg/stg

D

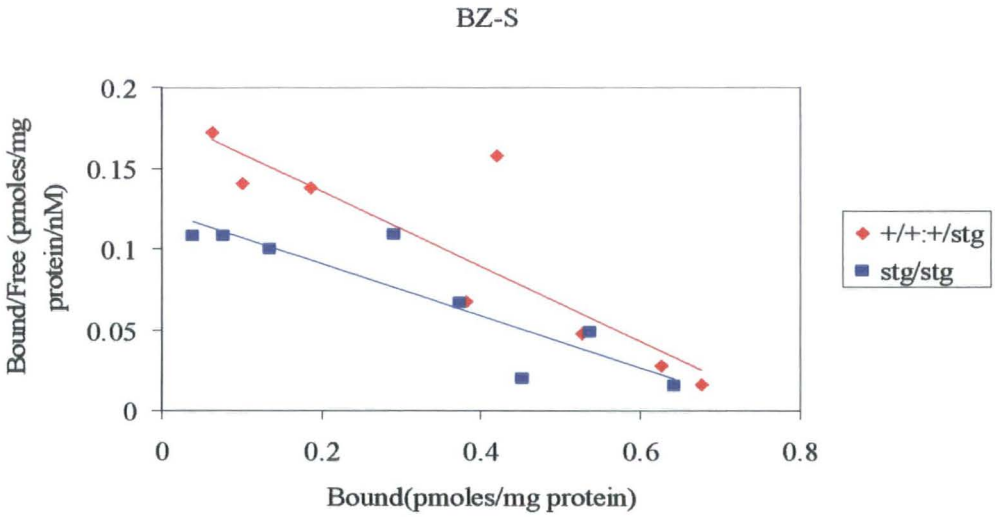
BZ-S
Bound/Free (pmoles/mg protein/nM)
0.2
0.15
0.1
0.05
0
0
0.2
0.4
0.6
0.8
Bound(pmoles/mg protein)
+/+:+/stg
stg/stg

E

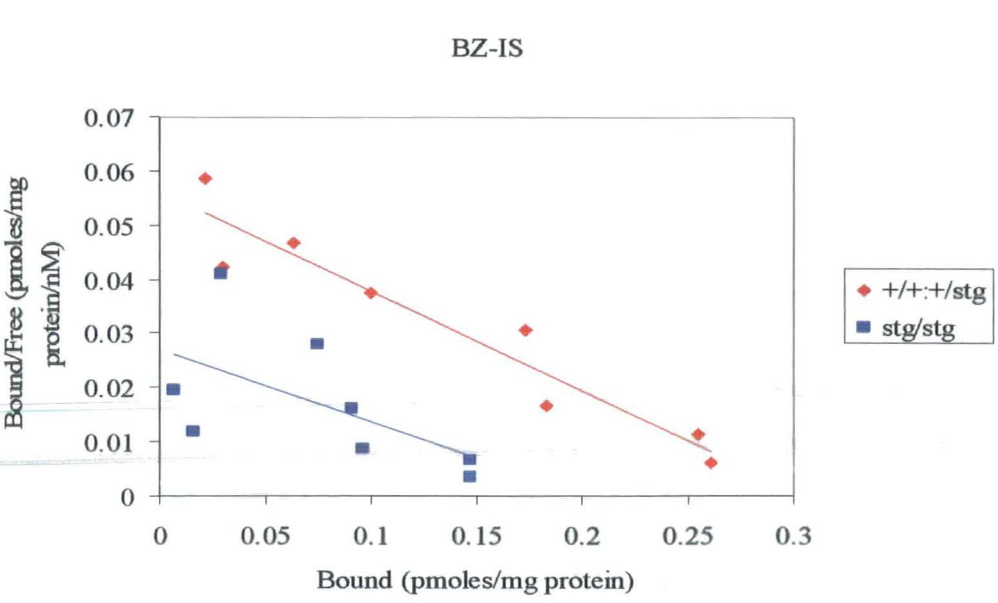
BZ-IS
Bound/Free (pmoles/mg protein/nM)
0.07
0.06
0.05
0.04
0.03
0.02
0.01
0
0
0.05
0.1
0.15
0.2
0.25
0.3
Bound (pmoles/mg protein)
+/+:+/stg
stg/stg

F

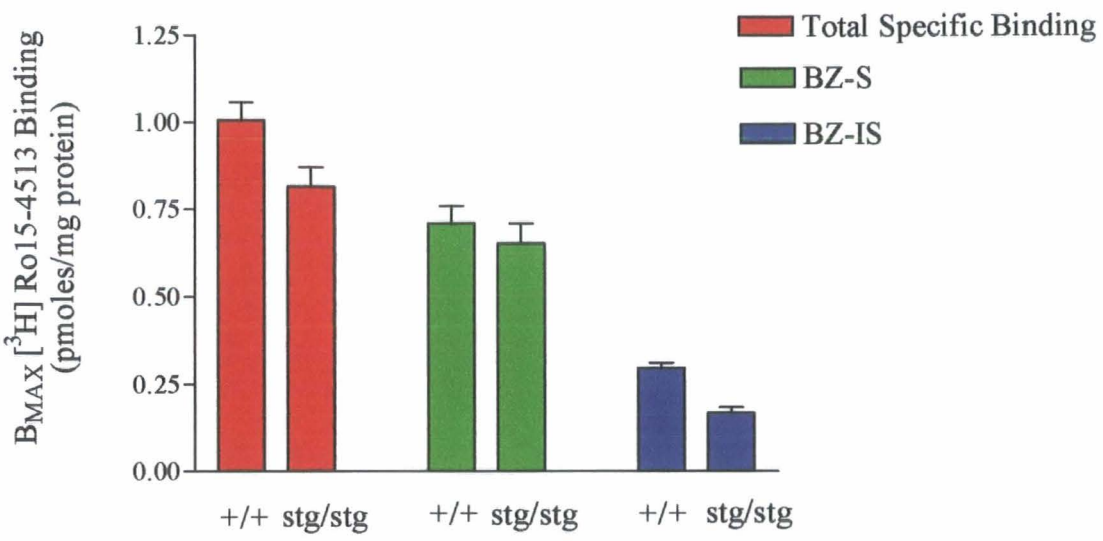

G

		+/+:+/stg	Stg/stg
Total Binding	B_{MAX} (pmoles/mg protein)	1.01 ± 0.05	0.82 ± 0.06
	K_D (nM)	3.76 ± 0.67	4.21 ± 0.95
BZ-S	B_{MAX} (pmoles/mg protein)	0.71 ± 0.08	0.65 ± 0.06
	K_D (nM)	3.31 ± 0.81	4.05 ± 1.19
BZ-IS	B_{MAX} (pmoles/mg protein)	0.30 ± 0.01	0.17 ± 0.02
	K_D (nM)	5.03 ± 0.76	5.09 ± 1.59

Figure 4.7. Total [^{3}H] Ro15-4513 binding (20 nM) to control (+/+:+/stg) and stargazer (stg/stg) adult mouse brain sections

A: Representative control and stargazer autoradiographs demonstrating high intensity of radiolabel in the cerebellum, cortex and hippocampus.

B: Standard curve of intensity versus radioactivity, constructed using ImageJ software to measure the intensity of [^{3}H] standards of known radioactivities (see Section 2.12.2.)

C: Column graph depicting the calculated radioactivities of the cerebellar granule cell layer of 6 control and 6 stargazer tissue sections, 10 measurements per section from n=2 mouse per strain.

D: Bar graph to demonstrate no significant decrease in total [^{3}H] Ro15-4513 binding in the cerebellar granule cell layer of the stargazer mutant mouse (90 ± 6% of control levels, p=0.07).

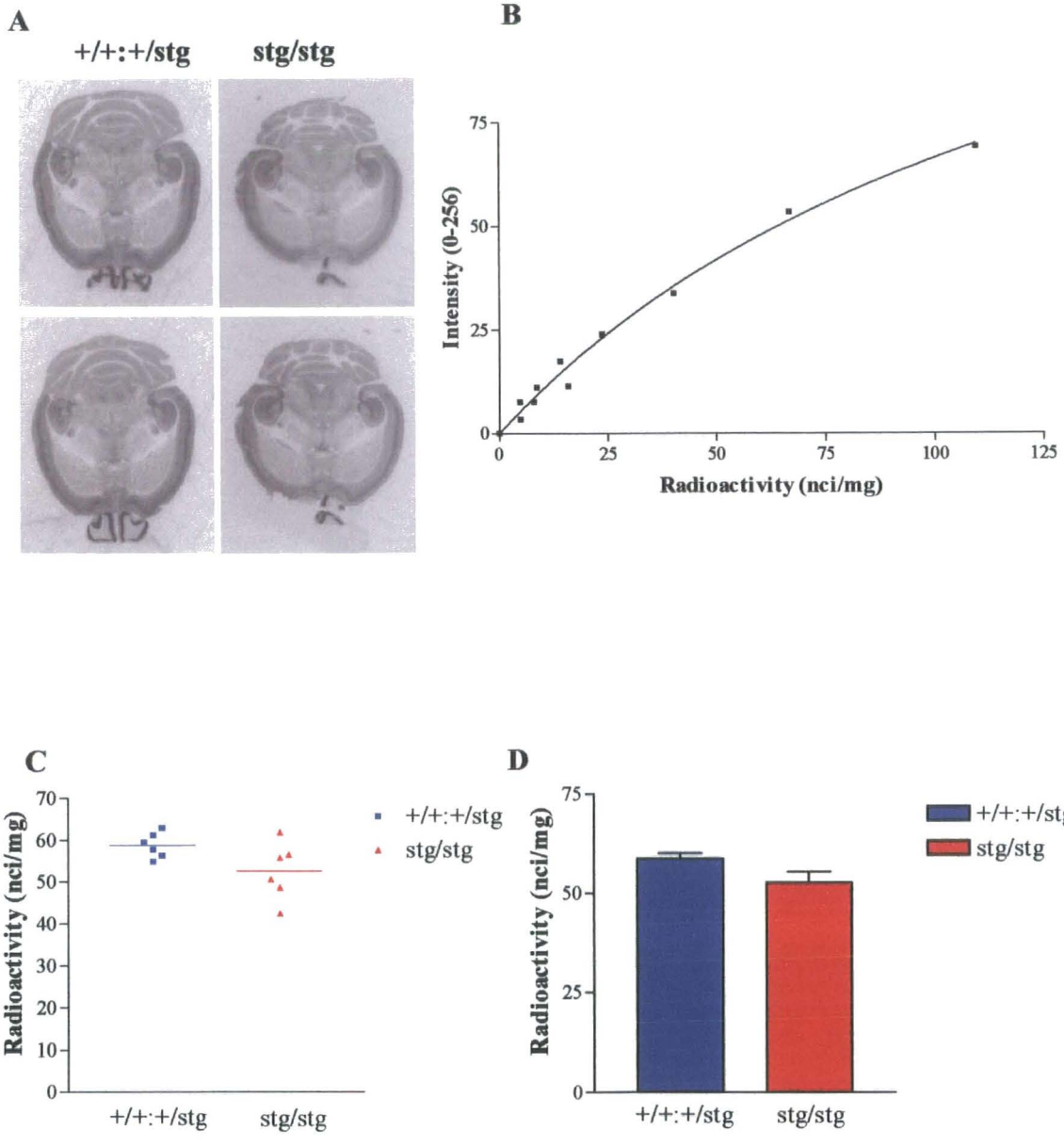
A
+/+:+/stg
stg/stg
B
Intensity (0-256)
75
50
25
0
0
25
50
75
100
125
Radioactivity (nci/mg)
C
Radioactivity (nci/mg)
70
60
50
40
30
20
10
0
+/+:+/stg
stg/stg
+/+:+/stg
stg/stg
D
Radioactivity (nci/mg)
75
50
25
0
+/+:+/stg
stg/stg
+/+:+/stg
stg/stg

Figure 4.8. [^{3}H] Ro15-4513 BZ-IS subtype binding (20 nM in the presence of 10 μM flunitrazepam) to control (+/+:+/stg) and stargazer (stg/stg) adult mouse brain sections

A: Representative control and stargazer autoradiographs demonstrating high intensity of radiolabel in the cerebellar granule cell layer. Autoradiographic film was processed to achieve the optimum signal in the CGC layer. Longer exposure times were required to achieve dentate gyrus labelling, see figure 7.3.

B: Standard curve of intensity versus radioactivity, constructed using ImageJ software to measure the intensity of [^{3}H] standards of known radioactivities (see section 2.12.2).

C: Column graph depicting the calculated radioactivities of the cerebellar granule cell layer of 5 control and 4 stargazer tissue sections, 10 measurements per section from n=2 mouse per strain.

D: Bar graph to demonstrate a significant decrease in the BZ-IS subtype of [^{3}H] Ro15-4513 binding in the cerebellar granule cell layer of the stargazer mutant mouse to 78 ± 10% of control levels, p=0.03.

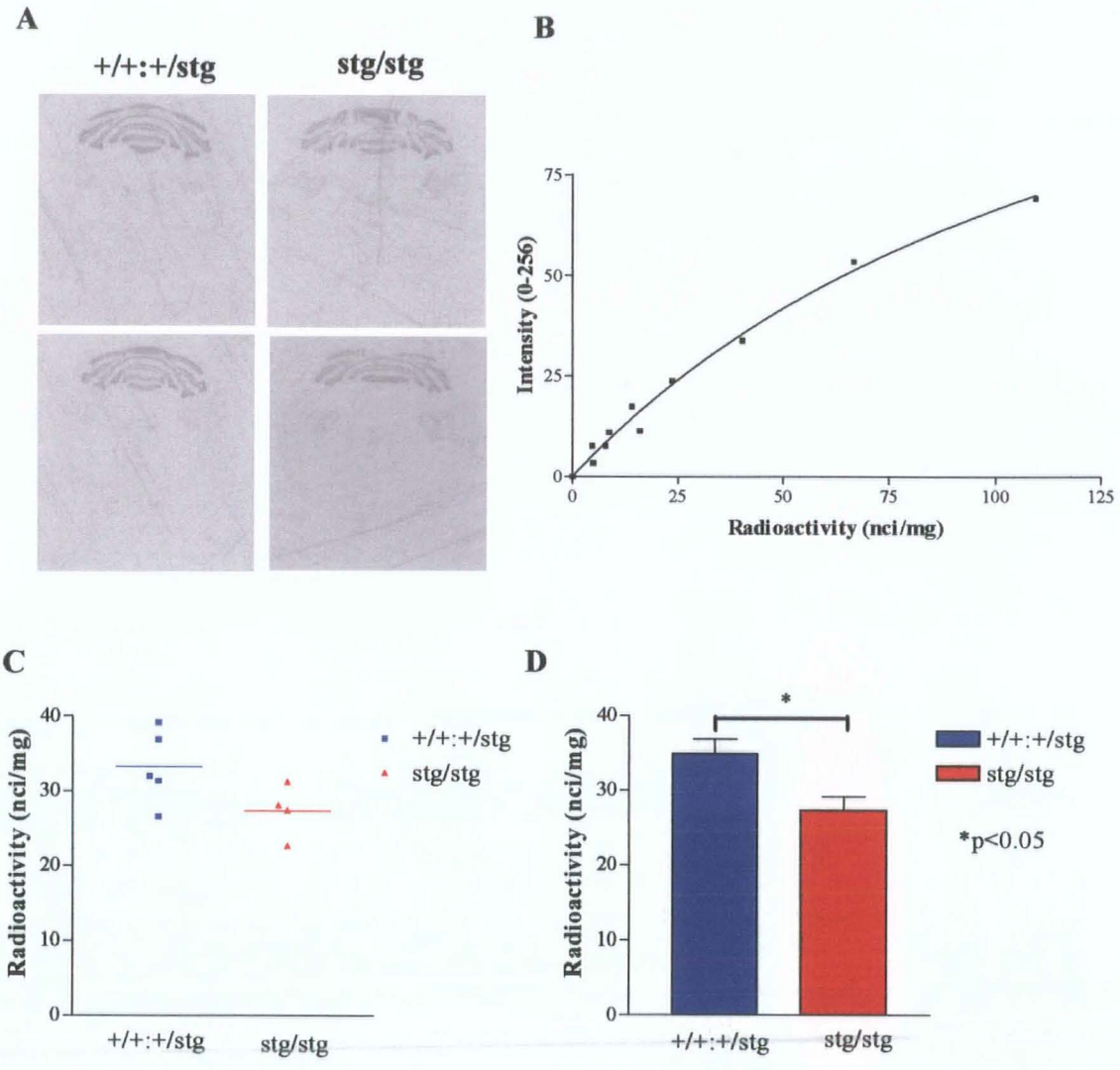
A
+/+:+/stg
stg/stg
B
Intensity (0-256)
75
50
25
0
0
25
50
75
100
125
Radioactivity (nci/mg)
C
Radioactivity (nci/mg)
40
30
20
10
0
+/+:+/stg
stg/stg
+/+:+/stg
stg/stg
D
Radioactivity (nci/mg)
*
40
30
20
10
0
+/+:+/stg
stg/stg
+/+:+/stg
stg/stg
*p<0.05

[^{3}H] Ro15-4513 binding was predominantly located in the cerebellum, cortex, olfactory bulbs and hippocampus. Quantification of the levels of radioactivity within the cerebellar granule cell layer of control and stargazer tissue sections revealed a slight decrease in total [^{3}H] Ro15-4513 binding in the CGC layer of the stargazer mutant that did not however reach statistical significance (90 ± 6% of control levels, p=0.07) (figure 4.7.).

In contrast, BZ-IS [^{3}H] Ro15-4513 binding was located solely in the CGC layer in control sections. Interestingly, in the stargazer mutant, BZ-IS binding was also observed in the dentate gyrus, an observation discussed in detail in chapter 7. Upon quantification of the levels of BZ-IS binding in the CGC layer, a significant decrease to 78 ± 10% of control levels was detected in the stargazer mutant, p=0.03 (figure 4.8.). Hence receptor autoradiographic studies also concur with radioligand binding studies on cerebellar membrane homogenates such that a significant decrease in α6 subunit-containing GABAR is observed in the stargazer mutant cerebellum.

4.3.3.3. [^{3}H] Flunitrazepam

[^{3}H] flunitrazepam was employed at a concentration of 5 nM in receptor autoradiographic studies on adult control and stargazer tissue sections, in order to determine any abnormalities in the BZ-S subtype (α1βγ2) of GABAR in the stargazer mutant CGC layer. The major areas of BZ-S expression observed by [^{3}H] flunitrazepam binding were noted in the cerebellum, cerebral cortex, olfactory bulbs and hippocampus. Quantification of radioactivity in the CGC layer of control and stargazer sections revealed a slight increase in BZ-S subtype of receptor binding in the stargazer mutant to 113 ± 8% of control levels which failed to reach statistical significance (p=0.19) (figure 4.9.).

4.3. DISCUSSION

[^{3}H] muscimol acts as a GABA mimetic and hence binds to the GABA binding site of the GABAR.

Figure 4.9. [^{3}H] Flunitrazepam binding (5 nM) to control (+/+:+/stg) and stargazer (stg/stg) adult mouse brain sections

A: Representative control and stargazer autoradiographs demonstrating high intensity of radiolabel in the cerebellum, hippocampus and cortex.

B: Standard curve of intensity versus radioactivity, constructed using ImageJ software to measure the intensity of [^{3}H] standards of known radioactivities (seeSection 2.12.2.).

C: Column graph depicting the calculated radioactivities of the cerebellar granule cell layer of 6 control and 6 stargazer tissue sections, 10 measurements per section from n=2 mouse per strain.

D: Bar graph to demonstrate no significant decrease in [^{3}H] flunitrazepam binding in the cerebellar granule cell layer of the stargazer mutant mouse (113 ± 8% of control levels, p=0.19).

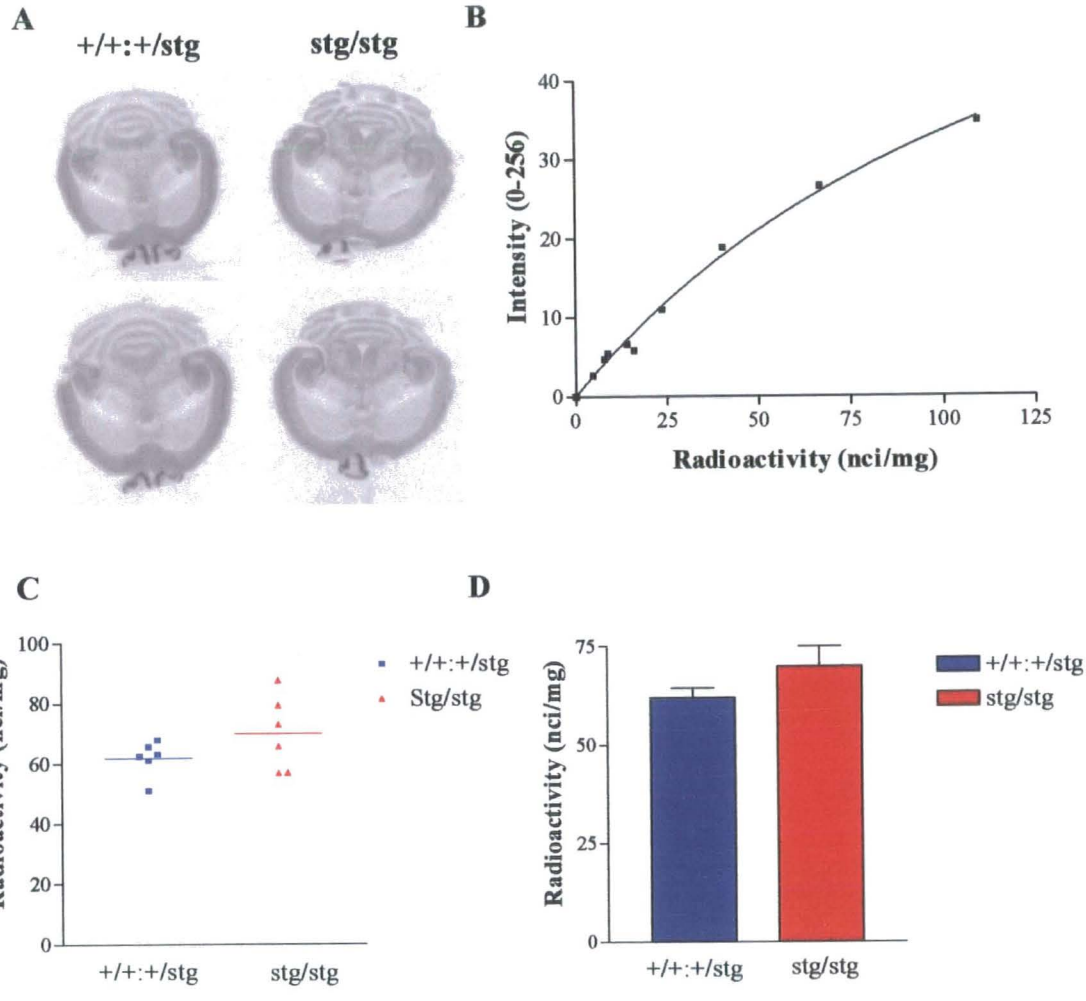
A
+/+:+/stg
stg/stg
B
Intensity (0-256)
Radioactivity (nci/mg)
C
Radioactivity (nci/mg)
+/+:+/stg
Stg/stg
D
Radioactivity (nci/mg)
+/+:+/stg
stg/stg

The GABA binding site is situated on the interface between α and β subunits. Consequently, the ligand binds to all GABAR which in the cerebellum includes α1β2/3γ2, α6β2/3γ2, α1α6β2/3γ2, α6β2/3δ and α1α6β2/3δ subunit combinations.

Radioligand binding studies on cerebellar membrane homogenates demonstrated a loss of [^{3}H] muscimol binding to 70 ± 10% of control levels in the stargazer mutant. This indicates either a uniform loss (by 30%) of all GABAR subtypes expressed (α1βγ2, α6βγ2, α1α6βγ2, α6βδ and α1α6βδ) or a selective loss of a particular subtype in the stargazer cerebellum. However, receptor autoradiography to control and stargazer tissue sections revealed a reduction in [^{3}H] muscimol binding to 54 ± 10% of control levels in the stargazer mutant. Discrepancies in the percentage reductions obtained by both methods can be explained a number of ways. Receptor autoradiography allows for the accurate quantification of radioactivity within separate layers of the cerebellum, in this case, the level of radioligand binding in the cerebellar granule cell layer was determined. In comparison, a cerebellar membrane homogenate is composed of the whole structure of the cerebellum, including the Purkinje cell layer, molecular layer and CGC layer. As a result, differences in specific GABAR subtypes in separate cellular layers may be masked.

It has been widely reported that [^{3}H] muscimol selectively highlights only certain types of GABAR by receptor autoradiography (Quirk *et al.*, 1995; Jones *et al.*, 1997; Mihalek *et al.*, 1999; Korpi *et al.*, 2002b). Korpi *et al.*, in 2002b proposed that [^{3}H] muscimol in autoradiography selectively binds to the GABAR α6 subunit-containing subtypes (α6βγ2+α6βδ). A lot of evidence has been gathered on this disparity in [^{3}H] muscimol binding on membrane preparations and receptor autoradiography from studies on knockout animals. Jones *et al.*, in 1997 reported a complete loss of [^{3}H] muscimol binding in the cerebellar granule cell layer of the α6 knockout mouse. Korpi *et al.*, in 2002a demonstrated a loss of [^{3}H] muscimol binding in double knockout animals, where the GABAR α6 and δ subunits were absent, but the restoration of ligand binding in the CGC layer in the presence of the α6 subunit, but not the δ subunit alone. It was suggested that

a factor exists specifically associated with the α1/α2/α3/α5βγ2 GABAR on native membranes that prevents muscimol binding in receptor autoradiography (Korpi *et al.*, 2002a).

The selectivity of [^{3}H] muscimol for the cerebellar α6 subunit-containing GABARs in receptor autoradiography suggests that the loss of [^{3}H] muscimol binding (54 ± 10% of control levels) in the stargazer mutant is due to a loss of α6 subunit-containing receptors in the cerebellar granule cell layer. This is further supported by the dramatic reductions in the protein expression of the α6 and δ subunits in the stargazer cerebellum found by western blotting, which were reduced to 39 ± 22% and 36 ± 21% of control levels respectively (see section 3.2.2.). Thompson *et al.*, in 1998 also reported a dramatic reduction in α6 subunit expression, to 23 ± 8% of control levels. Interestingly the γ2 subunit is relatively spared (81 ± 26% of control levels).

[^{3}H] Ro15-4513 is a partial inverse agonist at the benzodiazepine binding site of the GABAR, which is located between the α and γ subunits. Consequently, the ligand is selective for γ subunit-containing GABAR which in the cerebellum include α1β2/3γ2, α6β2/3γ2 and α1α6β2/3γ2. It is possible to further subdivide these GABAR according to their sensitivity to benzodiazepines. The addition of flunitrazepam, a benzodiazepine agonist, acts to distinguish the benzodiazepine-insensitive (BZ-IS) subtype of receptor, namely α6 subunit-containing GABAR in the cerebellum. The benzodiazepine-sensitive subtype of receptor is predominantly the α1 subunit-containing receptors in the cerebellum and can be determined by the subtraction of the BZ-IS population of receptors from the total level of radioligand binding obtained.

Based upon the dramatic reductions in the protein expression of the α6 subunit observed in the stargazer cerebellum by western blotting, it would be predicted that this reduction would result in a loss of the BZ-IS subtype of [^{3}H] Ro15-4513 binding. Radioligand binding to cerebellar membrane homogenates demonstrated a reduction to 57 ± 13% of control levels in BZ-IS binding in the stargazer cerebellum. This reduction was also observed in the receptor autoradiographic

studies, where a significant decrease in BZ-IS binding was observed in the CGC layer of the stargazer mutant, to 78 ± 10% of control levels, p=0.03. Thompson *et al.*, in 1998 also reported a dramatic loss of the BZ-IS subtype of [^{3}H] Ro15-4513 binding in the stargazer mutant, to 38 ± 10% of control levels. This reported loss is significantly greater than the decrease in BZ-IS binding observed in the current study. A possible explanation for such a discrepancy is the difference in the background strain of mice used in the studies. C57BL/6J animals were employed in the initial study, whereas in the current investigations, C3B6Fe$^+$ mice were used, which is essentially the background strain of the stargazer mutant. Therefore, any differences in reported results may be due to strain variability (see section 3.3.2.).

Determination of the total levels of [^{3}H] Ro15-4513 binding in control and stargazer cerebellum revealed no significant difference between the two strains, with calculated reductions to 81 ± 10% of control levels in the stargazer mutant on cerebellar membranes and to 90 ± 6% by receptor autoradiography. Therefore, there is no significant difference in the total number of γ2-containing GABAR in the stargazer mutant cerebellum. Western blotting further corroborates these findings, which revealed a decrease to 81 ± 26% of control levels in γ2 subunit protein expression in the stargazer mutant.

The BZ-S subtype of receptor, representing α1βγ2 GABAR was not significantly affected in cerebellar membrane homogenates, being 92 ± 15% of control levels in the stargazer mutant. Likewise [^{3}H] flunitrazepam binding which highlights the BZ-S subtype of receptor in autoradiography was not significantly different in the CGC layer of stargazer compared to controls (113 ± 8% of control levels). The protein expression levels of the GABAR α1 subunit also concur with the BZ-S radioligand binding results, such that no significant difference in the expression levels were found between the two mouse strains (72 ± 34% of control levels, n=3, p=0.062).

Pöltl *et al.*, in 2003 identified the contributions of each GABAR subtype to the mouse cerebellar GABAR population by immunodepletion by immunoaffinity

chromatography and western blotting. GABAR γ2 subunit containing receptors were found to represent 68% of total GABAR in the cerebellum, while GABAR δ subunit-containing receptors contributed 29% of total GABAR with the remaining 3% attributable to minor GABAR populations. [^{3}H] muscimol when used in receptor autoradiography binds to GABAR α6 subunit-containing receptors only (Mihalek *et al.*, 1999; Korpi *et al.*, 2002a). Therefore, in the cerebellum these would include α1α6βγ2, α6βγ2, α1α6ββδ and α6βδ GABAR, which contribute 22%, 7%, 10% and 18% to the total number of GABAR in the cerebellum respectively (Pöltl *et al.*, 2003). Hence, by extrapolation, α1α6βγ2 and α6βγ2 contribute 51% of the total GABAR signal obtained by [^{3}H] muscimol autoradiography. α1α6ββδ and α6βδ contribute 49% of total signal.

The BZ-IS subtype of [^{3}H] Ro15-4513 autoradiography was shown to be reduced by 22% in the stargazer mutant CGC layer, conferred by α1α6βγ2 and α6βγ2. Therefore, by extrapolation, this reduction would represent a loss of 11% of the total [^{3}H] muscimol autoradiography signal. However, [^{3}H] muscimol autoradiography revealed a 47% decrease in binding in the stargazer CGC layer, which is not fully accountable by a loss of 11% of binding due to γ2 subunit containing GABAR. Therefore, it could be predicted that there is a loss of 36% of the total signal attributable to δ subunit containing GABAR, resulting in a 73% loss of total δ subunit containing GABAR, making this the major subtype abnormality so far observed in the stargazer cerebellum.

In conclusion, possible abnormalities in the GABAR profile of the stargazer mutant mouse were determined by radioligand binding techniques to both cerebellar membrane homogenates and tissue sections by receptor autoradiography. [^{3}H] muscimol binding to cerebellar membranes revealed a decrease to 70 ± 10% of control levels, suggesting a loss of total GABAR in the stargazer cerebellum. Receptor autoradiography using [^{3}H] muscimol, which is selective for α6 subunit-containing receptors, revealed a decrease to 54 ± 10% of control levels in the CGC layer of the stargazer mutant. Total levels of [^{3}H] Ro15-4513 binding were not found to differ significantly between control and stargazer animals. However, upon further pharmacological dissection, the BZ-IS

subtype of receptor, conferred by α6βγ2 and α1α6βγ2 receptors was found to be reduced to 57 ± 13% of control levels in cerebellar membrane homogenates and to 78 ± 10% of control levels in the CGC layer by receptor autoradiography. By difference analysis, if there is a dramatic decrease in the total number of GABAR as revealed by a loss of [^{3}H] muscimol binding, yet the total level of [^{3}H] Ro15-4513 binding is unchanged, this implies that the major GABAR abnormality in the stargazer mutant cerebellum is due to a deficit of α6βδ subunit-containing GABARs.

CHAPTER 5. ARE THE CEREBELLAR $GABA_A$ RECEPTOR DEFICITS OBSERVED IN STARGAZER MUTANT MICE DUE TO COMPROMISED AMPA RECEPTOR EXPRESSION?

5.1. INTRODUCTION

Previous results of this study identified a dramatic and relatively selective reduction in the expression of the cerebellar granule cell-specific $GABA_A$ receptor (GABAR) α6, δ but not γ2 subunits in the stargazer mutant mouse cerebellum, to 39 ± 22%, 36 ± 21% and 81 ± 26% of control levels, respectively (see section 3.3.2.). These observations were compatible with a reduction in [^{3}H] muscimol binding by *in situ* autoradiography to 54 ± 10% of control levels in the stargazer cerebellar granule cell (CGC) layer, suggesting a dramatically lower level of expression of α6βδ receptors in the stargazer mutant (see section 4.3.2.2.; 4.4).

In order to investigate the mechanisms that link failure to express an AMPA receptor (AMPAR) trafficking/targeting protein with a selective influence on the inhibitory profile of CGCs, it was necessary to utilise a dynamic model system which can recapitulate the mechanisms governing GABAR expression and trafficking seen *in vivo*. Since the expression of CGC-specific GABAR subunits α6 and δ have been shown to be selectively reduced in the stargazer mutant, cultured CGCs were utilised in the current study. Furthermore, it has been widely reported that the expression of GABAR *in vivo* can be successfully reproduced in cultured cerebellar granule cells (CGCs) (Beattie & Siegel, 1993; Thompson *et al.*, 1994; 1996; Zheng *et al.*, 1994; Behringer *et al.*, 1996).

The majority of previous studies have utilised rat CGCs, which have an absolute requirement for depolarising conditions (25 mM KCl) for survival and maintenance in culture, as under non-depolarising conditions they rapidly undergo apoptosis and degenerate (Gallo *et al.*, 1987). Gault and Siegel in 1997 demonstrated that the expression and maintenance of the GABAR δ subunit is

modulated by KCl-mediated depolarisation in cultured rat CGCs. GABAR δ subunit mRNA was not detected in cultures maintained at physiological levels of KCl (5 mM). Whereas, following depolarisation with 25 mM KCl which activated L-type voltage-gated calcium channels, transcription of the GABAR δ gene was increased. In terms of rat CGC development this is in accordance with what is observed *in vivo*, i.e. KCl-mediated depolarisation appears to direct **rat** CGCs along an appropriate path of neuronal development.

Intriguingly, the contrary appears to apply to mouse CGCs (Mellor *et al.*, 1998; Ives *et al.*, 2002a). CGCs derived from some mouse strains do not require depolarising conditions for survival (Mellor *et al.*, 1998; Fujikawa *et al.*, 2000). Under basal culture conditions (5 mM KCl) these neurons are electrically active (Mellor *et al.*, 1998). Furthermore, Ives *et al.*, in 2002 have reported that mouse CGCs maintained under 5 mM KCl culture conditions closely mimic the developmental expression profile of GABAR seen *in vivo*. Interestingly, Mellor *et al.*, in 1998 reported that if mouse CGCs are maintained under depolarising conditions (25 mM KCl) for prolonged periods of time (>3 DIV) as used to maintain rat CGCs, they become electrically silent, in that they do not exhibit spontaneous action potentials, miniature excitatory postsynaptic currents (mEPSCs) or miniature inhibitory postsynaptic currents (mIPSCs). In addition, KCl-mediated depolarisation induced a switch in GABAR subunit expression, such that an immature GABAR profile was achieved. Therefore, under KCl-mediated depolarising conditions, the GABAR profile of **mouse** CGCs does not mirror the expression profile seen in maturing CGCs *in vivo* (Ives *et al.*, 2002a). Clearly this implies that electrical activity of CGCs is important in orchestrating the developmental maturation and expression levels of GABARs, that is characterised by the emergence of the α6 and δ subunits-that are compromised in stargazer mutant mice.

More recently, a number of groups have reported that expression of GABAR subunit mRNAs in mouse CGCs is affected by depolarisation following activation of ionotropic glutamate receptors (e.g. by kainic acid, a non-NMDA receptor agonist) (Engblom *et al.*, 2003; Martikainen *et al.*, 2004). However,

effects reported on GABAR δ subunit expression following kainic acid-treatment are controversial. Martikainen *et al.*, in 2004 reported a reduction in δ subunit mRNA expression to 28% of control levels following AMPAR activation compared to 5K by RT-PCR. In contrast, Engblom *et al.*, in 2003 report no effect on GABAR δ subunit mRNA levels following kainic acid-mediated depolarisation, compared to 5K controls. Observations reporting GABAR δ subunit mRNA modulation following kainic acid treatment, acting to activate AMPAR and kainate receptors are not compatible with our previous observations of GABAR δ subunit protein expression in the stargazer mutant cerebellum, where we observed a significant reduction in GABAR δ subunit expression, in a CGC which fails to express AMPAR at the cell surface. Is the deficit in AMPAR expression in stargazer CGCs responsible for aberrant expression of δ subunit-containing GABARs?

Previous studies have been unable to distinguish if kainic acid depolarisation-induced effects on GABAR expression occurred as a consequence of AMPA or kainate receptor activation. The stargazer mutant mouse provides an invaluable tool to allow for the distinction between the effect of activating each type of receptor, CGCs only express TARPγ2 of the family of transmembrane AMPA receptor regulatory proteins (TARPs) and therefore rely exclusively on this protein for surface trafficking and targeting of AMPARs in CGCs. In stargazer mice, where TARPγ2 is not expressed, CGCs from this mouse can be regarded as AMPAR 'incompetent', but kainate receptor 'competent' (Hashimoto *et al.*, 1999), as kainate receptors are relatively unaffected by the mutation (Chen *et al.*, 2003). Therefore, only kainate receptors would be activated in response to kainic-acid mediated depolarisation in stg/stg CGCs whilst CGCs derived from control mice are AMPA and kainate receptor competent.

The aims of this chapter were to firstly characterise the developmental profile of mouse cultured CGCs in terms of the GABAR subunits they express and their migration and morphology at different time points in culture. Secondly, to determine the effects of depolarisation on the GABAR profile and the morphology and cellular migration of CGCs in culture. Finally, to re-investigate

the effects of kainic acid-mediated depolarisation on the expression of the GABAR δ subunit in culture (Engblom *et al.*, 2003; Martikainen *et al.*, 2004). Furthermore, to determine if the effects on δ subunit expression observed *in vivo* in the stargazer could be attributed to differential activation of AMPA or kainate receptors by comparing expression in control and stargazer CGCs.

5.2. RESULTS

In order to study the effects of excitatory inputs on the expression and trafficking of the GABAR subunits, it was first necessary to characterise the culture system in terms of the development of expression of the GABAR subunits with time *in vitro*, the patterns of maturation, migration and morphology in culture and the survival and maintenance of mouse CGCs in response to depolarisation.

5.2.1. Developmental profile of the morphology and migration of mouse CGCs in culture

Figure 5.1. depicts the development of mouse CGCs under 5K culture conditions with time, in terms of their morphology, migration and cellular arrangement. Cerebella were dissected from P6-7 mouse neonates and CGCs cultured from them according to standard procedures (see section 2.14). CGCs were fixed with 4% paraformaldehyde in 0.2 M phosphate buffer at 2 day intervals in culture from 1 days *in vitro* (DIV) to 7 DIV and viewed using a Nikon diaphot 300 microscope. Images were taken at x200 magnification.

Figure 5.1.A demonstrates CGCs at 1 DIV, where the cells had adhered to the poly-L-lysine coated surface of the culture dish and had begun to elongate and form neuronal processes. At 3 DIV, the CGCs were beginning to form complex networks of neuronal processes, with a bipolar morphology characteristic of CGCs in culture (see figure 5.1.B). By 5 DIV, there was evidence that the CGCs had begun to migrate towards each other to from cellular aggregates, with numerous processes extruding from a central core of cell bodies (see figure 5.1.C). At 7 DIV, the abundance of cellular aggregates was greatly increased,

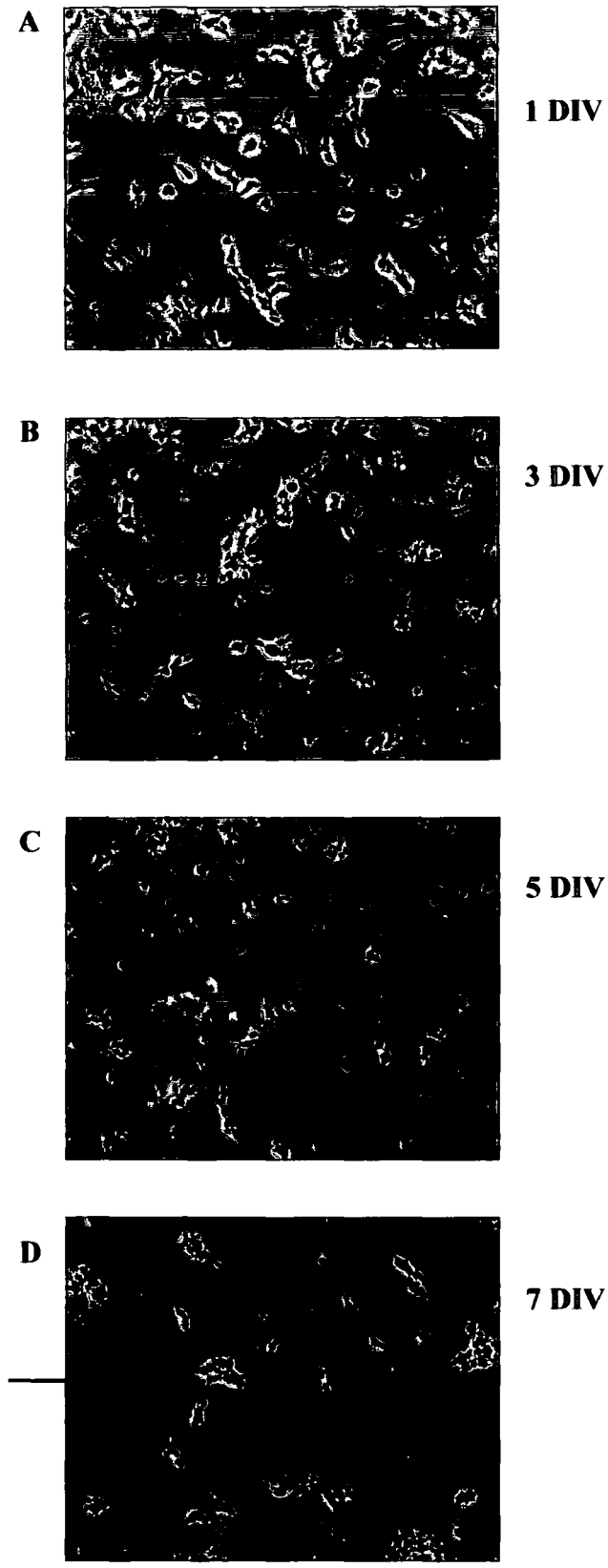

Figure 5.1. Development of adult mouse control (+/+:+/stg) cerebellar granule cells (CGCs) in culture

A: CGCs at 1 Day in vitro (DIV).
B: CGCs at 3 DIV, note the elaboration of neuronal processes.
C: CGCs at 5 DIV. CGCs begin to migrate towards each other to form the cellular aggregates.
D: CGCs at 7 DIV, note the abundance of cellular aggregates, indicated with an arrow.

with compact aggregates connected by large cables of neuronal processes (see figure 5.1.D).

5.2.2. Developmental expression of GABAR subunits in culture

The expression of the GABAR subunits was determined in CGCs derived from P6-7 control (+/+:+/stg) mouse neonates cultured by standard methods and harvested at 2 day intervals from 1 DIV to 9 DIV for western blot analysis.

5.2.2.1. GABAR α1 subunit expression

Figure 5.2.A represents western blot analysis of cultured control CGCs harvested at 2 day intervals *in vitro* and probed with anti-GABAR α1 subunit-specific antibody at 1 μg/ml. Expression of the α1 subunit appeared at low levels at 1 DIV and continued to increase until a plateau was reached at 7 DIV. Two immunoreactive bands were highlighted with the anti-GABAR α1 antibody. The higher molecular weight species has previously been shown to correspond to the α1 subunit (Mr 53 000 Da) (Thompson *et al.*, 1996). The lower molecular weight band is likely to be a proteolytically processed fragment of the mature α1 subunit (Duggan *et al.*, 1991).

5.2.2.2. GABAR α6 subunit expression

Expression of the GABAR α6 subunit became evident at low levels at 3 DIV and increased to plateau at 5-7 DIV. Two further bands were identified by the anti-GABAR α6 subunit antibody at 1 μg/ml which may represent cross-reacting proteins, differentially glycosylated forms of the subunit or in the case of the immunoreactive band highlighted at a lower molecular weight than the α6 subunit, a degradation product (see figure 5.2.B).

Figure 5.2. Developmental profile for the expression of GABAR subunits in cultured cerebellar granule cells

Control CGCs cultured under basal conditions (5 mM KCl) harvested at 2 day intervals from 1 DIV to 9 DIV and subjected to western blot analysis (10 μg protein per gel lane) using subunit-specific antibodies compared to adult control cerebellar membranes (+/+ cblm).

A: GABAR α1 subunit

B: GABAR α6 subunit

C: GABAR β2 subunit

D: GABAR β3 subunit

E: GABAR δ subunit

F: GABAR γ2 subunit

G: AMPAR GluR2 subunit

H: TARPγ2

I: β-actin

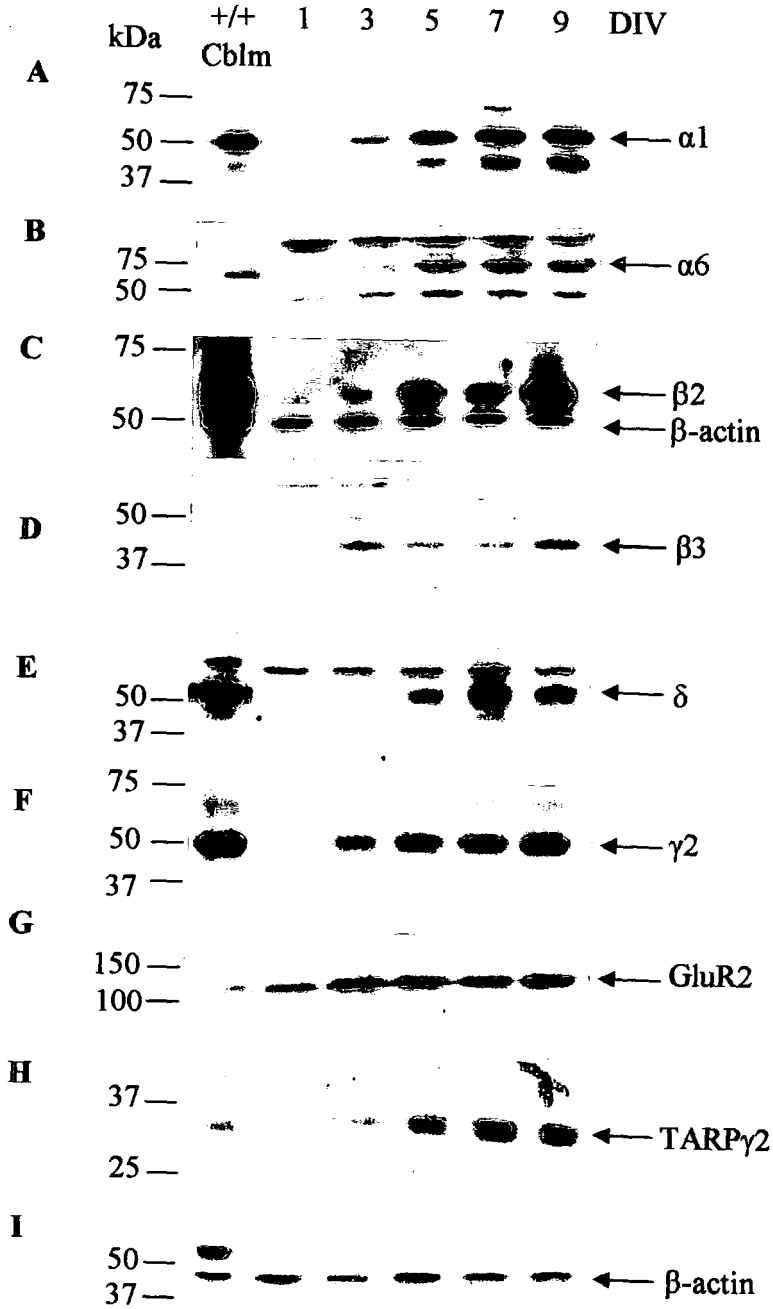
kDa
+/+
Cblm
1
3
5
7
9
DIV
A
75
50
37
α1
B
75
50
α6
C
75
50
β2
β-actin
D
50
37
β3
E
50
37
δ
F
75
50
37
γ2
G
150
100
GluR2
H
37
25
TARPγ2
I
50
37
β-actin

5.2.2.3. GABAR β2 subunit expression

Figure 5.2.C demonstrates CGCs subjected to immunoblotting and probed with anti-GABAR β2 subunit-specific antibody at 0.5 μg/ml. Expression of the β2 subunit appeared at low levels at 1-3 DIV and increased to reach a peak at 7-9 DIV.

5.2.2.4. GABAR β3 subunit expression

CGCs subjected to immunoblotting and probed with an anti-GABAR β3 subunit-specific antibody at 0.5 μg/ml demonstrated a low level of expression at 1 DIV which increased with time in culture, to plateau at 3-5 DIV (see figure 5.2.D).

5.2.2.5. GABAR δ subunit expression

Expression of the GABAR δ subunit appeared at 5 DIV and peaked at 7-9 DIV. Immunoblot probed with anti-GABAR δ subunit antibody at 1 μg/ml highlighted an immunoreactive species corresponding to the δ subunit (Mr 54 0000 Da) and a protein of higher molecular weight which as discussed earlier is most likely a cross-reacting, non-δ subunit protein (see figure 5.2.E).

5.2.2.6. GABAR γ2 subunit expression

Figure 5.2.F shows western blot analysis of cultured CGCs probed with anti-GABAR γ2 subunit-specific antibody at 1 μg/ml which highlighted one band with Mr 45 000-50 000 Da, corresponding to the GABAR γ2 subunit. Expression of the GABAR γ2 subunit appeared at low levels at 1 DIV and increased in expression, to peak at 7-9 DIV.

In order to conduct experiments to compare GABAR subunit modulation between control and stargazer CGCs, it was necessary to determine the point at which TARPγ2, the AMPAR auxiliary protein ablated in the stargazer mutant, is

expressed in a control neuron. Furthermore, to determine the time point in culture when expression of AMPAR subunits occurs in control CGCs.

5.2.2.7. TARPγ2 expression

Western blot analysis of cultured CGCs probed with anti-pan TARP antibody at 1 μg/ml highlighted a single immunoreactive species with a molecular weight of approximately 36 000 Da, corresponding to TARPγ2. Expression of TARPγ2 appeared at 3 DIV at low levels and increased in expression to plateau at 7-9 DIV (see figure 5.2.G).

5.2.2.8. AMPAR GluR2 subunit expression

In order to determine the presence of AMPAR subunits in cultured mouse CGCs, expression of the GluR2 subunit was characterised by western blotting, using an anti-AMPAR GluR2 antibody at 1:500 dilution. Figure 5.2.H shows expression of the GluR2 subunit consistently at all time points in culture.

5.2.2.9. Expression of β-actin in cultured CGCs

Following the characterisation of the expression of the principal GABAR subunits in culture, expression of β-actin was determined, to ensure that equal levels of protein were analysed per time point sample (Figure 5.2.I)

Western blot analysis of the principal GABAR subunits in culture demonstrated markers of mature CGCs, GABAR α6 and δ subunits were expressed at high levels in culture between 7-9 DIV, corresponding to P13/14-P15/16, when these subunits are expressed *in vivo* (see figure 1.2.). Cells demonstrated migration in culture to form compact cellular aggregates, previously proven to correlate with GABAR α6 subunit expression (Ives *et al.*, 2002a). Furthermore, cell viability was high at 7 DIV, with the generation of >95% pure primary CGC population. Therefore, for all subsequent experiments, CGCs were used for further experimentation at 7 DIV.

5.2.3. Effects of depolarisation on the migration and maturation of adult control (+/+:+/stg) and stargazer (stg/stg) mouse CGCs in culture

Figure 5.3. demonstrates the cellular arrangement, maturation and morphology of control and stargazer CGCs in culture in response to depolarisation mediated by KCl and kainic acid (7 DIV). Cerebella were simultaneously dissected from age-matched control and stargazer mice at P6-7 and cultured by standard methods. CGCs were treated at 1 DIV with KCl (fc=25 mM) or kainic acid (100 μM), fixed with 4% paraformaldehyde in 0.2 M phosphate buffer at 7 DIV and viewed under a Nikon diaphot 300 microscope. Images were taken at x200 magnification.

Figure 5.3.A&B represent control (A) and stargazer (B) CGCs cultured under normal physiological KCl concentrations (5 mM). CGCs derived from both mouse strains formed cellular aggregates, connected by thick cables of neuronal processes. Upon depolarisation with KCl (fc=25 mM), both control and stargazer CGCs responded differently in culture. CGCs failed to migrate towards each other to from cellular aggregates, rather they appeared to remain stationary and formed a network of neuronal processes (figure 5.3. C&D). This is in agreement with, Ives *et al.*, in 2002 who also reported similar patterns of migration of CGCs cultured under KCl-mediated depolarising conditions.

Kainic acid-mediated depolarisation however, appeared to affect the migration of CGCs derived from control and stargazer mice differently. Stargazer CGCs more closely resembled CGCs cultured under 5 mM KCl conditions, forming compact cellular aggregates interconnected by a network of cables of processes (figure 5.3.F). In comparison, CGCs derived from control animals responded similarly to kainic acid-mediated as to KCl-induced depolarisation. Few cellular aggregates were observed in control CGCs cultured in the presence of kainic acid, rather a complex network of neuronal processes was evident interspersed with numerous cell bodies (figure 5.3.E).

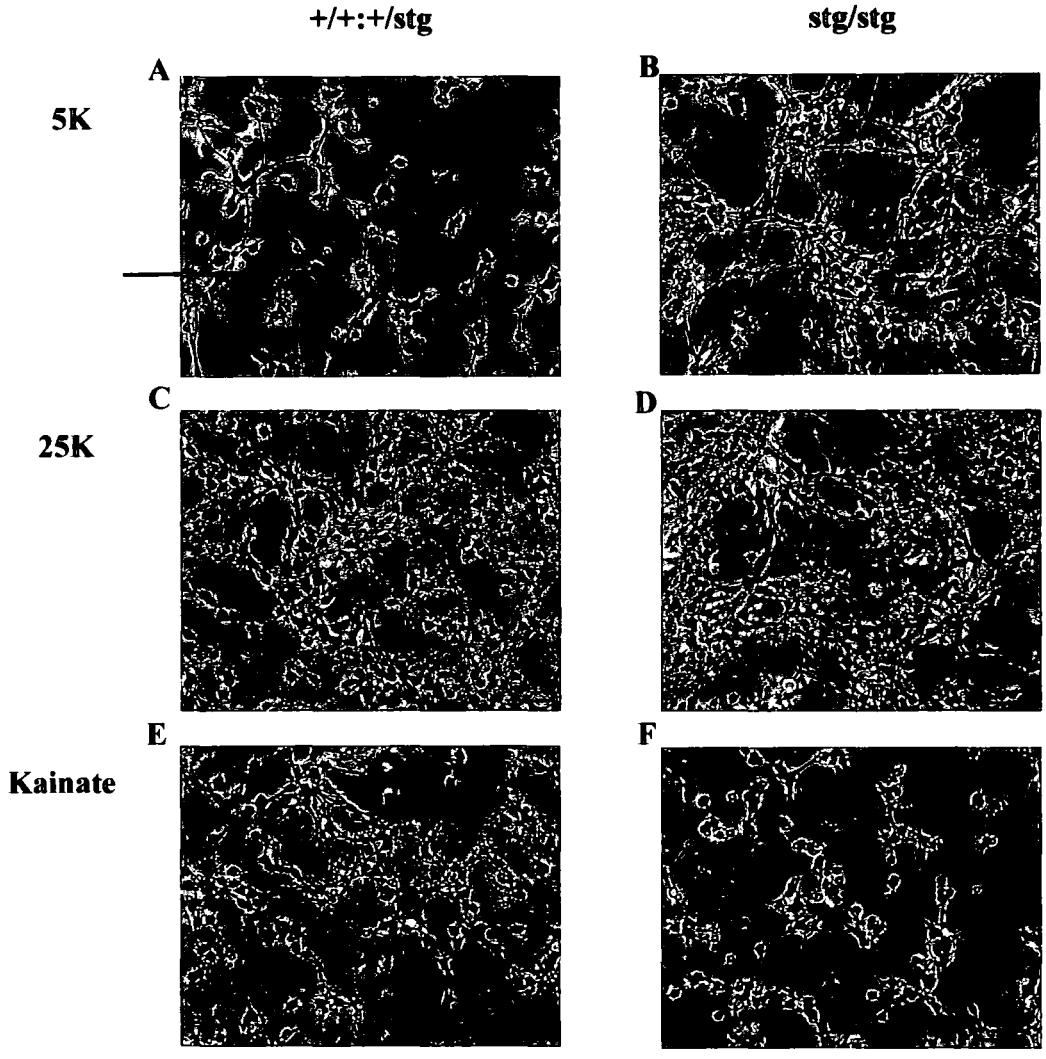

Figure 5.3. The effects of culture conditions on the cellular arrangement and morphology of cerebellar granule cells (CGCs) in culture

A&B: CGCs cultured under physiological conditions (5 mM KCl, '5K')
C&D: CGCs cultured under depolarising conditions (25 mM KCl, '25K')
E&F: CGCs cultured in the presence of kainic acid (100 μM 'Kainate')
Arrow indicates cellular aggregate.
Scale bar: 0.05 mm

5.2.4. Effects of KCl-mediated depolarisation on GABAR subunit expression in control and stargazer CGCs.

Previous findings in the lab have indicated a role for neuronal activity in the regulation of GABAR subunit expression in cultured mouse CGCs (Ives *et al.*, 2002a). In order to confirm and extend previous observations, control and stargazer CGCs were cultured simultaneously from age-matched littermates, treated at 1 DIV with KCl (fc=25 mM) and harvested at 7 DIV for western blot analysis.

5.2.4.1. Control CGCs

In agreement with previous findings in this lab (Ives *et al.*, in 2002a), expression of the GABAR α1 subunit protein was found to be dramatically reduced in control CGCs cultured under 25K conditions to 7 ± 15% of 5K levels ($p=0.01$). Western blot analysis of cultured control CGCs subjected to KCl-mediated depolarisation probed with anti-GABAR α6 subunit-specific antibody revealed a dramatic reduction in α6 subunit expression to 25 ± 1% of 5K levels. Ives *et al.*, in 2002 also reported a dramatic loss of expression of the α6 subunit in control CGCs following KCl-mediated depolarisation (to 3 ± 2% of 5K levels).

Immunoblotting results indicated differential modulation of the expression of the GABAR β subunits in response to KCl-mediated depolarisation. The expression of the β2 subunit was undetectable by immunoblotting following KCl-mediated depolarisation (figure 5.4.). In contrast, β3 subunit expression was increased dramatically (251 ± 29% of 5K levels, $p<0.01$). These observations are in agreement with Ives *et al.*, in 2002 who reported that the β2 subunit was undetectable under 25K conditions while β3 subunit levels were increased to 167 ± 8% of 5K levels.

To extend previous studies, expression levels of the GABAR γ2 and δ subunits were quantified in control CGCs following KCl-mediated depolarisation. A

Figure 5.4. Effects of KCl-mediated depolarisation on the expression of GABAR subunits in cultured control and stargazer CGCs

A: Western blot analysis of GABAR subunit expression in cultured control (+/+:+/stg) CGCs (7 DIV) treated in the absence (5K) and presence of increased extracellular KCl (25 mM). Note the **reduction** in expression of the GABAR α1, α6 and γ2 subunits following KCl-mediated depolarisation. Furthermore, an **up-regulation** of β3 and δ subunit expression was observed in response to KCl-mediated depolarisation. Data represents mean ± SEM from n=3 cultures as presented in figure 5.6.

B: Western blot analysis of GABAR subunit expression in cultured stargazer (stg/stg) CGCs (7 DIV) treated in the absence (5K) and presence of increased extracellular KCl (25 mM). Note the **reduction** in expression of the GABAR α1, α6 and γ2 subunits following KCl-mediated depolarisation. Furthermore, an **up-regulation** of β3 and δ subunit expression was observed in response to KCl-mediated depolarisation. Data represents mean ± SEM from n=3 cultures as presented in figure 5.6.

A: Control CGCs

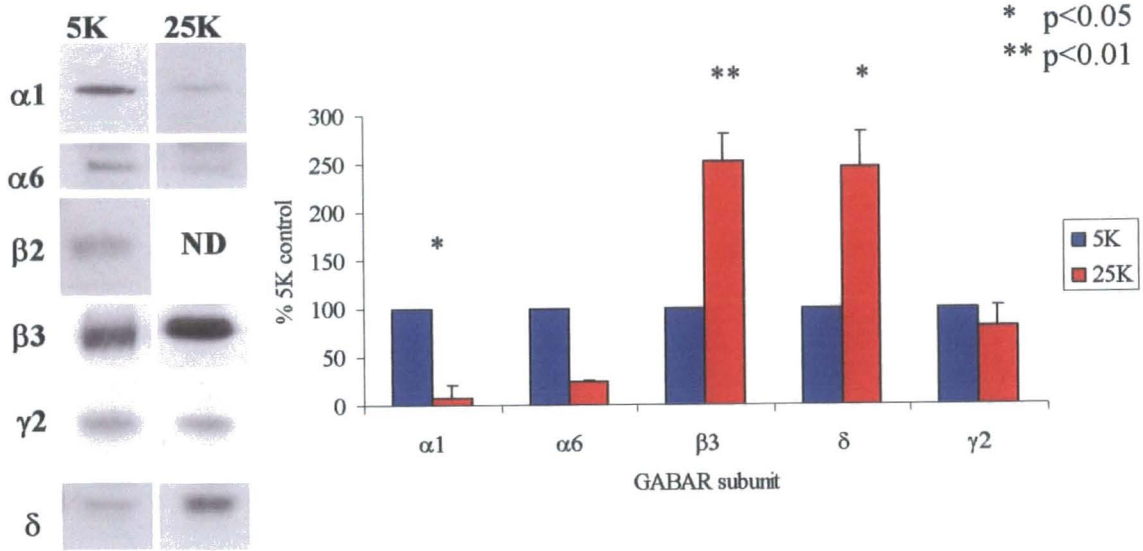

B: Stargazer CGCs

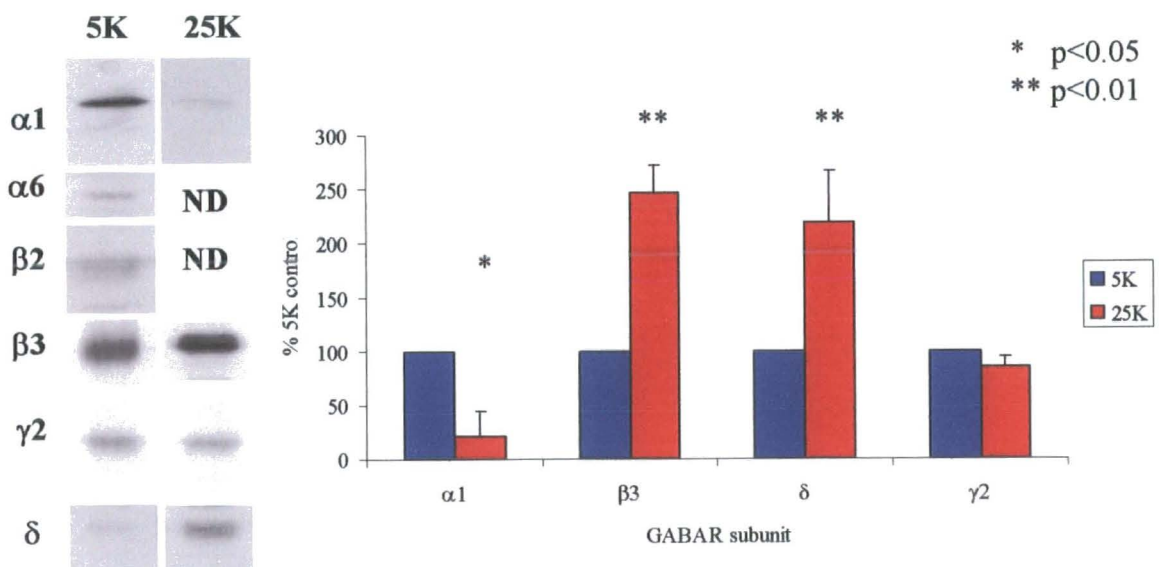

slight reduction in expression of the GABAR γ2 subunit was observed to 81 ± 21%, which however failed to reach statistical significance, p=0.36. In contrast, the expression of the δ subunit protein was dramatically increased to 245 ± 36% of 5K levels, p=0.02.

5.2.4.2. Stargazer CGCs

A significant reduction in GABAR α1 subunit expression was observed in stargazer CGCs upon KCl-mediated depolarisation, to 21 ± 23% of 5K levels (p=0.05). GABAR α6 subunit expression was not detectable following KCl-mediated depolarisation. Regulation of β subunit expression was differentially modulated in response to KCl-mediated depolarisation, as observed in control CGCs, such that expression of the GABAR β2 subunit was undetectable. Conversely, expression of the β3 subunit was increased to 246 ± 26% of 5K levels ($p<0.01$). GABAR γ2 subunit expression was not significantly different from 5K levels, 85 ± 10%, p=0.28 of 5K levels respectively. Under 25 mM KCl culture conditions, expression of the δ subunit protein was dramatically increased in stargazer CGCs (220 ± 47% of 5K levels, $p<0.01$) (figure 5.4.).

5.2.4.3. GABAR subunit expression following KCl-mediated depolarisation in control and stargazer CGCs

KCl-mediated depolarisation acted to modulate the expression of GABAR subunit expression similarly in both control and stargazer CGCs. Expression of the GABAR α1 subunit was dramatically reduced in control and stargazer CGCs, to 7 ± 15% and 21 ± 23% of 5K levels respectively. GABAR α6 subunit expression was also similarly reduced to 25 ± 1% in control CGCs and was undetectable in stargazer CGCs. GABAR β subunit expression was differentially modulated in both control and stargazer CGCs, where β2 subunit expression was not detectable upon KCl-mediate depolarisation, while β3 subunit expression was dramatically increased to 251 ± 29% and 246 ± 26% of 5K levels in control and stargazer CGCs respectively. GABAR γ2 subunit expression was reduced to 81 ± 21% of 5K levels in control CGCs and 85 ± 10% in stargazer CGCs, which

did not however reach statistical significance. A dramatic up-regulation of GABAR δ subunit expression was observed in both control and stargazer CGCs, to 245 ± 36% and 220 ± 47% of 5K levels respectively.

Previous observations in the current study demonstrated a significant reduction in GABAR α6 and δ subunit expression in the stargazer mutant CGC layer *in vivo* (see section 3.3.2.). Treatment with increased extracellular KCl (fc=25 mM) acted to down-regulate α6 subunit expression in both control and stargazer CGCs *in vitro*. However, expression of the GABAR δ subunit was dramatically up-regulated in CGCs derived from both mouse strains. Loss of AMPAR expression in stargazer mutant CGCs correlates with differential electrical activity of CGCs. Comparison of GABAR expression in control and stargazer CGCs can be correlated with comparison of 5K (electrically active) and 25K (electrically inactive). Therefore, it is possible to conclude that increased extracellular KCl-mediated depolarisation does not mimic *in vivo* GABAR subunit regulation in the stargazer mutant. However, it is possible to conclude that the downstream signalling cascades responsible for inducing regulation of expression of the GABAR subunits following KCl-mediated depolarisation are intact in stargazer CGCs, as similar GABAR subunit modulation was observed in both mouse strains.

5.2.5. Effects of kainic acid-mediated depolarisation on GABAR subunit expression in control and stargazer CGCs.

The mechanism by which KCl-mediated depolarisation regulates GABAR subunit expression has yet to be resolved. However, it was conceivable that depolarising KCl concentrations could evoke glutamate release, subsequently activating glutamate receptors. Previous studies have reported modulatory effects of kainic acid treatment (non-NMDA receptor agonist) on GABAR subunit expression in cultured mouse CGCs (Engblom *et al.*, 2003; Martikainen *et al.*, 2004). In order to assess the possible contribution of AMPAR/Kainate receptor activation on GABAR expression, control and stargazer CGCs were cultured

from age-matched littermates, treated at 1 DIV with kainic acid (100 μM) and harvested at 7 DIV for immunoblotting.

5.2.5.1. Control CGCs

Kainic acid–mediated depolarisation acted to dramatically reduce the levels of expression of the GABAR α1 subunit protein in control CGCs to 29 ± 22% of 5K levels ($p<0.01$). When control CGCs were cultured in the presence of the non-NMDA receptor antagonist, CNQX (20 μM), kainic acid treatment did not act to reduce the expression of the α1 subunit in control CGCs (121 ± 21% of 5K levels, $p=0.34$). Therefore, it is possible to conclude that kainic acid is acting via AMPA and/or kainate receptors to regulate GABAR α1 subunit expression.

GABAR α6 subunit expression was reduced to 27 ± 0.3% of 5K levels, in control CGCs cultured in the presence of kainic acid. Kainic acid-mediated depolarisation differentially regulated expression of the β subunits, resulting in undetectable levels of GABAR β2 subunit expression, while a significant increase in β3 subunit protein levels were noted, to 167 ± 30% of 5K levels, $p=0.04$ (see figure 5.5.). Kainic acid-induced depolarisation caused a significant reduction in GABAR γ2 subunit expression in control CGCs (44 ± 21% of 5K levels, $p=0.03$). The effects of kainic acid-mediated depolarisation resulted in a significant increase in expression of GABAR δ subunit in control CGCs (246 ± 40% of 5K levels). CGCs cultured in the presence of kainic acid and CNQX resulted in GABAR δ subunit expression levels similar to those at 5K (118 ± 35% of 5K levels, $p=0.16$).

5.2.5.2. Stargazer CGCs

No significant effect on GABAR α1 subunit expression upon kainic acid treatment was observed in stargazer CGCs (86 ± 29% of 5K levels, $p=0.63$). GABAR α6 subunit expression was also not modulated in response to kainic acid-mediated depolarisation in stargazer CGCs (100 ± 2% of control levels). β2 and β3 subunit protein levels were unaffected by AMPAR activation, 64 ± 46%

Figure 5.5. Effects of kainic acid depolarisation on the expression of GABAR subunits in cultured control and stargazer CGCs

A: Western blot analysis of GABAR subunit expression in cultured control (+/+:+/stg) CGCs (7 DIV) treated in the absence (5K) and presence of kainic acid (100 μM). Note the **reduction** in expression of the GABAR α1, α6 and γ2 subunits following kainic acid treatment. Furthermore, an **up-regulation** of β3 and δ subunit expression was observed in response to AMPAR activation. Data represents mean ± SEM for n=3 cultures as presented in figure 5.6.

B: Western blot analysis of GABAR subunit expression in cultured stargazer (stg/stg) CGCs (7 DIV) treated in the absence (5K) and presence of kainic acid (100 μM). Note the **reduction** in expression of the GABAR γ2 subunit following kainic acid treatment. Kainic acid treatment did not affect GABAR α1, α6, β3 or δ expression levels. Data represents mean ± SEM for n=3 cultures as presented in figure 5.6.

A: Control CGCs

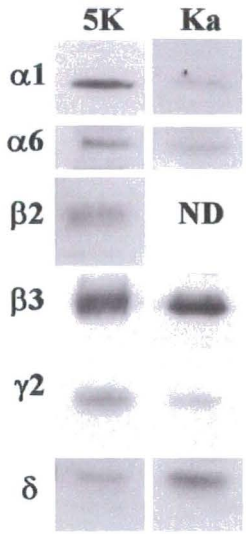

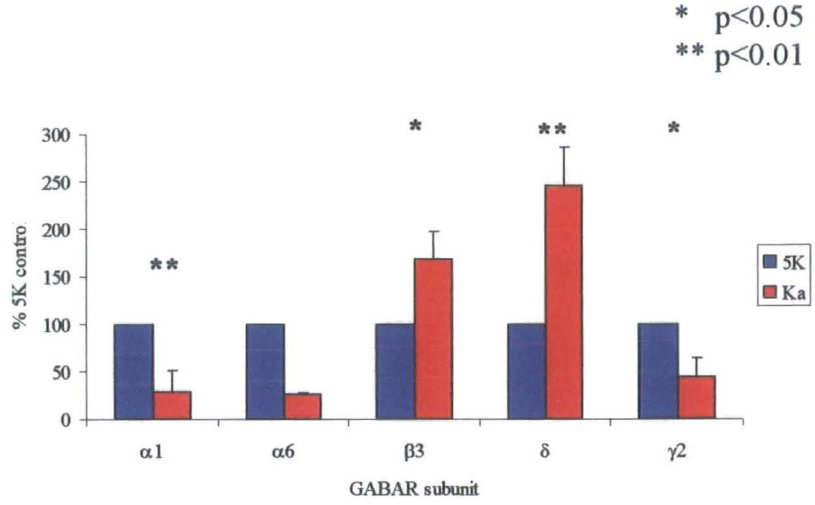

B: Stargazer CGCs

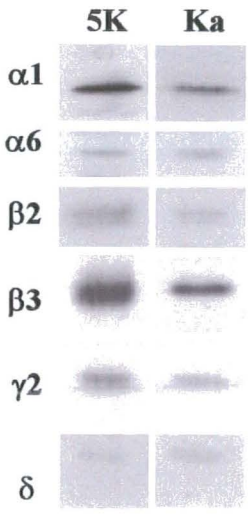

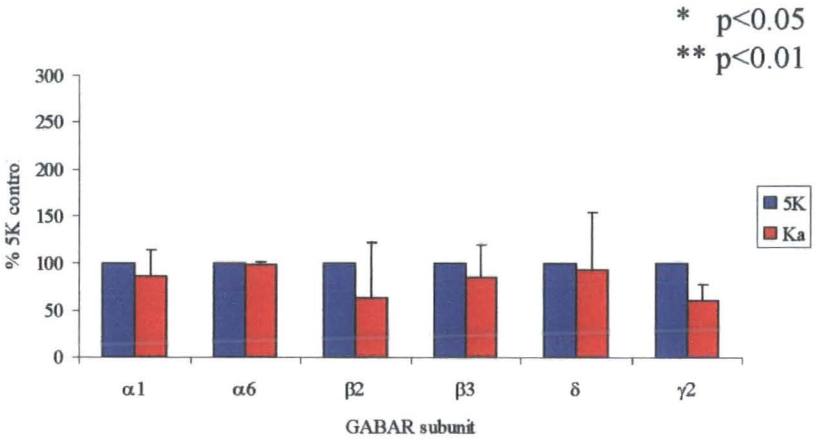

and 85 ± 35% of 5K levels, respectively. No effect on expression of the δ subunit was noted in stargazer CGCs (93 ± 61% of 5K levels) Kainic acid induced depolarisation caused a significant reduction in GABAR γ2 subunit expression in stargazer CGCs (61 ± 18% of 5K levels, p=0.05). Hence, it can be concluded that expression of the γ2 subunit is modulated by activation of kainate receptors and not AMPAR (see figure 5.5.).

5.2.5.3. GABAR subunit expression following kainate-mediated depolarisation in control and stargazer CGCs

In contrast to the effects of KCl-mediated depolarisation, kainic acid-mediated depolarisation acted to regulate the expression of the GABAR subunits differently in control and stargazer CGCs. Expression of the GABAR α1 subunit was dramatically reduced in control CGCs (to 29 ± 22% of 5K levels), while no significant effect on expression of the subunit in CGCs derived from the stargazer mutant were noted (to 86 ± 29% of 5K levels). Similarly, GABAR α6 subunit expression was reduced in control CGCs (to 27 ± 0.3% of 5K levels), which was not reciprocated in stargazer CGCs (to 100 ± 2% of 5K levels). GABAR β3 subunit expression levels were increased to 167 ± 30% of 5K levels in control CGCs, while protein levels were 85 ± 35% of 5K levels in stargazer CGCs. Expression of the GABAR δ subunit were up-regulated in control CGCs, to 246 ± 40% of 5K levels, which was not observed in stargazer CGCs (93 ± 61% of 5K levels). Therefore, it is possible to conclude that activation of AMPAR in control CGCs resulted in the modulation of GABAR α1, α6, β3 and δ subunit expression levels, since these effects were not observed in stargazer CGCs, which are AMPAR-incompetent.

In contrast, the expression of the GABAR γ2 subunit was down-regulated in response to kainic acid-mediated depolarisation in both control and stargazer CGCs, to 44 ± 21% and 61 ± 18% of 5K levels respectively. Hence, it is possible to conclude that the regulation of the GABAR γ2 subunit occurred as a result of kainate receptor activation, since stargazer CGCs are AMPAR-incompetent, and kainate receptor-competent.

Figure 5.6. Expression of $GABA_A$ Receptor subunits in control and stargazer CGCs (7 DIV) under polarised (5K) and depolarised (25K and Kainate-treated) culture conditions.

CGCs (7 DIV) derived from control (+/+:+/stg) and stargazer (stg/stg) mice, in the absence (5K) and presence of increased extracellular KCl (25K, 25 mM), kainic acid (Ka, 100 μM) or kainic acid (100 μM) and CNQX (20 μM). 10 μg protein per gel lane, data represents n=3 cultures.

A: Western blot analysis of cultured CGC material probed with anti-GABAR α1 subunit specific antibody at 1 μg/ml.
B: Western blot analysis of cultured CGC material probed with anti-GABAR α6 subunit specific antibody at 2 μg/ml.
C: Western blot analysis of cultured CGC material probed with anti-GABAR β2 subunit specific antibody at 0.5 μg/ml.
D: Western blot analysis of cultured CGC material probed with anti-GABAR β3 subunit specific antibody at 0.5 μg/ml.
E: Western blot analysis of cultured CGC material probed with anti-β-actin specific antibody at 1:2000 dilution.
F: Western blot analysis of cultured CGC material probed with anti-GABAR γ2 subunit specific antibody at 1 μg/ml.
G : Western blot analysis of cultured CGC material probed with anti-GABAR δ subunit specific antibody at 1 μg/ml.
H : Western blot analysis of cultured CGC material probed with anti-β-actin specific antibody at 1:2000 dilution.

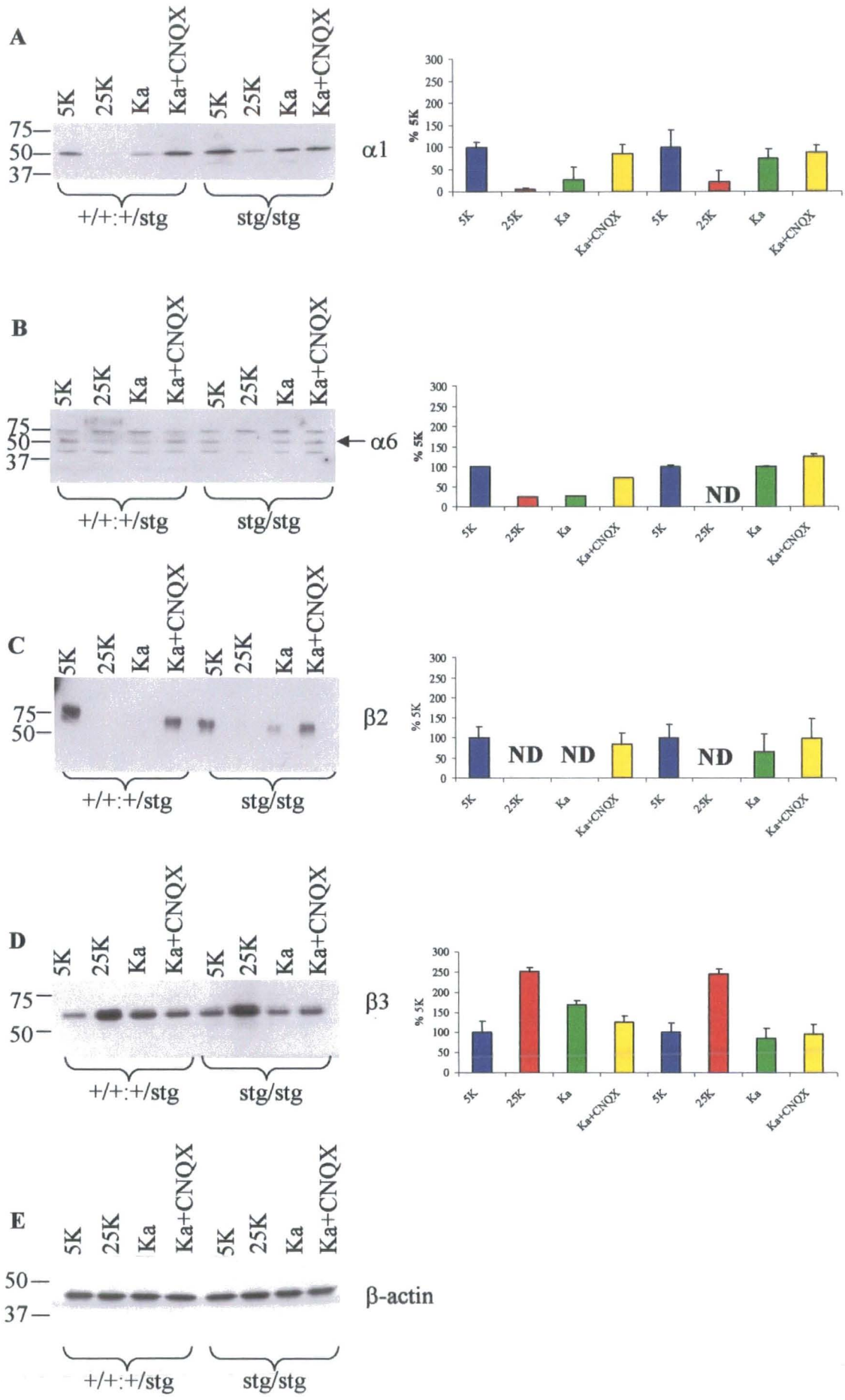
A
5K
25K
Ka
Ka+CNQX
5K
25K
Ka
Ka+CNQX
75
50
37
+/+:+/stg
stg/stg
α1
% 5K
300
250
200
150
100
50
0
5K
25K
Ka
Ka+CNQX
5K
25K
Ka
Ka+CNQX
B
5K
25K
Ka
Ka+CNQX
5K
25K
Ka
Ka+CNQX
75
50
37
α6
+/+:+/stg
stg/stg
% 5K
300
250
200
150
100
50
0
ND
5K
25K
Ka
Ka+CNQX
5K
25K
Ka
Ka+CNQX
C
5K
25K
Ka
Ka+CNQX
5K
25K
Ka
Ka+CNQX
75
50
β2
+/+:+/stg
stg/stg
% 5K
300
250
200
150
100
50
0
ND
ND
ND
5K
25K
Ka
Ka+CNQX
5K
25K
Ka
Ka+CNQX
D
5K
25K
Ka
Ka+CNQX
5K
25K
Ka
Ka+CNQX
75
50
β3
+/+:+/stg
stg/stg
% 5K
300
250
200
150
100
50
0
5K
25K
Ka
Ka+CNQX
5K
25K
Ka
Ka+CNQX
E
5K
25K
Ka
Ka+CNQX
5K
25K
Ka
Ka+CNQX
50
37
β-actin
+/+:+/stg
stg/stg

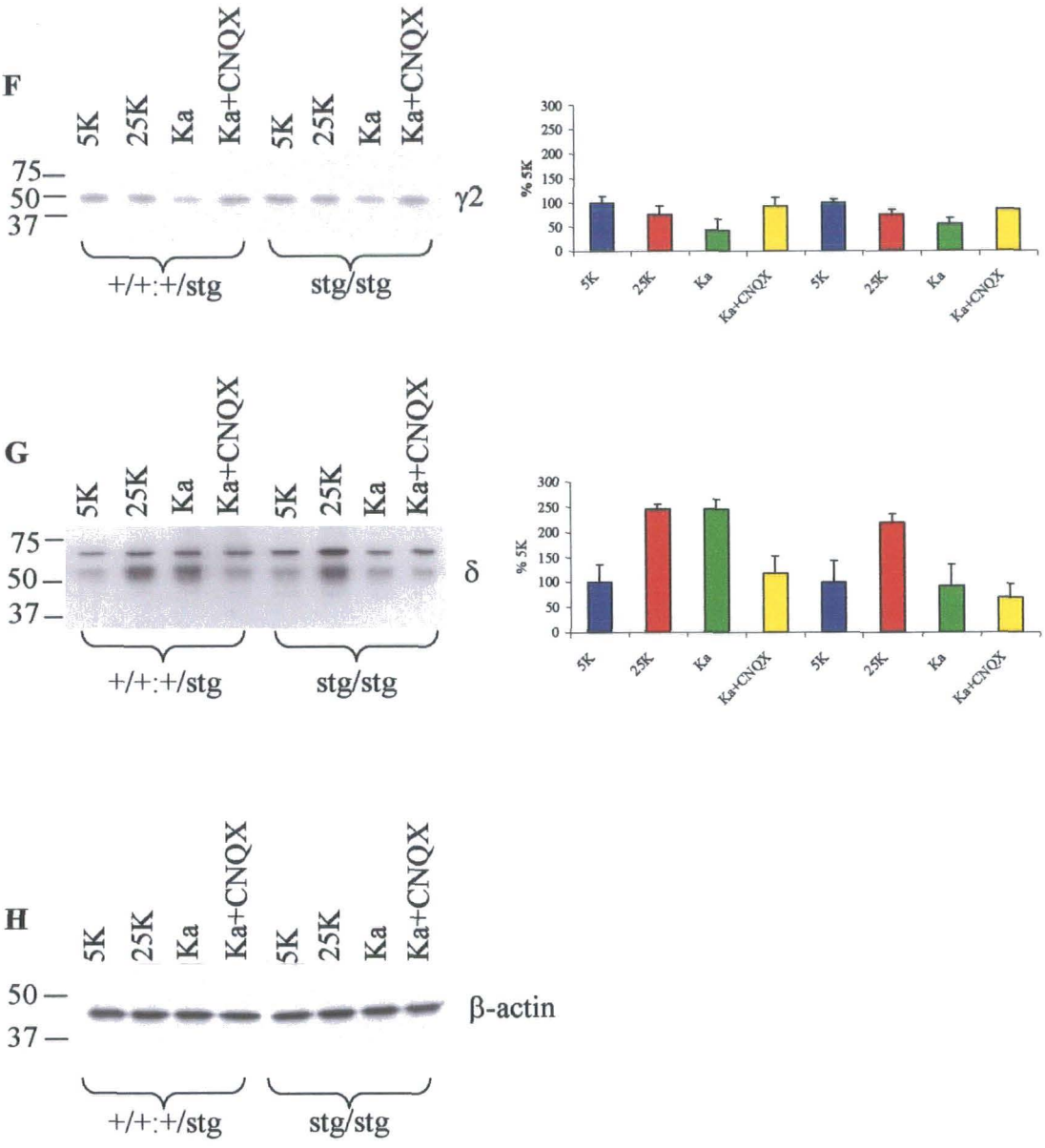
F
5K
25K
Ka
Ka+CNQX
5K
25K
Ka
Ka+CNQX
75
50
37
γ2
+/+:+/stg
stg/stg
% 5K
300
250
200
150
100
50
0
5K
25K
Ka
Ka+CNQX
5K
25K
Ka
Ka+CNQX
G
5K
25K
Ka
Ka+CNQX
5K
25K
Ka
Ka+CNQX
75
50
37
δ
+/+:+/stg
stg/stg
% 5K
300
250
200
150
100
50
0
5K
25K
Ka
Ka+CNQX
5K
25K
Ka
Ka+CNQX
H
5K
25K
Ka
Ka+CNQX
5K
25K
Ka
Ka+CNQX
50
37
β-actin
+/+:+/stg
stg/stg

The effects of KCl-mediated depolarisation on GABAR subunit expression were largely mirrored by kainic acid-mediated depolarisation, except in stargazer CGCs. Clearly the mechanism by which KCl-mediated depolarisation induces effects on GABAR subunit expression are not due to glutamate release and its subsequent activation of non-NMDA receptors though the downstream signalling mechanisms must be very similar. Since these also occur in stargazer CGCs it implies that KCl-mediate depolarisation bypasses the requirement for functional AMPARs to induce its effects. These will be discussed later. The only instance where KCl-mediated depolarisation and kainic acid-mediated depolarisation do not parallel each other is in the case of the GABAR γ2 subunit, which is down-regulated by kainic acid treatment and unaffected by KCl. The γ2 subunit appears unique in that it is the only subunit which appears to be influenced by kainate receptors of the subunits tested, through a mechanism that is not paralleled by simple depolarisation. Details of this mechanism are still yet to be resolved.

5.3. DISCUSSION

The aim of this chapter was to firstly characterise the mouse CGC culture system in terms of their morphological maturation and migration in culture by examination of CGCs at 2 day intervals from 1-7 DIV. Secondly, to determine the GABAR expression profile by western blot analysis of mouse control CGCs harvested at 2 day intervals from 1-9 DIV to establish whether these would constitute a good model system for studying developmental regulation of GABAR expression *in vitro*. The criteria required were that they switch on GABAR subunits with a temporal profile as seen *in vivo* (Laurie *et al.*, 1992) and that they expressed TARPγ2 protein. Thirdly, to investigate the modulation of expression of GABAR subunits by depolarisation, to confirm and extend previously reported effects of KCl-mediated depolarisation and kainic acid-induced depolarisation on GABAR subunit expression (Gault and Siegel., 1997, 1998; Mellor *et al.*, 1998; Ives *et al.*, 2002a; Engblom *et al.*, 2003; Martikainen *et al.*, 2004). Ultimately the aim here was to establish whether impaired AMPAR activity in stargazer CGCs (AMPAR-incompetent and kainate receptor-

competent) was responsible for the GABAR deficits reported in stargazer cerebellum *in vivo* (see results chapters 3 and 4).

5.3.1. Characterisation of the cell culture system

During the maturation of the cerebellum, CGC precursors migrate from the external granule cell layer (EGL) to the internal granule cell layer (IGL) and once in their adult positions form synapses with glutamatergic mossy fibre afferents and GABAergic Golgi II interneurons. Synaptogenesis coincides with a developmental switch in the expression of GABAR subunits at P6-7 *in vivo*, from α2 and α3 subunits, characteristic of the juvenile GABAR complement, to α1, α6 and δ subunits (Laurie *et al.*, 1992; Mellor *et al.*, 1998). Concomitantly there is a selective enrichment of the benzodiazepine-insensitive (BZ-IS) subtype of GABAR, characteristic of α6βγ2 receptors which correlates with the temporal up-regulation of the α6 subunit (Thompson & Stephenson, 1994; Wisden *et al.*, 1996).

Western blot analysis of mouse CGCs cultured under basal 5K conditions, collected at 2 day intervals from 1-9 DIV demonstrated a developmental increase in GABAR α1, β2 and γ2 subunits with time from 1 DIV to plateau at 7-9 DIV, in agreement with observations reported in rat CGCs by Thompson & Stephenson in 1994. In contrast, expression of the α6 and δ subunits did not occur until 3-5 DIV, but also demonstrated a time dependent increase in expression, with expression levels reaching a plateau at 7-9 DIV. These findings are further supported by the work of Thompson & Stephenson in 1994 who demonstrated a time-dependent enrichment of BZ-IS binding sites in rat CGCs with time in culture, corresponding to an increase in GABAR α6 subunit expression. Furthermore, Zheng *et al.*, in 1994 reported that positive modulation of GABA action by diazepam was decreased in rat CGCs from 5-20 DIV, corresponding to an increase in expression of α6 subunit containing receptors.

At 5-7 DIV, CGCs were shown to have migrated in culture to form compact cellular aggregates, interconnected by large cables of neuronal processes,

mimicking the migration of CGC precursors from the EGL to the IGL and the formation of synapses with glutamatergic mossy fibres *in vivo*. Hence it can be concluded that mouse CGCs cultured under basal conditions (5 mM KCl) undergo a maturation process as expected of CGCs *in vivo*, providing a model system with which to study the expression, trafficking and targeting of GABAR subunits.

Furthermore, TARPγ2 protein was expressed by control CGCs at 3-5 DIV as expected *in vivo*. Interestingly, western blot analysis of time point samples demonstrated the expression of the AMPAR GluR2 subunit in culture before the expression of TARPγ2, a protein known to be involved in the targeting and anchoring of AMPAR at the synapse (Chen *et al.*, 2000). This is an interesting observation, as it suggests the production of AMPAR subunits before the expression of proteins (TARPγ2) necessary for cell surface trafficking and targeting of functional AMPA receptors. Future work would involve western blot analysis to determine if there is the presence of other TARP isoforms, such as TARPγ4, known to be expressed in CGCs *in vivo* (Tomita *et al.*, 2003), early in the development of CGCs in culture.

Other groups have also reported minimal expression of AMPAR at the cell surface in the absence of TARPγ2 (Chen *et al.*, 2003, Vandenberghe *et al.*, 2005). Vandenberghe *et al.* in 2005 suggested that this may be explained by induction of the unfolded protein response (UPR). The unfolded protein response is triggered by accumulation of unfolded and unassembled proteins in the endoplasmic reticulum (ER), which leads to the increased transcription of genes encoding ER chaperones, such as Ig binding protein (BiP) (Vandenberghe *et al.*, 2005). BiP acts to bind to mis-folded or misassembled proteins and helping fold and assemble AMPAR.

Vandenberghe *et al.* also demonstrated that the UPR is induced in stargazer CGCs. Expression levels of BiP were found to be increased in stargazer CGCs, but not in wild type or heterozygote mice. AMPAR in the stargazer mutant have also been reported to show an immature ER-type glycosylation pattern (Tomita

et al., 2003). Furthermore, genistein, a tyrosine kinase inhibitor known to prevent full expression of the UPR reduced residual AMPA currents in stargazer CGCs.

5.3.2. Modulation of the GABAR subunits by depolarisation

The underlying mechanisms responsible for the temporal regulation of GABAR subunit expression are unknown to date, but could result from activation of ionotropic glutamate receptors, intrinsic pre-programmed factors or environmental cues. However, it has been widely reported that each GABAR subunit is independently regulated (Zheng *et al.*, 1994; Behringer *et al.*, 1996).

Gault and Siegel in 1997 reported modulatory effects on the expression of the δ subunit by potassium-mediated depolarisation in rat CGCs. Under 25K conditions, the group reported an increase in the expression of the δ subunit mRNA, proposed to result from activation of L-type calcium channels and an increase in intracellular calcium levels to cause either increased transcription of the δ subunit gene directly or indirectly by phosphorylation of transcription factors.

In a later study in 1998, the group used rat CGCs maintained at 5 mM potassium levels, in the narrow window before cellular degeneration and apoptosis, to show that activation of NMDA receptors causing an influx of calcium also acted to increase δ subunit mRNA levels. This increase in expression was also increased further by removal of the magnesium block from NMDAR which was suggested could be removed indirectly by activation of non-NMDAR. Increased intracellular calcium was proposed to cause activation of transcription factors, or immediate early genes to result in increased transcription of δ gene. However, we have employed the NMDAR antagonist, MK-801 to block calcium influx via NMDAR in the presence of kainic acid and observed no negative modulation of the GABAR δ subunit (C.L.Thompson, personal communication).

In the current study, the level of expression of the GABAR δ subunit protein was found to be dramatically increased in response to KCl-mediated depolarisation in

control CGCs (245 ± 36% of 5K levels, p=0.02). A number of groups have also reported effects of kainic acid treatment on mouse CGCs to cause depolarisation by activation of excitatory inputs via AMPA and kainate receptors. Martikainen *et al.*, 2004 reported an increase in the levels of δ subunit mRNA under 25K culture conditions, in agreement with Gault and Siegel 1997,1998 and observations herein, but a decrease in δ subunit mRNA in response to kainic acid-mediated depolarisation. The findings of the current study however, demonstrated a dramatic increase in GABAR δ subunit protein in response to kainic acid treatment (246 ± 40% of 5K levels). This difference in δ subunit protein and mRNA levels may result from differences in mouse strain utilised in each study, as discussed in section 3.3.2. Preliminary results in the laboratory suggest an increase in GABAR δ subunit mRNA expression following kainic acid treatment compared to 5K controls (J.H. Ives, personal communication).

It has been shown previously that under 25K culture conditions, mouse CGCs are developmentally arrested in terms of their GABAR profile (Ives *et al.*, 2002a). Ives *et al.*, in 2002 reported a decrease in GABAR α6 subunit expression under 25K culture conditions, correlated with a failure of migration of the cells to form cellular aggregates. Immunocytochemistry revealed no α6 subunit expression unless CGCs were arranged in compact cellular aggregates as under basal, 5K conditions. Decreased levels of α6 subunit expression were observed following KCl-mediated depolarisation in the current study, but also following kainic acid treatment (25 ± 1% and 27 ± 0.3% of 5K levels respectively). These observations were also mirrored in the failure of CGCs derived from both control and stargazer mice to form cellular aggregates in culture, rather, cells remained stationary and formed networks of neuronal processes.

The reported modulation of the GABAR α6 subunit in the current study was based on western blot analysis of material from one culture, due to the degradation of the anti-GABAR α6 subunit-specific antibody available in the laboratory and problems encountered with culturing the CGCs, which was later identified as a problem with the trypsin inhibitor used during the protocol. Therefore, preliminary results marry with previously reported effects on α6

subunit expression however, further work would be necessary to confirm these observations.

The GABAR δ subunit has been shown to preferentially co-assemble with the α6 subunit in the cerebellum (Quirk *et al.*, 1994; Jechlinger *et al.*, 1998; Sun *et al.*, 2004). Consequently, it raises the question, that if the expression levels of the α6 subunit decrease and the levels of the δ subunit increase with kainic acid treatment, what is the fate of the δ subunit? Is it assembled into receptors? Does it reach the cell surface? Which subunits does it co-assemble with? It may be possible that expression of an α subunit normally expressed in immature CGCs is increased following kainic acid treatment. Based on our knowledge that δ preferentially co-assembles with GABAR α4 and α6 subunits, the α4 subunit may be inappropriately expressed following kainic acid treatment. This issue is addressed in chapter 6.

Differential regulation of β subunit expression was noted following KCl and kainic acid mediated depolarisation of control CGCs, such that increases to 251 ± 29% and 167 ± 30% of 5K levels in GABAR β3 subunit expression levels were observed respectively. In contrast, dramatic reductions in β2 subunit expression were observed upon KCl and kainic acid treatment of control CGCs to undetectable levels. These findings may reflect co-assembly of the β subunits with different α subunits, suggesting preferential co-assembly of the β2 subunit with the α1 subunit (Benke *et al.*, 1994). Ives *et al.*, in 2002 similarly reported differential modulation of the β subunits in response to KCl-mediated depolarisation, such that expression levels of β3 subunit were increased (167 ± 50% of 5K levels) whereas, the β2 subunit was undetectable by immunoblotting.

5.3.3. Mechanisms of GABAR subunit protein modulation in response to kainic acid-mediated depolarisation

Treatment of cultured mouse CGCs with kainic acid, to cause activation of excitatory receptors and hence depolarisation demonstrated differential modulation of the principal GABAR subunits in mouse CGCs. The effects

observed on the expression of each GABAR subunit varied, such that decreased expression of the GABAR α1, α6, β2 and γ2 subunits was noted, with an increase in the expression of the β3 and δ subunits. Kainic acid-mediated GABAR subunit modulation was reversed in the presence of CNQX. Therefore, it can be concluded that kainic acid was acting via non-NMDA (AMPA and kainate) receptors to cause GABAR subunit modulation. GABAR α1, α6, β2, β3 and δ subunits expression levels were modulated in control CGCs only. Therefore, AMPAR activation caused the modulation of expression of the above subunits. GABAR γ2 subunit modulation was observed in both control and stargazer CGCs. Therefore, it is possible to conclude that these effects were caused by activation of kainate receptors, as it has been previously reported that the stargazer mutant possesses no functional AMPA receptors at the cell surface (Hashimoto *et al.*, 1999; Chen *et al.*, 1999, 2000, 2003).

5.3.4. Conclusions

Results of the current investigation indicate that CGCs derived from control and stargazer mice follow a pattern of development, as expected of CGCs *in vivo*, thereby providing a model system for the investigation of the factors affecting the expression, trafficking and targeting of the GABAR subunits. Depolarisation either by KCl or kainic acid treatment demonstrated the differential modulation of the principal GABAR subunits in mouse CGCs. As previously reported, CGCs cultured under 25 mM KCl, demonstrated a decrease in the expression of the GABAR subunits indicative of a mature CGC, the α1 and α6 subunits (Mellor *et al.*, 1998; Ives *et al.*, 2002a; Engblom *et al.*, 2003).

Furthermore, depolarisation mediated by kainic acid treatment also acted to decrease α1 and α6 subunit expression in control CGCs. However, expression of the δ subunit was found to be dramatically increased under both KCl and kainic acid induced depolarisation in control CGCs, but only under KCl-induced depolarisation in stargazer CGCs. Therefore, it is possible to conclude that activation of AMPA receptors is responsible for initiating the up-regulation of the δ subunit protein.

CHAPTER 6. INVESTIGATING THE MECHANISMS LINKING AMPA RECEPTOR ACTIVITY TO $GABA_A$ RECEPTOR EXPRESSION USING CULTURED CEREBELLAR GRANULE CELLS

6.1. INTRODUCTION

Previous results of this study have demonstrated that the stargazer mutation results in compromised expression of $\alpha6\beta\delta$ $GABA_A$ receptors (GABAR) in the cerebellar granule cell (CGC) layer, which would be predicted to result in a loss of GABAR-mediated, extrasynaptic tonic inhibition. Furthermore, results also showed a modulation of expression of the GABAR δ subunit by activation of excitatory inputs in the form of AMPA receptors (AMPAR) in cultured control CGCs.

The aim of the experiments described in this chapter was to further determine the mechanism by which activation of AMPA receptors acts to cause modulation of the GABAR δ subunit in cultured cerebellar granule cells. Secondly, to evaluate the effects of depolarisation on the GABAR subtypes expressed in cultured control CGCs and finally to investigate the effects of electrical activity on the expression of TARPγ2, the AMPAR auxiliary protein, whose expression is ablated by the stargazer mutation.

6.2. RESULTS

6.2.1. Modulation of GABAR δ subunit expression by depolarisation

Figure 6.1.A demonstrates western blot analysis of cultured cerebellar granule cells, derived from age-matched (P6-7) control and stargazer mice, cultured under basal KCl concentrations (5 mM KCl) and under depolarising conditions mediated both by increased extracellular KCl (25 mM KCl) and kainic acid (100 μM) treatment and probed with anti-GABAR δ subunit specific antibody.

Expression of the δ subunit was found to be increased to 245 ± 36% and 220 ± 47% of 5K levels, $p<0.01$ in control and stargazer CGCs respectively upon KCl-mediated depolarisation. In contrast, kainic acid-mediated depolarisation caused an increase in expression of the δ subunit in control CGCs (246 ± 40% of 5K levels, $p=0.02$) that was reversed by co-application of the non-NMDA receptor antagonist CNQX (20 μM, figure 6.1A). Expression in stargazer CGCs was unaffected (93 ± 61% of 5K levels) by kainic acid (100 μM) treatment proving that AMPA receptor activation plays a role in the modulation of GABAR δ subunit expression in CGCs (see sections 5.2.4 and 5.2.5.).

If expression of the GABAR δ subunit is increased in control CGCs following kainic acid treatment, while its preferential subunit partner, α6 is dramatically reduced, it raises the question as to whether the δ subunit contributes to assembled GABAR under such culture conditions if so, we would expect δ to be trafficked to the cell surface.

The next aim was to determine if the increase in GABAR δ subunit expression in control CGCs upon AMPAR activation resulted in increased expression of the subunit at the cell surface. Subsequently GABAR subunit expression at the CGC cell surface and within intracellular compartments was analysed using biotinylation assays. Control and stargazer CGCs (7 DIV) were incubated with 1 mg/ml sulpholink-NHS-SS-biotin in order to biotinylate cell surface proteins. Biotinylated CGCs were subsequently solubilised using solubilisation buffer (see section 2.15), incubated with streptavidin beads to separate out the biotinylated cell surface proteins. This allowed for the separation of intracellular proteins which are retained in the supernatant, from the cell surface proteins which become bound to the streptavidin beads. Surface proteins were then eluted from the streptavidin beads by incubation in 2x sample buffer containing 20 mM DTT. Samples were then subjected to western blot analysis and probed with anti-GABAR δ subunit specific antibody at 1 μg/ml.

Figure 6.1.B shows an immunoblot of biotinylated control (+/+:+/stg) and stargazer (stg/stg) CGCs 7 DIV cultured under basal culture conditions (5 mM

Figure 6.1. Expression of the GABAR δ subunit under depolarising conditions

A: Western blot analysis of control and stargazer CGCs (7 DIV) cultured in the absence ('5K', 5 mM KCl) and presence ('25K', 25 mM) of increased extracellular potassium, kainic acid ('Ka', 100 μM) or kainic acid (100 μM) and CNQX ('Ka + CNQX', 20 μM). Note increased δ subunit expression under 25 mM culture conditions in control and stargazer CGCs, but only in control CGCs under kainic acid treatment. Data represents n=3 cultures, as in figure 5.6.
B: Immunoblot of control and stargazer CGCs (7 DIV) cultured in the presence and absence of kainic acid (100 μM). 'Bound' fraction represents protein found at the cell surface. 'Unbound' fraction represents proteins located intracellularly. Note the increased expression of the GABAR δ subunit at the cell surface and within the cell interior of control CGCs treated with kainic acid (100 μM). n=2 cultures.

A

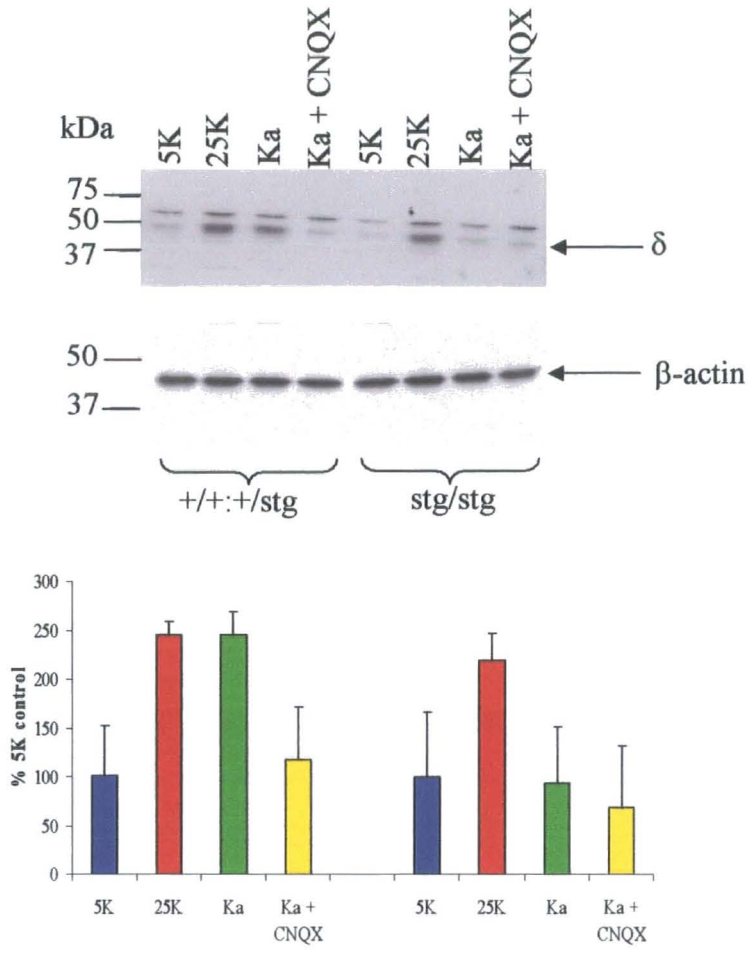
kDa
5K
25K
Ka
Ka + CNQX
5K
25K
Ka
Ka + CNQX
75
50
37
δ
50
37
β-actin
+/+:+/stg
stg/stg
% 5K control
300
250
200
150
100
50
0
5K
25K
Ka
Ka + CNQX
5K
25K
Ka
Ka + CNQX

B

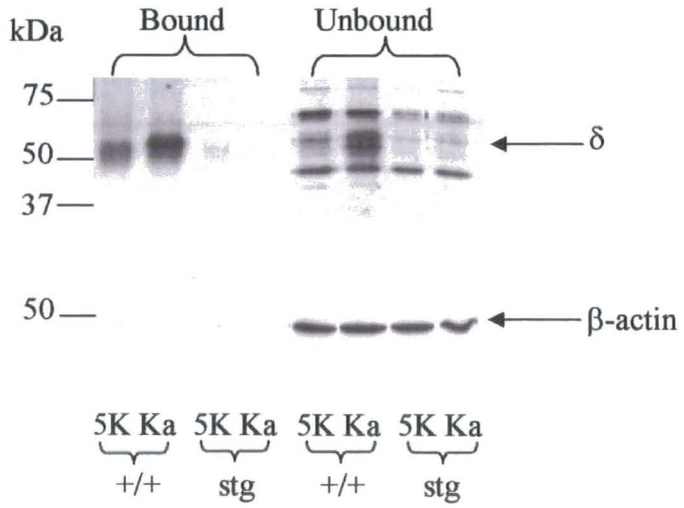
kDa
Bound
Unbound
75
50
37
δ
50
β-actin
5K Ka
5K Ka
5K Ka
5K Ka
+/+
stg
+/+
stg

KCl) and following kainic acid treatment (100 μM). Expression of the δ subunit was found to be increased both at the cell surface and intracellularly upon AMPAR activation in control CGCs. Expression of GABAR δ subunit was dramatically reduced in stargazer CGCs (stg/stg) under basal KCl levels both at the cell surface and intracellularly compared to control CGCs (+/+:+/stg). However, upon kainic acid treatment (100 μM), expression of the δ subunit was undetectable in stargazer CGCs at the cell surface, with minimal amounts detected in the intracellular pool.

6.2.2. Expression of GABAR α subunits under depolarising conditions

Expression of the principal α subunits detected in cultured mouse CGCs at 7 DIV, namely GABAR α1 and α6, have previously been quantified following KCl and kainic acid-mediated depolarisation in cultured control and stargazer mouse CGCs (see section 5.2.4.). Results demonstrated a near total loss of α1 and α6 subunit protein in control CGCs under 25 mM KCl concentrations (7 ± 15% and 25 ± 1% of 5K levels respectively). AMPAR activation was observed also to cause a significant reduction in α1 (29 ± 22% of 5K levels) and α6 (27 ± 0.3% of 5K levels) subunit expression. These observations imply a dramatic loss of the principal GABAR α subunits expected of a mature CGC following depolarisation by KCl and kainic acid treatment. Furthermore, if an increase in GABAR δ subunit expression occurs upon depolarisation, with which α subunit is the δ subunit co-assembling?

CGCs derived from P6-7 age-matched control and stargazer mice were cultured simultaneously according to standard methods (see section 2.14.). At 1 DIV, CGCs were treated with KCl (fc=25 mM), kainic acid (100 μM) or kainic acid (100 μM) and CNQX (20 μM). CGCs (7 DIV) were harvested for western blot analysis to compare total protein expression or following cell surface protein biotinylation assays in order to compare the proportion of proteins of interest that were expressed at the CGC surface versus intracellular compartments.

Figure 6.2. Expression of the principal GABAR α subunits in cultured control CGCs under depolarising conditions

Western blot analysis of the principal GABAR α subunits expressed by cultured control CGCs in the presence and absence of increased extracellular KCl (25 mM), kainic acid (100 μM) or kainic acid (100 μM) and CNQX (20 μM).

A: Note the **reduction** in α1 subunit expression following 25K and kainic acid treatment.

B: Note the dramatic **increase** in α4 subunit expression following 25K and kainic acid treatment.

C: Note the dramatic **reduction** in α6 subunit expression following 25K and kainic acid treatment.

D: Expression of β-actin in the presence and absence of increased extracellular KCl (25 mM), kainic acid (100 μM) or kainic acid (100 μM) and CNQX (20 μM).

CGCs (7 DIV) were subjected to biotinylation assays to determine the relative proportions of proteins of interest that were expressed at the cell surface ('Bound') versus that retained within intracellular compartments ('Unbound').

E: Note an **increase** in α4 subunit expression at the cell surface following kainic acid depolarisation.

F: A dramatic **reduction** in cell surface expression of the α6 subunit was observed following kainic acid treatment.

G: No non-specific binding of β-actin was observed in the 'bound' fractions following biotinylation. Furthermore, equal protein loading of 'unbound' fractions was observed.

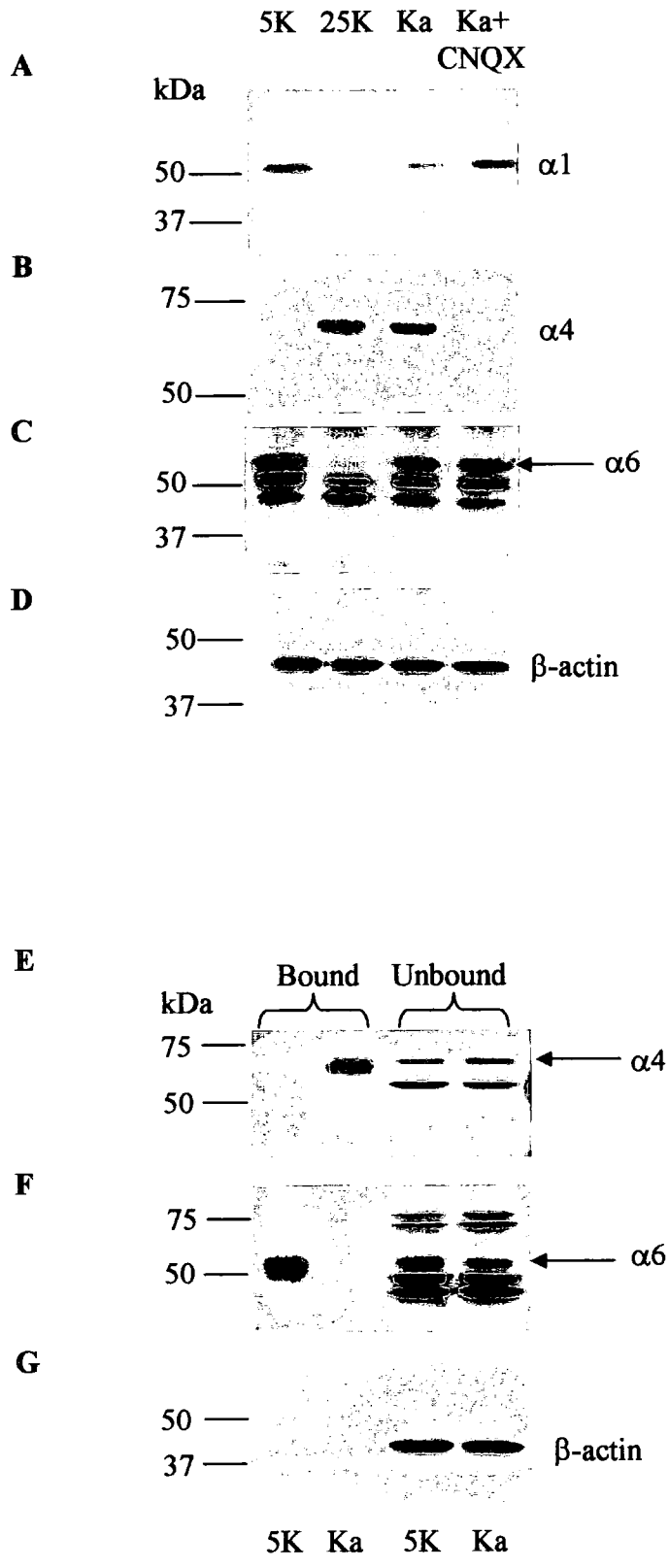
5K
25K
Ka
Ka+
CNQX
A
kDa
50
37
α1
B
75
50
α4
C
50
37
α6
D
50
37
β-actin
E
Bound
Unbound
kDa
75
50
α4
F
75
50
α6
G
50
37
β-actin
5K
Ka
5K
Ka

Figure 6.2. A-D summarise western blot analysis of GABAR α subunit expression in cultured control CGCs at 7 DIV under basal (5K) and depolarised (25K and Kainate-treated) culture conditions. Results demonstrate that a dramatic decrease in GABAR α1 (figure 6.2.A) and α6 (figure 6.2.C) subunit expression, as reported in section 5.2.4., but a significant increase in GABAR α4 subunit expression occurred following culture under depolarising culture conditions (figure 6.2.B).

Furthermore, western blot analysis of cell surface expressed protein from CGCs cultured under 5K and AMPAR-activated conditions revealed that GABAR α4 subunit at the cell surface was increased following kainic acid treatment (figure 6.2.E), with a concomitant decrease in α6 subunit expression at the cell surface (figure 6.2.F). Expression of β-actin was restricted to 'unbound' fractions, therefore, cell integrity was maintained throughout the assay as intracellular proteins were not biotinylated and no non-specific proteins present in the intracellular fraction were bound to the streptavidin beads upon separation of cell surface from intracellular proteins (figure 6.2.G). Results therefore suggest an up-regulation of expression of the GABAR α4 subunit in response to depolarisation. Furthermore, since this subunit reaches the neuronal cell surface it is probably assembled into a GABAR.

6.2.3. Radioligand binding to control CGCs (7 DIV) under polarised (5K) and depolarised (kainic acid-mediated) culture conditions

Ives *et al.*, in 2002 reported a switch in GABAR pharmacological subtypes expressed in cultured control CGCs upon depolarisation (25K). The BZ-S subtype of GABAR was found to switch from predominantly type I pharmacology, compatible with a GABAR profile found in a mature CGC, to type II BZ-S pharmacology, predictive of GABAR α2/α3/α5βγ2. Furthermore, an increase in zolpidem-insensitive binding was observed, corresponding to increased expression of α5 subunit-containing GABARs.

In order to confirm and extend the reported differences in GABAR profiles following KCl-mediated depolarisation by Ives *et al.*, in 2002 and determine if such rearrangements occur following kainic acid depolarisation, radioligand binding studies were carried out on 7 DIV control CGCs cultured under basal polarised (5K) and depolarised (25K and Kainic acid-mediated) conditions.

6.2.3.1. [^{3}H] muscimol binding

[^{3}H] muscimol binding was performed on intact CGCs (7 DIV) cultured under 5K and kainate-treated conditions. [^{3}H] muscimol was employed at a concentration of 40 nM, with non-specific binding determined in the presence of 0.2 mM GABA. Figure 6.3.A demonstrates that there was no significant difference in the amount of ligand bound in pmoles per mg protein between 5K and kainate-treated CGCs (0.11 ± 0.05 and 0.11 ± 0.04 pmoles/mg protein, respectively n=3, p=0.83) (figure 6.3.A.). [^{3}H] muscimol binds to both γ2 and δ subunit-containing GABAR in cultured CGCs. Therefore, it is possible to conclude that the total number of GABAR does not differ under basal, polarised and kainate-mediated depolarised culture conditions.

6.2.3.2. [^{3}H] Ro15-4513 binding

[^{3}H] Ro15-4513 binding was conducted on intact control CGCs (7 DIV) cultured under 5K, 25K and kainate-treated conditions. [^{3}H] Ro15-4513 was utilised at a concentration of 40 nM, with non-specific binding determined in the presence of 10 μM Ro15-1788. BZ-IS binding was determined in the presence of 10 μM flunitrazepam and BZ-S binding was calculated by subtraction of the BZ-IS subtype from total [^{3}H] Ro15-4513 binding.

The abundance of [^{3}H] Ro15-4513 binding sites was significantly reduced in both 25K and kainate-treated CGCs to 64 ± 14% (0.40 ± 0.07 pmoles/mg protein, n=3) and 59 ± 14% (0.36 ± 0.06 pmoles/mg protein, n=3) of 5K levels (0.62 ± 0.06 pmoles/mg protein, n=3) respectively. A significant reduction in the BZ-S subtype of binding was also noted in kainate-treated CGCs, to 64 ± 23%

Figure 6.3. Radioligand binding to control (+/+:+/stg) mouse cerebellar granule cells (7 DIV) cultured under non-depolarising (5K) and depolarising (25K and Kainate-treated) conditions

A: [^{3}H] muscimol binding to intact cultured control mouse CGCs (7 DIV) following 5K and kainate acid (100 μM) treatment. Note no significant difference in total [^{3}H] muscimol binding between 5K and kainate-treated CGCs, p=0.83, n=3.

B: [^{3}H] Ro15-4513 binding to intact cultured control mouse CGCs (7 DIV) under 5K and depolarised (25K and kainate-treated) conditions. Significant reductions in total [^{3}H] Ro15-4513 binding were observed in both 25K and kainate-treated (100 μM) CGCs (decreased to 64 ± 14% (p=0.008) and 59 ± 14% (p=0.006) of 5K levels, respectively). A dramatic reduction in BZ-S subtype of binding in kainate-treated CGCs was also observed to 64 ± 23% of 5K levels, p=0.03. Notably, a total loss of BZ-IS subtype of [^{3}H] Ro15-4513 binding was observed in 25K CGCs, but no significant difference in kainate-treated CGCs from 5K levels (p=0.10).

A

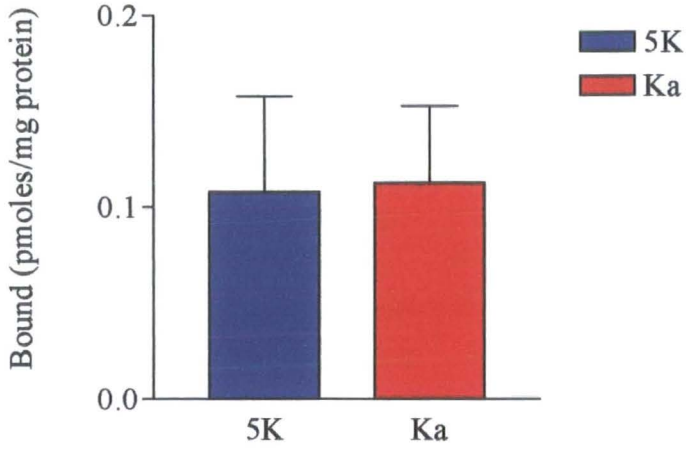

	Bound (pmoles/mg protein)
5K	0.11 ± 0.05
Kainate	0.11 ± 0.04

B

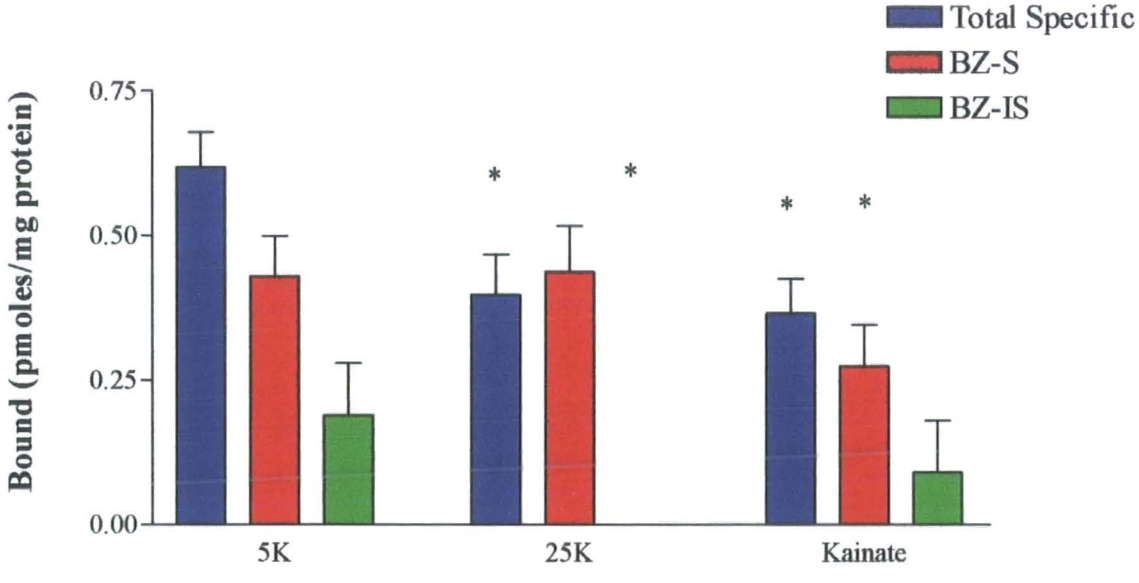

	Total binding (pmoles/mg protein)	BZ-S (pmoles/mg protein)	BZ-IS (pmoles/mg protein)
5K	0.62 ± 0.06	0.43 ± 0.07	0.19 ± 0.09
25K	0.40 ± 0.07	0.44 ± 0.08	0.00 ± 0.10
Kainate	0.36 ± 0.06	0.27 ± 0.07	0.09 ± 0.09

(0.27 ± 0.07 pmoles/mg protein, n=3) of 5K levels (0.43 ± 0.07 pmoles/mg protein, n=3). Most notably, a total loss of the BZ-IS subtype of binding was observed in 25K CGCs, while no significant difference in BZ-IS binding was found in kainate-treated CGCs (p=0.10, n=3) (figure 6.3.B).

6.2.4. Activation of L-type voltage-gated calcium channels following AMPA receptor activation leads to an increase in GABAR δ subunit expression in kainate treated CGCs

Results of the current investigation have demonstrated that expression of the GABAR δ subunit in cultured control mouse CGCs is increased by KCl-mediated depolarisation. Gault and Siegel in 1997 proposed that the increase in expression of the GABAR δ subunit in response to KCl-mediated depolarisation could be blocked by preventing the intracellular calcium influx through L-type voltage-gated calcium channels.

Figure 6.4.A demonstrates the expression of the GABAR δ subunit in the presence and absence of kainic acid (100 μM) and increasing concentrations of nifedipine, an L-type calcium channel blocker (0.1-10 μM). Results show that if calcium entry into the CGC via L-type calcium channels is blocked with nifedipine at a concentration of 1-10 μM, the kainic acid induced increase in GABAR δ subunit protein was inhibited. Nifedipine was employed at a concentration of 10 μM for future experimentation.

Figure 6.4.B demonstrates the effect of application of kainic acid (100 μM) and nifedipine (10 μM) applied at 1 DIV, kainic acid acts to activate AMPA receptors, causing an influx of calcium via L-type calcium channels, to result in an increase in GABAR δ subunit expression which can be blocked by treatment with nifedipine (10 μM).

Furthermore, figure 6.4.B illustrates that the effect of nifedipine to completely reverse the kainic acid-induced effects on GABAR subunits is not unique to the

Figure 6.4. Expression of the GABAR δ subunit in the presence of kainic acid and nifedipine

A: GABAR δ subunit expression in the presence of kainic acid ('Ka', 100 μM) and dose response treatment with the L-type calcium channel blocker, Nifedipine (n=1).

Lane 1: 5K

Lane 2: 5K+Ka (100 μM)

Lane 3: 5K+Ka+Nifedipine (0.1 μM)

Lane 4: 5K+Ka+Nifedipine (1 μM)

Lane 5: 5K+Ka+Nifedipine (10 μM)

B: Treatment of control CGCs with kainic acid (100 μM) in the presence and absence of nifedipine (10 μM) at 1 DIV. Western blots of this material were probed with anti-GABAR α1, α4, α6, β3, δ, γ2 subunit-specific antibodies and β-actin specific antibody. Note the reversal of the δ and β3 subunit up-regulation and the partial reversal of the α4 subunit depolarisation-mediated up-regulation in the presence of nifedipine (10 μM).

A

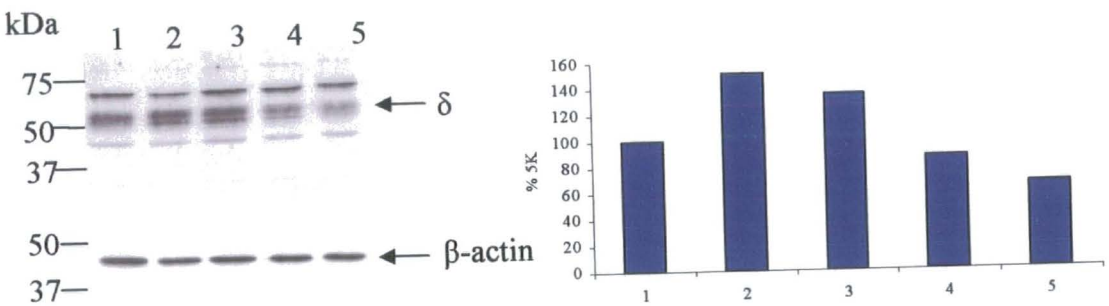
kDa
1 2 3 4 5
75
50
37
δ
50
37
β-actin
% 5K
160
140
120
100
80
60
40
20
0
1 2 3 4 5

B

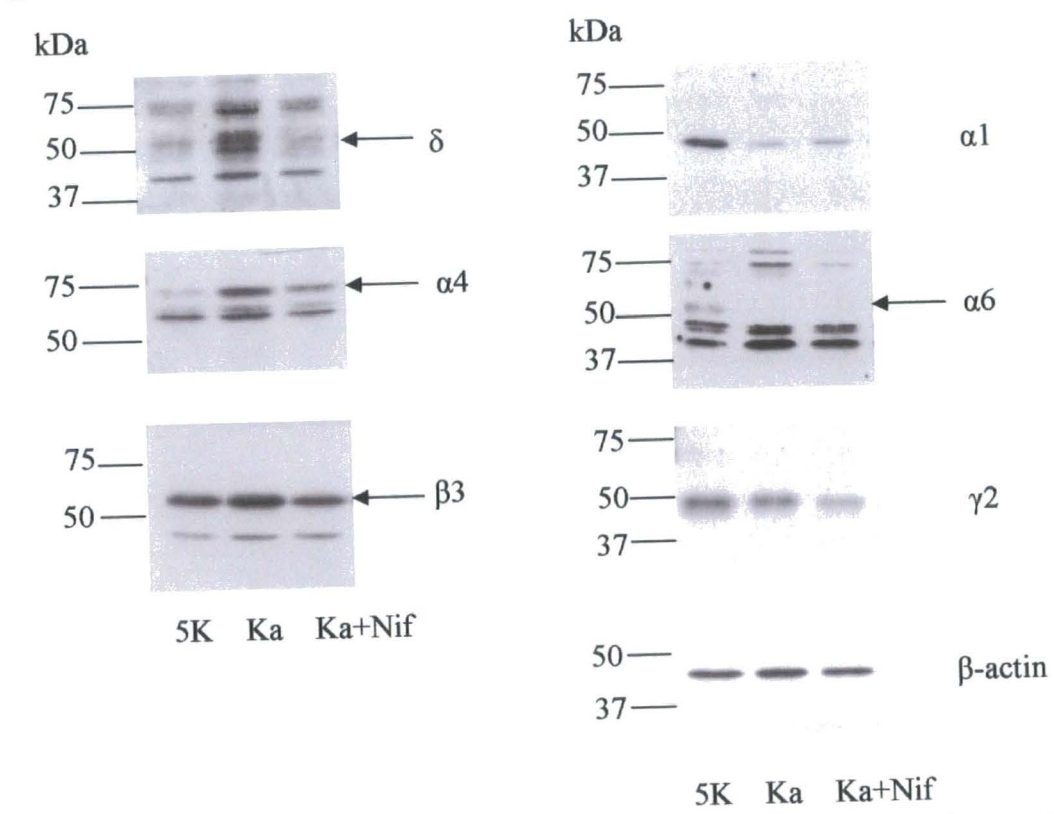
kDa
75
50
37
δ
75
50
α4
75
50
β3
5K Ka Ka+Nif
kDa
75
50
37
α1
75
50
37
α6
75
50
37
γ2
50
37
β-actin
5K Ka Ka+Nif

Figure 6.5. Reversal of kainic acid depolarisation-mediated up-regulation of GABAR δ subunit expression with L-type calcium channel blockers nifedipine and verapamil

A: Control CGCs treated at 1 DIV as detailed below, harvested at 7 DIV, and subjected to western blot analysis, probed with anti-GABAR δ subunit-specific antibody at 3 μg/ml. Note the increase in expression of the δ subunit in response to treatment with kainic acid (100 μM), which is reversed by treatment with L-type calcium channel blockers, nifedipine and verapamil (10 μM) (n=1).
B: Immunoblot as in A, reprobed with anti-β-actin antibody (1:2000 dilution) to determine protein loading.

Lane 1: 5K
2: Kainate treated (100 μM)
3: Kainate and nifedipine (10 μM)
4: Kainate and verapamil (10 μM)
5: Kainate and CNQX (20 μM)
6: 5K and Nifedipine
7: 5K and verapamil
8: 5K and CNQX

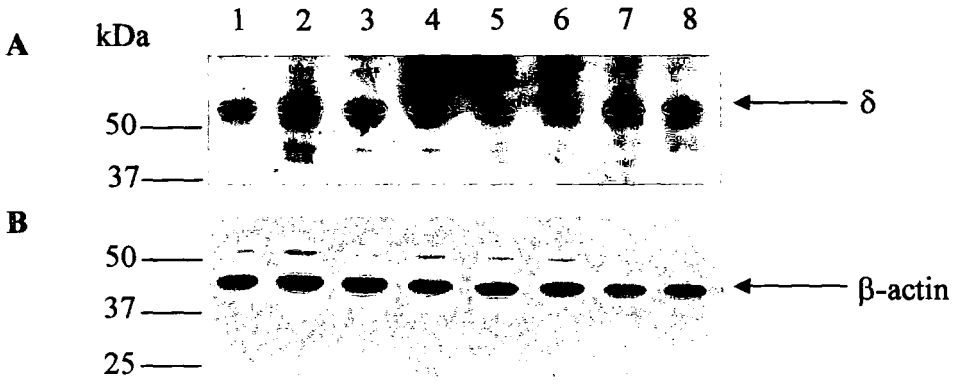
A
kDa
1 2 3 4 5 6 7 8
50
37
δ
B
50
37
25
β-actin

GABAR δ subunit, as treatment with nifedipine also completely reverses the kainic acid-mediated up-regulation of GABAR β3 subunit to 5K levels. However, nifedipine treatment acted to only partially reverse the kainate-mediated up-regulation of GABAR α4 subunit expression. Furthermore, nifedipine treatment did not act to reverse the kainic acid-mediated down regulation of GABAR α1, α6 or γ2 subunits, thereby suggesting that a number of mechanisms are in operation to modulate GABAR subunit expression in response to kainic acid-mediated depolarisation.

In order to further confirm the action of nifedipine, to reverse the kainic acid mediated modulation of the GABAR δ subunit, a further L-type calcium channel blocker was employed, verapamil. Control CGCs were treated at 1 DIV with kainic acid in the presence or absence of nifedipine (10 μM), verapamil (10 μM) and CNQX (20 μM). CGCs cultured under basal (5 mM KCl) culture conditions were also treated with each compound, in order to rule out any effects on the GABAR δ subunit in the absence of kainic acid. Figure 6.5. shows western blot analysis demonstrating an increase in GABAR δ subunit expression upon kainic acid treatment, which was inhibited by treatment with nifedipine, verapamil and CNQX. None of the drugs were shown to have a major effect on δ subunit expression when applied to 5K CGCs in the absence of kainic acid. Therefore, it is possible to conclude that the modulation of the GABAR δ subunit in response to kainic acid mediated depolarisation occurs as a consequence of AMPA receptor activation, causing an influx of calcium into the cell via L-type calcium channels.

6.2.5. Effects of depolarisation on TARPγ2 expression

We had earlier shown that TARPγ2, the protein ablated in stargazer CGCs, was expressed in control CGCs at 3-5 DIV, hence why we have conducted these studies at 7 DIV. We decided to investigate whether these depolarisation regimes had any affect on TARPγ2 expression, since we assumed that in its presence AMPARs would be expressed and responsive to kainic acid. Figure 6.6.A illustrates the effects of both KCl and kainic acid-mediated depolarisation on the

Figure 6.6. Effects of AMPA receptor activation on the expression of AMPA receptor subunit GluR2 and TARPγ2

A: Expression of GluR2 and TARPγ2 following KCl and kainic acid-mediated depolarisation in control CGCs (7 DIV). Note the reduction in molecular weight of TARPγ2 upon KCl-mediated depolarisation and the reduction in expression of TARPγ2 following kainic acid treatment.

CGCs (7 DIV) were subjected to biotinylation assays to determine the relative proportions of proteins of interest that were expressed at the cell surface ('Bound') versus that retained within intracellular compartments ('Unbound').
B: Expression of the AMPAR GluR2 subunit and TARPγ2 at the cell surface of control CGCs following kainic acid treatment (100 μM). Note the reduction in GluR2 and TARPγ2 expression levels and the reduction in molecular weight of TARPγ2 at the cell surface in kainate-treated CGCs. Furthermore, note the reduction in expression of TARPγ2 expression intracellularly following AMPAR activation. TARPγ2^{a} represents the native form of protein, TARPγ2^{b} represents a modified form of the protein.

A

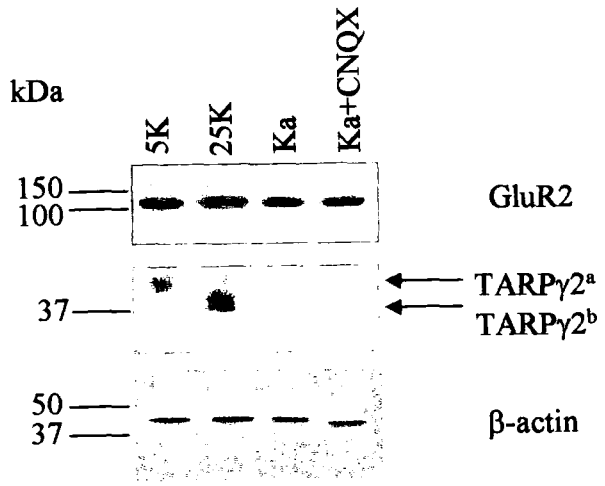
kDa
5K
25K
Ka
Ka+CNQX
150
100
GluR2
37
TARPγ2a
TARPγ2b
50
37
β-actin

B

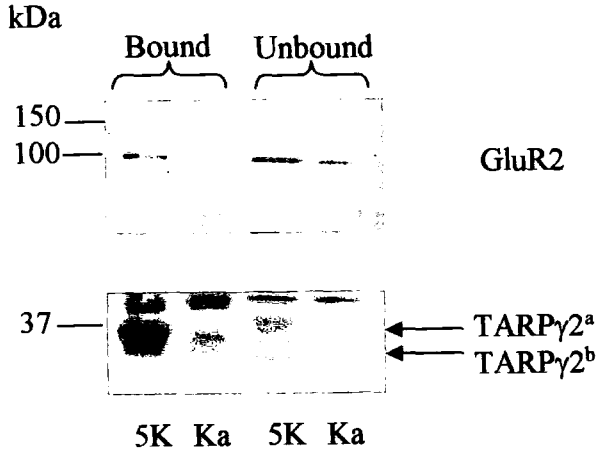
kDa
Bound
Unbound
150
100
GluR2
37
TARPγ2a
TARPγ2b
5K Ka 5K Ka

expression of TARPγ2 protein in cultured control CGCs (7 DIV). Upon KCl-induced depolarisation, the levels of total protein appear unaffected, but interestingly the molecular weight of TARPγ2 was decreased, suggesting either dephosphorylation or deglycosylation of the protein. In contrast, kainic acid treatment (100 μM) of CGCs resulted in a near total loss of TARPγ2 protein expression.

Figure 6.6.B demonstrates western blot analysis of biotinylated CGCs cultured under basal, polarised (5K) and kainic acid-mediated depolarised conditions (7 DIV) and probed for the expression of TARPγ2 and the AMPA receptor subunit, GluR2. Results indicate a dramatic decrease in the expression of TARPγ2 at the cell surface upon kainic acid treatment (100 μM), with a reduction in molecular weight of the protein at the cell surface, correlating with observations following KCl- mediated depolarisation. Furthermore, expression of the GluR2 subunit was found to be reduced at the cell surface, while total protein levels appeared unaffected by depolarisation.

6.3. DISCUSSION

Two methods of inducing depolarisation in CGCs were utilised in the current study, increasing the extracellular KCl levels to 25 mM and treatment with kainic acid (100 μM). By increasing the extracellular KCl levels to 25 mM, this acts to alter sodium and potassium ion fluxes and inhibit or potentially reverse outward K^+ movement. Consequently, this causes a switch in the equilibrium potential for K^+, causing it to become less negative. As a result, the cell membrane is unable to repolarise and the cells become electrically silent. Kainic acid is an ionotropic glutamate receptor agonist, hence it acts to activate excitatory AMPA and kainate receptors on the cell surface to cause increased permeability to Na^+ and K^+ ions and hence depolarisation.

Depolarisation mediated by both KCl and kainic acid has been shown to cause effects on the expression of the GABAR δ subunit (Gault & Siegel 1997, 1998; Martikainen *et al.*, 2004). The focus of the current study was to begin to

determine the mechanism by which kainic acid-mediated depolarisation acts to cause modulation of the δ subunit, as previous studies have been unable to distinguish between activation of AMPA receptors or kainate receptors. Stargazer mutant CGCs provide an invaluable tool, as they do not possess functional AMPAR at the cell surface, whereas kainate receptors seem to be relatively spared by the mutation (Hashimoto *et al.*, 1999; Chen *et al.*, 2000, 2003). Hence, by comparison of control and stargazer CGCs, it was possible to distinguish between activation of different excitatory receptors.

The aims of the current chapter were to determine the mechanism by which activation of AMPA receptors acts to cause modulation of the GABAR δ subunit in cultured cerebellar granule cells. Secondly, to evaluate the effects of depolarisation on the GABAR subtypes expressed in cultured control CGCs and finally to investigate the effects of electrical activity on the expression of TARPγ2, the AMPAR auxiliary protein, whose expression is ablated by the stargazer mutation. Results indicated an increase in GABAR δ subunit expression following activation of AMPAR by kainic acid treatment in control CGCs, which was not observed in CGCs derived from the stargazer mutant. Since the stargazer mutant CGCs are essentially AMPAR-incompetent, this identified a role for AMPAR activation in the modulation of GABAR subunit expression. Biotinylation assays determined that the increased level of GABAR δ subunit was indeed expressed at the cell surface in cultured control CGCs. Radioligand binding studies further supported an up-regulation of δ subunit-containing GABAR following kainic acid treatment, as evidenced by a reduction in [^{3}H] Ro15-4513 binding (γ2 subunit-containing GABAR) in kainic acid treated CGCs and no difference in [^{3}H] muscimol binding (γ2 and δ subunit-containing GABAR).

Treatment with the L-type calcium channel blockers, nifedipine and verapamil implicated the influx of calcium via L-type calcium channels as a result of AMPAR activation to cause the depolarisation induced up-regulation of δ subunit protein.

6.3.1. Is GABAR δ subunit assembled into receptors following kainic acid depolarisation, when its receptor partner, α6 is down-regulated?

Results of the current study indicated a dramatic up-regulation of GABAR δ subunit expression upon kainic acid treatment in control CGCs. However, a significant reduction in GABAR α6 subunit expression was also noted, the preferential subunit partner for the δ subunit in CGCs. Therefore, this raises the question as to whether the δ subunit is retained intracellularly or if the subunit is assembled into receptors and trafficked to the cell surface.

In order to address this question, biotinylation assays were conducted on control CGCs (7 DIV) cultured under basal conditions and in the presence of kainic acid (100 μM). Results demonstrated that the GABAR δ subunit is indeed expressed at the cell surface under both conditions (figure 6.2). Kainic acid-mediated depolarisation results in an increase in total GABAR δ subunit protein levels, but also an increase in GABAR δ subunit expression at the cell surface. From heterologous cell expression studies, it has been shown that GABAR α and γ subunits and presumably δ alone are unable to traffick to the neuronal cell surface unless co-assembled into αβ, αβγ or αβδ combinations (Connolly *et al.*, 1996a, 1996b, 1999a). Therefore, if expression levels of the GABAR δ subunit is increased at the cell surface following kainic acid treatment, with which α subunit does the δ subunit co-assemble?

6.3.2. Which GABAR α subunit does the δ subunit co-assemble with under depolarising conditions?

6.3.2.1. Kainic acid mediated depolarisation

Results of the current study demonstrated a dramatic increase in expression of the GABAR δ subunit upon kainic acid depolarisation. However, total expression levels of the GABAR α1 and α6 subunits were significantly reduced upon depolarisation to 29 ± 22% and 27 ± 0.3% of 5K levels, with a concomitant

decrease in GABAR α6 subunit expression at the cell surface. Radioligand binding studies using [^{3}H] Ro15-4513 indicated that the levels of BZ-IS binding were slightly reduced in kainic acid-depolarised CGCs (0.09 ± 0.09 pmoles/mg protein) to 5K CGCs (0.19 ± 0.09 pmoles/mg protein), which however did not reach statistical significance (figure 6.3).

Western blot analysis indicated a dramatic up-regulation of expression of the GABAR α4 subunit upon depolarisation mediated by kainic acid (figure 6.2). Biotinylation experiments also revealed a dramatic increase in cell surface expression of the α4 subunit in kainic acid treated CGCs. Therefore, it is possible to conclude that under kainic acid depolarisation, there is a selective up-regulation of α4 subunit expression. Sur *et al.*, in 1999 reported that in rat thalamus there was a preferential co-assembly of α4 subunits with δ subunits. Immunoprecipitations using anti-α4 serum precipitated 20% of [^{3}H] muscimol binding sites and only 7% of [^{3}H] Ro15-4513 binding sites.

Consequently, it is possible to suggest that the δ subunit preferentially co-assembles with α4 subunits under depolarising conditions in CGCs. In support of this observation, total [^{3}H] Ro15-4513 binding was reduced to 59 ± 14% of 5K levels, indicating a loss of γ2 subunit-containing GABAR (figure 6.3.B). No significant difference in total [^{3}H] muscimol binding was observed in kainate-treated CGCs, indicating that the total number of GABAR (γ2 and δ subunit containing receptors) does not differ between basal, polarised and kainate-induced depolarised CGCs (figure 6.3.A). Therefore, it is possible to conclude that if the total number of GABAR is unchanged, while there is a significant decrease in γ2 subunit containing GABAR, there is an up-regulation of δ subunit containing GABAR under kainic acid mediated depolarisation. This up-regulation of GABAR may be in the form of α4βδ receptors. In order to test this hypothesis, future work would involve immunoprecipitations of α4 subunit-containing GABAR from kainate-treated CGCs and probing the precipitated material for the presence of the GABAR δ subunit and vice versa.

6.3.2.2. KCl-mediated depolarisation

KCl-mediated depolarisation has also been shown to cause an increase in the expression of the GABAR δ subunit to 245 ± 36% of 5K levels in control CGCs. Furthermore, western blot analysis demonstrated a dramatic reduction in α1 and α6 subunit expression (7 ± 15% and 25 ± 1% of 5K levels respectively). In agreement with observations following kainic acid depolarisation, expression of the GABAR α4 subunit was found to be dramatically increased (figure 6.2). However, radioligand binding studies utilising [^{3}H] Ro15-4513 indicated the total loss of BZ-IS subtype of GABAR, conferred by GABAR α6 and α4 subunits upon KCl-mediated depolarisation, whereas following depolarisation mediated by kainic acid treatment, levels of BZ-IS binding were unchanged. This observation suggests differential regulation of GABAR assembly between depolarisation mechanisms.

6.3.3. Are CGCs cultured under kainic acid-mediated depolarisation developmentally arrested in terms of the pharmacology of the BZ-S subtype of GABAR?

[^{3}H] Ro15-4513 binding studies on basal polarised, KCl and kainic acid-mediated depolarised CGCs indicated differential modulation of the BZ-S subtype of GABAR between depolarisation methods. The levels of BZ-S binding in 25K CGCs was not significantly different from that observed in 5K CGCs. However, in kainate-treated CGCs, BZ-S levels of binding were found to be reduced to 64 ± 23% of 5K levels. Ives *et al.*, in 2002 reported a switch in BZ-S subtype pharmacology from type I, conferred by GABAR α1 subunit expression, to type II pharmacology, indicative of an up-regulation of expression of α2 and α3 subunits in KCl-mediated depolarised CGCs. Results of the current study are in support of these observations, BZ-S subtype of binding was not decreased, while expression of the GABAR α1 subunit was reduced to 7 ± 15% of 5K levels, suggesting an alternative α subunit co-assembles with the GABAR γ2 subunit to confer BZ-S pharmacology.

No evidence of such a switch in BZ-S pharmacology was found in kainate-treated CGCs. Levels of BZ-S binding were reduced to 64 ± 23% of 5K levels, which correlated with a significant reduction in GABAR α1 subunit expression (29 ± 22% of 5K levels, $p<0.01$).

6.3.4. Modulation of GABAR δ subunit expression by activation of AMPAR to cause calcium influx via L-type calcium channels

Results of chapter 5 indicated a possible modulation of GABAR δ subunit expression by kainic acid-mediated depolarisation. Kainic acid is an ionotropic glutamate receptor agonist, acting at excitatory AMPA and kainate receptors, to cause depolarisation. Comparison of responses observed in control and stargazer CGCs indicated a dramatic up-regulation of GABAR δ subunit expression in control CGCs upon kainic acid treatment, while expression of the subunit in stargazer CGCs remained at basal levels (section 5.2.4.). Since stargazer CGCs do not possess functional AMPAR at the cell surface, it can be concluded that activation of AMPAR by kainic acid treatment results in the positive modulation of expression of the GABAR δ subunit.

In order to determine the downstream consequence of activation of AMPAR in the mechanism resulting in increased GABAR δ subunit expression, the possible involvement of calcium influx was investigated. Gault and Siegel in 1997 reported the involvement of calcium entry via L-type calcium channels in the modulation of GABAR δ subunit expression following KCl-mediated depolarisation. Therefore, in order to test the possibility that such a mechanism existed upon kainic acid-mediated depolarisation, calcium influx via L-type calcium channels was blocked by employing two types of L-type calcium channel blocker, nifedipine, a 1,4-dihydropyridine and verapamil, a phenylalkylamine at a concentration of 10 μM.

Results indicated that nifedipine and verapamil reversed the increase in GABAR δ subunit expression following kainic acid treatment. Furthermore, in order to test the specificity of action of the drugs employed on the expression of the δ

subunit, each compound was applied to CGCs cultured under 5K conditions. None of the compounds tested acted alone to cause modulation of the δ subunit expression. Therefore, the basal, constitutive level of expression of the δ subunit is independent of AMPAR activity and L-type calcium channel activation (figure 6.5).

Therefore it can be concluded that activation of AMPAR causing an increase in intracellular calcium levels via L-type calcium channels did act to modulate expression levels of GABAR δ subunit.

Further work is necessary to elucidate the exact mechanism by which AMPAR mediated, L-type voltage-gated calcium channel-dependent calcium influx evokes effects on GABAR δ subunit expression. GABAR are subject to phosphorylation which can regulate functional desensitisation, open channel probability, aggregation of receptors at the synapse and assembly of subunits (Swope *et al.*, 1992). The latter two could conceivably result in an apparent increase in expression of the phosphorylated subunit. Mckernan *et al.*, in 1996 reported that there are residues in the GABAR δ subunit sequence that are predictive substrates for phosphorylation e.g. by protein kinase C. Results of biotinylation assays in the current study indicate that phosphorylation of the δ subunit may occur following kainic acid treatment, as the surface expressed protein appeared to have an increased molecular weight when subjected to immunoblotting (figure 6.1.). Dephosphorylation assays on biotinylated, kainate-treated CGCs would be needed to confirm the above observation.

Alternatively depolarisation-mediated calcium influx could activate kinases, such as protein kinase A, protein kinase C or calcium/calmodulin-dependent kinase II (CaMKII) and/or phosphatases, such as PP1 or PP2, which may act to modulate the activity of transcription factors, which could cause increased δ subunit transcription. Gault and Siegel in 1997 and 1998 suggested that the activation of transcription factors leads to increased GABAR δ subunit expression following KCl-mediated depolarisation. Indeed initial observations in the lab suggest the

up-regulation of GABAR δ subunit mRNA expression in kainate-treated CGCs (J.H. Ives, personal communication).

6.3.5. What are the effects of depolarisation on TARPγ2 expression?

We were intrigued to find that TARPγ2 protein expression levels were compromised upon kainic acid-mediated depolarisation, furthermore this resulted in a decrease in expression of TARPγ2 at the cell surface. In addition, the molecular weight of the protein appeared to be decreased at the cell surface (figure 6.6). Expression levels of the total AMPAR subunit GluR2 expressed in cultured CGCs were relatively unaffected by kainic acid treatment. However, the levels of expression at the cell surface were dramatically reduced (figure 6.6.).

TARPγ2 has been shown to regulate synaptic AMPAR by two distinct mechanisms. The C-terminal tail of the TARPγ2 protein possesses a type I PDZ-binding domain which has been shown to interact with PDZ proteins, such as PSD-95 at the synapse, and hence regulate synaptic targeting of AMPAR (Chen *et al.*, 2000). TARPγ2 also interacts with AMPAR to traffick receptors to the cell membrane, an interaction which does not require the PDZ binding domain of the protein. Tomita *et al.*, in 2004 reported that neuronal activity acted to increase the endocytosis of AMPAR. Furthermore, that depolarisation by increased extracellular KCl acted to decrease the surface levels of AMPAR/TARP complexes, in a CNQX sensitive fashion (Tomita *et al.*, 2004). Endogenous agonist at excitatory synapses was also found to disrupt the association of AMPAR with TARPs. Therefore, kainic acid treatment of CGCs would be predicted to disrupt the association of GluR2 with TARPγ2 and increase the endocytosis of the AMPAR subunit. Consequently, less GluR2 and TARPγ2 would be expressed at the cell surface. This indeed is what we have shown herein, that chronic activation of AMPARs in a neuronal context results in down-regulation of AMPAR cell surface expression as well as TARPγ2 expression. We assume that during this period of AMPAR activity coincides with GABAR δ expression.

In 2005, Tomita *et al.*, reported that TARPγ2 is heavily phosphorylated at a set of conserved serine residues within its C-terminal tail. This phosphorylation is dynamically regulated by synaptic activity, such that activation of CaMKII and PKC causes phosphorylation of the protein, while activation of PP1 and PP2B causes dephosphorylation. Phosphorylation was shown to facilitate the synaptic targeting of TARPγ2, dependent on the interaction of the C-terminal tail of TARPγ2 to PDZ domains of PSD-95. Therefore, a reduction in the molecular weight of stargazin at the cell surface, following depolarisation likely represents the dephosphorylation of the protein and the redistribution of receptors between synaptic and non-synaptic sites. We have a model system here to test this hypothesis.

6.3.6. Conclusions

Results of the current study indicated a role for excitatory neurotransmission in the modulation of GABAergic inhibition in culture CGCs. Results indicated an increase in GABAR δ subunit expression following kainic acid-mediated depolarisation in control CGCs, which was not observed in CGCs derived from the stargazer mutant. Since the stargazer mutant CGCs are essentially AMPAR-incompetent, this identified a role for AMPAR activation in the modulation of GABAR subunit expression. Furthermore, biotinylation assays determined that the increased level of GABAR δ subunit was indeed expressed at the cell surface in cultured control CGCs.

Radioligand binding studies demonstrated no significant difference in [^{3}H] muscimol binding between basal (5K) and kainate-treated CGCs, suggesting that the total number of GABAR does not differ between the two treatment groups. However, if considered with a reduction in total [^{3}H] Ro15-4513 binding observed in kainate-treated CGCs, indicative of the contribution of γ2 subunit-containing GABAR, these results further support an increase in δ subunit-containing GABAR in response to kainic acid-mediated depolarisation.

Treatment with the L-type calcium channel blockers, nifedipine and verapamil implicated the influx of calcium via L-type calcium channels as a result of AMPAR activation to cause the depolarisation induced up-regulation of δ subunit protein. The failure of nifedipine treatment to block the modulation of GABAR α1 and γ2 subunit expression also highlighted the existence of a number of mechanisms in the regulation of GABAR subunit expression in kainate-treated CGCs, further work would be necessary to ascertain the exact nature of such mechanisms.

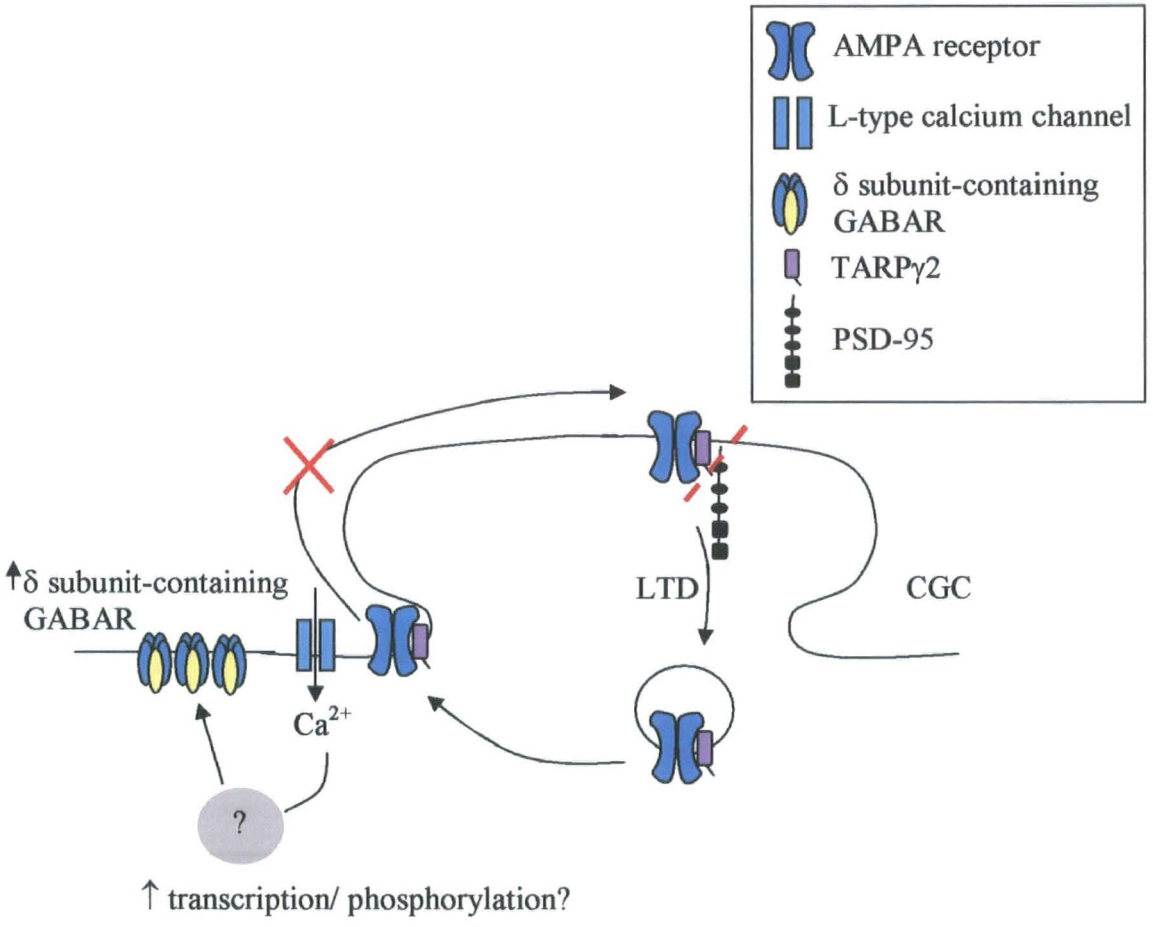

Figure 6.6. Schematic representation of the effects of kainic acid-mediated depolarisation on the expression of GABAR δ subunit and TARPγ2 in cultured control cerebellar granule cells (CGCs)

Kainic acid depolarisation acts to cause an influx in intracellular calcium via L-type voltage-gated calcium channels which results in an increase in cell surface expression of δ subunit-containing GABAR. Furthermore, depolarisation acts to disrupt the association of TARPγ2 with PSD-95 and results in the internalisation of AMPAR and TARPγ2. LTD: Long term depression.

CHAPTER 7. $GABA_A$ RECEPTOR EXPRESSION IN THE DENTATE GYRUS OF THE STARGAZER MUTANT MOUSE

7.1. INTRODUCTION

Cerebellar granule cells of the stargazer mutant are electrically silent as a result of failure to express TARPγ2 to cause a deficit in AMPAR expression at mossy fibre-granule cell synapses (Chen *et al.*, 2000). This in turn results in a near total ablation of brain-derived neurotrophic factor (BDNF) expression in CGCs and compromised TrkB signalling (Qiao *et al.*, 1996; 1998).

In contrast, granule cells of the dentate gyrus (DG) are not electrically silent in the stargazer mutant. The stargazer mutant exhibits spontaneous bilaterally symmetrical 6-7 per second spike-wave discharges (SWDs) in cortical and hippocampal brain areas, which represent ~20% of total waking electroencephalographic (EEG) activity (Qiao & Noebels, 1993). Onset of seizure activity has been shown to occur between postnatal days 16-18 (P16-18), with a frequency of ~150 bursts per hour (Qiao & Noebels, 1993). The spike-wave pattern of generalised synchronous activity has been shown to generate primarily in the thalamus and neocortex to activate synaptically linked brain areas, such as the hippocampus via the dentate gyrus.

A clear correlation has been shown between the accumulation of continuous seizure activity and an increase in mossy fibre sprouting in the inner molecular-granule cell layer of the dentate gyrus, reported to occur at 4-6 weeks following seizure onset (Qiao & Noebels, 1993). No significant cell death of granule cells in the dentate gyrus (DG), CA3 pyramidal cells or hilar polymorph cells was noted following non-convulsive seizures in the stargazer mutant (Qiao & Noebels, 1993), in contrast to convulsive seizure models such as kainic acid treatment, kindling and pentylenetetrazole (PTZ) which are associated with cellular injury, death and gliosis (Nahm & Noebels, 1998). Hypersynchronous activity has also been shown to induce axonal sprouting in the granule cell-

molecular layer of the dentate gyrus in these convulsive seizure models (Nahm & Noebels, 1998). Chronic depolarisation in convulsive seizure models also results in an adaptive modification of inhibitory neurotransmission to balance increased excitation, manifesting in alterations in the function, pharmacology, targeting and clustering of GABAR (Brooks-kayal *et al.*, 1998; Clark, 1998; Cohen *et al.*, 2003; Peng *et al.*, 2004).

Previous results in the laboratory have shown effects of electrical activity on the GABAR expression profiles of cultured CGCs (studies described herein and Ives *et al.*, 2002a) and a subunit specific down-regulation of expression of the GABAR α6 and β3 subunits to result in a loss of benzodiazepine-insensitive (BZ-IS) [^{3}H] Ro15-4513 binding in the stargazer mutant (herein and Thompson *et al.*, 1998). If a loss of electrical activity and a complete ablation of BDNF expression in stargazer CGCs causes GABAR rearrangements, it could be postulated that increased electrical activity and an increase in BDNF expression might evoke a reciprocal rearrangement of GABAR in stargazer dentate granule cells (DGCs). Furthermore, previous work herein has indicated a possible switch in the GABAR profile of the dentate gyrus of the stargazer mutant to favour expression of GABAR with a BZ-IS subtype of [^{3}H] Ro15-4513 pharmacology by receptor autoradiography, suggesting an increase in expression of α4βγ2 GABAR (see section 4.3.3.2; Figure 4.9.).

The aim of the current chapter was to characterise the expression profile of GABAR in control and stargazer DG by a combination of immunohistochemical, immunoblotting and radioligand binding techniques to determine any abnormalities in GABAR expression in the stargazer DG in response to high frequency SWDs and increased BDNF expression (Chaftez *et al.*, 1995; Nahm and Noebels, 1998; Koyama *et al.*, 2004; 2005).

7.2. RESULTS

7.2.1. GABA receptor switch from α4βδ to α4βγ2 in the DG of the stargazer mutant mouse

7.2.1.1. [^{3}H] Muscimol binding

The relative distribution of [^{3}H] muscimol binding (20 nM) was observed to be comparable in control and stargazer forebrain tissue sections, with the highest levels of binding in the hippocampus, cerebral cortex and striatum (figure 7.1.A). Quantification of the levels of [^{3}H] muscimol binding in the dentate gyrus revealed a significant decrease in the levels of binding in the stargazer mutant, to 79 ± 9% of control levels, n=30, p=0.01 (Figure 7.1. C&D). Since [^{3}H] muscimol has been shown to selectively bind only GABAR α6 in autoradiography (or its equivalent, α4 in the forebrain) either directly, or as a result of the presence of the δ subunit (Korpi *et al.*, 2002b), a reduction in [^{3}H] muscimol binding suggests a loss of α4βδ GABAR in the stargazer mutant DG.

7.2.1.2. Total [^{3}H] Ro15-4513 binding

In order to determine any possible abnormalities in expression of γ2 subunit-containing GABAR population, radioligand binding studies were conducted on control and stargazer tissue sections, using [^{3}H] Ro15-4513 at a concentration of 20 nM. Figure 7.2.A demonstrates the mapping of total [^{3}H] Ro15-4513 binding sites in control and stargazer tissue sections. The highest intensity of binding was observed in the hippocampus and cortex. Figure 7.2.C&D illustrate the calculated levels of total [^{3}H] Ro15-4513 binding in the dentate gyrus which revealed no significant difference in the levels of binding between control and stargazer tissue sections (104 ± 7% of control levels, p=0.55, n = 30, 6 sections per mouse strain, 5 measurements per section). Therefore, it is possible to conclude that the total levels of γ2 subunit-containing receptors expressed in the dentate gyrus do not differ between control and stargazer mice

Figure 7.1. [^{3}H] Muscimol binding (20 nM) to control (+/+:+/stg) and stargazer (stg/stg) adult mouse dentate gyrus

A: Representative control and stargazer autoradiographs demonstrating high intensity of radiolabel in the dentate gyrus and cortex.
B: Standard curve of intensity versus radioactivity, constructed using ImageJ software to measure the intensity of [^{3}H] standards of known radioactivities (see section 2.12.2).
C: Representative column graph depicting the calculated radioactivities of the dentate gyrus of 6 control and 6 stargazer tissue sections, 5 measurements per section from n=2 mice per strain.
D: Bar graph to demonstrate a significant decrease in [^{3}H] muscimol binding in the dentate gyrus of the stargazer mutant mouse, to 79 ± 9% of control levels, p=0.01.

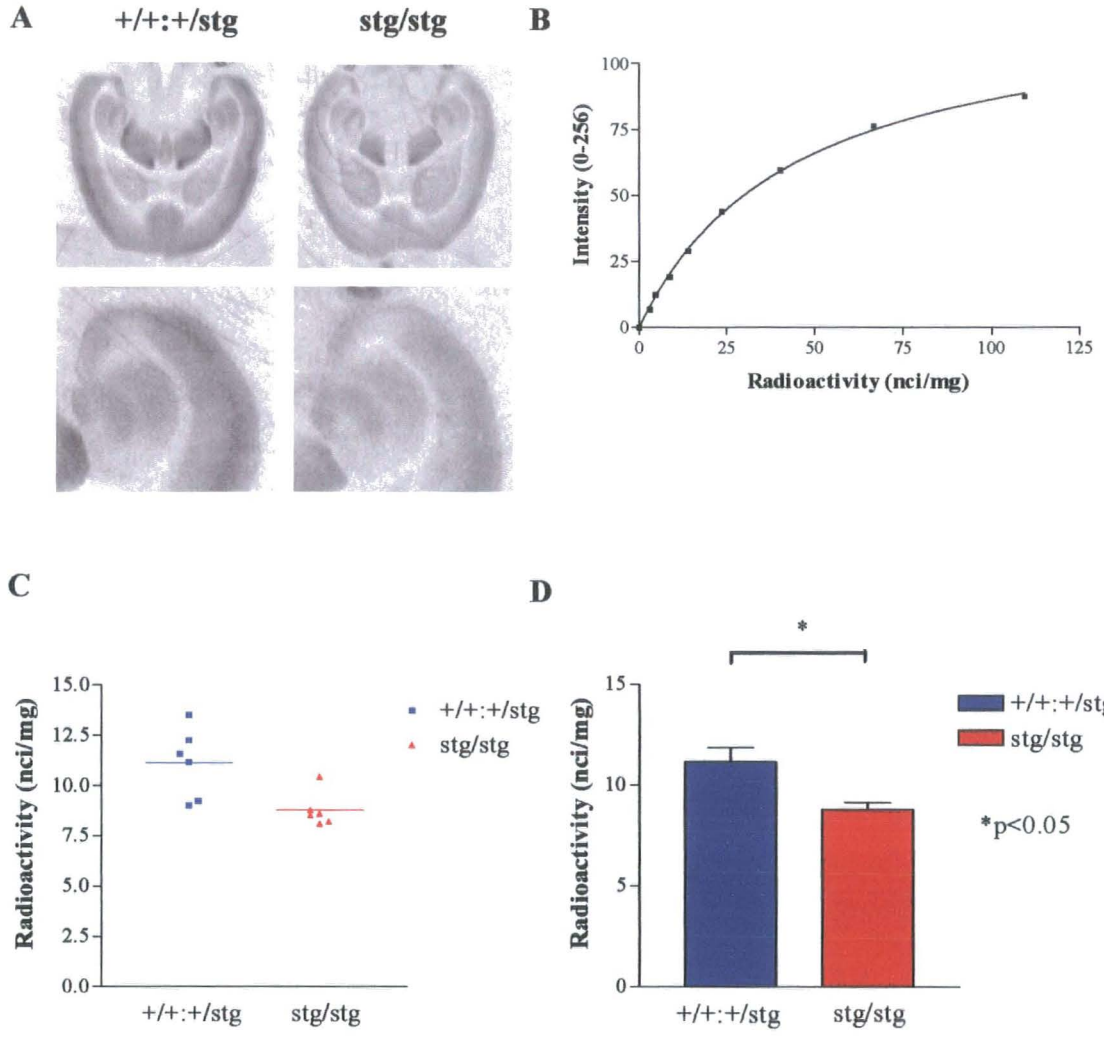
A
+/+:+/stg
stg/stg
B
Intensity (0-256)
100
75
50
25
0
0
25
50
75
100
125
Radioactivity (nci/mg)
C
Radioactivity (nci/mg)
15.0
12.5
10.0
7.5
5.0
2.5
0.0
+/+:+/stg
stg/stg
+/+:+/stg
stg/stg
D
*
Radioactivity (nci/mg)
15
10
5
0
+/+:+/stg
stg/stg
+/+:+/stg
stg/stg
*p<0.05

Figure 7.2. Total [^{3}H] Ro15-4513 binding (20 nM) to control (+/+:+/stg) and stargazer (stg/stg) adult mouse dentate gyrus

A: Representative control and stargazer autoradiographs demonstrating high intensity of radiolabel in the cortex and hippocampus.

B: Standard curve of intensity versus radioactivity, constructed using ImageJ software to measure the intensity of [^{3}H] standards of known radioactivities (see section 2.12.2).

C: Column graph depicting the calculated radioactivities of the dentate gyrus of 6 control and 6 stargazer tissue sections, 5 measurements per section from n=2 mice per strain.

D: Bar graph to demonstrate no significant decrease in total [^{3}H] Ro15-4513 binding in the dentate gyrus of the stargazer mutant mouse (104 ± 7% of control levels, p=0.55.

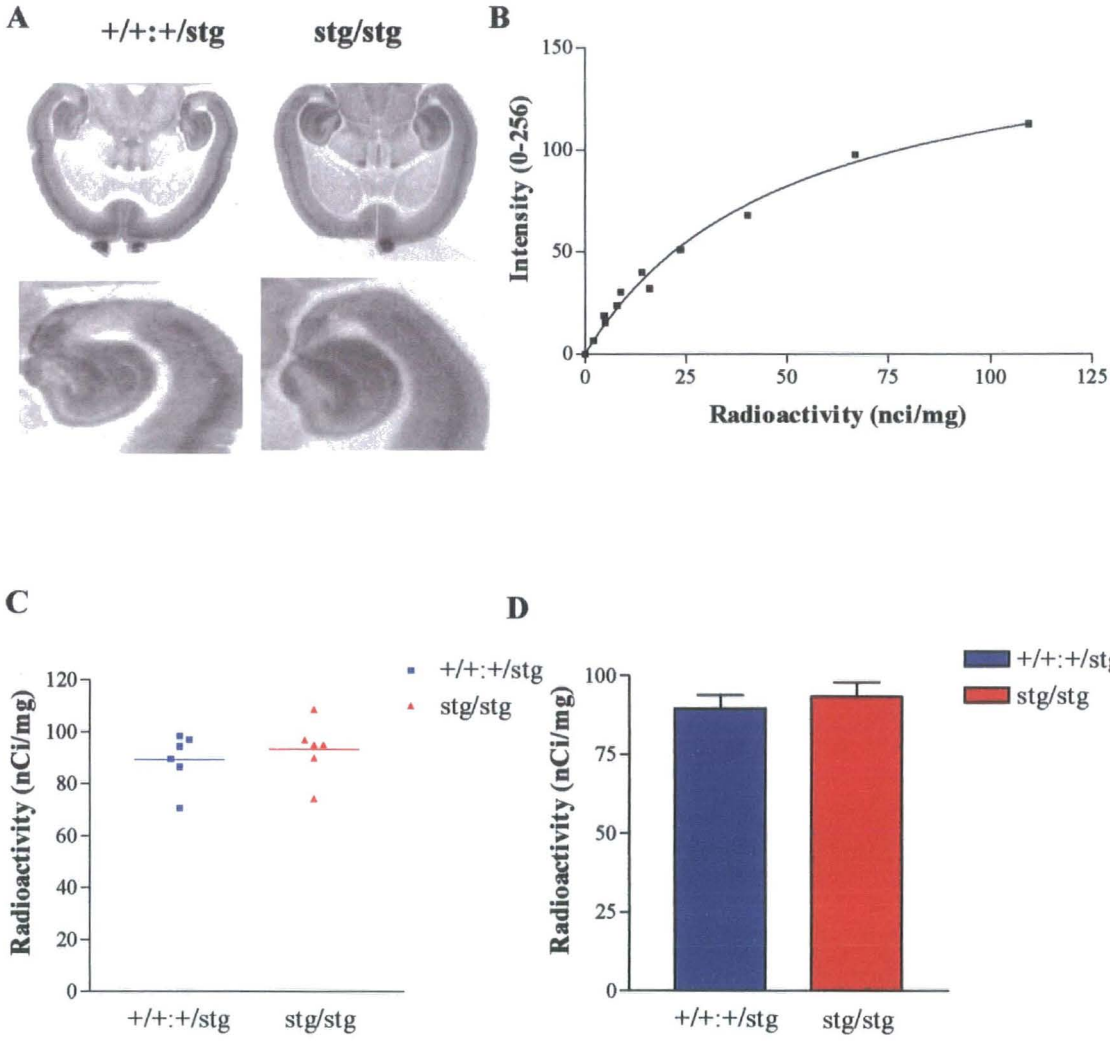
A
+/+:+/stg
stg/stg
B
Intensity (0-256)
150
100
50
0
0
25
50
75
100
125
Radioactivity (nci/mg)
C
Radioactivity (nCi/mg)
120
100
80
60
40
20
0
+/+:+/stg
stg/stg
+/+:+/stg
stg/stg
D
Radioactivity (nCi/mg)
100
75
50
25
0
+/+:+/stg
stg/stg
+/+:+/stg
stg/stg

7.2.1.3. Benzodiazepine-insensitive (BZ-IS) subtype of [^{3}H] Ro15-4513 binding

Levels of BZ-IS subtype of [^{3}H] Ro15-4513 binding were determined in the presence of 10 μM flunitrazepam. Interestingly, BZ-IS binding was not detected in control DG, with levels of binding not different from background film levels (figure 7.3.A). However, this subtype of binding was dramatically up-regulated in the stargazer DG which upon quantification yielded ~10 nCi/mg gray matter radioactivity ($p<0.01$, $n=25$). An increase in the BZ-IS subtype of binding suggests an increase in $\alpha4\beta\gamma2$ (or $\alpha6\beta\gamma2$) GABAR in the stargazer DG.

7.2.1.4. Benzodiazepine-sensitive (BZ-S) subtype of [^{3}H] Ro15-4513 binding

The contribution of the BZ-S subtype to total [^{3}H] Ro15-4513 binding was determined qualitatively by [^{3}H] flunitrazepam (5 nM) labelling of control and stargazer tissue sections. No qualitative differences were noted in the distribution of [^{3}H] flunitrazepam binding to control or stargazer sections. The highest levels of binding were observed in the hippocampus, cerebral cortex and striatum (figure 7.4.A). However, upon quantification of [^{3}H] flunitrazepam binding, the gray scale intensities of labelling in the dentate gyrus of control and stargazer sections fell above the highest calibration standard available. Consequently, since total [^{3}H] Ro15-4513 binding is equal to the sum of BZ-S and BZ-IS binding, the relative levels of BZ-S binding were calculated by the subtraction of BZ-IS binding from total [^{3}H] Ro15-4513 binding. By this method, the levels of BZ-S binding were calculated to not differ significantly between control and stargazer DG (94 ± 6% of control levels, $p=0.39$). Therefore, it is possible to conclude that the levels of $\alpha1/\alpha2\beta\gamma2$ GABAR were not different between control and stargazer DG.

Figure 7.3. [^{3}H] Ro15-4513 BZ-IS subtype (20 nM in the presence of 10 μM flunitrazepam) binding to control (+/+:+/stg) and stargazer (stg/stg) adult mouse dentate gyrus

A: Representative control and stargazer autoradiographs demonstrating high intensity of radiolabel in the dentate gyrus of the stargazer mutant.
B: Standard curve of intensity versus radioactivity, constructed using ImageJ software to measure the intensity of [^{3}H] standards of known radioactivities (see section 2.12.2).
C: Representative column graph depicting the calculated radioactivities of the dentate gyrus of 5 control and 5 stargazer tissue sections, 5 measurements per section from n=2 mice per strain.
D: Bar graph to demonstrate a significant increase in the BZ-IS subtype of [^{3}H] Ro15-4513 binding in the dentate gyrus of the stargazer mutant mouse of control levels, $p<0.01$.

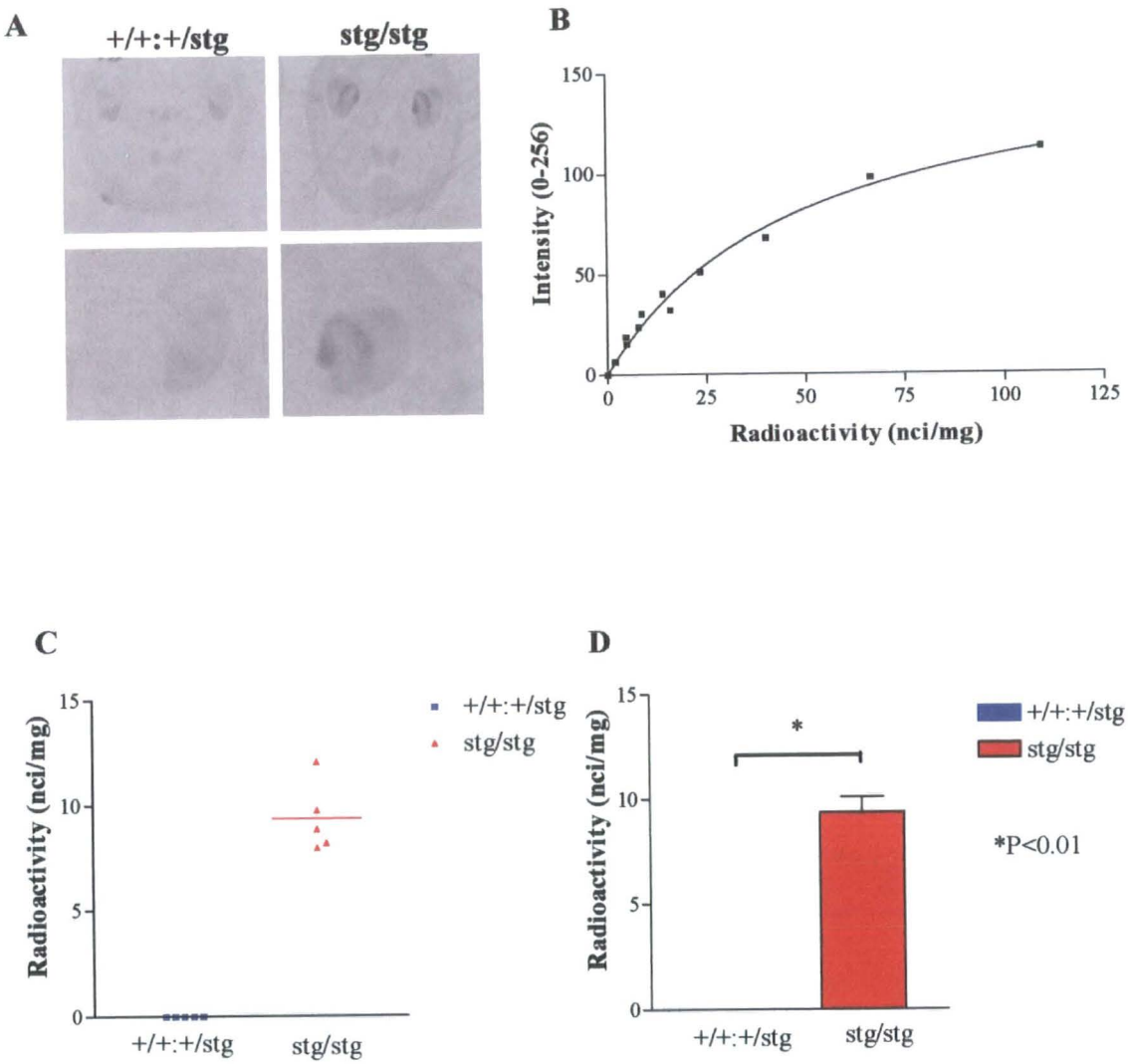
A
+/+:+/stg
stg/stg
B
Intensity (0-256)
150
100
50
0
0
25
50
75
100
125
Radioactivity (nci/mg)
C
Radioactivity (nci/mg)
15
10
5
0
+/+:+/stg
stg/stg
+/+:+/stg
stg/stg
D
Radioactivity (nci/mg)
15
10
5
0
*
+/+:+/stg
stg/stg
+/+:+/stg
stg/stg
*P<0.01

Figure 7.4. [^{3}H] Flunitrazepam binding (5 nM) to control (+/+:+/stg) and stargazer (stg/stg) adult mouse dentate gyrus

A: Representative control and stargazer autoradiographs demonstrating high intensity of radiolabel in the hippocampus and cortex.
B: Standard curve of intensity versus radioactivity, constructed using ImageJ software to measure the intensity of [^{3}H] standards of known radioactivities (see section 2.12.2).
C: Bar graph to demonstrate no significant decrease in [^{3}H] flunitrazepam binding in the cerebellar granule cell layer of the stargazer mutant mouse (94 ± 6% of control levels).

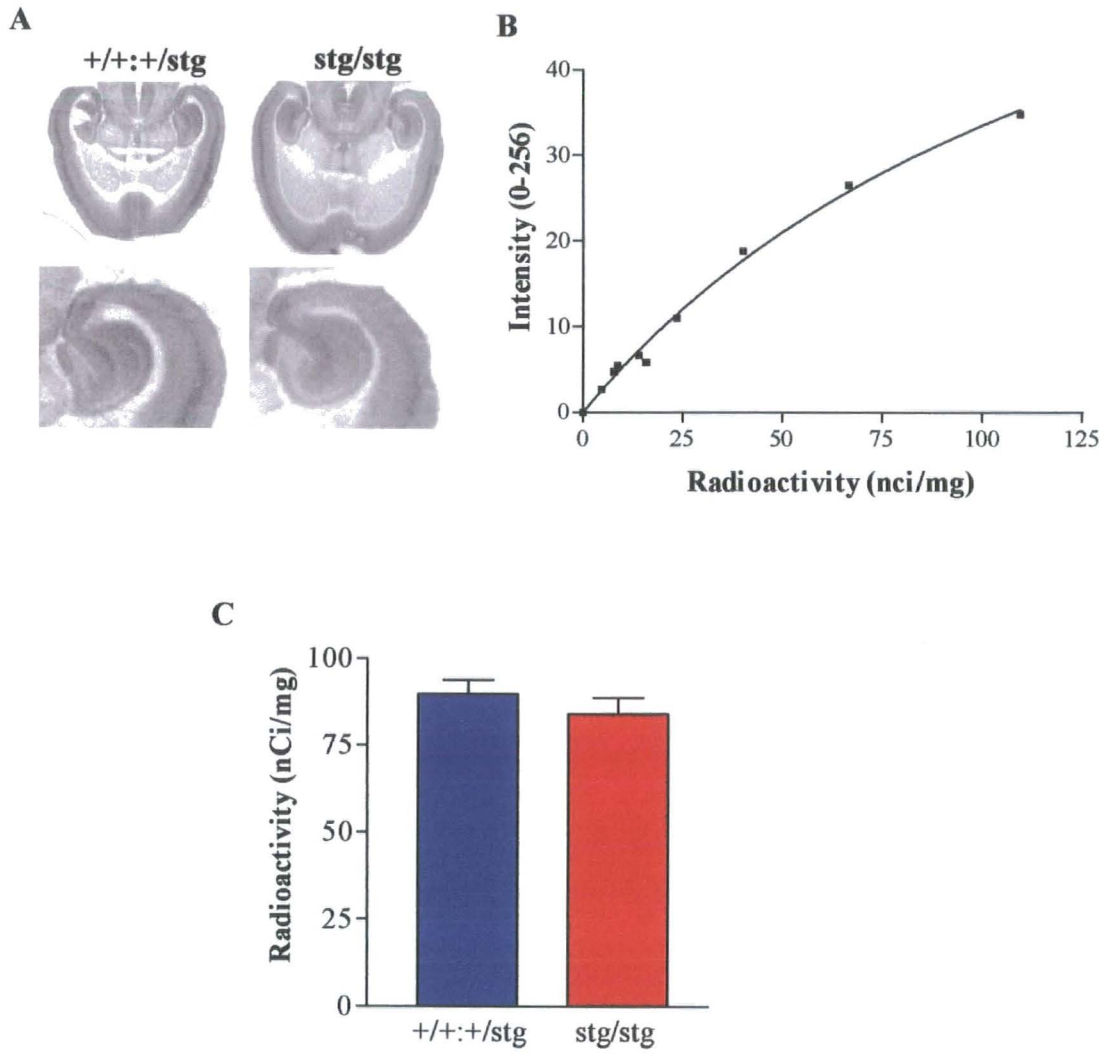
A
+/+:+/stg
stg/stg
B
Intensity (0-256)
40
30
20
10
0
0
25
50
75
100
125
Radioactivity (nci/mg)
C
Radioactivity (nCi/mg)
100
75
50
25
0
+/+:+/stg
stg/stg

7.2.2. Immunohistochemical mapping of GABAR subunit expression in the DG of control and stargazer mice

Receptor autoradiography revealed an increase in BZ-IS [^{3}H] Ro15-4513 binding in the stargazer DG. Therefore, in order to determine any alterations in the distribution and expression levels of GABAR subunits in the stargazer DG, GABAR expression was compared in control and stargazer DG by immunohistochemistry and quantitative western blotting.

7.2.2.1. α1 subunit expression

Paraformaldehyde perfusion-fixed adult mouse control and stargazer tissue sections were probed with anti-GABAR α1 subunit specific antibody at 0.25 μg/ml (see section 2.14 for method). Figure 7.5. demonstrates intense immunoreactivity in the stratum oriens, pyramidal cell layer and the stratum radiatum of the CA1and CA3. A high level of immunoreactive staining was also observed in the hilus and molecular layers of the dentate gyrus, with intense staining at the hilar surface of the granule cell layer. No apparent differences were noted in the levels of staining in stargazer compared to control tissue sections (n=4).

7.2.2.2. α4 subunit expression

GABAR α4 subunit immunostaining was detected in the pyramidal cell layer of the CA1 and CA3 and to a lesser extent in the stratum oriens using anti-GABAR α4 subunit specific antibody at 0.5 μg/ml (figure 7.6.). The most intense immunoreactivity was noted in the molecular layer of the dentate gyrus, with staining also observed in the granule cell layer and interneurons of the hilus. No immunoreactive staining was observed in the stratum radiatum of the CA1 and CA3 (n=5-8). A qualitative increase in immunostaining for the GABAR α4 subunit was observed in the molecular layer of the dentate gyrus in stargazer tissue sections compared to control sections.

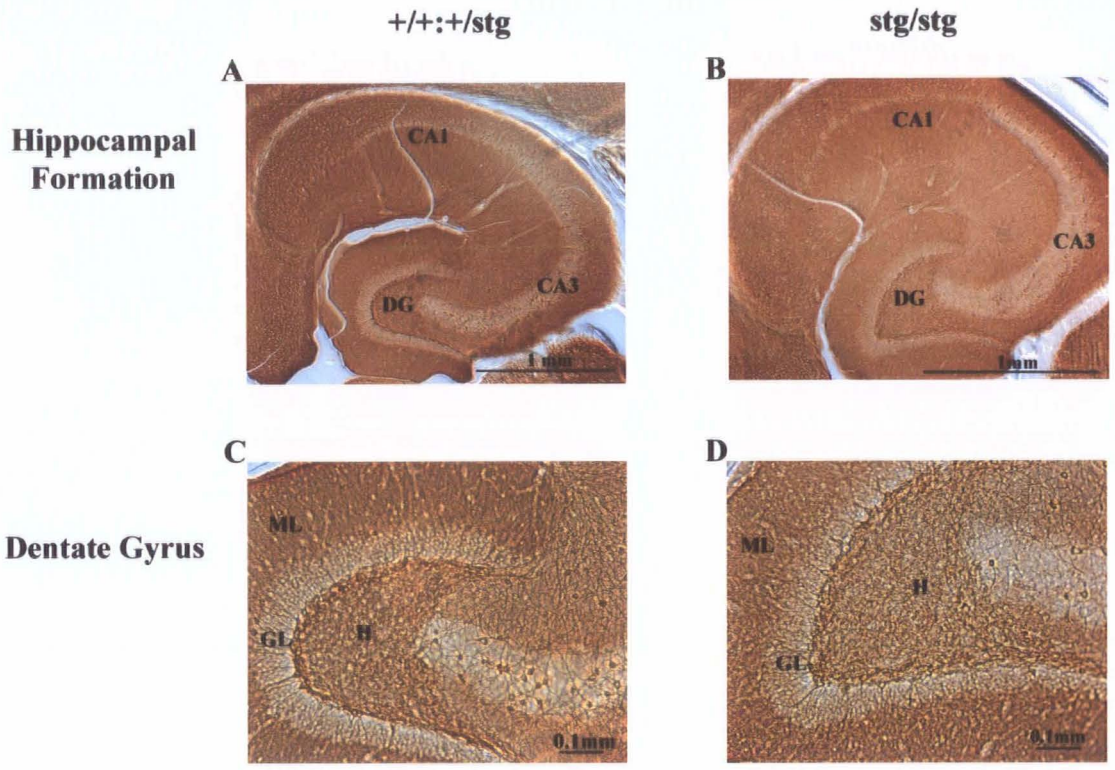

Figure 7.5. Immunohistochemical mapping of the $GABA_A$ receptor $\alpha 1$ subunit in adult mouse dentate gyrus

A&B: +/+:+/stg and stg/stg whole hippocampi respectively at x40 magnification
C&D: +/+:+/stg and stg/stg brain sections respectively at x100 magnification

Note the intense staining in the granule cell layer (GL), molecular layer (ML) and hilus (H) of the dentate gyrus (DG) in both control and stargazer tissue sections.

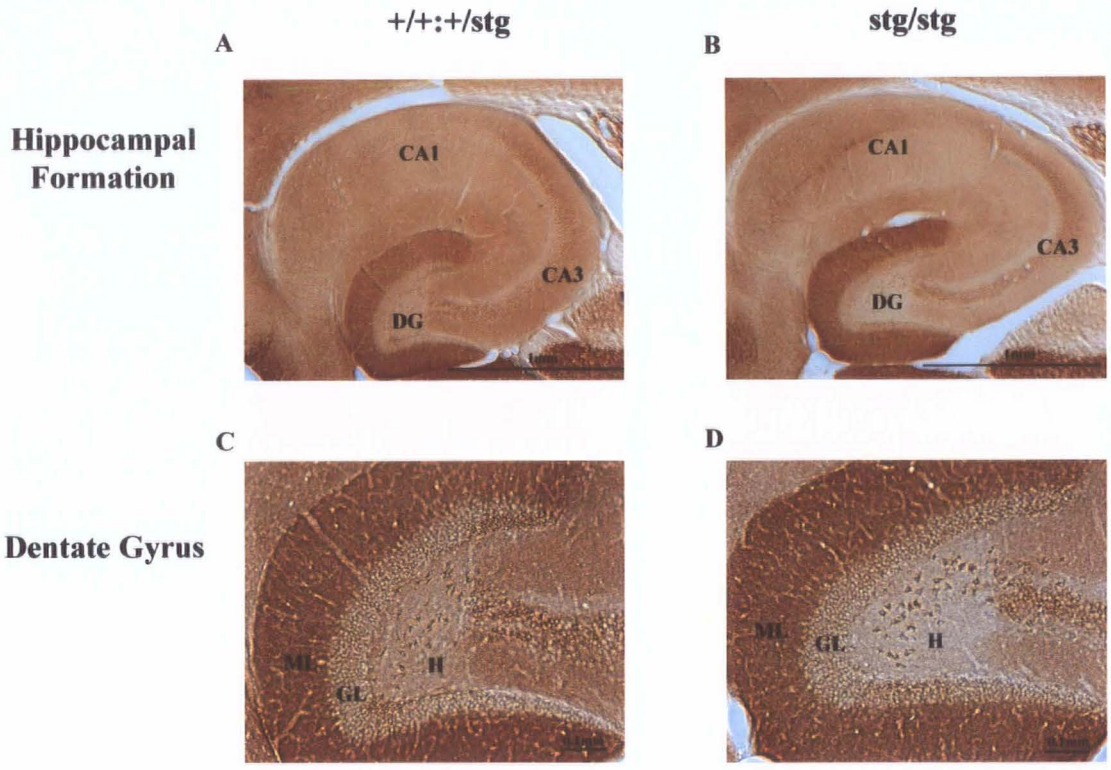

Figure 7.6. Immunohistochemical mapping of the $GABA_A$ receptor α4 subunit in adult mouse dentate gyrus

A&B: +/+:+/stg and stg/stg whole hippocampi respectively at x40 magnification
C&D: +/+:+/stg and stg/stg brain sections respectively at x100 magnification

Note the intense staining in the molecular layer (ML) and hilus (H) in control dentate gyrus (DG) which is greatly reduced in the molecular layer of the stargazer dentate gyrus.

7.2.2.3. β2 subunit expression

Anti-GABAR β2 subunit specific antibody was employed at a concentration of 0.5 μg/ml in order to map the subunit expression in the hippocampus. High levels of immunoreactivity were detected in the stratum oriens and stratum radiatum of the CA1 and to a lesser extent in the stratum oriens and radiatum of the CA3. Intense immunoreactivity was observed in the molecular layer of the DG, with immunoreactive staining noted in the hilus and granule cell layer (figure 7.7.). No immunoreactive staining was noted in the pyramidal cell layer of the CA1 or CA3 (n=4). An increase in β2 subunit immunoreactivity was noted in the molecular layer of the dentate gyrus in stargazer tissue sections compared to control levels of staining.

7.2.2.4. β3 subunit expression

Figure 7.8. demonstrates immunohistochemical staining of control and stargazer tissue sections with anti-GABAR β3 subunit specific antibody at 0.5 μg/ml. Intense immunoreactivity was observed in the molecular layer of the dentate gyrus, with high levels of staining in the stratum oriens and stratum radiatum of the CA3 and to a lesser extent in the stratum oriens and radiatum of the CA1 and stratum lacunosum moleculare. No immunoreactivity was detected in the hilus or granule cell layer of the dentate gyrus or pyramidal cell layer of the CA1 and CA3 (n=5-8) (figure 7.8.). Increased levels of immunoreactivity were detected in the molecular layer of the stargazer mutant tissue sections when compared to control sections.

7.2.2.5. δ subunit expression

GABAR δ subunit immunoreactivity in the hippocampus was determined immunohistochemically using anti-GABAR δ subunit specific antibody at 0.25 μg/ml. In order to visualise immunoreactive staining in the dentate gyrus, tissue sections were subjected to antigen retrieval prior to immunohistochemical staining, in order to boost specific antibody binding

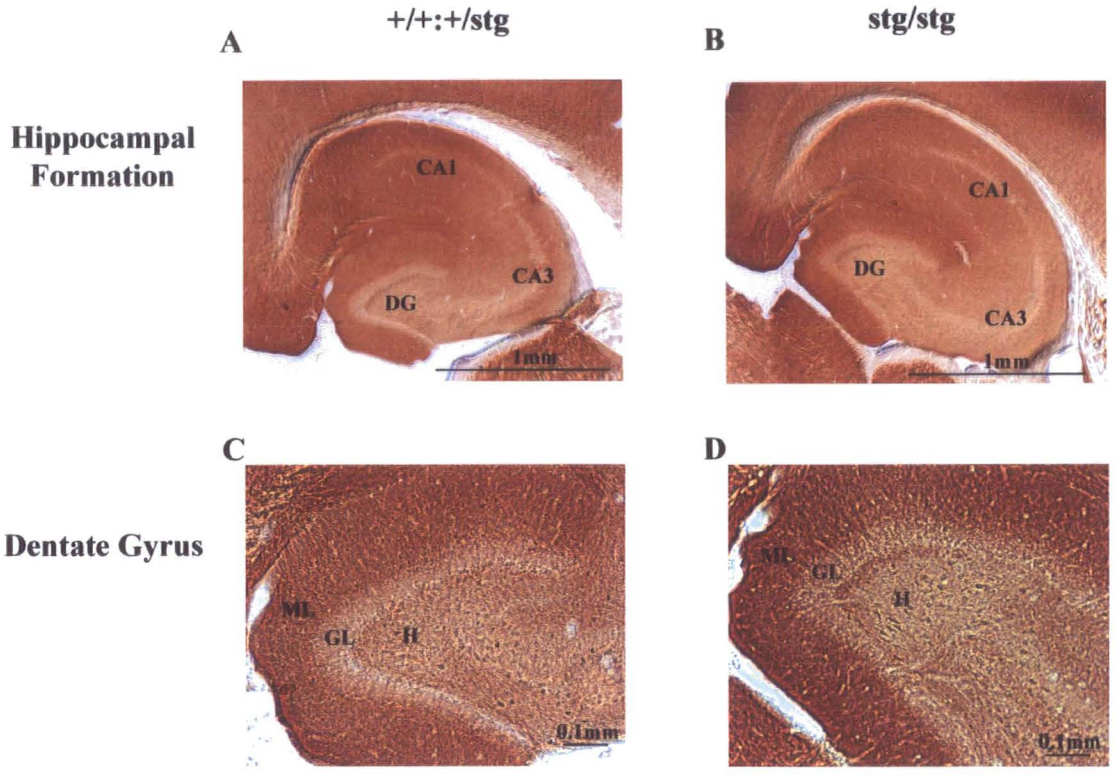

Figure 7.7. Immunohistochemical mapping of the $GABA_A$ receptor β2 subunit in adult mouse dentate gyrus

A&B: +/+:+/stg and stg/stg whole hippocampi respectively at x40 magnification
C&D: +/+:+/stg and stg/stg brain sections respectively at x100 magnification

Note the intense staining in the molecular layer (ML) and hilus (H) in control dentate gyrus (DG) which is slightly increased in the molecular layer of the stargazer dentate gyrus.

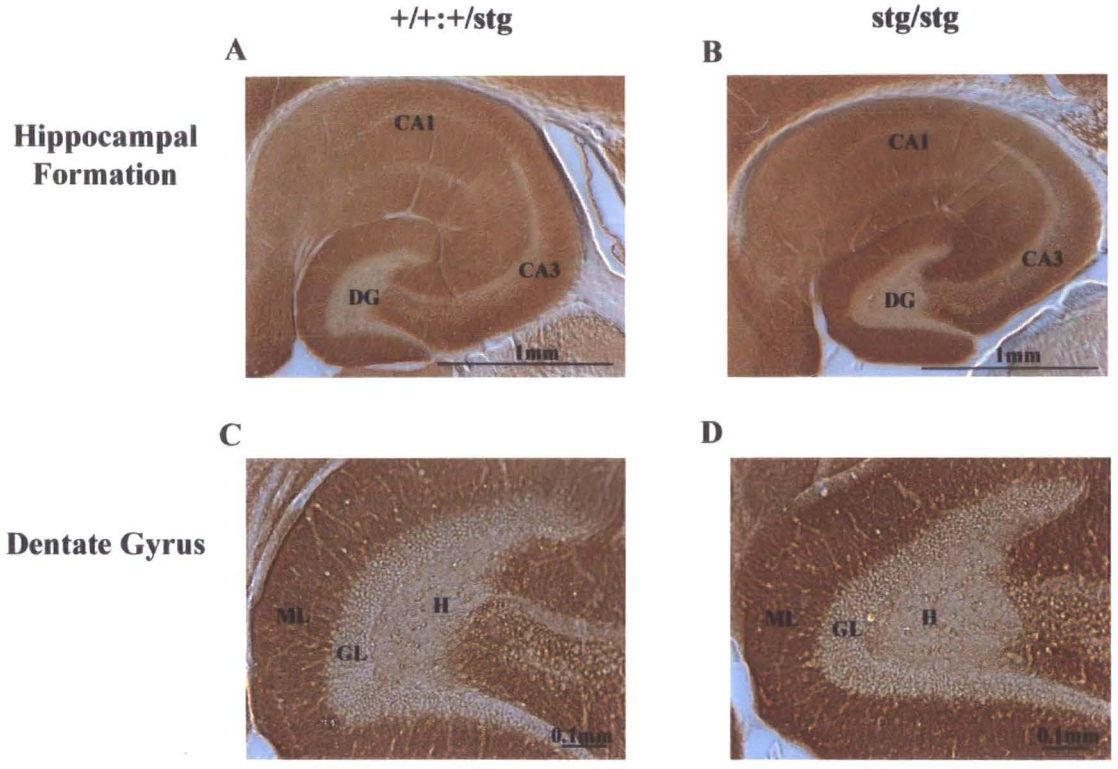

Figure 7.8. Immunohistochemical mapping of the $GABA_A$ receptor β3 subunit in adult mouse dentate gyrus

A&B: +/+:+/stg and stg/stg whole hippocampi respectively at x40 magnification
C&D: +/+:+/stg and stg/stg brain sections respectively at x100 magnification

Note the intense staining in the molecular layer (ML) and hilus (H) in control dentate gyrus (DG) which is greatly increased in the molecular layer of the stargazer dentate gyrus.

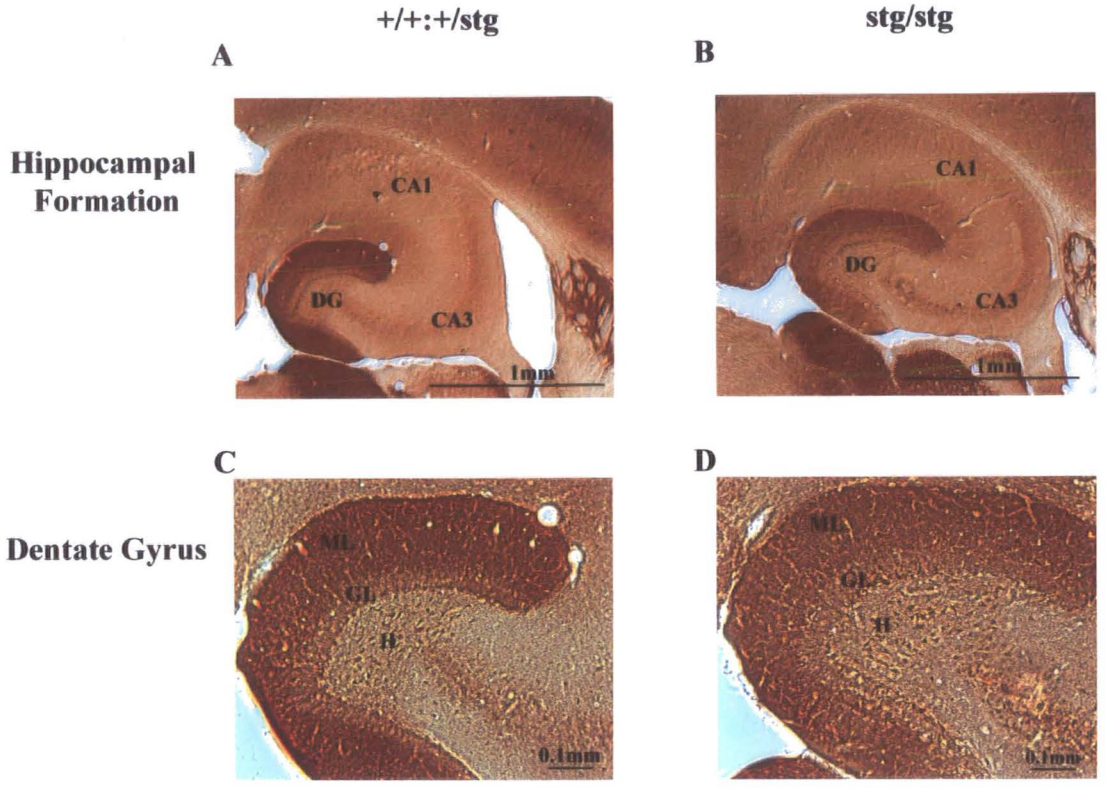

Figure 7.9. Immunohistochemical mapping of the $GABA_A$ receptor δ subunit in adult mouse dentate gyrus

A&B: +/+:+/stg and stg/stg whole hippocampi respectively at x40 magnification
C&D: +/+:+/stg and stg/stg brain sections respectively at x100 magnification

Note the intense staining in the granule cell layer (GL), molecular layer (ML) and hilus (H) of control dentate gyrus (DG) which is greatly decreased in the molecular layer of the stargazer dentate gyrus.

(see section 2.13.3. for method). Consistent differences in expression levels of the δ subunit were not obtained in 5-10 tissue sections. However, in some instances expression of the subunit appeared to be reduced in stargazer DG compared to controls. The highest levels of immunoreactivity were consistently observed in the molecular layer of the dentate gyrus, with high levels in the granule cell layer. Immunoreactive staining was also noted in the hilus, stratum lacunosum moleculare, stratum oriens of the CA1and pyramidal cell layer of the CA1 and CA3. No immunoreactive staining was noted in the stratum radiatum of the CA1 and CA3 or the stratum oriens of the CA3 (n=5-10). Figure 7.9. demonstrates a qualitative decrease in immunoreactivity in the molecular layer of the dentate gyrus in stargazer mutant sections compared to controls.

7.2.2.6. γ2 subunit expression

Figure 7.10. demonstrates immunohistochemical staining of the hippocampal formation using an anti-GABAR γ2 subunit-specific antibody at a concentration of 2 μg/ml. The highest levels of staining were observed in the molecular layer of the dentate gyrus and the pyramidal cell layer of the CA2. Immunoreactivity for the γ2 subunit was also noted in the hilus, dentate granule cell layer and the stratum oriens and stratum lacunosum moleculare of the CA1. No differences in intensity of staining were noted between control and stargazer sections (n=5-8).

Table 7.1. summarises the patterns of immunoreactive staining of the GABAR subunits in the hippocampus and the qualitative differences observed between control and stargazer tissue sections.

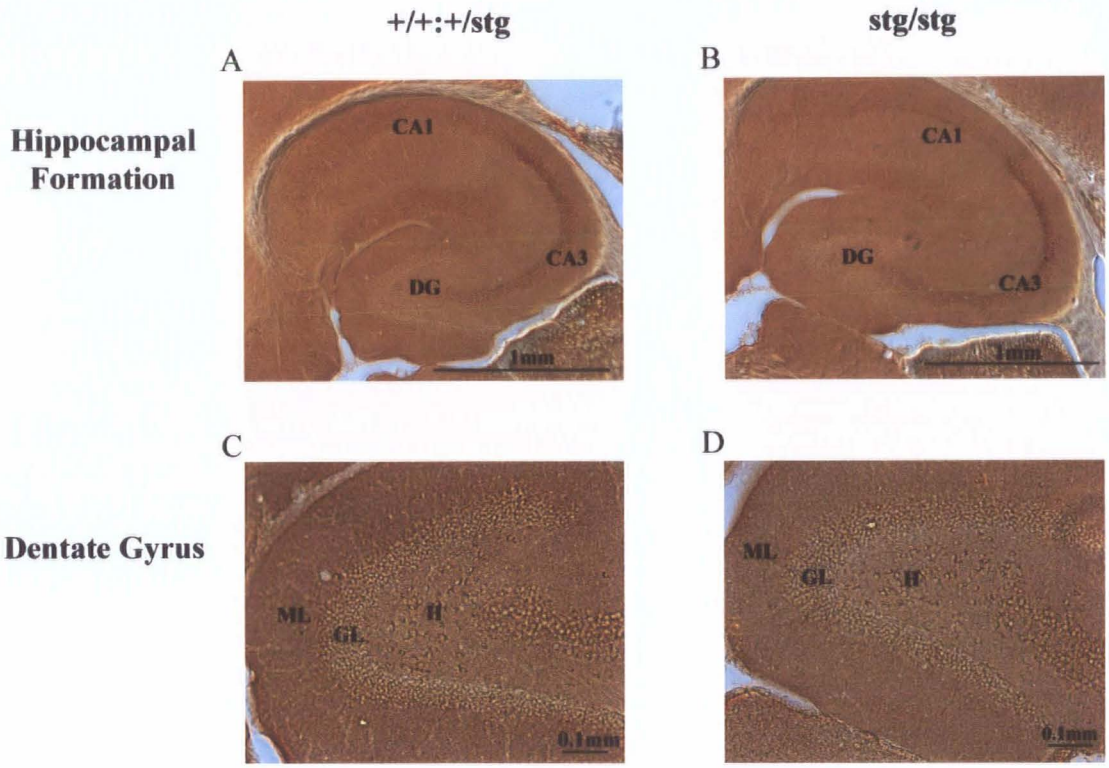

Figure 7.10. Immunohistochemical mapping of the $GABA_A$ receptor γ2 subuni in adult mouse dentate gyrus

A&B: +/+:+/stg and stg/stg whole hippocampi respectively at x40 magnification
C&D: +/+:+/stg and stg/stg brain sections respectively at x100 magnification

Note the intense staining in the molecular layer (ML) and hilus (H) of control and stargazer dentate gyrii (DG).

Table 7.1. Quantitative comparison of GABAR subunit expression in adult control and stargazer hippocampus

GABAR SUBUNIT	CA1				CA2			CA3			DG			STAINING IN STARGAZER DENTATE GYRUS COMPARED TO CONTROLS
	SO	PL	SR	SLM	SO	PL	SR	SO	PL	SR	H	GL	ML	
α1	+++	+++	+++	++	-	+	+	+++	+++	+++	++	++	++	=
α4	+	++	-	+	++	+	-	+	++	-	+	+	+++	↑↑
β2	++	-	++	++	+	-	+	+	-	+	++	+	+++	↑
β3	+	-	+	+	+	-	+	++	-	++	-	-	+++	↑↑
δ	+	+	-	+	-	+	-	-	+	-	+	++	+++	↓
γ2	+	-	-	+	-	++	-	-	-	-	+	+	++	=

+: Weak staining ++: Moderate staining +++: Strong staining -: No specific staining. DG: Dentate gyrus, GL: Granule cell layer, H: Hilus, ML: Molecular layer, PL: Pyramidal cell layer, SLM: Stratum lacunosum moleculare, SO: Stratum oriens, SR: Stratum radiatum

7.2.3. Quantitative western blot analysis of GABAR subunit expression in the control and stargazer DG

Immunohistochemical mapping of GABAR subunits in the dentate gyrus consistently revealed a qualitative up-regulation in expression of the α4, β2 and β3 subunits in the stargazer mutant mouse. Consistent changes in the expression levels of the GABAR α1, γ2 or δ subunits were not observed between control and stargazer tissue sections. However, in some instances, expression of the δ subunit appeared to be reduced in the molecular layer of the stargazer DG compared to controls (figure 7.9.).

In order to determine exact differences in GABAR subunit expression levels, western blot analysis was conducted on SDS-solubilised control and stargazer DG in order to accurately quantify any differences in expression.

7.2.3.1. α4 subunit expression

Expression of the GABAR α4 subunit was determined in SDS-solubilised control and stargazer DG probed with anti-GABAR α4 subunit specific antibody at 0.5 μg/ml. Immunoreactive band intensities were quantified by image densiometry using ImageJ software. Results were normalised to β-actin levels to accommodate changes in protein loading. Expression of the α4 subunit was found to be significantly up-regulated in the stargazer mutant DG to 137 ± 12% of control levels ($n=7$, $p<0.01$).

7.2.3.2. β3 subunit expression

GABAR β3 subunit expression was determined in control and stargazer DG by immunoblotting using anti-GABAR β3 subunit specific antibody at 0.5 μg/ml. Quantification of expression levels revealed a dramatic up-regulation of expression of the subunit in stargazer DG to 139 ± 28% of control levels ($n=6$, $p=0.03$).

Figure 7.11. Quantification of expression of GABAR α4 and β3 subunits in control (+/+:+/stg) and stargazer (stg/stg) dentate gyrus

A: Western blot analysis of control and stargazer SDS-solubilised DG probed for expression of GABAR α4, β3, δ, γ2, NMDAR NR1, AMPAR GluR2 and β-actin.

B: Quantification of expression of GABAR α4 and β3 subunits in control and Stargazer DG. Expression of the α4 and β3 subunits were found to be increased to 137 ± 12%, p=0.0003 (n=7) and 139 ± 28%, p=0.026 (n=6) of control levels respectively.

A

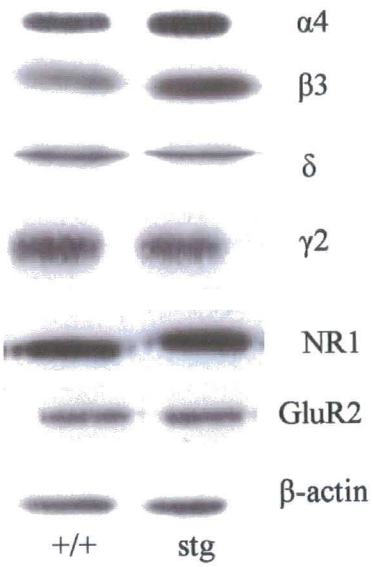
α4
β3
δ
γ2
NR1
GluR2
β-actin
+/+
stg

B

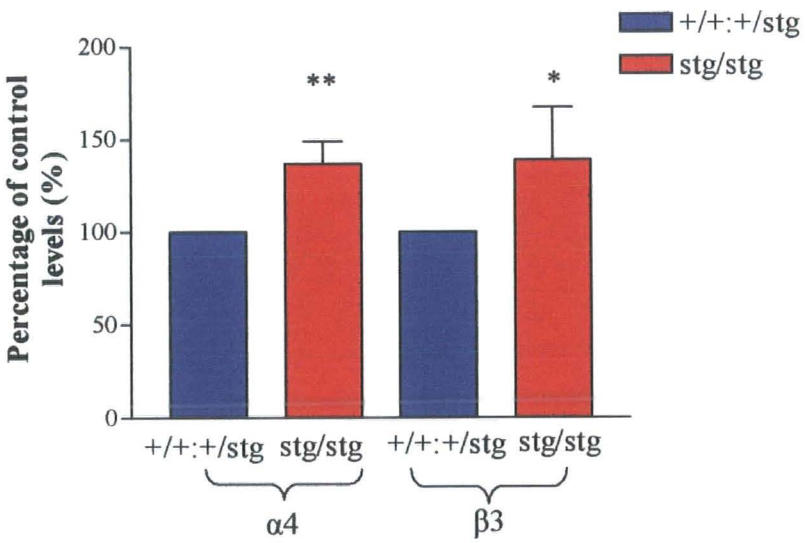
+/+:+/stg
stg/stg
Percentage of control levels (%)
200
150
100
50
0
**
*
+/+:+/stg
stg/stg
+/+:+/stg
stg/stg
α4
β3

7.2.4. Expression of TARPs in the dentate gyrus of control and stargazer mice

Figure 7.12.A demonstrates western blot analysis of forebrain membranes (10 μg per lane) from control (+/+:+/stg) and stargazer (stg/stg) mice probed with a C-terminally directed anti-TARPγ2 antibody at a concentration of 4 μg/ml. Immunoblot demonstrates the presence of three immunoreactive bands at 36-41 kDa, ~48 kDa and ~55 kDa. The 36-41 kDa band corresponds to stargazin (TARPγ2) protein (Ives *et al.*, 2004), which was shown to be absent in stargazer forebrain membranes. The ~48 and ~55 kDa bands correspond in molecular weight to TARPs γ4 and γ8 respectively (Sharp *et al.*, 2001). Interestingly, both the 48 and 55 kDa immunoreactive species were present in both control and stargazer forebrain membranes.

Heterologous expression of the TARP isoforms in human embryonic kidney 293 cells (HEK-293) and subjected to western blot analysis carried out by other lab members revealed that the anti-TARPγ2 antibody recognised TARPγ3 and γ8 and can therefore be referred to as an anti-pan TARP antibody.

Immunohistochemical staining of paraformaldehyde-perfusion fixed control and stargazer tissue sections using an anti-pan TARP antibody at 0.5 μg/ml indicated differential staining of the dentate gyrus (DG). Figure 7.12.B&C demonstrates intense immunoreactivity in the CA1, with a high level of staining in the CA3 and dentate gyrus in control tissue sections (B). Expression of TARP isoforms in the CA1 and CA3 were found to be reduced in stargazer tissue sections with a more profound reduction in staining observed in the DG, suggesting a loss of TARP isoform expression in the hippocampus of the stargazer mutant mouse (C).

In order to determine the identity of the TARP isoforms expressed in the dentate gyrus, the brain structure was dissected from control tissue, SDS-solubilised and subjected to western blot analysis probed with anti-pan TARP antibody at 4 μg/ml.

Figure 7.12. Expression of TARPs in the adult mouse control (+/+:+/stg) and stargazer (stg/stg) dentate gyrus

𝔸: Control and stargazer forebrain membranes subjected to western blot analysis and probed for the expression of stargazin using anti-TARPγ2 antibody directed to the C-terminus at 4 μg/ml. Expression of TARPγ2 (36-41 kDa) was only detected in control forebrain material.
A number of immunoreactive bands were detected in both control and stargazer forebrain membranes of ~55 kDa, ~48 kDa and 36-41 kDa.
𝔹&ℂ: Immunohistochemical mapping of TARPs in the dentate gyrus of control (B) and stargazer (C) tissue sections using anti-pan TARP antibody at 0.5 μg/ml. Note the reduction in intensity of staining in the DG of the stargazer mutant.(Courtesy of P. Tiwari).
𝔻: Western blot analysis of control DG probed with anti-pan TARP antibody at 4 μg/ml. Notice the absence of TARPγ2 expression in control DG. (Courtesy of P. Donoghue).

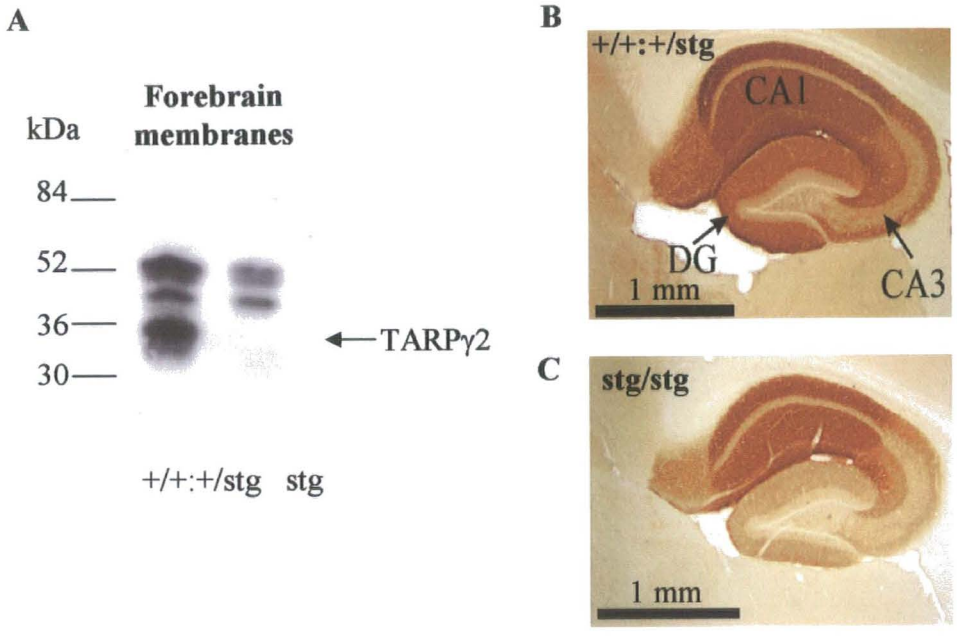
A
Forebrain membranes
kDa
84
52
36
30
TARPγ2
+/+:+/stg
stg
B
+/+:+/stg
CA1
DG
CA3
1 mm
C
stg/stg
1 mm
D
+/+
DG
kDa
55
TARPγ8
36

Figure 7.12.D demonstrates the presence of a single immunoreactive species expressed in control DG with a molecular weight of ~55 kDa, corresponding to TARPγ8. Stargazin (TARPγ2) protein expression was demonstrated in control cerebellar membranes, which was absent in stargazer cerebellar membranes AND control DG.

7.2.5. Quantification of TARP γ8 expression in the dentate gyrus of the control and stargazer mice

Figure 7.13.A demonstrates quantitative western blot analysis of control and stargazer DG probed for the expression of TARPγ8. Expression of TARPγ8 was found to be reduced to 77±1% of control levels in the stargazer DG (n=2). In order to determine if the immunoreactive species (~55 kDa), corresponding to TARPγ8 was an AMPAR interacting protein, DG were dissected from control animals, triton X-100 solubilised and immunoprecipitated using anti-pan TARP antibody (100 μg). Figure 7.13.C illustrates the co-immunoprecipitation of AMPAR GluR2 subunit with anti-pan TARP antibody 55kDa immunoreactive species. Therefore it is possible to conclude that TARPγ8 does function as an AMPAR interacting protein in the dentate gyrus.

7.3. DISCUSSION

7.3.1. GABAR plasticity in the dentate gyrus of the stargazer mutant

Inhibitory GABAergic networks adapt to changes in the strength of their excitatory inputs. Results herein identify that cerebellar granule cells of the stargazer mutant mouse *in vivo* demonstrate a loss of GABAR α6 and δ subunit expression, to result in a significant reduction in [^{3}H] muscimol binding to 70 ± 10% of control levels (see section 4.3.2.1.). This selective loss of GABAR subtype occurs as a consequence of the stargazer mutation, to cause a failure to express TARPγ2 and a near complete ablation of AMPAR expression at the mossy fibre-granule cell synapse. Hence, a loss of excitatory input *in vivo* causes an adaptation in GABAR expression in the cerebellar granule cell layer.

Figure 7.13. Expression of TARPγ8 in stargazer dentate gyrus

A: Western blot analysis of control and stargazer DG material probed with anti-pan TARP antibody at 4 μg/ml.

B: Immunoprecipitation of control DG Triton-soluble material with anti-pan TARP antibody (100 μg), demonstrating the association of TARPγ8 with AMPAR GluR2 subunit.(Courtesy of P. Donoghue).

DG: Dentate gyrii, IP: Immunoprecipitated protein, UB: Unbound material.

A

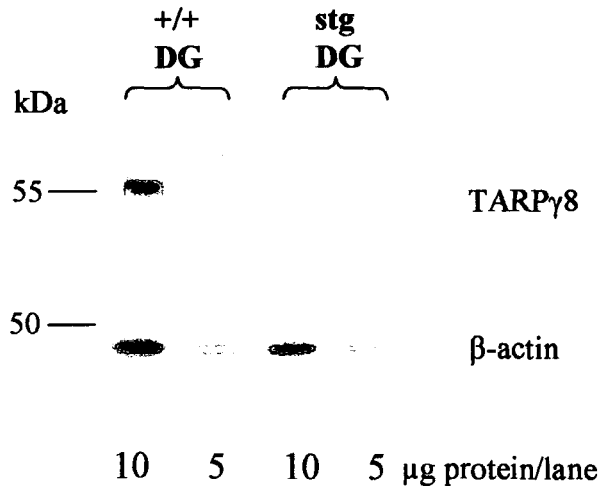
+/+
DG
stg
DG
kDa
55
TARPγ8
50
β-actin
10
5
10
5 μg protein/lane

B

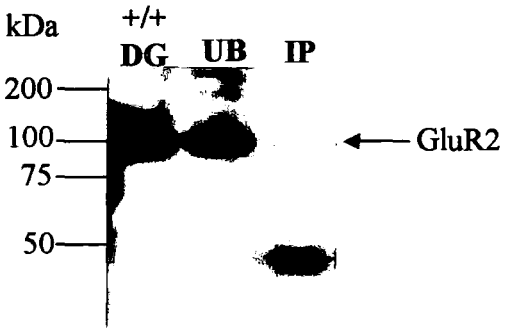
kDa
+/+
DG
UB
IP
200
100
75
50
GluR2

In contrast, the dentate gyrus of the stargazer mutant receives high frequency (6-7 Hz) spike-wave discharges, which could be postulated to cause the reverse response to that seen in the CGC layer of the mutant, where excitatory inputs are reduced, which is indeed what was observed.

In the current study, the levels of GABAR α4 and β3 subunits were found to be significantly increased in the DG of the stargazer mutant compared to controls (figure 7.11). Furthermore, the levels of BZ-IS [^{3}H] Ro15-4513 binding were shown to be up-regulated in the stargazer DG, indicative of α4βγ2 GABAR, a subtype of binding not observed in the control DG (figure 7.2.1.3.). Expression of the BZ-S subtype of binding was not significantly affected, represented by α1/α2βγ2 GABAR in the DG, highlighting the specificity of the GABAR switch observed in the stargazer DG.

The α4 subunit has been reported to preferentially co-assemble with the GABAR δ subunit in the thalamus of control mice (Sur *et al.*, 1999), unless the ability to form GABAR containing the δ subunit is compromised, as in the δ knockout mouse, where α4βδ receptors are replaced by α4βγ2 GABAR (Mihalek *et al.*, 1999; Korpi *et al.*, 2002a; Sun *et al.*, 2004). In the current study, the levels of [^{3}H] muscimol binding in the stargazer DG were significantly reduced, to 79 ± 9% of control levels. [^{3}H] muscimol in autoradiography highlights α4βδ GABAR in the forebrain (Korpi *et al.* 2002b). Therefore, it is possible to conclude that α4βγ2 GABAR arise in the DG of the stargazer mutant, at the expense of α4βδ GABAR.

Immunohistochemical studies indicated a possible down-regulation of expression of the GABAR δ subunit in the molecular and granule cell layers of the stargazer DG (figure 7.9.). A reduction in the expression of the δ subunit would have been in agreement with the reduction in [^{3}H] muscimol binding observed in the stargazer DG. Furthermore, if the γ2 and δ subunits compete for assembly with the α4 subunit in the forebrain, a reduction in δ subunit expression would also favour the up-regulation of BZ-IS subtype of binding observed in the stargazer DG. However, this result was variable between sections immunohistochemically

stained for δ subunit immunoreactivity. Further experiments were conducted to examine the possible role of age or gender in the variability in δ immunostaining observed. Gender could be a factor influencing δ subunit expression, as the levels of the δ subunit have been shown to fluctuate with the oestrus cycle in female rats (Griffiths *et al.*, 2005). However, none of these factors could explain the variability observed (data not shown). No variability was observed in autoradiographic studies in that all stargazer DG sections showed the GABAR subtype switch. Therefore, further studies using a dynamic cell system would be required to determine how the switch from α4βδ to α4βγ2 GABAR occurs in the stargazer.

7.3.2. Is the GABAR plasticity observed in the stargazer DG as a consequence of the mutation in the failure of TARPγ2 expression, or in response to the hyper-excitability entering the dentate gyrus?

The effects observed on GABAR expression could be postulated to occur as a consequence of failure to express TARPγ2 in the thalamocortical pathways resulting in seizure activity entering the hippocampus (Qiao and Noebels., 1993). Conversely, if TARPγ2 is normally expressed in the DG acting to regulate inhibitory networks in the control hippocampus, the stargazer hippocampus would therefore experience hyper-excitability.

Previous studies have reported the expression of TARPγ2 isoform in the cerebellum, CA3, dentate gyrus, cerebral cortex, thalamus and olfactory bulb (Sharp *et al.*, 2001; Tomita *et al.*, 2003). Western blot analysis of control and stargazer forebrain membranes, probed with anti-TARPγ2 antibody revealed that the 36-41 kDa band which corresponds to TARPγ2 in molecular weight and was observed in control cerebellar membranes, was absent from stargazer forebrain. Surprisingly, two other immunoreactive bands at ~48 and ~55 kDa were observed in both control and stargazer forebrain (figure 7.12.). Upon further characterisation of the antibody by other lab members, by recombinant expression of the TARP isoforms in HEK-293 cells, it was revealed that the

antibody cross-reacted with TARPγ3 and γ8 and could therefore be referred to as a pan-TARP antibody.

In order to confirm the identity of the immunoreactive species highlighted by the anti-pan TARP antibody, the dentate gyrus was excised from control and stargazer forebrain and subjected to western blot analysis. Results demonstrated that indeed the TARPγ2 isoform was not expressed in control DG, rather the immunoreactive band at ~55 kDa was the prominent immunoreactive species. Further analysis using an anti-TARPγ8 specific antibody revealed that the ~55 kDa band corresponded to TARPγ8, the levels of which were reduced to 77 ± 1% of control levels in the stargazer mutant DG, consistent with immunostaining differences observed using the anti-TARP antibody (figure 7.12.). Furthermore, immunoprecipitation assays using the anti pan-TARP and TARPγ8 antibodies confirmed that TARPγ8 does indeed interact with the AMPAR GluR2 subunit in the control DG (figure 7.13.).

Consequently it is possible to conclude that the mossy fibre sprouting, down-regulation of TARPγ8 and GABAR rearrangements occur as a consequence of failed TARPγ2 expression elsewhere in the stargazer mutant brain.

7.3.3. What are the implications for a switch to BZ-IS subtype of GABAR?

A switch from expression of the δ subunit-containing GABAR to γ2 subunit-containing GABAR has the potential to result in a switch in location of receptor from extrasynaptic to synaptic location. Therefore, resulting in an adaptation in inhibitory response to accommodate increased hyper-excitability entering the DG to maintain cell viability. In the stargazer mutant, mossy fibre release of zinc and glutamate to give high extracellular zinc concentrations acts on zinc-insensitive GABAR. Unlike in temporal lobe epilepsy models, where a switch to δ subunit-containing GABAR which are zinc sensitive causes blockade of the GABA response and zinc-mediated failure of inhibition, acting to promote seizure generation (Cohen *et al.*, 2003).

The GABAR switch observed in the current study is not uniform in all absence epilepsy models, but rather is unique to the stargazer mutant. Autoradiographic studies were carried out on tottering mouse tissue sections, where no increased BZ-IS binding was observed in the dentate gyrus (data not shown). A possible explanation for such a difference between absence models, when the tottering mouse DG experiences the same SWDs, but at a lower burst frequency is that there is a threshold level of excitability required to cause rearrangements of GABAR profile, not reached in the tottering mouse.

7.3.4. Conclusions

In conclusion, the current study has demonstrated a switch in GABAR expression from $\alpha4\beta\delta$ to $\alpha4\beta\gamma2$ in the stargazer DG. This switch was not observed in autoradiographic studies in the tottering mutant, hence it can be concluded that this GABAR rearrangement is not a common feature of absence epilepsy models. The switch was found not to be caused by the failure to express TARP$\gamma2$ in the stargazer DG, rather can be predicted to occur as a consequence of hyper-excitability and failed TARP $\gamma2$ expression elsewhere in afferent pathway (thalamocortical networks), as the DG does not normally express TARP$\gamma2$, TARP$\gamma8$ appears to be the predominant TARP in control mouse DG. The switch from extrasynaptic (δ subunit-containing GABAR) to potentially synaptic ($\gamma2$ subunit-containing GABAR) location of GABAR may provide a homeostatic mechanism which neurons can employ to balance increased excitatory inputs.

CHAPTER 8. SUMMARY AND FUTURE WORK

The stargazer mutant mouse is an animal model of human absence epilepsy and cerebellar ataxia. The stargazer mutation results in the complete ablation of expression of TARPγ2, an AMPA receptor auxiliary subunit. Results of the current study provide evidence for the involvement of TARPγ2 in the regulation of expression and trafficking of specific $GABA_A$ receptor (GABAR) subtypes in the cerebellum and hippocampal formation.

Qualitative differences in GABAR subunit expression were determined using immunohistochemical techniques. Decreases in the α6, β2, β3, and δ subunits were observed in all cerebellar folia of the stargazer mutant cerebellum when compared to controls. The expression of the GABAR subunits were quantified in adult control and stargazer mouse cerebellum and revealed decreases in expression of the GABAR α6, β2, β3 and δ subunits in the stargazer mutant to 39 ± 22%, 45 ± 42%, 77 ± 42% and 36 ± 21% of control levels respectively. The abnormal GABAR profile expressed in the stargazer cerebellum is not a consequence of failed cerebellar maturation as an immature complement of receptors were not found to be expressed in adult stargazer (e.g. α2/α3/α5 subunit-containing receptors), as determined by zolpidem displacement of [^{3}H] Ro15-4513 binding. This demonstrates that the development of the GABAR profile of the stargazer mutant cerebellum is not impaired, rather, the levels of expression of the α6 and δ subunit-containing GABARs present in the mature cerebellum, are dramatically reduced.

Possible abnormalities in the GABAR profile of the stargazer mutant mouse were determined by radioligand binding techniques to both cerebellar membrane homogenates and tissue sections by receptor autoradiography. [^{3}H] muscimol binding to cerebellar membranes revealed a decrease to 70 ± 10% of control levels, a loss of 30% of total GABAR (γ2 and δ containing subpopulations) in the stargazer cerebellum. Receptor autoradiography using [^{3}H] muscimol, which is selective for α6 subunit-containing receptors, revealed a decrease to 54 ± 10% of control levels in the CGC layer of the stargazer mutant indicating that the loss of

GABAR is entirely accommodated by the loss of CGC-specific α6βγ2 and α6βδ GABAR subtypes. Total levels of [^{3}H] Ro15-4513 binding were not found to differ significantly between control and stargazer animals. However, upon further pharmacological dissection, the BZ-IS subtype of receptor, conferred by α6βγ2 and α1α6βγ2 receptors was found to be reduced to 57 ± 13% of control levels in cerebellar membrane homogenates and to 78 ± 10% of control levels in the CGC layer by receptor autoradiography. By difference analysis, if there is a dramatic decrease in the total number of GABAR as revealed by a loss of [^{3}H] muscimol binding, and the total level of [^{3}H] Ro15-4513 binding is not changed, the loss of GABAR must be due to a dramatic loss of α6βδ receptors reduced by 76%. In CGCs, activation of δ-subunit containing GABARs mediates >95% of the total GABAR-mediated inhibition in these neurons (Cope *et al.*, 2005). Thus in stargazer CGCs we would estimate a loss of 78% of GABA-mediated inhibition potential.

CGCs derived from control and stargazer mice follow a pattern of development, as expected of CGCs *in vivo*, thereby providing a model system for the investigation of the factors affecting the expression, trafficking and targeting of the GABAR subunits. Depolarisation either by KCl or kainic acid treatment demonstrated the differential modulation of the principal GABAR subunits in mouse CGCs. As previously reported, CGCs cultured under 25 mM KCl, demonstrated a decrease in the expression of the GABAR subunits indicative of a mature CGC, the α1 and α6 subunits (Mellor *et al.*, 1998; Ives *et al.*, 2002a; Engblom *et al.*, 2003).

Furthermore, depolarisation mediated by kainic acid treatment also acted to decrease α1 and α6 subunit expression in control CGCs. However, expression of the δ subunit was found to be dramatically increased under both KCl and kainic acid-induced depolarisation in control CGCs, but only under KCl-induced depolarisation in stargazer CGCs. The studies described herein demonstrated that AMPAR activation resulted in L-type voltage-gated calcium channel-dependent up-regulation of GABAR δ subunit expression and cell surface trafficking which was not detected in CGCs derived from stargazer animals. Offering a partial

explanation for the abnormalities observed *in vivo*. The KCl-mediated depolarisation studies do however indicate that the signalling pathways linking depolarisation to GABAR δ subunit up-regulation are still intact in the CGCs of the stargazer.

Future work would involve blocking downstream signalling pathways following calcium influx through L-type voltage-gated calcium channels, using pathway inhibitors of PKA, PKC, CaM Kinases, MAP kinase, in order to further dissect the signalling pathways involved in the modulation of GABAR subunit expression and trafficking in cultured CGCs. Furthermore, the levels of GABAR subunit mRNA present in 5K and kainate CGCs needs to be quantified, to determine if increased transcription of the GABAR δ subunit gene was responsible for increased GABAR δ subunit expression. In addition, cultured control CGCs treated in the absence (5 mM KCl) and presence of increased extracellular KCl (25 mM) or kainic acid (100 μM) could be immunofluorescently stained with anti-GABAR δ subunit-specific and L-type voltage-gated calcium channel-specific antibodies to determine where the increased expression of the δ subunit localises within the CGC following depolarisation and furthermore if the δ subunit co-localises with L-type voltage-gated calcium channels.

Conflicting reports exist as to the electrical activity of mouse CGCs under 5K culture conditions. Mellor *et al.*, in 1998 reported that CGCs maintained under 5K culture conditions were electrically active in that they exhibited spontaneous action potentials, mEPSCS and mIPSCs. Engblom *et al.*, in 2003 reported that no spontaneous action potentials were observed in CGCs cultured under 5K conditions. Hence, the cells were considered to be electrically silent. The group suggested that the conflicting reports resulted from differences in the age of the CGCs in culture. Mellor *et al.* recorded electrical activity in mouse CGCs at 15 DIV. In contrast, the neurons recorded from by Engblom *et al.* were at 7 DIV, suggesting that the necessary features for spontaneous electrical activity, such as functional synapses and voltage-gated sodium channels were less developed at 7-8 DIV.

Results of the current study, are in support of Engblom *et al.*, as CGCs employed in current investigations were also utilised at 7 DIV. Upon treatment of CGCs cultured under basal conditions (5 mM KCl) with CNQX (20 μM), the levels of for example the δ subunit protein observed by western blotting would be expected to be lower than that obtained in untreated cells if the CGCs were spontaneously active, which was not the case for the GABAR δ subunit. CGCs are a good model system to begin to study mechanisms of trafficking and targeting of GABAR, but the whole cerebellar circuitry is not intact, therefore, in order to study the system as a whole, it would be necessary to employ cerebellar slices.

The current study has also demonstrated a switch in GABAR expression from α4βδ to α4βγ2 in the stargazer dentate gyrus (DG). This switch was not observed in autoradiographic studies in the tottering mutant. Hence it can be concluded that this GABAR rearrangement is not a common feature of absence epilepsy models. The switch was found not to be caused by the failure to express TARPγ2 in the stargazer DG, rather can be predicted to occur as a consequence of hyper-excitability and failed TARPγ2 expression elsewhere in afferent pathway (thalamocortical networks), as the DG does not normally express TARPγ2, but TARPγ8 is the predominant TARP in control mice. The switch from extrasynaptic (δ subunit-containing GABAR) to synaptic (γ2 subunit-containing GABAR) location of GABAR provides a homeostatic mechanism which neurons can employ to balance increased excitatory inputs.

Future work would involve electrophysiological studies on control compared to stargazer dentate granule cells (DGGCs), to determine if the proposed decrease in α4βδ GABAR in the stargazer DGGCs is evident by a loss of tonic currents. Lesion of the thalamocortical pathway in the control mouse would allow for the quantification of GABAR subunit levels in the DG, to determine if the GABAR switch observed in the stargazer mutant occurs as a result of failed TARPγ2 expression elsewhere in the afferent pathway.

In conclusion, the results of this study support the hypothesis that neural networks in both the cerebellum and the hippocampus are able to undergo homeostatic GABAergic plasticity in response to alterations in excitatory inputs.

PUBLICATIONS

Payne H.L., Ives J.H., Tiwari P., Lucocq J.M., Sieghart W., Thompson C.L., (2006) Expression and cell surface trafficking of extrasynaptic δ-containing $GABA_A$ receptors is compromised in cerebellar granule cells of the ataxic mouse, stargazer (Manuscript in preparation).

Kaja S., **Payne H.L.,** Crawford A.R., Hann V., Ives J.H., Thompson C.L., (2006) Cerebellar granule cell-specific $GABA_A$ receptor expression is impaired in the epileptic and ataxic mouse mutant tottering. (Manuscript in preparation).

Payne H.L., Donoghue P.S., Tiwari P., Ives J.H., Hann V.H., Sieghart W., Thompson C.L., (2006) Abnormal $GABA_A$ Receptor subtypes are expressed in the dentate gyrus of the stargazer mutant mouse. (Manuscript in preparation).

Payne H.L., Donoghue P.S., Ives J.H., Sieghart W., Thompson C.L., (2005) Seizure activity in the dentate gyrus induces a switch in $GABA_A$ receptor expression profile in stargazer but not tottering mice. *British Neuroscience Assoc. Abstr.*, vol 18, P21

Hann V., Ives J.H., Fung S., **Payne H.L.,** Wafford K., Thompson C.L., (2005) AMPA receptors (AMPARs), Stargazin and Microtubule-associated protein 1–LC2 (MAP1-LC2) form a tripartite protein complex *in vivo*. *British Neuroscience Assoc. Abstr.*, vol 18, P19

Ives J.H., Fung S., Tiwari P., **Payne H.L.,** Thompson C.L., (2004) Microtubule-associated Protein Light Chain 2 Is a Stargazin-AMPA Receptor Complex-interacting Protein *in vivo*. *Journal of Biological Chemistry* 279(30):31002-31009

Payne H.L., Ives J.H., Sieghart W., Thompson C.L., (2004) AMPA and Kainate receptors mediate mutually exclusive effects on $GABA_A$ receptor expression in cultured mouse cerebellar granule cells. Fens abstracts A080.3

Thompson C.L., Fung S., **Payne H.L.,** Ives J.H., (2004) Microtubule-associated protein 1A/1B is a stargazin interacting protein *in vivo*. Fens abstracts A184.11

Ives J.H., Tiwari P., Sieghart W., Lucocq J.M., Young C.E., **Payne H.L.,** Thompson C.L., (2003) Cerebellar granule cell-specific $GABA_A$ receptor abnormalities in stargazer mice. *British Neurosci. Assoc. Abstr.* Vol 17, P26.15

Tiwari P., Ives J.H., Sieghart W., **Payne H.L.,** Wright M., Thompson C.L., (2003) $GABA_A$ receptor expression in the granule cells of the dentate gyrus is impaired in the epileptic mutant mouse, Stargazer. *British Neurosci. Assoc. Abstr.* Vol 17, P58.05.

Appendix 1. Expression of the GABAR α6 subunit in response to depolarisation in cultured CGCs (7 DIV)

A: Quantification of expression levels of the GABAR α6 subunit in response to depolarisation mediated by increased extracellular KCl (25 mM) and kainic acid treatment (100 μM). n=1

B: Quantification of expression levels of the GABAR α6 subunit in response to depolarisation mediated by increased extracellular KCl (25 mM) and kainic acid treatment (100 μM), including data as presented in figure 5.6, n=2.

C: Summary of quantification of GABAR α6 subunit expression levels. Note a significant reduction in GABAR α6 subunit expression in response to KCl and kainic acid mediated depolarisation in control CGCs (13 ± 0.5% and 16 ± 2% of 5K levels respectively, $p<0.05$). In contrast, GABAR α6 subunit expression was not detectable in stargazer CGCs upon KCl-mediated depolarisation whereas expression levels were not affected by kainic acid-mediated depolarisation (82 ± 16% of 5K levels, $p=0.20$).

A

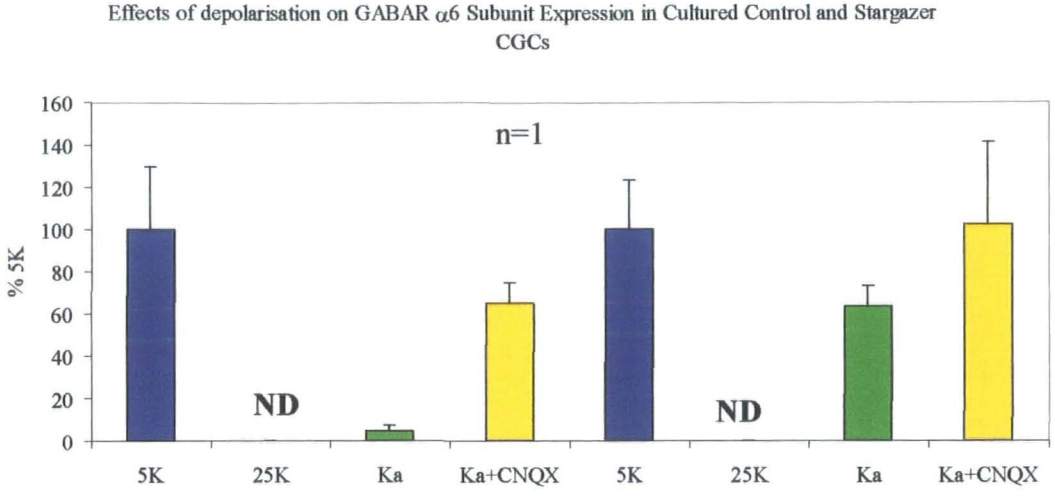

B

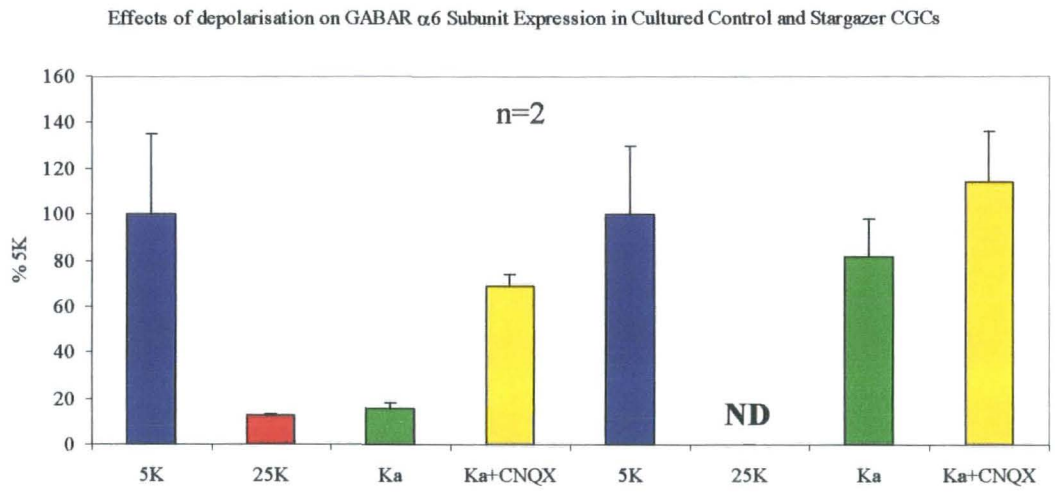

C

		% 5K	SEM	P value (compared to 5K)
Control	5K	100	35	
	25K	13	0.5	0.015
	Ka	16	2	0.019
	Ka+CNQX	69	5	0.312
Stg	5K	100	30	
	25K	0	0	0.005
	Ka	82	16	0.203
	Ka+CNQX	114	22	0.964

Appendix 2. Dentate granule cells of the stargazer mutant mouse exhibit reduced tonic currents and decreased potentiation in response to neurosteroids compared to age-matched control mice

GABAR-mediated tonic currents were significantly lower in the dentate granule cells of stargazer mice (6-8 week old male mice) compared to control animals (3.5 ± 0.7 pA vs 7.5 ± 0.2 pA respectively; $n = 4\text{-}5$; $P<0.05$). Dentate granule cells from the stargazer mutant exhibited decreased potentiation of tonic currents in response to the neurosteroid, THDOC (100 nM), (11.1 ± 2.6pA vs 19.8 ± 1.0pA; $n = 4\text{-}5$; $P<0.05$), correlating with a loss of the GABAR δ subunit-containing, neurosteroid-sensitive subtype of GABAR.

Conducted by W.M.K Connelly and G. Lees of the Department of Pharmacology & Toxicology, Otago School of Medical Sciences, University of Otago, PO Box 913, Dunedin, New Zealand.

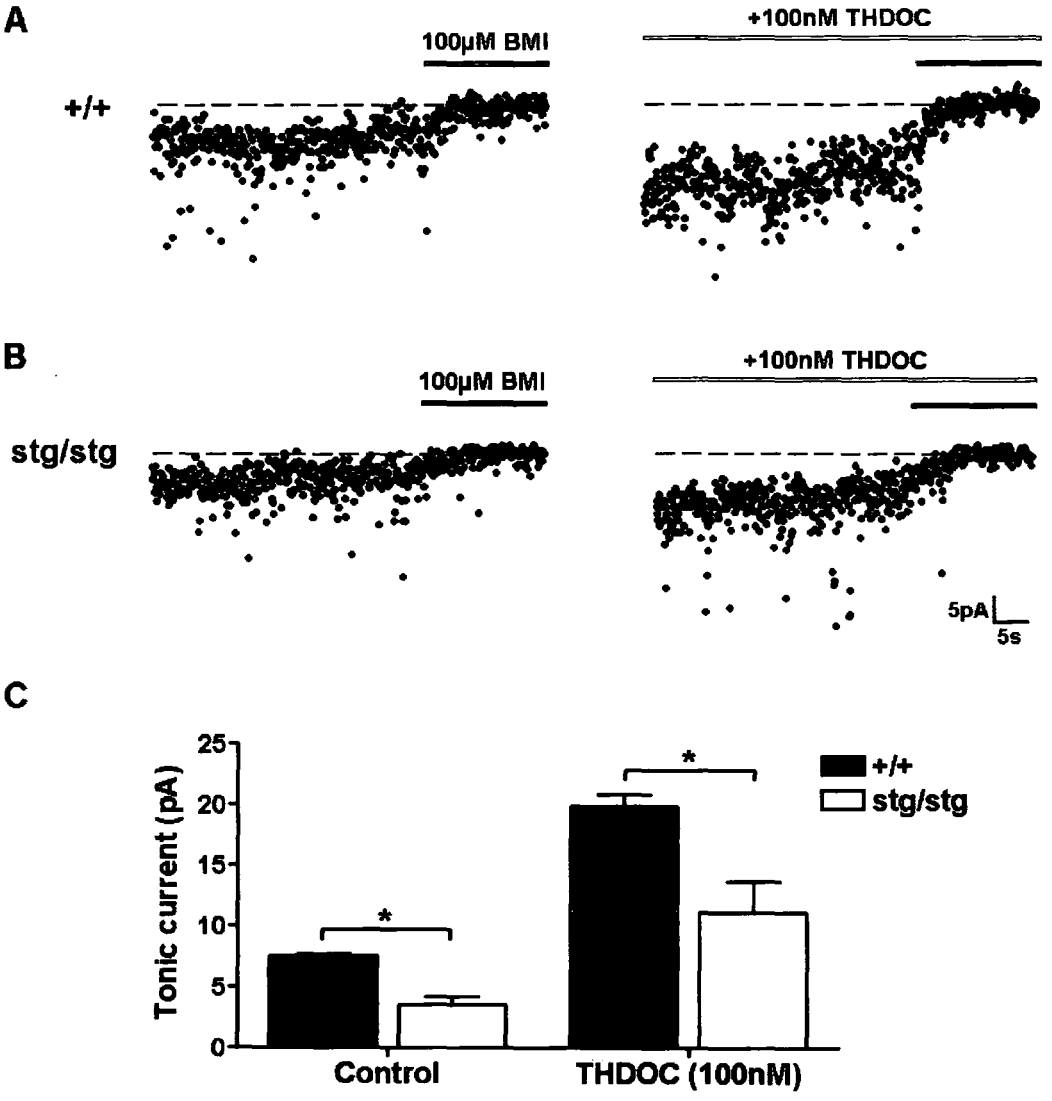
A
100μM BMI
+100nM THDOC
+/+
B
100μM BMI
+100nM THDOC
stg/stg
5pA
5s
C
Tonic current (pA)
25
20
15
10
5
0
*
*
+/+
stg/stg
Control
THDOC (100nM)

REFERENCES

Alldred M.J., Mulder-Rosi J., Lingenfelter S.E., Chen G., Luscher B., (2005) Distinct γ2 subunit domains mediate clustering and synaptic function of postsynaptic $GABA_A$ receptors and gephyrin. *Journal of Neuroscience* 25(3):594-603

Archibold K., Perry M.J., Molnar E., Henley J.M., (1998) Surface expression and metabolic half-life of AMPA receptors in cultured rat cerebellar granule cells. *Neuropharmacology* 37:1345-1353

Barnard E.A., Skolnick P., Olsen R.W., Mohler H., Sieghart W., Biggio G., Braestrup C., Bateson A.N., Langer S.Z., (1998) International Union of Pharmacology.XV. Subtypes of γ-Aminobutyric $Acid_A$ Receptors: Classification on the basis of subunit structure and receptor function. *Pharmacological Reviews* 50(2):292-313

Beattie C.E., Siegel R.E., (1993) Developmental cues modulate $GABA_A$ receptor subunit mRNA expression in cultured cerebellar granule neurons. *Journal of Neuroscience* 13(4):1784-1792

Beck M., Brickley K., Wilkinson H.L., Sharma S., Smith M., Chazot P.L., Pollard S., Stephenson F.A., (2002) Identification, molecular cloning, and characterisation of a novel GABAA receptor-associated protein, GRIF-1. *Journal of Biological Chemistry* 277(33):30079-30090

Bedford F.K., Kittler J.T., Muller E., Thomas P., Uren J.M., Merlo D., Wisden W., Triller A., Smart T.G., Moss S.J., (2001) $GABA_A$ receptor cell surface number and subunit stability are regulated by the ubiquitin-like protein Plic-1. *Nature Neuroscience* 4(9): 908-916

Behringer K.A., Gault L.M., Siegel R.E., (1996) Differential regulation of $GABA_A$ receptor subunit mRNAs in rat cerebellar granule neurons: Importance of environmental cues. *Journal of Neurochemistry* 66:1347-1353

Benke D., Mertens S., Trzeciak A., Gillessen D., Mohler H., (1991) Identification and immunohistochemical mapping of $GABA_A$ receptor subtypes containing the δ-subunit in rat brain. *Federation of European Biochemical Societies Letters* 283(1):145-149

Bettler B., Mülle C., (1995) Review: Neurotransmitter receptors II: AMPA and kainate receptors. *Neuropharmacology* 34(2):123-139

Bollan K., King D., Robertson L.A., Brown K., Taylor P.M., Moss S.J., Connolly C.N., (2003) $GABA_A$ receptor composition is determined by distinct assembly signals within α and β subunits. *Journal of Biological Chemistry* 278(7):4747-4755

Bollan K., Robertson L.A., Tang H., Connolly C.N., (2003) Multiple assembly signals in γ-aminobutyric acid (type A) receptor subunits combine to drive receptor construction and composition. *Biochemical Society Transactions* 31(4):875-879

Borghesani P.R., Peyrin J.M., Klein R., Rubin J., Carter A.R., Schwarz P.M., Luster A., Corfas G., Segal R.A., (2002) BDNF stimulates migration of cerebellar granule cells. *Development* 129:1435-1442

Braithwaite S.P., Meyer G., Henley J.M., (2000) Interactions between AMPA receptors and intracellular proteins. *Neuropharmacology* 39:919-930

Brandon N.J., Uren J.M., Kittler J.T., Wang H., Olsen R., Parker P.J., Moss S.J., (1999) Subunit-specific association of protein kinase C and the receptor for activated C kinase with GABA type A receptors. *Journal of Neuroscience* 19(21):9228-9234

Bredt D.S., Nicoll R.A., (2003) AMPA receptor trafficking at excitatory synapses. *Neuron* 40:361-379

Brickley K., Smith M.J., Beck M., Stephenson F.A., (2005) GRIF-1 and OIP106, members of a novel gene family of coiled-coil domain proteins: association *in vivo* and *in vitro* with kinesin. *Journal of Biological Chemistry* 280(15):14723-14732

Brickley S.G., Cull-Candy S.G., Farrant M., (1996) Development of a tonic form of synaptic inhibition in rat cerebellar granule cells resulting from persistent activation of $GABA_A$ receptors. *Journal of Physiology* 497(3):753-759

Brickley S.G., Cull-candy S.G., Farrant M., (1999) Single-channel properties of synaptic and extrasynaptic $GABA_A$ receptors suggest differential targeting of receptor subtypes. *Journal of Neuroscience* 19(8):2960-2973

Brodie M.J., Schachter S.C., Kwan P., (2005) Fast facts: Epilepsy. Third Edition, Health Press, Oxford, UK.

Brooks-kayal A.R., Shumate M.D., Jin H., Rikhter T.Y., Coulter D.A., (1998) Selective changes in single cell $GABA_A$ receptor subunit expression and function in temporal lobe epilepsy. *Nature Medicine* 4(10):1166-1172

Brown N., Kerby J., Bonnert T.P., Whiting P.J., Wafford K.A., (2002) Pharmacological characterisation of a novel cell line expressing human $\alpha_4\beta_3\delta$ $GABA_A$ receptors. *British Journal of Pharmacology* 13697):965-974

Burgess D.L., Davis C.F., Gefrides L.A., Noebels J.L., (1999) Identification of three novel Ca^{2+} channel γ subunit genes reveals molecular diversification by tandem and chromosome duplication. *Genome research* 9:1204-1213

Chaftez R.S., Nahm W.K., Noebels J.L., (1995) Aberrant expression of neuropeptide Y in hippocampal mossy fibers in the absence of local cell injury following onset of spike-wave synchronisation. *Molecular Brain Research* 31:111-121

Chen L., Bao S., Qiao X., Thompson R.F., (1999) Impaired cerebellar synapse maturation in *waggler*, a mutant mouse with a disrupted neuronal calcium channel γ subunit. *Proceedings of the National Academy of Sciences of the United States of America* 96(21):12132-12137

Chen L., Chetkovich D.M., Petralia R.S., Sweeney N.T., Kawasaki Y., Wenthold R.J., Bredt D.S., Nicoll R.A., (2000a) Stargazin regulates synaptic targeting of AMPA receptors by two distinct mechanisms. *Nature* 408(6815):936-943

Chen L., Wang H., Vicini S., Olsen R.W., (2000b) The gamma-aminobutyric acid type A ($GABA_A$) receptor-associated protein (GABARAP) promotes $GABA_A$ receptor clustering and modulates channel kinetics. *Proceedings of the National Academy of Sciences of the United States of America* 97(21):11557-11562

Chen L., El-Husseini A., Tomita S., Bredt D.S., Nicoll R.A., (2003) Stargazin differentially controls the trafficking of α-amino-3-hydroxyl-5-methyl-4-isoxazoleproprionate and kainate receptors. *Molecular Pharmacology* 64(3):703-706

Chetkovich D.M., Chen L., Stocker T.J., Nicoll R.A., Bredt D.S. (2002) Phosphorylation of the postsynaptic density-95 (PSD-95)/Discs Large/Zona Occludens-1 binding site of Stargazin regulates binding to PSD-95 and synaptic targeting of AMPA receptors. *Journal of Neuroscience* 22(14):5791-5796

Choi J., Ko J., Park E., Lee J., Yoon J., Lim S., Kim E., (2002) Phosphorylation of Stargazin by protein kinase A regulates its interaction with postsynaptic density-95 (PSD-95). *Journal of Biological Chemistry* 277(14):12359-12363

Chu P., Robertson H.M., Best P.M., (2001) Calcium channel γ subunits provide insights into the evolution of this gene family. *Gene* 280:37-48

Clark M., (1998) Sensitivity of the rat hippocampal $GABA_A$ receptor α4 subunit to electroshock seizures. *Neuroscience Letters* 250:17-20

Cohen A.S., Lin D.D., Quirk G.L., Coulter D.A., (2003) Dentate granule cell $GABA_A$ receptors in epileptic hippocampus: enhanced synaptic efficacy and altered pharmacology. *European Journal of Neuroscience* 17:1607-1616

Connolly C.N., Krishek B.J., McDonald B.J., Smart T.G., Moss S.J., (1996a) Assembly and cell surface expression of heteromeric and homomeric γ-Aminobutyric Acid Type A Receptors. *Journal of Biological Chemistry* 271(1):89-96

Connolly C.N., Wooltorton J.R.A., Smart T.G., Moss S.J., (1996b) Subcellular localisation of γ-Aminobutyric acid type A receptors is determined by receptor β subunits. *Proceedings of the National Academy of Sciences of the United States of America* 93:9899-9904

Connolly C.N., Kittler J.T., Thomas P., Uren J.M., Brandon N.J., Smart T.G., Moss S.J., (1999a) Cell surface stability of γ-aminobutyric acid type A receptors. *Journal of Biological Chemistry* 274(51):36565-36572

Connolly C.N., Uren J.M., Thomas P., Gorrie G.H., Gibson A., Smart T.G., Moss S.J., (1999b) Subcellular localization and endocytosis of homomeric γ2 subunit splice variants of γ-aminobutyric acid type A receptors. *Molecular and Cellular Neuroscience* 13:259-271

Cope D.W., Hughes S.W., Crunelli V., (2005) $GABA_A$ receptor-mediated tonic inhibition in thalamic neurons. *Journal of Neuroscience* 25(50):11553-11563

Cuadra A.E., Kuo S., Kawasaki Y., Bredt D.S., Chetkovich D.M., (2004) AMPA Receptor Synaptic Targeting Regulated by Stargazin Interactions with the Golgi-Resident PDZ Protein nPIST. *Journal of Neuroscience* 24(34):7491-7502

Dakoji S., Tomita S., Karimzadegan S., Nicoll R.A., Bredt D.S., (2003) Interaction of transmembrane AMPA receptor regulatory proteins with multiple membrane associated guanylate kinases. *Neuorpharmacology* 45:849-856

Das K.P., Chao S.L., White L.D., Haines W.T., Harry G.J., Tilson H.A., Barone S., (2001) Differential patterns of nerve growth factor, brain-derived neurotrophic factor and neurotrophin-3 mRNA and protein levels in developing regions of rat brain. *Neuroscience* 103(3):739-761

Dev K.K., Nishimune A., Henley J.M., Nakanishi S., (1999) The protein kinase Ca binding protein PICK1 interacts with short but not long form alternative splice variants of AMPA receptor subunits. *Neuropharmacology* 38:635-644

Dong H., O'Brien R.J., Fung E.T., Lanahan A.A., Worley P.F., Huganir R.L., (1997) GRIP: a synaptic PDZ domain-containing protein that interacts with AMPA receptors. *Nature* 386:279-284

Duggan M.J., Pollard S., Stephenson F.A., (1991) Immunoaffinity purification of $GABA_A$ receptor alpha-subunit iso-oligomers. Demonstration of receptor populations containing alpha1 alpha2, alpha1 alpha3, and alpha2, alpha3 subunit pairs. *Journal of Biological Chemistry* 266(36):24778-24784

Dutton G.R., Isolation, culture and use of viable central nervous system perikarya. *Methods in Neurosciences*, Vol 2 (1990), Academic Press.

Ebert V., Scholze P., Sieghart W., (1996) Extensive heterogeneity of recombinant gamma-aminobutyric acid A receptors expressed in alpha 4 beta 3 gamma 2 transfected human embryonic kidney 293 cells. *Neuropharmacology* 35(9-10):1323-1330

Elmiariah S.B., Crumling M.A., Parsons T.D., Balice-Gordon R.J., (2004) Postsynaptic TrkB-mediated signalling modulates excitatory and inhibitory neurotransmitter receptor clustering at hippocampal synapses. *Journal of Neuroscience* 24(10):2380-2393

Engblom C., Johansen F.F., Kristiansen U., (2003) Actions and interactions of extracellular potassium and kainate on expression of 13 γ-aminobutyric acid type A receptor subunits in cultured mouse cerebellar granule neurons. Journal of *Biological Chemistry* 278(19):16543-16550

Fujikawa N., Tominaga-yoshino K., Okabe M., Ogura A., (2000) Depolarization-dependent survival of cultured mouse cerebellar granule neurons is strain-restrained. *European Journal of Neuroscience* 12:1838-1842

Gallo V., Kingsbury A., Balazs R., Jorgensen O.S., (1987) The role of depolarization in the survival and differentiation of cerebellar granule cells in culture. *Journal of Neuroscience* 7(7):2203-2213

Gao W.Q., Zheng J.L., Karihaloo M., (1995) Neurotrophin-4/5 (NT-4/5) and brain-derived neurotrophic factor (BDNF) act at later stages of cerebellar granule cell differentiation. *Journal of Neuroscience* 15(4):2656-2667

Gault L.M., Siegel R.E., (1997) Expression of the $GABA_A$ receptor δ subunit is selectively modulated by depolarisation in cultured rat cerebellar granule neurons. *Journal of Neuroscience* 17(7):2391-2399

Gault L.M., Siegel R.E., (1998) NMDA receptor stimulation selectively initiates $GABA_A$ receptor δ subunit mRNA expression in cultured rat cerebellar granule neurons. *Journal of Neurochemistry* 70:1907-1915

Green P.J., Warre R., Hayes P.D., McNaughton N.C.L., Medhurst A.D., Pangalos M., Duckworth D.M., Randall A.D., (2001) Kinetic modification of the α_{1I} subunit-mediated T-type Ca^{2+} channel by a human neuronal Ca^{2+} channel γ subunit. *Journal of Physiology* 533.2:467-478

Griffiths J.L., Lovick T.A., (2005) GABAergic neurones in the rat periaqueductal grey matter express alpha4, beta1 and delta $GABA_A$ receptor subunits: plasticity of expression during the estrous cycle. *Neuroscience* 136(2):457-466

Hall R.A., Soderling T.R., (1997) Quantitation of AMPA receptor surface expression in cultured hippocampal neurons. *Neuroscience* 78(2):361-371

Harney S.C., Frenguelli B.G., Lambert J.J., (2003) Phosphorylation influences neurosteroid modulation of synaptic $GABA_A$ receptors in rat CA1 and dentate gyrus neurones. *Neuropharmacology* 45:873-883

Hashimoto K., Fukaya M., Qiao X., Sakimura K., Watanabe M., Kano M., (1999) Impairment of AMPA receptor function in cerebellar granule cells of ataxic mutant mouse Stargazer. *Journal of Neuroscience* 19(14):6027-6036

Hayashi T., Umemori H., Mishina M., Yamamoto T., (1999) The AMPA receptor interacts with and signals through the protein tyrosine kinase Lyn. *Nature* 397:72-76

Henley J.M., (2003) Proteins interactions implicated in AMPA receptor trafficking: a clear destination and an improving route map. *Neuroscience research* 45:243-254

Huh K., Wenthold R.J., (1999) Turnover analysis of glutamate receptors identifies a rapidly degraded pool of the *N*-methyl-D-Aspartate receptor subunit, NR1, in cultured cerebellar granule cells. *Journal of Biological Chemistry* 274(1):151-157

Isaac J.T.R., (2003) Postsynaptic silent synapses: evidence and mechanisms. *Neuropharmacology* 45:450-460

Ives J.H., Drewery D.L., Thompson C.L., (2002a) Neuronal activity and its influence on developmentally regulated $GABA_A$ receptor expression in cultured mouse cerebellar granule cells. *Neuropharmacology* 43:715-725

Ives J.H., Drewery D.L., Thompson C.L., (2002b) Differential cell surface expression of $GABA_A$ receptor α_1, α_6, β_2 and β_3 subunits in cultured mouse cerebellar granule cells – influence of cAMP-activated signalling. *Journal of Neurochemistry* 80:317-327

Ives J.H., Fung S., Tiwari P., Payne H.L., Thompson C.L., (2004) Microtubule-associated Protein Light Chain 2 is a Stargazin-AMPA Receptor Complex-interacting Protein *in vivo*. *Journal of Biological Chemistry* 279(30):31002-31009

Jacob T.C., Bogdanov Y.D., Magnus C., Saliba R.S., Kittler J.T., Haydon P.G., Moss S.J., (2005) Gephyrin regulates the cell surface dynamics of synaptic $GABA_A$ receptors. *Journal of Neuroscience* 25(45):10469-10478

Jechlinger M., Pelz R., Tretter V., Klausberger T., Sieghart W., (1998) Subunit composition and quantitative importance of hetero-oligomeric receptors: $GABA_A$ receptors containing α_6 subunits. *Journal of Neuroscience* 18(7):2449-2457

Jiao Y., Sun Z., Lee T., Fusco F.R., Kimble T.D., Meade C.A., Cuthbertson S., Reiner A., (1999) A simple and sensitive antigen retrieval method for free-floating and slide-mounted tissue sections. *Journal of Neuroscience Methods* 93:149-162

Jones A., Korpi E.R., McKernan R.M., Pelz R., Nusser Z., Mäkelä R., Mellor J.R., Pollard S., Bahn S., Stephenson F.A., Randall A.D., Sieghart W., Somogyi P., Smith A.J.H., Wisden W., (1997) Ligand-gated ion channel subunit partnerships:$GABA_A$ receptor α_6 subunit gene inactivation inhibits δ subunit expression. *Journal of Neuroscience* 1794):1350-1362

Jovanovic J.N., Thomas P., Kittler J.T., Smart T.G., Moss S.J., (2004) Brain-derived neurotrophic factor modulates fast synaptic inhibition by regulating $GABA_A$ receptor phosphorylation, activity and cell-surface stability. *Journal of Neuroscience* 24(2):522-530

Keller C.A., Yuan X., Panzanelli P., Martin M.L., Alldred M., Sassoe-Pognetto M., Luscher B., (2004) The γ2 subunit of $GABA_A$ receptors is a substrate for palmitoylation by GODZ. *Journal of Neuroscience* 24(26):5881-5891

Kittler J.T., Rostaing P., Schiavo G., Fritschy J., Olsen R., Triller A., Moss S.J., (2001a) The subcellular distribution of GABARAP and its ability to interact with NSF suggest a role for this protein in the intracellular transport of $GABA_A$ receptors. *Molecular and Cellular Neuroscience* 18:13-25

Kittler J.T., Moss S.J., (2001b) Neurotransmitter receptor trafficking and the regulation of synaptic strength. *Traffic* 2:437-448

Kittler J.T., Moss S.J., (2003) Modulation of $GABA_A$ receptor activity by phosphorylation and receptor trafficking: implications for the efficacy of synaptic inhibition. *Current Opinion in Neurobiology* 13:341-347

Kittler J.T., Thomas P., Tretter V., Bogdanov Y.D., Haucke V., Smart T.G., Moss S.J., (2004) Huntingtin-associated protein 1 regulates inhibitory synaptic transmission by modulating γ-aminobutyric acid type A receptor membrane trafficking. *Proceedings of the National Academy of Sciences of the United States of America* 101(34):12736-12741

Klugbauer N., Dai S., Specht V., Lacinová L., Marais E., Bohn G., Hofmann F., (2000) A family of γ-like calcium channel subunits. *Federation of European Biochemical Societies Letters* 470:189-197

Kneussel M., Brandstätter J.H., Laube B., Stahl S., Müller U., Betz H., (1999) Loss of postsynaptic $GABA_A$ receptor clustering in gephyrin-deficient mice. *Journal of Neuroscience* 19(21):9289-9297

Kneussel M., Haverkamp S., Fuhrmann J.C., Wang H., Wassle H., Olsen R.W., (2000) The γ-Aminobutyric Acid Type A receptor-associated protein GABARAP interacts with gephyrin but is not involved in receptor anchoring at the synapse. *Proceedings of the National Academy of Sciences of the United States of America* 97(15):8594-8599

Kneussel M., Brandstätter J.H., Gasnier B., Feng G., Sanes J.R., Betz H., (2001) Gephyrin-independent clustering of postsynaptic $GABA_A$ receptor subtypes. *Molecular and Cellular Neuroscience* 17:973-982

Kneussel M., (2002) Dynamic regulation of $GABA_A$ receptors at synaptic sites. *Brain Research Reviews* 39:74-83

Korpi E.R., Koikkalainen P., Vekovischeva O.Y., Makela R., Kleinz R., Uusi-oukari M., (1998) Cerebellar granule-cell specific $GABA_A$ receptors attenuate benzodiazepine-induced ataxia: evidence from α6-subunit-deficient mice. *European Journal of Neuroscience* 11:233-240

Korpi E.R., Mihalek R.M., Sinkkonen S.T., Hauer B., Hevers W., Homanics G.E., Sieghart W., Lüdders H., (2002a) Altered receptor subtypes in the forebrain of $GABA_A$ receptor δ subunit-deficient mice: recruitment of γ_2 subunits. *Neuroscience* 109(4):733-743

Korpi E.R., Gründer G., Lüddens H., (2002b) Drug Interactions at $GABA_A$ Receptors. *Progress in Neurobiology* 67:113-159

Koyama R., Yamada M.K., Fujisawa S., Katoh-Semba R., Matsuki N., Ikegaya Y., (2004) brain-derived neurotrophic factor induces hyperexcitable re-entrant circuits in the dentate gyrus. *Journal of Neuroscience* 24(33):7215-7224

Koyama R., Ikegaya Y., (2005) To BDNF or not to BDNF: That if the epileptic hippocampus. *The Neuroscientist* 11(4):282-287

Krishek B.J., Xie X., Blackstone C., Huganir R.L., Moss S.J., Smart T.G., (1994) Regulation of $GABA_A$ receptor function by protein kinase C phosphorylation. *Neuron* 12:1081-1095

Laurie D.J., Wisden W., Seeburg P.H., (1992) The distribution of thirteen GABAA receptor subunit mRNAs in the rat brain. III. Embryonic and postnatal development. *Journal of Neuroscience* 12(11):4151-4172

Leil T.A., Chen Z., Chang C.S., Olsen R.W., (2004) $GABA_A$ receptor-associated protein traffics $GABA_A$ receptors to the plasma membrane in neurons. *Journal of Neuroscience* 24(50):11429-11438

Leroy C., Poisbeau P., Keller A.F., Nehlig A., (2004) Pharmacological plasticity of $GABA_A$ receptors at dentate gyrus synapses in a rat model temporal lobe epilepsy. *Journal of Physiology* 557.2:473-487

Letts V.A., Felix R., Biddlecome G.H., Arikkath J., Mahaffey C.L., Valenzuela A., Bartlett II F.S., Mori Y., Campbell K.P., Frankel W.N., (1998) The mouse Stargazer gene encodes a neuronal Ca^{2+}-channel γ subunit. *Nature Genetics* 19:340-347

Letts V.A., Kang M., Mahakkey C.L., Beyer B., Tenbrink H., Campbell K.P., Frankel W.N., (2003) Phenotypic heterogeneity in the stargazin allelic series. *Mammalian Genome* 14:506-513

Letts V.A., (2005a) Stargazer-A mouse to seize! *Epilepsy Currents* 5(5):161-165

Lin Y.F., Angelotti T.P., Dudek E.M., Browning M.D., McDonald R.L (1996) Enhancement of recombinant $\alpha 1\beta 1\gamma 2L$ γ-aminobutyric acid A receptor whole-cell currents by protein kinase C is mediated through phosphorylation of both $\beta 1$ and $\gamma 2L$ subunits. *Molecular Pharmacology* 50:185-195

Liu S.J., Cull-Candy S.G., (2005) Subunit interaction with PICK1 and GRIP controls Ca2+ permeability of AMPARs at cerebellar synapses. *Nature Neuroscience* 8(6):768-775

Loup F., Wieser H.G., Yonekawa Y., Aguzzi A., Fritschy J.M., (2000) Selective alterations in $GABA_A$ receptor subtypes in human temporal lobe epilepsy. *Journal of Neuroscience* 20(14):5401-5419

Lowry O.H., Rosebrough N.J., Farr A.L., Randall R.J., (1951) Protein measurements with the folin phenol reagent. *Journal of Biological Chemistry* 193: 265-275

Lüscher B., Keller C.A., (2004) Regulation of $GABA_A$ receptor trafficking, channel activity, and functional plasticity of inhibitory synapses. *Pharmacology and Therapeutics* 102:195-221

Lynd-Balla E., Pilcher W.H., Joseph S.A., (2004) AMPA Receptor alterations precede mossy fiber sprouting in young children with temporal lobe epilepsy. *Neuroscience* 126:105-114

Malenka R.C., Nicoll R.A., (1999) Long-term potentiation – a decade of progress? *Science* 285:1870-1874

Malinow R., Malenka R.C., (2002) AMPA Receptor Trafficking and Synaptic Plasticity. *Annual Reviews Neuroscience* 25:103-126

Mammen A.L., Huganir R.L., O'Brien R.J., (1997) Redistribution and stabilization of cell surface glutamate receptors during synapse formation. *Journal of Neuroscience* 17(19):7351-7358

Martikainen I.K., Lauk K., Moykkynen T., Holopainen I.E., Korpi E.R., Uusi-oukari M., (2004) Kainate down-regulates a subset of $GABA_A$ receptor subunits expressed in cultured mouse cerebellar granule cells. *Cerebellum* 3(1):27-38

McDonald B.J., Moss S.J., (1994) Differential phosphorylation of intracellular domains of γ-aminobutyric acid type A receptor subunits by calcium/calmodulin type 2-dependent protein kinase and cGMP-dependent protein kinase. *Journal of Biological Chemistry* 269(27):18111-18117

McDonald B.J., Amato A., Connolly C.N., Benke D., Moss S.J., Smart T.G., (1998) Adjacent phosphorylation sites on $GABA_A$ receptor β subunits determine regulation by cAMP-dependent protein kinase. *Nature Neuroscience* 1(1):23-28

McKernan R.M., Whiting P.J., (1996) Which $GABA_A$-receptor subtypes really occur in the brain? *Trends in Neurosciences* 19:139-143

Mehta A.K., Ticku M.K., (1999) Prevalence of the $GABA_A$ receptor assemblies containing α_1-subunit in the rat cerebellum and cerebral cortex as determined by immunoprecipitation: lack of modulation by chronic ethanol administration. *Molecular Brain Research* 67:194-199

Mellor J.R., Merlo D., Jones A., Wisden W., Randall A.D., (1998) Mouse cerebellar granule cell differentiation: Electrical activity regulates the $GABA_A$ receptor α6 subunit gene. *Journal of Neuroscience* 18(8):2822-2833

Mihalek R.M., Banerjee P.K., Korpi E.R., Quinlan J.J., Firestone L.L., Mi Z., Lagenaur C., Tretter V., Sieghart W., Anagnostaras S.G., Sage J.R., Fanselow M.S., Guidotti A., Spigelman I., Li Z., Delorey T.M., Olsen R.W., Homanics G.E., (1999) Attenuated sensitivity to neuroactive steroids in γ-aminobutyric acid type A receptor delta subunit knockout mice. *Proceedings of the National Academy of Sciences of the United States of America* 96(22):12905-12910

Mohler H., Knoflach F., Paysan J., Motejlek K., Benke D., Luscher B., Fritschy J.M., (1995) Heterogeneity of GABAA-receptors: Cell-specific expression, pharmacology and regulation. *Neurochemical Research* 20(5):631-636

Moss S.J., Smart T.G., (2001) Constructing inhibitory synapses. *Nature Reviews Neuroscience* 2(4):240-250

Moss F.J., Viard P., Davies A., Bertaso F., Page K.M., Graham A., Canti C., Plumpton M., Plumpton C., Clare J.J., Dolphin A.C., (2002) The novel product of a five-exon stargazin-related gene abolishes $Ca_V2.2$ calcium channel expression. *European molecular biology organisation* 21(7):1514-1523

Nahm W.K., Noebels J.L., (1998) Nonobligate role of early or sustained expression of immediate-early gene proteins c-Fos, c-Jun, and Zif/268 in hippocampal mossy fiber sprouting. *Journal of Neuroscience* 18(22):9245-9255

Nakagawa T., Sheng M., (2000) A stargazer foretells the way to the synapse. *Science* 290(5500):2270-2271

Nishimune A., Isaac J.T.R., Molnar E., Noel J., Nash S.R., Tagaya M., Collingridge G.L., Nakanishi S., Henley J.M., (1998) NSF binding to GluR2 regulates synaptic transmission. *Neuron* 21:87-97

Noebels J.L., Qiao X., Bronson R.T., Spencer C., Davisson M.T., (1990) Stargazer: a new neurological mutant on chromosome 15 in the mouse with prolonged cortical seizures. *Epilepsy Research* 7:129-135

Nusser Z., Sieghart W., Somogyi P., (1998) Segregation of different $GABA_A$ receptors to synaptic and extrasynaptic membranes of cerebellar granule cells. *Journal of Neuroscience* 18(5):1693-1703

Peng Z., Hauer B., Mihalek R.M., Homanics G.E., Sieghart W., Olsen R.W., Houser C.R., (2002) $GABA_A$ receptor changes in δ subunit-deficient mice: Altered expression of α4 and γ2 subunits in the forebrain. *Journal of Comparative Neurology* 446:179-197

Peng Z., Huang C.S., Stell B.M., Mody I., Houser C.R., (2004) Altered Expression of the δ Subunit of the $GABA_A$ Receptor in a Mouse Model of Temporal Lobe Epilepsy. *Journal of Neuroscience* 24(39):8629-8639

Peng Z., Houser C.R., (2005) Temporal patterns of Fos expression in the dentate gyrus after spontaneous seizures in a mouse model of temporal lobe epilepsy. *Journal of Neuroscience* 25(31):7210-7220

Pirker S., Schwarzer C., Wieselthaler A., Sieghart W., Sperk G., (2000) $GABA_A$ receptors: Immunocytochemical distribution of 13 subunits in the adult rat brain. *Neuroscience* 101(4):815-850

Poisbeau P., Cheney M.C., Browning M.D., Mody I., (1999) Modulation of synaptic $GABA_A$ receptor function by PKA and PKC in adult hippocampal neurons. *Journal of Neuroscience* 19(2):674-683

Pollard S., Duggan M.J., Stephenson F.A., (1993) Further evidence for the existence of alpha subunit heterogeneity within discrete gamma-aminobutyric acid A receptor subpopulations. *Journal of Biological Chemistry* 268(5):3753-3757

Pollard S., Thompson C.L., Stephenson F.A., (1995) Quantitative characterisation of α_6 and $\alpha_1\alpha_6$ subunit-containing native γ-aminobutyric acid A receptors of adult rat cerebellum demonstrates two α subunits per receptor oligomer. *Journal of Biological Chemistry* 270(36):21285-21290

Pöltl A., Hauer B., Fuchs K., Tretter V., Sieghart W., (2003) Subunit composition and quantitative importance of $GABA_A$ receptor subtypes in the cerebellum of mouse and rat. *Journal of Neurochemistry* 87:1444-1455

Priel A., Kolleker A., Ayalon G., Gillor M., Osten P., Stern-Bach Y., (2005) Stargazin reduces desensitization and slows deactivation of the AMPA-type glutamate receptors. *Journal of Neuroscience* 25(10):2682-2686

Qiao X., Noebels J.L., (1993) Developmental analysis of hippocampal mossy fiber outgrowth in a mutant mouse with inherited spike-wave seizures. *Journal of Neuroscience* 13(11):4622-4635

Qiao X., Hefti F., Knusel B., Noebels J.L., (1996) Selective failure of brain-derived neurotrophic factor mRNA expression in the cerebellum of stargazer, a mutant mouse with ataxia. *Journal of Neuroscience* 16(2):640-648

Qiao X., Chen L., Gao H., Bao S., Hefti F., Thompson R.F., Knusel B., (1998) Cerebellar brain derived neurotrophic factor-TrkB defect associated with impairment of eyeblink conditioning in Stargazer mutant mice. *Journal of Neuroscience* 18(17):6990-6999

Qiao X., Meng H., (2003) Nonchannel functions of the calcium channel γ subunit: Insight from research on the Stargazer mutant. *Journal of Bioenergetics and Biomembranes* 35(6):661-670

Quirk K., Gillard N.P., Ragan C.I., Whiting P.J., McKernan R.M., (1994) Model of subunit composition of γ-aminobutyric acid A receptor subtypes expressed in rat cerebellum with respect to their α and γ/δ subunits. *Journal of Biological Chemistry* 269(23):16020-16028

Quirk K., Whiting P.J., Ragan C.I., McKernan R.M., (1995) Characterisation of δ-subunit containing $GABA_A$ receptors from rat brain. *European Journal of Pharmacology-Molecular Pharmacology Section 290*:175-181

Rathenberg J., Kittler J.T., Moss S.J., (2004) Palmitoylation regulates the clustering and cell surface stability of $GABA_A$ receptors. *Molecular and Cellular Neuroscience* 26:251-257

Rogers C.J., Twyman R.E., MacDonald R.L., (1994) Benzodiazepine and beta-carboline regulation of single GABAA receptor channels of mouse spinal neurons in culture. *Journal of Physiology* 475:69-82

Rouach N., Byrd K., Petralia R.S., Elias G.M., Adesnik H., Tomita S., Karimzadegan S., Kealey C., Bredt D.S., Nicoll R.A., (2005) TARP γ-8 controls hippocampal AMPA receptor number, distribution and synaptic plasticity. *Nature Neuroscience* 8(11):1525-1533

Rousset M., Cens T., Restituito S., Barrere C., Black III J.L., McEnery M.W., Charnet P., (2001) Functional roles of γ2, γ3 and γ4, three new Ca^{2+} channel subunits, in P/Q-type Ca^{2+} channel expressed in *Xenopus* oocytes. *Journal of Physiology* 532.3:583-593

Sans N., Racca C., Petralia R.S., Wang Y., McCallum J., Wenthold R.J., (2001) Synapse-associated protein 97 selectively associates with a subset of AMPA receptors early in their biosynthetic pathway. *Journal of Neuroscience* 21(19):7506-7516

Sarto I., Wabnegger L., Dögel E., Sieghart W., (2002) Homologous sites of $GABA_A$ receptor α1, β3, γ2 subunits are important for assembly. *Neuropharmacology* 43:482-491

Sassoe-Pognetto M., Fritschy J., (2000) Gephyrin, a major postsynaptic protein of GABAergic synapses. *European Journal of Neuroscience* 12:2205-2210

Schnell E., Sizemore M., Karimzadegan S., Chen L., Bredt D.S., Nicoll R.A., (2002) Direct interactions between PSD-95 and stargazing control synaptic AMPA receptor number. *Proceedings of the National Academy of Sciences of the United States of America* 99(21):13902-13907

Segal R.A., Takahashi H., McKay R.D.G., (1992) Changes in neurotrophin responsiveness during the development of cerebellar granule neurons. *Neuron* 9:1041-1052

Sharp A.H., Black J.L., Dubel S.J., Sundarraj S., Shen J.P., Yunker A.M.R., Copeland T.D., Mcenery M.W., (2001) Biochemical and anatomical evidence for specialised voltage-dependent calcium channel γ isoform expression in the epileptic and ataxic mouse, Stargazer. *Neuroscience* 105(3):599-617

Shen L., Liang F., Walensky L.D., Huganir R.L., (2000) Regulation of AMPA receptor GluR1 subunit surface expression by a 4.1 N-linked actin cytoskeletal association. *Journal of Neuroscience* 20:7932-7940

Shumate M.D., Lin D.D., Gibbs III J.W., Holloway K.L., Coulter D.A., (1998) $GABA_A$ receptor function in epileptic human dentate granule cells: comparison to epileptic and control rat. *Epilepsy Research* 32:114-128

Sieghart W., Eichinger A., Richards J.G., Mohler H., (1987) Photoaffinity labelling of benzodiazepine receptor proteins with the partial inverse agonist [^{3}H] Ro15-4513: A biochemical and autoradiographic study. *Journal of Neurochemistry* 48(1):46-52

Sieghart W., Fuchs K., Tretter V., Ebert V., Jechlinger M., Hoger H., Adamiker D., (1999) Structure and subunit composition of $GABA_A$ receptors. *Neurochemistry International* 34:379-385

Sinkkonen S.T., Vekovischeva O.Y., Moykkynen T., Ogris W., Sieghart W., Wisden W., Korpi E.R., (2004) Behavioural correlates of an altered balance between synaptic and extrasynaptic $GABA_A$ergic inhibition in a mouse model. *European Journal of Neuroscience* 20:2168-2178

Slany A., Zezula J., Tretter V., Sieghart W., (1995) Rat β3 subunits expressed in human embryonic kidney 293 cells form high affinify [^{35}S] t-butylbicyclophosphorothionate binding sites modulated by several allosteric ligands of γ-aminobutyric acid type A receptors. *Molecular Pharmacology* 48:385-391

Smart T.G., (1997) Regulation of excitatory and inhibitory neurotransmitter-gated ion channels by protein phosphorylation. *Current Opinion in Neurobiology* 7:358-367

Smart T.G., (1998) in Frontiers in Neurobiology: Amino Acid Neurotransmission. Edited by F.A. Stephenson and A.J. Turner. Portland Press (London)

Song I., Kamboj S., Xia J., Dong H., Liao D., Huganir R.L., (1998) Interaction of the N-ethylmaleimide-sensitive factor with AMPA receptors. *Neuron* 21:393-400

Song I., Huganir R.L., (2002) Regulation of AMPA receptors during synaptic plasticity. *Trends in Neurosciences*. 25(11):578-588

Sperk G., Schwarzer C., Tsunashima K., Fuchs K., Sieghart W., (1997) $GABA_A$ receptor subunits in the rat hippocampus I: immunocytochemical distribution of 13 subunits. *Neuroscience* 80(4):987-1000

Spigelman I., Li Z., Banerjee P.K., Mihalek R.M., Homanics G.S., Olsen R.W., (2002) Behaviour and physiology of mice lacking the $GABA_A$-receptor δ subunit. *Epilepsia* 43(Suppl. 5):3-8

Spigelman I., Li Z., Liang J., Cagetti E., Samzadeh S., Mihalek R.M., Homanics G.E., Olsen R.W., (2003) Reduced inhibition and sensitivity to neurosteroids in hippocampus of mice lacking the $GABA_A$ receptor δ subunit. Journal of *Neurophysiology* 90:903-910

Srivastava S., Osten P., Vilim F.S., Khatri L., Inman G.J., States B.A., Daly C., DeSouza S., Abagyan R., Valtschanoff J.G., Weinberg R.J., Ziff E.B., (1998) Novel anchorage of GluR2/3 to postsynaptic density by an AMPA receptor binding protein ABP. *Neuron* 21:581-591

Stell B.M., Brickley S.G., Tang C.Y., Farrant M., Mody I., (2003) Neuroactive steroids reduce neuronal excitability by selectively enhancing tonic inhibition mediated by δ subunit-containing $GABA_A$ receptors. *Proceedings of the National Academy of Sciences of the United States of America* 100(24):14439-14444

Sun C., Sieghart W., Kapur J., (2004) Distribution of α1, α4, γ2, and δ subunits of $GABA_A$ receptors in hippocampal granule cells. *Brain Research* 1029:207-216

Sur C., Farrar S.J., Kerby J., Whiting P.J., Atack J.R., McKernan R.M., (1999) Preferential coassembly of α4 and δ subunits of the γ-aminobutyric $acid_A$ receptor in rat thalamus. *Molecular Pharmacology* 56:110-115

Swope S.L., Moss S.J., Blackstone C.B., Huganir R.L., (1992) Phosphorylation of ligand-gated ion channels: a possible mode of synaptic plasticity. *Federation of American Societies for experimental biology* 6:2514-2523

Tehrani M.H.J., Baumgartner B.J., Barnes E.M., (1997) Clathrin-coated vesicles from bovine brain contain uncoupled $GABA_A$ receptors. *Brain Research* 776:195-203

Thompson C.L., Bodewitz G., Stephenson F.A., Turner J.D., (1992) Mapping of $GABA_A$ receptor α5 and α6 subunit-like immunoreactivity in rat brain. *Neuroscience Letters* 144:53-56

Thompson C.L., Stephenson F.A., (1994) $GABA_A$ receptor subtypes expressed in cerebellar granule cells: a developmental study. *Journal of Neurochemistry* 62: 2037-2044

Thompson C.L., Pollard S., Stephenson F.A., (1996) Developmental regulation of expression of $GABA_A$ receptor α_1 and α_6 subunits in cultured rat cerebellar granule cells. *Neuropharmacology* 35(9/10):1337-1346

Thompson C.L., Tehrani M.H., Barnes E.M., Stephenson F.A., (1998) Decreased expression of $GABA_A$ receptor α_6 and β_3 subunits in stargazer mutant mice: a possible role for brain-derived neurotrophic factor in the regulation of cerebellar $GABA_A$ receptor expression. *Molecular Brain Research* 60:282-290

Thompson C.L., Razzini G., Pollard S., Stephenson F.A., (2000) Cyclic AMP-mediated regulation of $GABA_A$ receptor subunit expression in mature rat cerebellar granule cells: Evidence for transcriptional and translational control. *Journal of Neurochemistry* 74:920-931

Thompson R.F., (1990) Neural mechanisms of classical conditioning in mammals. *Philos Trans R Soc Lond B Biol Sci* 329:161-170

Tomita S., Nicoll R.A., Bredt D.S., (2001) PDZ protein interactions regulating glutamate receptor function and plasticity. *Journal of Cell Biology* 153(5):F19-F23

Tomita S., Chen L., Kawasaki Y., Petralia R.S., Wenthold R.J., Nicoll R.A., Bredt D.S., (2003) Functional studies and distribution define a family of transmembrane AMPA receptor regulatory proteins. *Journal of Cell Biology* 161(4):805-816

Tomita S., Fukata M., Nicoll R.A., Bredt D.S., (2004) Dynamic interaction of stargazin-like TARPs with cycling AMPA receptors at synapses. *Science* 303:1508-1511

Tomita S., Stein V., Stocker T.J., Nicoll R.A., Bredt D.S., (2005a) Bidirectional synaptic plasticity regulated by phosphorylation of stargazin-like TARPs. *Neuron* 45:269-277

Tomita S., Adesnik H., Sekiguchi M., Zhang W., Wada K., Howe J.R., Nicoll R.A., Bredt D.S., (2005b) Stargazin modulates AMPA receptor gating and trafficking by distinct domains. *Nature* 435(7045):1052-1058

Tretter V., Haver B., Nusser Z., Mihalek R.M., Hoger H., Homanics G.E., Somogyi P., Sieghart W., (2001) Targeted disruption of the $GABA_A$ receptor δ subunit gene leads to an up-regulation of γ_2 subunit-containing receptors in cerebellar granule cells. *Journal of Biological Chemistry* 276(13):10532-10538

Turetsky D., Garringer E., Patneau D.K., (2005) Stargazin modulates native AMPA receptor functional properties by two distinct mechanisms. *Journal of Neuroscience* 25(32):7438-7448

Turner D.M., Sapp D.W., Olsen R.W., (1991) The benzodiazepine/alcohol antagonist Ro15-4513: Binding to a $GABA_A$ receptor subtype that is insensitive to diazepam. *Journal of Pharmacology and Experimental Therapeutics* 257(3):1236-1242

Uusi-Oukari M., (1992) Characterisation of two cerebellar binding sites of [^{3}H] Ro15-4513. *Journal of Neurochemistry* 59:568-574

Vandenberghe W., Nicoll R.A., Bredt D.S., (2005a) Stargazin is an AMPA receptor auxiliary subunit. *Proceedings of the National Academy of Sciences of the United States of America* 102(2):485-490

Vandenberghe W., Nicoll R.A., Bredt D.S., (2005b) Interaction with the Unfolded Protein Response reveals a role for stargazin in biosynthetic AMPA receptor transport. *Journal of Neuroscience* 25(5):1095-1102

Wang H., Olsen R.W., (2000) Binding of the $GABA_A$ receptor-associated protein (GABARAP) to microtubules and microfilaments suggests involvement of the cytoskeleton in GABARAP-$GABA_A$ receptor interaction. *Journal of Neurochemistry* 75:644-655

Wei W. Zhang N., Peng Z., Houser CR., Mody I., (2003) Perisynaptic localization of δ subunit-containing $GABA_A$ receptors and their activation by GABA spillover in the mouse dentate gyrus. *Journal of Neuroscience* 23(33):10650-10661

Wingrove P.B., Safo P., Wheat L., Thompson S.A., Wafford K.A., Whiting P.J., (2002) Mechanism of α-subunit selectivity of benzodiazepine pharmacology at γ-aminobutyric acid type A receptors. *European Journal of Neuroscience* 437:31-39

Wisden W., Korpi E.R., Bahn S., (1996) The Cerebellum: A model for studying $GABA_A$ receptor diversity. *Neuropharmacology* 35(9/10):1139-1160

Wisden W., Cope D., Klausberger T., Hauer B., Sinkkonen S.T., Tretter V., Lujan R., Jones A., Korpi E.R., Mody I., Sieghart W., Somogyi P., (2002) Ectopic expression of the $GABA_A$ receptor α6 subunit in hippocampal pyramidal neurons produces extrasynaptic receptors and an increased tonic inhibition. *Neuropharmacology* 43:530-549

Xia J., Zhang X., Staudinger J., Huganir R.L., (1999) Clustering of AMPA receptors by the synaptic PDZ domain-containing protein PICK1. *Neuron* 22:179-187

Yamada M.K., Nakanishi K., Ohba S., Nakamura T., Ikegaya Y., Nishiyama N., Matsuki N., (2002) Brain-derived neurotrophic factor promotes the maturation of GABAergic mechanisms in cultured hippocampal neurons. *Journal of Neuroscience* 22(17):7580-7585

Yamasaki M., Ohno-Shosaku T., Fukaya M., Kano M., Watanabe M., Sakimura K., (2004) A novel action of stargazin as an enhancer of AMPA receptor activity. *Neuroscience Research* 50:369-374

Zheng T.M., Zhu W.J., Puia G., Vicini S., Grayson D.R., Costa E., Caruncho H.J., (1994) Changes in γ-aminobutyric type A receptor subunit mRNAs, translation product expression, and receptor function during neuronal maturation *in vitro. Proceedings of the National Academy of Sciences of the United States of America* 91:10952-10956

Zhou Q., Xiao M., Nicoll R.A., (2001) Contribution of cytoskeleton to the internalization of AMPA receptors. *Proceedings of the National Academy of Sciences of the United States of America* 98(3):1261-1266

Zhu W.J., Wang J.F., Kreuger K.E., Vicini S., (1996) δ subunit inhibits neurosteroid modulation of $GABA_A$ receptors. *Journal of Neuroscience* 16(21):6648-6656